SURFACE PLASMON RESONANCE IMAGING AS A SCREENING PLATFORM IN BIOPHARMACEUTICAL DEVELOPMENT

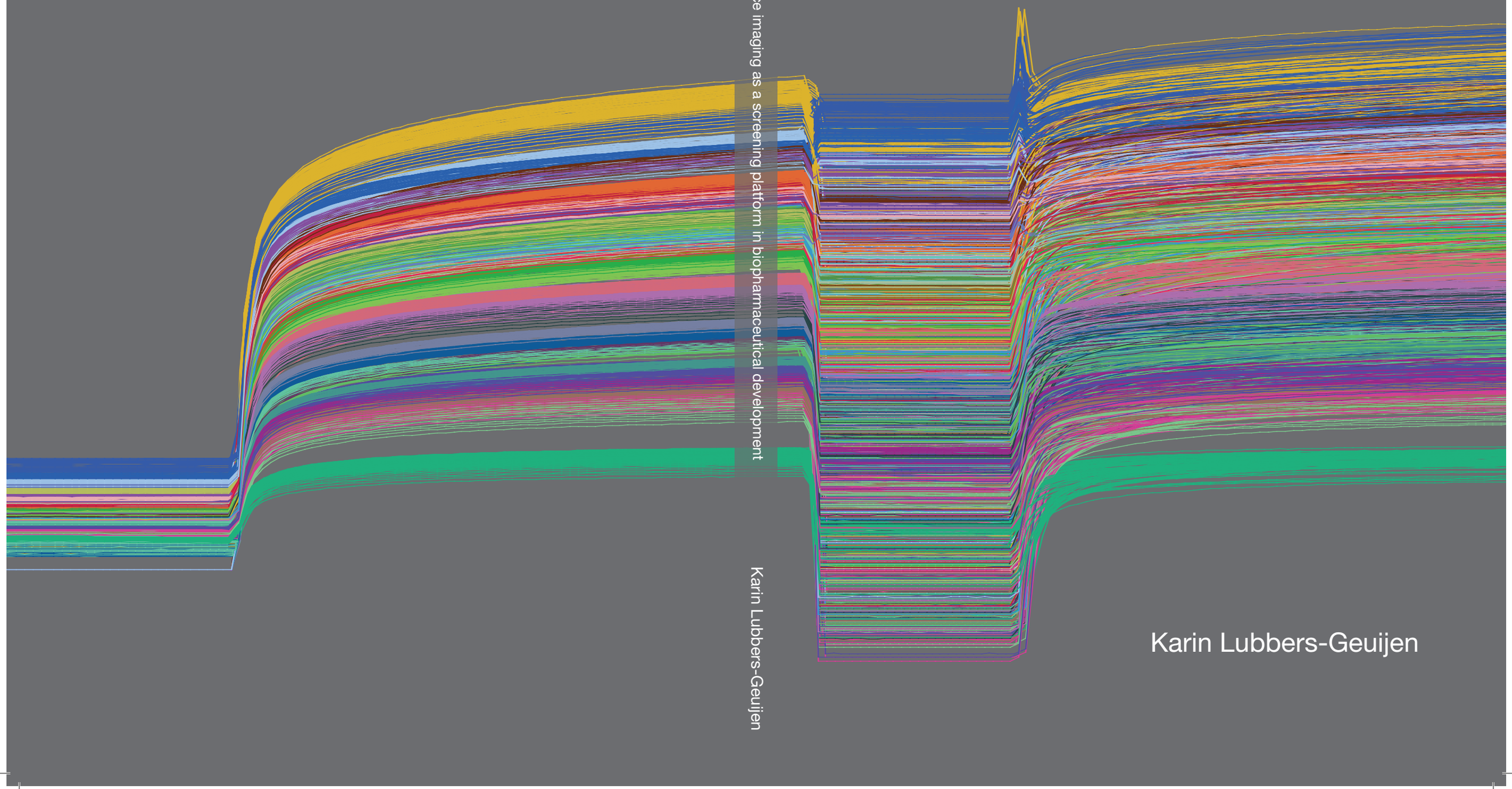

Surface plasmon resonance imaging as a screening platform in biopharmaceutical development

Karin Lubbers-Geuijen

Karin Lubbers-Geuijen

Propositions

1. Size matters: protein aggregates influence SPR analyses.
   (this thesis)

2. Sugars are not always sweet, because glycan binding studies are challenging.
   (this thesis)

3. The reflectivity - incidence angle curve in SPR closely matches the four years of a PhD trajectory.

4. Technological innovations are a worldwide threat when not used for the intended applications.

5. Every child exhibits a natural perseverance that fades during the years, unless one challenges him/herself.

6. Children's behavior is a balance between nature and nurture.

Propositions belonging to the thesis entitled:
Surface plasmon resonance imaging as a screening platform in biopharmaceutical development

Karin Lubbers-Geuijen
2017

Surface plasmon resonance imaging as a screening platform in biopharmaceutical development

Karin Lubbers-Geuijen

Thesis committee

Promotors

Prof. Dr M.H.M Eppink

Special Professor Biorefinery with Focus on Mild Separation Technologies of Complex Biomolecules

Wageningen University & Research

Co-promotors

Dr R.B.M. Schasfoort

Associate professor, Faculty of Science and Technology, Medical Cell BioPhysics

University of Twente, Enschede

Dr D.F. Egging

Project leader, Preclinical department, Bioanalysis group

Synthon Biopharmaceuticals BV, Nijmegen

Other members

Prof. Dr M.W.F. Nielen, Wageningen University & Research

Prof. Dr G.W. Somsen, VU Amsterdam

Prof. Dr M.W.J. Prins, Eindhoven University of Technology

Dr G. Vidarsson, Sanquin, Amsterdam

This research was conducted under the auspices of the Graduate School VLAG (Advanced studies in Food Technology, Agrobiotechnology, Nutrition and Health Sciences)

Surface plasmon resonance imaging as a screening platform in biopharmaceutical development

Karin Lubbers-Geuijen

Thesis

submitted in fulfillment of the requirements for the degree of doctor
at Wageningen University
by the authority of the Rector Magnificus,
Prof. Dr A.P.J. Mol,
in the presence of the
Thesis Committee appointed by the Academic Board
to be defended in public
on Monday 28 August 2017
at 11 a.m. in the Aula.

K.P.M. Lubbers-Geuijen

Surface plasmon resonance imaging as a screening platform in biopharmaceutical development,

246 pages.

PhD thesis, Wageningen University, Wageningen, the Netherlands (2017)

With references, with summaries in English and Dutch

ISBN: 978-94-6343-211-5

DOI: 10.18174/415645

Contents

Abbreviations and terminology

ADC	antibody drug conjugate
ADCC	antibody-dependent cell-mediated cytotoxicity
AEX	anion-exchange chromatography
AF4	asymmetrical flow field flow fractionation
AUC	analytical ultracentrifugation
BHK	baby hamster kidney
BLI	biolayer interferometry
CCF	cell culture filtrate
CD	circular dichroism
CDC	complement-dependent cytotoxicity
CE-LIF	capillary electrophoresis – laser induced fluorescence
CE-MS	capillary electrophoresis – mass spectrometry
CE-SDS	capillary electrophoresis – sodium dodecyl sulfate
CEX	cation-exchange chromatography
CFM	continuous flow microspotter
CHO	chinese hamster ovary
cIEF	capillary isoelectric focusing
CIP	cleaning-in-place
CQA	critical quality attribute
CV	column volumes
CZE	capillary zone electrophoresis
DBC	dynamic binding capacity
DSC	differential scanning calorimetry
DSP	downstream processing
ELISA	enzyme-linked immunosorbent assay
EPO	erythropoietin
ER	endoplasmic reticulum
FcRn	neonatal Fc receptor
FTIR	fourier transform infrared spectroscopy
GC-MS	gas chromatography – mass spectrometry
HCP	host cell protein

HDX-MS	hydrogen-deuterium exchange mass spectrometry
HEK	human embryonic kidney
HIC	hydrophobic interaction chromatography
HILIC-FLD	hydrophilic liquid chromatography – fluorescence detection
HPAEC-PAD	High-performance anion exchange chromatography - pulsed amperometric detection
HTS	high-throughput screening
IEC	ion-exchange chromatography
IEF	isoelectric focusing
IgG	immunoglobulin G
IMAC	immobilized-metal affinity chromatography
KCA	KanCapA (protein A ligand)
LC-FLC	liquid chromatography – fluorescence detection
LC-MS	liquid chromatography – mass spectrometry
LO	light obscuration
MALDI-MS	matrix-assisted laser desorption ionization – mass spectrometry
MFI	micro-flow imaging
MS	mass spectrometry
MS	MabSelect (protein A ligand)
MSS	MabSelectSure (protein A ligand)
NMR	nuclear magnetism resonance
NPLC-FLC	normal phase liquid chromatography – fluorescence detection
PTM	post-translational modification
R_{eq}	response at equilibrium
RP-HPLC	reversed phase high-pressure liquid chromatography
ROI	region of interest
RU	resonance units
SDS-PAGE	sodium dodecyl sulfate – polyacrylamide gel electrophoresis
SEC	size-exclusion chromatography
SPR/SPRi	surface plasmon resonance, surface plasmon resonance imaging
rhEPO	recombinant human erythropoietin
USP	upstream processing

CHAPTER 1

General introduction and thesis outline

Chapter 1

Abstract

Development of biopharmaceutical products requires extensive research on a multitude of steps that are involved in the delivery of a final product. In this chapter, a general introduction on biopharmaceuticals is provided, including two examples of biopharmaceutical products (erythropoietin and monoclonal antibodies) that have been studied throughout this research. The following paragraphs will highlight a typical production process for biopharmaceuticals consisting of both upstream and downstream processing. In addition, product characterization using a variety of analytical tools is required to determine the product quality, based on several critical quality attributes of biopharmaceuticals that need to be assessed. An overview of the most widely applied analytical tools, including the product characteristics that can be determined, is provided. This is followed by a more detailed description of the principles of Surface Plasmon Resonance (SPR) and SPR imaging (SPRi), which was the main analytical technology that has been applied in this research. The use and potential applications of SPRi during various steps in biopharmaceutical development have been explored and will be further discussed throughout this work.

Biopharmaceuticals

The biopharmaceutical market is growing year by year, ever since the introduction of the very first biological therapeutics.[1,2] In 1982 recombinant human insulin was approved as the first therapeutic recombinant protein.[1,2] Since that date, many more products have been developed and approved, including hormones, growth factors and monoclonal antibodies.[3] Currently, biopharmaceuticals occupy approximately a quarter of the total pharmaceutical market, with annual sales exceeding the blockbuster status of $1 billion for several of them.[3] Annual sales of biologics reached $163 billion in 2016 (lamerie.com, press release 17 March 2017), which was a growth of 5.8% compared to 2015. Whereas in the early days these biological products were extracted from a natural source, today recombinant proteins are the main source of an ever expanding market.[3] Recombinant proteins are produced in living cells that were genetically modified in order to produce the protein of interest. The choice for a particular type of cell line is often determined by the required characteristics of the end product, mainly based on glycosylation, which is best produced in mammalian cells.

On-going efforts are made to improve the production and purification of biopharmaceuticals, resulting in higher yields while reducing production costs. These improvements may lead to processes that alter the quality of the proteins, and therefore extensive monitoring of product quality during process optimization is performed.

The following sections will briefly introduce erythropoietin and monoclonal antibodies, two types of therapeutic proteins that were subject for method development using SPRi in this research, aiming at rapid screening methodologies.

Erythropoietin

Erythropoietin (EPO) was developed as a biotherapeutic to stimulate the production of red blood cells in patients with renal failure.[4] EPO is a glycoprotein hormone which is naturally synthesized by the kidney and regulates red blood cell production (Figure 1.1). The production of EPO by recombinant technology became available after the sequencing of the human gene responsible for natural EPO production[5] and transfection of this gene into producing mammalian cell lines. Recombinant human EPO (rhEPO) was approved in 1988 by the FDA as a therapeutic protein for treatment of anemia.[4,6] rhEPO acts as a medium to increase hemoglobin and hematocrit levels in patients with deficient red blood cell production. For this same reason, rhEPO has also been abused as a performance-enhancing

drug in sports and its use has been prohibited by the World Anti-Doping Agency (WADA) and the International Olympic Committee (IOC).[7,8]

Since the patent on the original rhEPO product has expired, a large number of biosimilars[1] from competitors have entered the market.[3] Some of these biosimilar products are quite different from the natural EPO or the original rhEPO, for example in terms of sialylation, which may lead to faster plasma clearance, since the level of sialylation is directly correlated to the *in vivo* half-life of EPO.[9] Therefore, full characterization of biosimilar products and comparability with the innovator product are required to determine the quality.

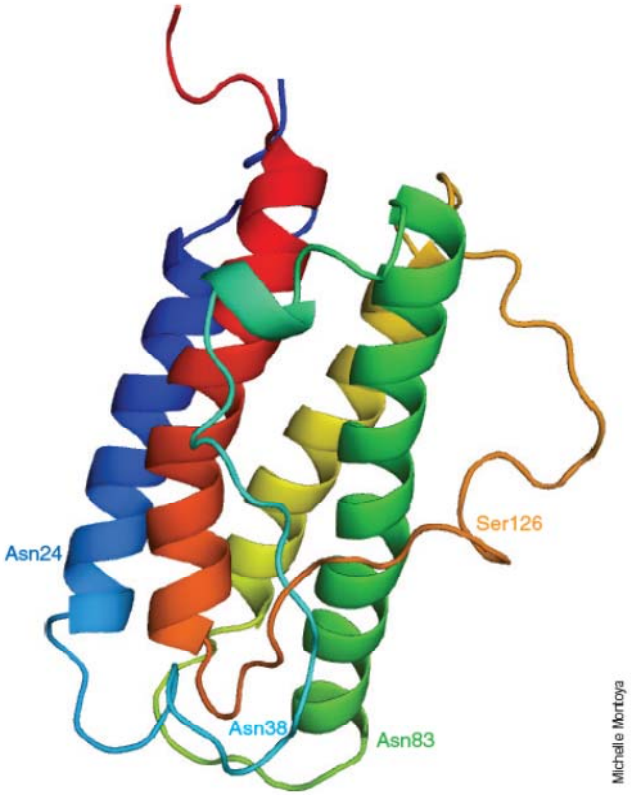

Figure 1.1 *Protein structure of erythropoietin including the four potential glycosylation sites (reprinted from Walsh and Jefferis, Nature biotechnology [10])*

[1] Here we refer to biosimilars as any copy of the original product. Several definitions of biosimilars / biosimilarity across different countries may apply. In Europe a biosimilar is a product that has been approved by the EMA and is comparable in safety and efficacy.

Furthermore, the administration of therapeutic proteins to patients can have severe side-effects, such as generation of neutralizing antibodies as has been the case for rhEPO.[11] These neutralizing antibodies may not only block the activity of the recombinant protein, but also of the endogenous protein. Immunogenic responses may be influenced by structural differences in the protein, storage conditions, contaminants or dosage forms.[12] In case of rhEPO, the immunogenicity response of patients may cause a complete absence of red blood cell precursors in the bone marrow, known as pure red cell aplasia (PRCA). No explicit cause for the increase in PRCA cases could be identified, and this was most likely a multifactorial cause.[13]

One of the most important characteristics of rhEPO is proper glycosylation; the attachment of sugar groups to several amino acid side groups. EPO glycosylation consists of three N-linked glycosylation sites (Asn-24, Asn-38 and Asn-83) and one O-linked glycosylation site (Ser-126) (Figure 1.1).[14] The molecular weight of the EPO protein alone is 18 kDa, and is increased to approximately 33-39 kDa because of the heavy glycosylation on the four glycosites.[15] Proper glycosylation of the rhEPO molecule is important for its biological activity, *in vivo* clearance rate and determines the stability and correct folding of the protein.[16] Especially, sialylation of the glycans (presence of terminal sialic acid) significantly impacts the *in vivo* bioactivity.

Extending the *in vivo* half-life of rhEPO has mainly focused on ways to improve sialylation levels on the molecules. Zhang et al.[17] have identified the genes that are responsible for sialylation of rhEPO in six different cell lines. They found that BHK and CHO cell lines were most effective in sialylation of rhEPO. Another strategy that has been applied is the introduction of novel erythropoiesis-stimulating agents, such as darbepoietin alfa. These compounds are analogues of rhEPO, but exhibit additional N-linked glycosylation sites and therefore have higher sialylation content. The major benefit is an extended serum half-life and increased *in vivo* activity, because of the presence of additional glycans and especially additional sialylation.[18] Another way to improve the sialylation of rhEPO was demonstrated by Meininger et al.[19] who were able to separate low-sialylated rhEPO variants from high-sialylated rhEPO variants by serotonin affinity chromatography.

In summary, sialylation of rhEPO is one of the most important characteristics of the molecule which can be improved at the molecular level, by amino acid mutations to include additional N-glycosylation sites, at the upstream processing by optimizing the culture conditions or during the downstream processing by applying novel selective purification methodologies.

Monoclonal antibodies

One of the main classes of therapeutic proteins nowadays is monoclonal antibodies, so far only of the immunoglobulin G (IgG) type.[10] These antibodies consist of 2 heavy and 2 light chains, connected via disulfide bridges, resulting in a protein of approximately 150 kDa.[20] An IgG has a typical Y-shaped protein structure, with a variable domain at both light chain – heavy chain connections (Fab region), and an Fc region consisting of the lower constant regions of the heavy chains (Figure 1.2). The main advantage of IgGs as a therapeutic protein is the specific binding to a target antigen by the complementary-determining regions (CDRs) in the variable domain of the molecule.

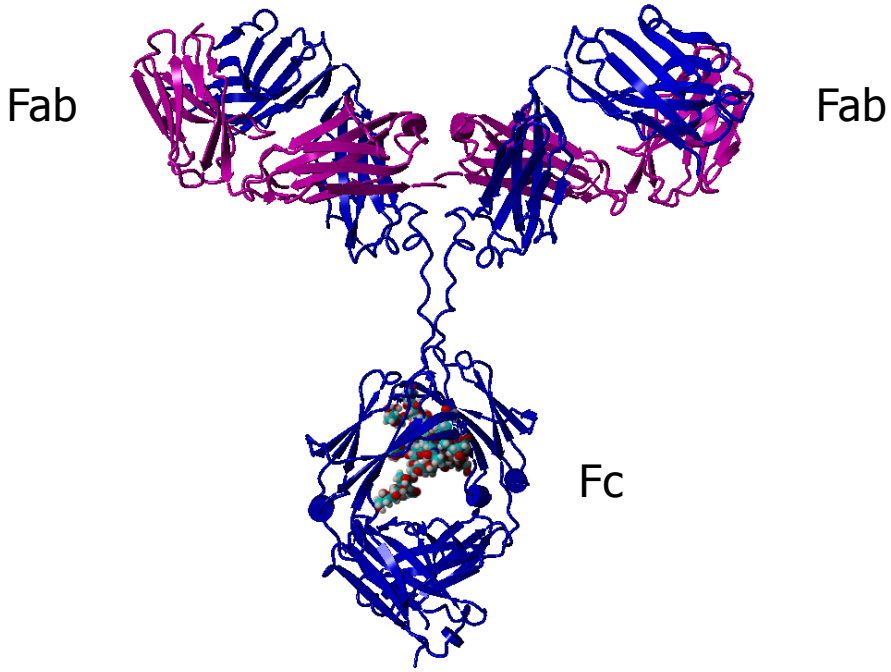

Figure 1.2 *Protein structure of an IgG molecule, with light chains in purple and heavy chains in blue, In the Fc region two N-glycosylation sites are present and corresponding glycans are shown.*

IgGs have a relatively stable structure, because of the various interchain and intrachain disulfide bonds. Four subclasses of IgGs exist (IgG1, IgG2, IgG3 and IgG4), with a 95% sequence homology. The major differences in amino acid sequence between the four IgG subclasses is found in the hinge region and the upper CH2 domain, which is important for the Fc effector functions of the antibodies, such as IgG – Fcγ receptor binding and binding

to complement C1q.[21] The Fc region is involved in clearance mechanisms like antibody-dependent cell-mediated cytotoxicity (ADCC) and phagocytosis by binding to various Fcγ receptors and complement-dependent cytotoxicity (CDC) by binding to C1q. Additionally, the relatively long half-life of antibodies in a human body is mainly due to binding of the Fc tail to the neonatal Fc receptor (FcRn) which is responsible for preventing lysosomal degradation of the antibodies.[22,23]

The stable expression and production of IgGs by mammalian cell lines (e.g. CHO or HEK cell lines) have improved the availability,[24,25] and the specific capture of IgG on protein A has further improved purification of these molecules.[26-28] All these factors combined (specificity, long serum half-life, stable production and selective capture) have contributed to the success of developing and manufacturing therapeutic antibodies.

Nowadays, many variations of the traditional IgG are being developed, such as bi-specifics,[29,30] antibody-drug conjugates (ADCs)[31] and Fc-fusion therapeutics.[32] Bi-specifics take advantage of the specific binding of two different Fab arms of the molecule to two different antigens. Antibody-drug conjugates (ADCs) combine the specificity of an antibody with the strong killing effect of cytotoxic drugs.[31,33,34] Fc-fusion therapeutics use the Fc region of an antibody fused to another specific target binding polypeptide.[32] As mentioned, the Fc region of an IgG molecule is responsible for the circulation and long serum half-life. By conjugating such an Fc region to other molecules, the serum half-life of these molecules can be increased as well, although Suzuki et al.[22] found that Fc-fusion proteins do not necessarily have a serum half-life that is comparable to that of IgG antibodies.

Process development

Before the biopharmaceutical is available as a therapeutic product, upstream and downstream process development is required. The upstream development covers the choice of a proper organism and cell line, which is transfected with the DNA sequence of the desired protein, and the development and optimization of a bioreactor process, including medium and process parameters. The selected, transfected cell line is cultured in large scale bioreactors and is able to produce the protein of interest, preferably in large quantities.[25,35] Then the next step is the recovery of the produced protein from the bioreactor harvest, using a variety of purification techniques during the downstream processing. Throughout all these steps, the product quality and yield is monitored using analytical methods to choose the most optimal conditions. Product quality is defined in terms of critical quality attributes

(CQAs), i.e. attributes that may affect safety and efficacy, such as purity and potency, and consistency between batches must always be kept within predefined ranges.

Upstream processing

Upstream process development consists of cell line development and clone selection, bioreactor design, optimization and scale-up.[36] Selection of a proper organism (prokaryotic or eukaryotic system) and the selection of a high-producing and stable clonal cell line of the selected organism are the first steps of a successful USP process. Mammalian cell lines are often selected because of their ability to produce proteins with most of the desired post-translational modifications (mainly glycosylation) and the available expertise for these cell types. Proteins produced in mammalian cell lines, such as CHO, BHK or HEK cells, are mostly human-like in structure, exhibit preferred post-translational modifications and meanwhile, the proteins are secreted by the cells, simplifying isolation of the product. The drawbacks of mammalian cell lines include slow growth, low cell densities, expensive media and relatively low productivity. However, recent advances have led to increased productivity.

A typical upstream process scheme (Figure 1.3) consists of the thawing of a vial of cells from the working cell bank, followed by pre-culturing in T-flasks or small shake flasks.[37] The culture is then scaled-up until inoculated into the seed bioreactor, followed by further scale-up into the production bioreactor, which is typically a 1000 - 15000 liter bioreactor in full manufacturing production. Different types of bioreactors are available nowadays, including stirred-tank reactors, wave reactors or orbital shaken reactors.[35] A new trend in bioreactors is the use of single-use bioreactor systems.[38] The bioreactor type at small scale has to be representative for the bioreactor at large scale, and therefore careful downscaling of the bioreactor is required.[39] The development of the upstream processes has been advanced by the introduction of micro-bioreactors, which can be operated simultaneously in order to rapidly screen different culture parameters.[25,39] Much research and development at small scale is performed, in which growth and feed medium and bioreactor conditions, such as temperature, pH and dissolved oxygen, have to be optimized.[36] Optimization further includes the establishment of the ideal culturing length in days; longer culture times may generate higher titers, however, cell viabilities may go down and these have to be balanced.

Furthermore, composition of the growth and feed medium, and the feed strategy may affect the productivity and product quality.[35] Different feed strategies exist, such as batch,

fed-batch, continuous or perfusion production, or combination of these.[35,36,38] In batch or fed-batch strategies the cells are allowed to grow and produce during a specified period, after which the entire bioreactor contents are harvested. In continuous or perfusion strategies, cells are kept in the bioreactor and are continuously supplied with nutrients, while the product is regularly extracted for further purification and processing.[38] The choice for any of these strategies has an impact on the following step, the downstream processing, and must therefore be evaluated. Overall, the bioreactor process and the growth and feed medium composition must be well-controlled, in order to guarantee a representative and reproducible process which generates a biopharmaceutical product with similar quality attributes batch after batch.

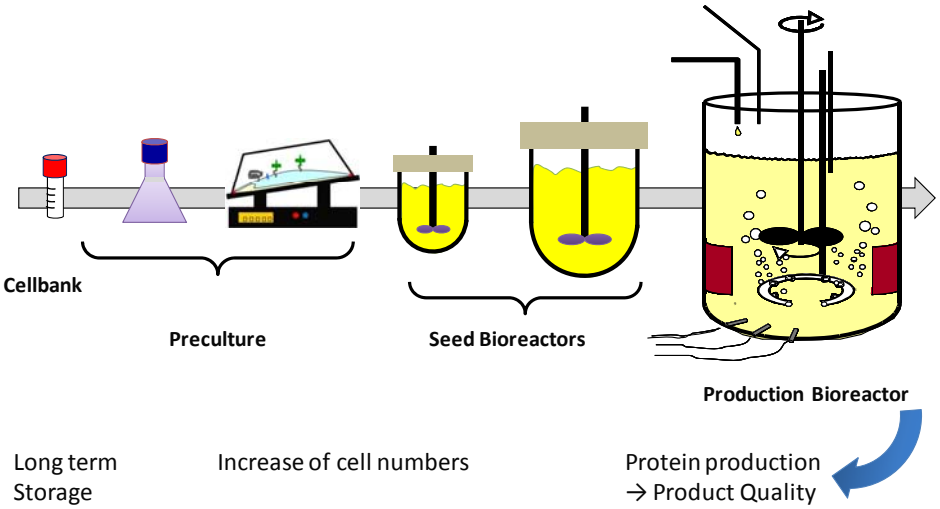

Figure 1.3 *Flow scheme of a typical upstream process*

Downstream processing

The main goal of downstream processing is to separate the protein of interest from the biomass, such as cells and impurities resulting in a highly pure product at high yield.[36] The DSP process consists of particulate removal, product isolation and concentration, various purification steps and a final polishing and fill/finish step (Figure 1.4). Initial clarification to remove cell broth (in case of batch or fed-batch processes) can be established by depth filtration or centrifugation, which is often still considered part of the USP process.[35] This is mostly followed by one or more chromatographic steps, such as affinity chromatography, HIC or IEC (CEX or AEX), to further purify the product. Several types of impurities may be

present and can be removed by applying various filtration and chromatographic steps, defined as unit operations. The types of impurities that can be expected are divided into host impurities (i.e. viruses, HCPs or DNA), product impurities (i.e. N-terminal and C-terminal variants, denatured proteins, aggregates or fragments) and process impurities (i.e. medium components, metals and column leakage material).[36,40] Furthermore, virus inactivation and virus removal are an important aspect of the DSP process.

In case of IgG purification, the first choice for purification is generally protein A chromatography, due to its high selectivity towards IgG, high capacity and the high purity after this initial step.[35] Furthermore, the acidic conditions that are used for protein A elution are useful to immediately continue with viral inactivation at low pH, reducing the need for additional buffer exchange. Drawbacks of protein A chromatography are the non-specific binding of certain impurities, such as medium components or HCPs to the resin,[41] the possibility of protein A leaching from the column, and the high costs for the resin. Further purification of antibodies, after the initial protein A step, often consist of CEX or AEX chromatography, or both, to further remove antibody variants (aggregates or charge variants) and remaining HCPs, DNA and leached protein A.

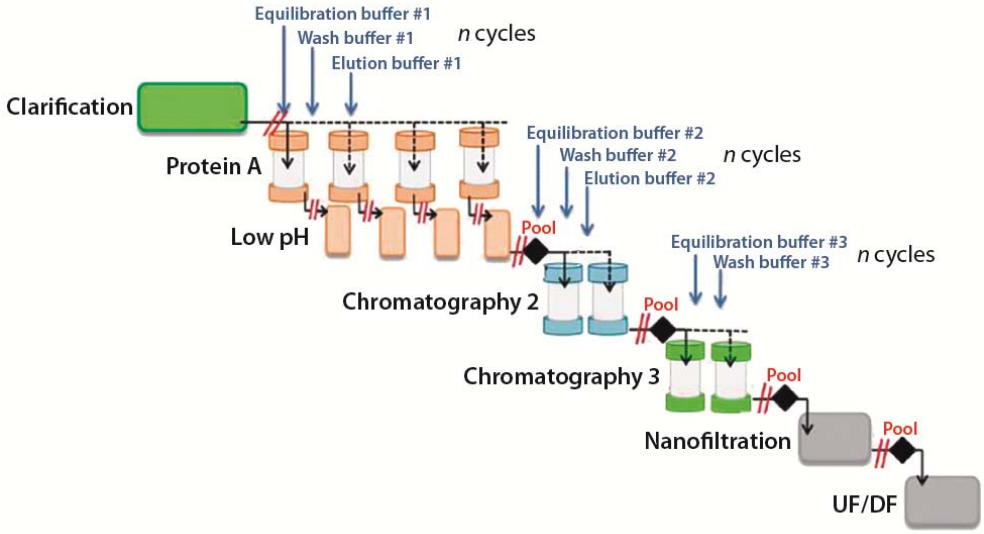

Figure 1.4 *Flow scheme of a typical downstream process for antibody purification (Reprinted from Mothes, Bioprocess international, May 11, 2016)* [42]

The final steps of the DSP process consist of several filtration steps, to obtain a product in the correct formulation buffer at high protein concentrations that are used for therapeutic dosage. These last steps are often performed by ultrafiltration and diafiltration. After the DSP process, sterile filling into the final form is the last step to obtain the final product.

The development of a purification process involves a multitude of unit operations, each of which needs to be developed and fine-tuned. High-throughput screening technologies, such as the use of robo-columns and filter plate screening, are implemented to increase the downstream process development at small scale.[39,43-45] Only low amounts of material are needed, which is beneficial in early stages as often limited material is available, and a broad range of parameters can be rapidly explored. Miniaturization and high-throughput screening technologies are often used these days to increase the process knowledge and process development and optimization for various chromatographic steps during the purification.

Recent developments in the DSP process involve the implementation of continuous processing, in line with continuous USP processes.[38] However, continuous purification schemes in DSP have not yet been widely applied at manufacturing scale.[46] Continuous downstream processing is applied by multicolumn approaches, such as connecting multiple columns in series,[42] continuous annular chromatography, simulated moving bed or countercurrent chromatography,[38,46] among other possible set-ups.

Product characterization

Traditionally, pharmaceutics were chemically synthesized and relatively easy characterized by a limited number of analytical methods. The complexity of modern biopharmaceuticals, caused by micro-heterogeneity inherent to a biological process, requires a broad panel of characterization methods, which are able to measure the structure, functional performance and other characteristics of these proteins.[47-49] The structure and composition of a biopharmaceutical product are analyzed and controlled throughout the entire process, from initial research up to manufacturing, which should give sufficient insights into the impact of process changes to the product quality. Generally, a certain level of heterogeneity is always present in a biopharmaceutical product, due to different post-translational modifications and minor structure differences, which require a large panel of characterization methodology to fully define the product (Table 1.1).

Table 1.1 *Characterization of biopharmaceuticals* [47-52]

Property	Purpose	Analytical technique
Primary structure	Molecular weight; amino acid sequence verification; single amino acid mutation	Intact MS; Peptide mapping; LC-MS
Higher order structures	Secondary, tertiary and quaternary structure; disulfide bridges	Spectroscopic techniques (CD, FTIR, NMR, intrinsic and extrinsic fluorescence); X-ray crystallography; HDX-MS; ion mobility MS; electron microscopy; DSC
Post-translational modifications (PTMs)	Oxidation; deamidation; C-terminal lysine variation; phosphorylation; sulphation; lipidation among many others	Peptide mapping; LC-MS; LC-UV; CZE; cIEF; IEC
PTM: glycosylation	Monosaccharide composition; glycan profiling; sialylation; fucosylation; galactosylation; mannosylation	HILIC-FLD; NPLC-FLD; LC-MS; CE-LIF; HPAEC-PAD
Charge heterogeneity	Acidic variants; basic variants	IEF; cIEF; IEC; CZE
Size heterogeneity	Monomer; low molecular weight variants; high molecular weight variants	SEC; CE-SDS; SDS-PAGE; AF4; AUC
Activity / biological performance	Potency; Target binding, FcγR binding (IgGs); FcRn binding (IgGs)	SPR; BLI; ELISA; cell-based assays (CDC, ADCC); animal studies
Product impurities	Aggregation; visible and subvisible particles	SDS-PAGE; CE-SDS; SEC; RP-HPLC; LO; MFI; visual inspection
Process impurities	Leachables; extractables; residual protein A (IgG); HCP; DNA	ELISA; SPR; LC; 2D-electrophoresis
Stability	Thermodynamic stability	DSC

Changes to the production process and, as a consequence, potentially also to the final product, are carefully monitored throughout the development of biopharmaceuticals. For example, various post-translational modifications may impact the activity or the stability, or may result in higher amounts of aggregates. In turn, this may lead to adverse effects, such as immunogenicity.[47] Small changes in secondary, tertiary or quaternary structure can affect the function and activity of the molecule.[48] The secondary structure is defined by α-helices, β-sheets and random coils, which can be studied by several spectroscopic techniques.[48] Tertiary structures define the folding of the protein into a three-dimensional structure, and quaternary structure describes the interaction of monomeric proteins, which is not present in all proteins. Furthermore, biological activity is measured to ensure a proper active protein.

We will further focus on protein glycosylation, mainly of rhEPO, and functional target binding and Fc region binding of IgGs because these topics have been studied throughout this research.

Glycosylation

Glycosylation is one of the most common post-translational modifications on proteins and can be one of the more critical modifications.[10,49] The functionality of a protein in binding to another protein, receptor or cell may be dependent on correct glycosylation. Mammalian cell lines that are often used to produce recombinant therapeutic proteins are capable of performing a cascade of reactions to glycosylate a protein (Figure 1.5). Glycosylation takes place in the ER and Golgi system, and many different forms of glycans may be attached to the protein. Various glycosidases, glycosyltransferases and other proteins are involved in the glycosylation process. Proper functionality depends on the type of glycosylation and in case of therapeutic proteins this must therefore be controlled conscientiously. However, the complex process of glycosylation leads to micro-heterogeneity in the produced protein, with potentially large impact on functionality and stability. Furthermore, certain non-human glycan structures should be kept at minor levels, as this may cause immunogenic responses. For example, two main variants of sialylation can be distinguished (N-glycolylneuraminic acid – Neu5Gc and N-acetylneuraminic acid – Neu5Ac), of which NeuGc is not found in humans and anti-NeuGc antibodies occur in all healthy humans. [53,54]

The complicated cascade of events that determine the final glycosylation of recombinant proteins, requires extensive analyses of the glycan forms to monitor product

changes during the complete development and marketing. Especially when using non-human cell lines, immunogenic glycans may be introduced to the protein, which can completely abolish the effectiveness of the therapeutic protein.[10] Additionally, proper glycosylation aids in protein production, protein stability, correct protein folding and biological activity / ligand recognition and binding. Mammalian cell lines are the first choice for production of glycosylated proteins, as these exhibit glycosylation patterns that are highly similar to those found in humans, whereas insect, yeast or plant expression systems may include glycans that are immunogenic to humans.[55] A large panel of analytical techniques is used on a regular basis to fully identify and measure glycosylation, glycoprofiling and individual glycans and monosaccharide composition (Table 1.2).

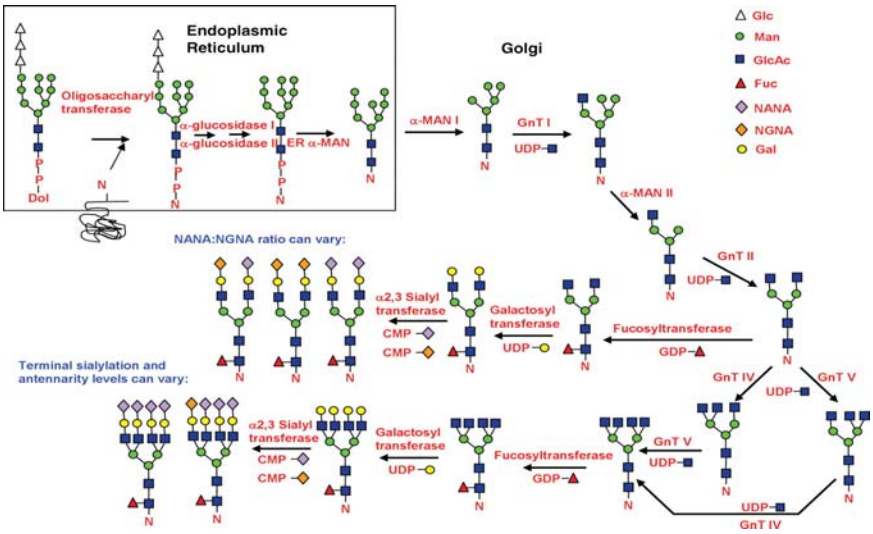

Figure 1.5 *Cascade of reactions to protein glycosylation (Reprinted from Hossler et al. Glycobiology 2009 [56])*

Numerous reports have been published about the analysis of rhEPO glycosylation. A broad range of analytical methods and strategies is applied to fully characterize rhEPO glycosylation, ranging from analysis of average glycoprofiles, to site-specific glycosylation identification and quantitation of sialic acid, specifically the difference between the nonhuman sialic acid *N*-glycolylneuraminic acid (Neu5Gc) and the human *N*-acetylneuraminic acid (Neu5Ac).[9,14]

Table 1.2 *Glycosylation analysis* [14,49,55,57]

Level	Purpose	Analytical technique
Intact glycoprotein	Charge distribution, glycoprofiling, identification of heterogeneity	MS, IEF, CZE, SDS-PAGE, cIEF, affinity-based arrays
Glycopeptides	Correlation of glycan composition with glycosylation site	AEX, HILIC, NP-HPLC, LC-MS,
Released glycans	Structural characterization, linkage	LC-FLD, LC-MS, CE-MS, CE-LIF, HPAEC-PAD, MALDI-MS
Monosaccharides	Identity and composition of monosaccharides	LC-MS, CE-MS, GC-MS

Current methodologies that are usually applied in the characterization of protein glycosylation involve the release and labeling of the glycans from the protein, followed by separation and detection.[9] This is a quite laborious process and development towards the characterization of glycosylation on intact glycoproteins has had the attention of many researchers during recent years. Intact glycoprotein analysis has generally been performed by mass spectrometric methods. Recently glycoprofiling / glycofingerprinting was performed with mass spectrometric methods, to compare biosimilars to innovator products.[58] Glycosylation site identification and site occupancy was determined by peptide mapping of rhEPO. The glycoforms were determined using released glycans, both with LC-MS methods.[59]

Nowadays, glycoprofiling can be performed on intact glycoproteins by a lectin array; however fluorescent labeling of glycoproteins is still necessary.[60] The glycoprofiling can be performed more rapidly and label-free using the specific binding characteristics of the N-glycans to for example lectins and monitoring them with imaging SPR.[61-64] These publications focus on small glycan structures rather than the higher-order structures of N-glycans found on glycoproteins or use a single lectin interaction to study glycan interactions.

Target binding and Fc-mediated binding

Protein functionality, or bio-activity, is of major importance for its use as a therapeutic agent. Target binding studies are necessary to test proper bio-activity *in vitro*, which represent the function of the protein in *in vivo* situations. These *in vitro* assays can be divided into cell-based assays and ligand-binding assays. In cell-based assays, the actual processes that take place in the body are mimicked with living cells. Cell-based assays have

a relatively large analytical variation due to the variation in the human pool of plasma that is used for these assays. Since most cellular events start with a proper binding to the receptor of interest, cell-based assays can partially be replaced by ligand-binding assays, where only the receptor or antigen of interest is used to study binding of the interaction partners (i.e. the biopharmaceutical protein). Label-free ligand-binding assays are often based on real-time measurement techniques, such as SPR or biolayer interferometry (BLI). The principle of SPR is further explained in the next paragraph.

Next to target binding, or antigen binding in case of antibodies, effector functions of antibodies are another important characteristic of therapeutic antibodies. The Fc region of the antibody can bind to different types of Fcγ receptors, the neonatal Fc receptor (FcRn) and to complement C1q which all may be required for the mode of action, depending on the type of therapeutic antibody. Most therapeutic antibodies require proper Fc tail functionality in order to be fully efficacious. Fcγ receptors are found on effector cells, such as macrophages or lymphocytes, in the human body and are responsible for clearance of pathogens, whereas proper FcRn functionality adds to the serum half-life of antibodies. These binding events can also be studied by ligand-binding assays, where the Fc receptors act as ligands.

Surface plasmon resonance imaging

Many techniques to study protein-protein interactions exist, all with their own advantages and drawbacks. Surface plasmon resonance (SPR) has become one of the most widely applied techniques ever since the availability of the first commercial instruments in the 1990s. Protein-protein interactions are measured in real-time and label-free using SPR.[65,66]

SPR is measured on a sensor which consists of a thin metal film, usually gold, and a prism or hemisphere attached to each other (Figure 1.6). Polarized light at a fixed wavelength shines through the prism or hemisphere, which generates surface plasmons by excitation of free electrons at the metal surface under a certain angle of incidence. Reflectivity of the incident light is measured and at a specific angle of incidence surface plasmons are excited and a dip in reflection occurs (the SPR angle) (Figure 1.6). The combination of refractive indices of both media, metal film thickness and the used wavelength together determine the SPR angle. The dip in the intensity of the reflected light, the SPR angle, will shift upon refractive index changes in an exponential decaying field at the metal side of the sensor, but only in the first ~ 200 nm from the surface (the

evanescent field). This means that only molecules (e.g. proteins) that bind to the sensor surface will generate a change in refractive index which changes the SPR-dip and this is measured. Molecules that pass the sensor surface but do not bind will not influence the refractive index and are not measured. This phenomenon can be followed in real-time, which results in kinetics data on the interaction, by measuring association and dissociation in time. However, a shift in refractive index, e.g. due to different buffer systems or bulk protein concentrations, can also be misinterpreted as binding. Therefore, SPR sensorgrams are normalized against a reference channel in which no ligand was immobilized and only the bulk effects are measured, which can be used to correct the signal.

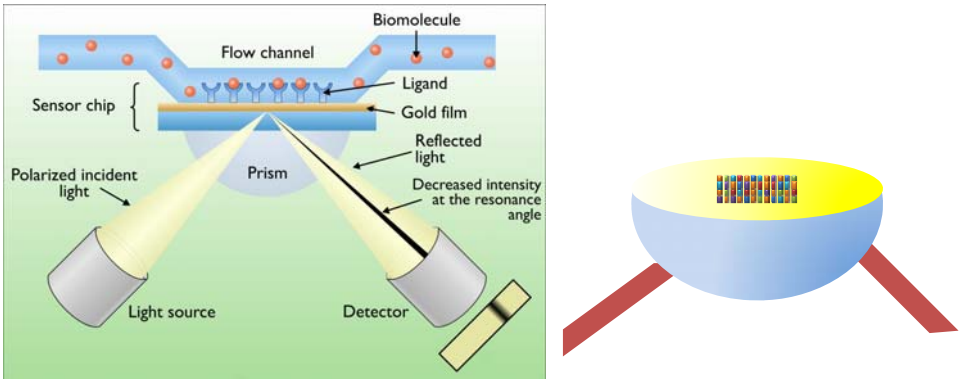

Figure 1.6 *Principle of surface plasmon resonance (left) and surface plasmon resonance imaging (right). In SPRi an array of ligands is printed on a sensor surface, followed by a similar detection principle as in SPR. (Reprinted from http://elte.prompt.hu/sites/default/files/tananyagok/IntroductionToPractical Biochemistry/ch08s07.html)*

Immobilization of one of the interaction partners (called the ligand) onto the sensor surface enables interaction measurements with a binding partner (the so-called analyte) when injected over this sensor surface. The association of analyte to ligand and dissociation of the formed complex is measured in real-time by SPR. The generated sensorgram, a plot of change in angle shift versus time, of the interaction is used to determine rate constants of the interaction (Figure 1.7). Injections of multiple analyte concentrations over the sensor surface allow the determination of association rate and dissociation rate of the complex and the affinity of the interaction. Complexes that have not dissociated may be broken by a regeneration procedure, in order to reuse the same surface for multiple sequential analyses.

SPR is a well-established and accepted technique nowadays, based on the numerous publications in biomolecular studies. The more traditional SPR instruments measure a limited number of interactions simultaneously (often only 4 channels of which 1 or 2 are used as reference). In the past 10-15 years, new SPR imaging (SPRi) systems have been commercialized and are becoming more popular, as they benefit from screening much more interactions simultaneously by immobilizing up to 100s of ligands on a single biosensor (Figure 1.6). This fits well in the high-throughput screening strategies that are applied more and more.[67] The number of publications on SPRi rapidly increased over the past five years.[68] Therefore, the SPRi technique has been used throughout this research, to study the implementation of SPRi in the development of biopharmaceuticals.

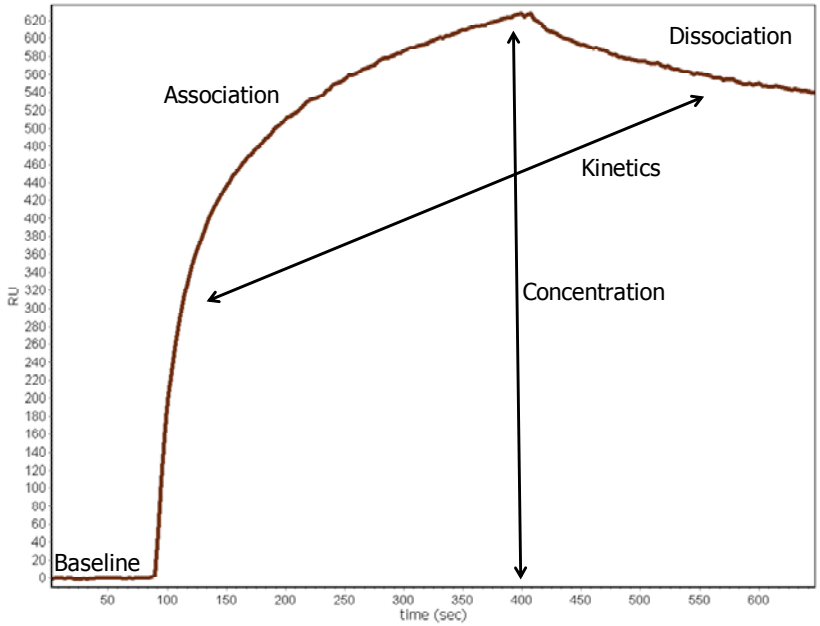

Figure 1.7 *Typical SPR sensorgram, indicating baseline, association and dissociation phase from which affinity and kinetics of the interaction can be determined*

Objectives and outline

Innovative new technologies are required to increase rapid process and product development in the biopharmaceutical industry. High-throughput screening (HTS) technologies that study one or more characteristics of a biopharmaceutical protein are useful to define the critical parameters in early stage, both in product characterization but also in process development and support. Novel developments are required to reduce product development time and costs, which may lead to faster development and approval of therapeutic proteins. Reduction of development costs may eventually lead to earlier marketing of therapeutic proteins, which in turn leads to more cost-efficient products. Additionally, the novel therapeutic protein is protected by patents that will expire, and the more rapidly a product is marketed, the more the innovator can reap the benefits of the patent protection period. On the other hand, biosimilar companies benefit if they are first-to-market, which may be accelerated by rapid developments using high-throughput screening technologies.

One way to achieve faster, yet fully understood, development of therapeutic proteins is by using innovative analytical methods. The described SPRi technology is one of the tools that are available to fulfil the requirement of high-throughput and label-free measurements, where possible directly from cell supernatant to study a variety of product characteristics and to support process developments. A major requirement for the reuse of SPR sensors for repeated analysis is the proper regeneration of the immobilized ligands at the surface. The choice for a suitable regeneration buffer can be quite time-consuming as certain protein-protein interactions cannot be regenerated by standard regeneration buffers, such as glycin-HCl. Especially in multiplexed SPR, where multiple different ligands with different types of interactions (i.e. electrostatic, hydrophobic or van der Waals interactions) can be immobilized onto a single sensor surface, it can be quite challenging to regenerate all ligands with a single regeneration buffer. The multiplexed capabilities of the SPRi technology enabled the development of a rapid regeneration buffer scouting as described in **Chapter 2**, where 48 different buffers could be simultaneously tested on a single sensor surface.

In **Chapter 3,** the SPRi technology has been applied to support the rapid development of an affinity chromatography step during the DSP process. The SPRi was used to screen for proper elution buffers, wash buffers and ligand re-usability in a miniaturized protein A chromatography set-up as an example. This may speed up the development of a downstream process, since many different buffers and conditions can be simultaneously

screened, while only minute quantities of ligand, analyte and buffer are required. Downstream processing is generally composed of one or more column purification steps, of which affinity chromatography is a highly specific technique to generate purified proteins with relatively high yields.

During USP development, certain product characteristics such as protein glycosylation and protein titer may be affected by variations that are applied to the pre-culturing or to the bioreactor process. Direct and rapid screening of protein glycosylation and titer are used to steer the entire process towards the desired end-product. In **Chapter 4** a glycan-fingerprinting method based on the specific interactions between certain monosaccharides and lectins has been described. This fingerprinting method has been applied to different brands of rhEPO and enabled the quantification of relative sialylation levels on rhEPO.

Target binding of biopharmaceutical products is inherent to the product quality and is often measured by ligand-binding studies. In case of IgGs, the Fc region functional binding additionally adds to proper functionality of the molecule. The Fc region of an IgG binds to Fc receptors on effector cells, which may be one of the modes of action. An SPRi method that studies IgG binding to immobilized Fc receptors has been developed. In order to study these Fc interactions, human Fcγ receptors had to be immobilized onto the SPR sensor surface. However, insufficient activity and stability of directly immobilized Fcγ receptors, likely due to the presence of lysines in the IgG binding region, limited the assay design. Therefore, a minimal labeling approach, described in **Chapter 5,** based on biotinylation of the Fcγ receptors was developed in order to improve Fcγ receptor activity and stability at the sensor surface. The minimal labeling approach included the identification of the most vulnerable binding sites in the Fcγ receptor structures, to possibly prevent labeling in the active binding site. The resulting multiplexed Fcγ receptor sensor, in combination with two additional methods using SPR and BLI, was used to set up a screening approach that could rapidly measure the various Fc tail interactions of an IgG as outlined in **Chapter 6**. Stressed IgG samples were then measured by all three screening methods, to verify the application of the method during in-process controls or early development.

This thesis covers the applicability of multiplexed SPR throughout the entire process of biopharmaceutical development, from process support up to product characterization. Several screening methodologies based on SPRi have been developed and optimized and the proof-of-concept has been demonstrated in a variety of applications.

References

1. Walsh, G. Biopharmaceutical benchmarks. Nat.Biotechnol. 2000; 18(8): 831-833
2. Human insulin receives FDA approval. FDA.Drug Bull. 1982; 12(3): 18-19
3. Walsh, G. Biopharmaceutical benchmarks 2014. Nat.Biotechnol. 2014; 32(10): 992-1000
4. Flaharty, K. K., Grimm, A. M., and Vlasses, P. H. Epoetin: human recombinant erythropoietin. Clin.Pharm. 1989; 8(11): 769-782
5. Lin, F. K., Suggs, S., Lin, C. H., Browne, J. K., Smalling, R., Egrie, J. C., Chen, K. K., Fox, G. M., Martin, F., Stabinsky, Z., and . Cloning and expression of the human erythropoietin gene. Proc.Natl.Acad.Sci.U.S.A 1985; 82(22): 7580-7584
6. Jones, E. H. Recombinant human erythropoietin. Am.J.Hosp.Pharm. 1989; 46(11 Suppl 2): S20-S23
7. Scott, J. and Phillips, G. C. Erythropoietin in sports: a new look at an old problem. Curr.Sports Med.Rep. 2005; 4(4): 224-226
8. Lundby, C., Robach, P., and Saltin, B. The evolving science of detection of 'blood doping'. Br.J.Pharmacol. 2012; 165(5): 1306-1315
9. Skibeli, V., Nissen-Lie, G., and Torjesen, P. Sugar profiling proves that human serum erythropoietin differs from recombinant human erythropoietin. Blood 15-12-2001; 98(13): 3626-3634
10. Walsh, G. and Jefferis, R. Post-translational modifications in the context of therapeutic proteins. Nat.Biotechnol. 2006; 24(10): 1241-1252
11. Schellekens, H. Immunologic mechanisms of EPO-associated pure red cell aplasia. Best.Pract.Res.Clin.Haematol. 2005; 18(3): 473-480
12. Schellekens, H. Factors influencing the immunogenicity of therapeutic proteins. Nephrol.Dial.Transplant. 2005; 20 Suppl 6 vi3-vi9
13. McKoy, J. M., Stonecash, R. E., Cournoyer, D., Rossert, J., Nissenson, A. R., Raisch, D. W., Casadevall, N., and Bennett, C. L. Epoetin-associated pure red cell aplasia: past, present, and future considerations. Transfusion 2008; 48(8): 1754-1762
14. Jiang, J., Tian, F., Cai, Y., Qian, X., Costello, C. E., and Ying, W. Site-specific qualitative and quantitative analysis of the N- and O-glycoforms in recombinant human erythropoietin. Anal.Bioanal.Chem. 31-7-2014;-
15. Yang, M. and Butler, M. Effects of ammonia on CHO cell growth, erythropoietin production, and glycosylation. Biotechnol.Bioeng. 20-5-2000; 68(4): 370-380
16. Dube, S., Fisher, J. W., and Powell, J. S. Glycosylation at specific sites of erythropoietin is essential for biosynthesis, secretion, and biological function. J.Biol.Chem. 25-11-1988; 263(33): 17516-17521
17. Zhang, P., Tan, D. L., Heng, D., Wang, T., Mariati, Yang, Y., and Song, Z. A functional analysis of N-glycosylation-related genes on sialylation of recombinant erythropoietin in six commonly used mammalian cell lines. Metab Eng 2010; 12(6): 526-536
18. Elliott, S., Egrie, J., Browne, J., Lorenzini, T., Busse, L., Rogers, N., and Ponting, I. Control of rHuEPO biological activity: the role of carbohydrate. Exp.Hematol. 2004; 32(12): 1146-1155
19. Meininger, M., Stepath, M., Hennig, R., Cajic, S., Rapp, E., Rotering, H., Wolff, M. W., and Reichl, U. Sialic acid-specific affinity chromatography for the separation of erythropoietin glycoforms using serotonin as a ligand. J.Chromatogr.B Analyt.Technol.Biomed.Life Sci. 15-2-2016; 1012-1013 193-203

20. Schroeder, H. W., Jr. and Cavacini, L. Structure and function of immunoglobulins. J.Allergy Clin.Immunol. 2010; 125(2 Suppl 2): S41-S52

21. Vidarsson, G., Dekkers, G., and Rispens, T. IgG subclasses and allotypes: from structure to effector functions. Front Immunol. 2014; 5 520-

22. Suzuki, T., Ishii-Watabe, A., Tada, M., Kobayashi, T., Kanayasu-Toyoda, T., Kawanishi, T., and Yamaguchi, T. Importance of neonatal FcR in regulating the serum half-life of therapeutic proteins containing the Fc domain of human IgG1: a comparative study of the affinity of monoclonal antibodies and Fc-fusion proteins to human neonatal FcR. J.Immunol. 15-2-2010; 184(4): 1968-1976

23. Wang, W., Lu, P., Fang, Y., Hamuro, L., Pittman, T., Carr, B., Hochman, J., and Prueksaritanont, T. Monoclonal antibodies with identical Fc sequences can bind to FcRn differentially with pharmacokinetic consequences. Drug Metab Dispos. 2011; 39(9): 1469-1477

24. Chartrain, M. and Chu, L. Development and production of commercial therapeutic monoclonal antibodies in Mammalian cell expression systems: an overview of the current upstream technologies. Curr.Pharm.Biotechnol. 2008; 9(6): 447-467

25. Li, F., Vijayasankaran, N., Shen, A. Y., Kiss, R., and Amanullah, A. Cell culture processes for monoclonal antibody production. MAbs. 2010; 2(5): 466-479

26. Hober, S., Nord, K., and Linhult, M. Protein A chromatography for antibody purification. J.Chromatogr.B Analyt.Technol.Biomed.Life Sci. 15-3-2007; 848(1): 40-47

27. Hahn, R., Schlegel, R., and Jungbauer, A. Comparison of protein A affinity sorbents. J.Chromatogr.B Analyt.Technol.Biomed.Life Sci. 25-6-2003; 790(1-2): 35-51

28. Liu, H. F., Ma, J., Winter, C., and Bayer, R. Recovery and purification process development for monoclonal antibody production. MAbs. 2010; 2(5): 480-499

29. Kontermann, R. E. and Brinkmann, U. Bispecific antibodies. Drug Discov.Today 2015; 20(7): 838-847

30. Chames, P. and Baty, D. Bispecific antibodies for cancer therapy: the light at the end of the tunnel? MAbs. 2009; 1(6): 539-547

31. Perez, H. L., Cardarelli, P. M., Deshpande, S., Gangwar, S., Schroeder, G. M., Vite, G. D., and Borzilleri, R. M. Antibody-drug conjugates: current status and future directions. Drug Discov.Today 2014; 19(7): 869-881

32. Czajkowsky, D. M., Hu, J., Shao, Z., and Pleass, R. J. Fc-fusion proteins: new developments and future perspectives. EMBO Mol.Med. 2012; 4(10): 1015-1028

33. Ornes, S. Antibody-drug conjugates. Proc.Natl.Acad.Sci.U.S.A 20-8-2013; 110(34): 13695-

34. Zolot, R. S., Basu, S., and Million, R. P. Antibody-drug conjugates. Nat.Rev.Drug Discov. 2013; 12(4): 259-260

35. Gronemeyer, P, Ditz, R, and Strube, J. Trends in upstream and downstream process development for antibody manufacturing. Bioengineering 1-10-2016;(1): 188-212

36. Faustino Jozala, A, Costa Geraldes, D, Lacalendola Tundisi, L, de Araujo Feitosa, V, Alexandre Breyer, C, Leite Cardoso, S, Gava Mazzola, P, de Oliveira-Nascimento, L, de Oliveira Rangel-Yagui, C, de Oliveira Magalhaes, P, Antonio de Oliveira, M, and Pessoa Jr, A. Biopharmaceuticals from microorganisms: from production to purification. Brazilian journal of microbiology 26-10-2016;(47): 51-63

37. Read, E. K., Park, J. T., Shah, R. B., Riley, B. S., Brorson, K. A., and Rathore, A. S. Process analytical technology (PAT) for biopharmaceutical products: Part I. concepts and applications. Biotechnol.Bioeng. 1-2-2010; 105(2): 276-284

38. Rathore, A. S., Agarwal, H., Sharma, A. K., Pathak, M., and Muthukumar, S. Continuous processing for production of biopharmaceuticals. Prep.Biochem.Biotechnol. 2015; 45(8): 836-849

39. Fernandes, P., Carvalho, F., and Marques, M. P. Miniaturization in biotechnology: speeding up the development of bioprocesses. Recent Pat Biotechnol. 2011; 5(3): 160-173

40. Read, E. K., Shah, R. B., Riley, B. S., Park, J. T., Brorson, K. A., and Rathore, A. S. Process analytical technology (PAT) for biopharmaceutical products: Part II. Concepts and applications. Biotechnol.Bioeng. 1-2-2010; 105(2): 285-295

41. Lintern, K., Pathak, M., Smales, C. M., Howland, K., Rathore, A., and Bracewell, D. G. Residual on column host cell protein analysis during lifetime studies of protein A chromatography. J.Chromatogr.A 26-8-2016; 1461 70-77

42. Mothes, B, Pezzini, J, Schroeder-Tittmann, K, and Villain, L. Accelerated, seamless antibody purification. BioProcess International 1-5-2017; 14(5): 34-58

43. Rege, K., Pepsin, M., Falcon, B., Steele, L., and Heng, M. High-throughput process development for recombinant protein purification. Biotechnol.Bioeng. 5-3-2006; 93(4): 618-630

44. Lacki, K. M. High-throughput process development of chromatography steps: advantages and limitations of different formats used. Biotechnol.J. 2012; 7(10): 1192-1202

45. Bergander, T., Nilsson-Valimaa, K., Oberg, K., and Lacki, K. M. High-throughput process development: determination of dynamic binding capacity using microtiter filter plates filled with chromatography resin. Biotechnol.Prog. 2008; 24(3): 632-639

46. Jungbauer, A. Continuous downstream processing of biopharmaceuticals. Trends Biotechnol. 2013; 31(8): 479-492

47. Berkowitz, S. A., Engen, J. R., Mazzeo, J. R., and Jones, G. B. Analytical tools for characterizing biopharmaceuticals and the implications for biosimilars. Nat.Rev.Drug Discov. 29-6-2012; 11(7): 527-540

48. Crommelin, D. J., Storm, G., Verrijk, R., de, Leede L., Jiskoot, W., and Hennink, W. E. Shifting paradigms: biopharmaceuticals versus low molecular weight drugs. Int.J.Pharm. 6-11-2003; 266(1-2): 3-16

49. Parr, M. K., Montacir, O., and Montacir, H. Physicochemical characterization of biopharmaceuticals. J.Pharm.Biomed.Anal. 25-10-2016; 130 366-389

50. Gahoual, R., Beck, A., Leize-Wagner, E., and Francois, Y. N. Cutting-edge capillary electrophoresis characterization of monoclonal antibodies and related products. J.Chromatogr.B Analyt.Technol.Biomed.Life Sci. 1-10-2016; 1032 61-78

51. Magil, S. G. Biopharmaceutical characterization techniques for early phase development of proteins. BioPharm International 15-9-2015;-

52. Visser, J., Feuerstein, I., Stangler, T., Schmiederer, T., Fritsch, C., and Schiestl, M. Physicochemical and functional comparability between the proposed biosimilar rituximab GP2013 and originator rituximab. BioDrugs. 2013; 27(5): 495-507

53. Ghaderi, D., Taylor, R. E., Padler-Karavani, V., Diaz, S., and Varki, A. Implications of the presence of N-glycolylneuraminic acid in recombinant therapeutic glycoproteins. Nat.Biotechnol. 2010; 28(8): 863-867

54. Ghaderi, D., Zhang, M., Hurtado-Ziola, N., and Varki, A. Production platforms for biotherapeutic glycoproteins. Occurrence, impact, and challenges of non-human sialylation. Biotechnol.Genet.Eng Rev. 2012; 28 147-175

55. Costa, A. R., Rodrigues, M. E., Henriques, M., Oliveira, R., and Azeredo, J. Glycosylation: impact, control and improvement during therapeutic protein production. Crit Rev.Biotechnol. 2014; 34(4): 281-299

56. Hossler, P., Khattak, S. F., and Li, Z. J. Optimal and consistent protein glycosylation in mammalian cell culture. Glycobiology 2009; 19(9): 936-949

57. Hashii, N., Harazono, A., Kuribayashi, R., Takakura, D., and Kawasaki, N. Characterization of N-glycan heterogeneities of erythropoietin products by liquid chromatography/mass spectrometry and multivariate analysis. Rapid Commun.Mass Spectrom. 30-4-2014; 28(8): 921-932

58. Harazono, A., Hashii, N., Kuribayashi, R., Nakazawa, S., and Kawasaki, N. Mass spectrometric glycoform profiling of the innovator and biosimilar erythropoietin and darbepoetin by LC/ESI-MS. J.Pharm.Biomed.Anal. 2013; 83 65-74

59. Kawasaki, N., Ohta, M., Hyuga, S., Hyuga, M., and Hayakawa, T. Application of liquid chromatography/mass spectrometry and liquid chromatography with tandem mass spectrometry to the analysis of the site-specific carbohydrate heterogeneity in erythropoietin. Anal.Biochem. 1-10-2000; 285(1): 82-91

60. Rosenfeld, R., Bangio, H., Gerwig, G. J., Rosenberg, R., Aloni, R., Cohen, Y., Amor, Y., Plaschkes, I., Kamerling, J. P., and Maya, R. B. A lectin array-based methodology for the analysis of protein glycosylation. J.Biochem.Biophys.Methods 10-4-2007; 70(3): 415-426

61. Reuel, N. F., Mu, B., Zhang, J., Hinckley, A., and Strano, M. S. Nanoengineered glycan sensors enabling native glycoprofiling for medicinal applications: towards profiling glycoproteins without labeling or liberation steps. Chem.Soc.Rev. 7-9-2012; 41(17): 5744-5779

62. Safina, G., Duran, IuB, Alasel, M., and Danielsson, B. Surface plasmon resonance for real-time study of lectin-carbohydrate interactions for the differentiation and identification of glycoproteins. Talanta 15-6-2011; 84(5): 1284-1290

63. Fais M, Karamanska R, Russell D A, and Field R A. Lectin and carbohydrate microarrays: New high-throughput method for glycoprotein, carbohydrate-binding protein and carbohydrate-active enzyme analysis. Journal of cereal science 26-6-2009; 50 306-311

64. Foley, K. J., Forzani, E. S., Joshi, L., and Tao, N. Detection of lectin-glycan interaction using high resolution surface plasmon resonance. Analyst 2008; 133(6): 744-746

65. de Mol, N. J. and Fischer, M. J. Surface plasmon resonance: a general introduction. Methods Mol.Biol. 2010; 627 1-14

66. Willander, M. and Al-Hilli, S. Analysis of biomolecules using surface plasmons. Methods Mol.Biol. 2009; 544 201-229

67. Ray, S., Mehta, G., and Srivastava, S. Label-free detection techniques for protein microarrays: prospects, merits and challenges. Proteomics. 2010; 10(4): 731-748

68. Puiu, M. and Bala, C. SPR and SPR Imaging: Recent Trends in Developing Nanodevices for Detection and Real-Time Monitoring of Biomolecular Events. Sensors.(Basel) 14-6-2016; 16(6):-

Chapter 1

CHAPTER 2

High-throughput and multiplexed regeneration buffer scouting for affinity-based interactions

The contents of this chapter have been published as:

Karin P.M. Geuijen, Richard B. Schasfoort, René H. Wijffels, Michel H.M. Eppink

High-throughput and multiplexed regeneration buffer scouting for affinity-based interactions

Analytical biochemistry (2014) 454, pg 38-40

Abstract

Affinity-based analyses on biosensors partly depend on regeneration between measurements. Regeneration is performed with a buffer that efficiently breaks all interactions between ligand and analyte, while maintaining the active binding site of the ligand. We demonstrated a regeneration buffer scouting using the combination of a continuous flow microspotter with a surface plasmon resonance imaging platform to simultaneously test 48 different regeneration buffers on a single biosensor. Optimal regeneration conditions are found within hours and consume little amounts of buffers, analyte and ligand. This workflow can be applied to any ligand that is coupled through amine, thiol or streptavidin immobilization.

Introduction

Surface plasmon resonance (SPR) is a widely applied and accepted method to study protein-protein interactions in real-time. Affinity between an immobilized ligand and a soluble analyte is measured when a reversible binding is established between the two interacting compounds. One of the key parameters in a successful SPR experiment is an adequate regeneration of the sensor surface after analyte binding. Regeneration is considered efficient and robust when all bound analyte is removed from the surface, activity of the surface is maintained after each cycle and when it can be performed in a reproducible way. Binding between analyte and ligand is established through, e.g., electrostatic forces, hydrophobic interactions or hydrogen bonds. A regeneration buffer can be chosen depending on the type of interactions that take place. However, multiple types of interactions between ligand and analyte can play a role and may influence each other, complicating the selection of a proper regeneration buffer.

Systematic screening of sensors for optimal regeneration conditions has been previously performed with the Drake-Klakamp methodology.[1] Alternatively, a multivariate cocktail approach may be applied.[2-4] Although the Drake-Klakamp methodology is a strategic approach it requires multiple experiments because only one regeneration buffer is screened at a time, either manually or in an automated fashion. Finding the best regeneration buffer may thus take many experiments with different buffers to be tested sequentially. The cocktail approach on the other hand screens mixtures of one type of buffer, reducing the number of experiments for initial screening. However, this may lead to complicated regeneration buffer systems or extensive further fine-tuning to find the best regeneration buffer increasing the number of experiments to be performed again. Additionally, both strategies may require multiple new sensors if the tested regeneration buffer destroys the ligand activity.

Here we demonstrate the use of a continuous flow microspotter (CFM) in combination with an SPR imaging instrument to rapidly screen many regeneration buffers simultaneously. The CFM has been developed to uniformly array proteins on a biosensor surface.[5] Here the microfluidics channels in the CFM are used for independent multiplexed surface regeneration, resulting in a buffer scouting with up to 48 different regeneration buffers that can be tested using a single sensor surface. The multiplexed regeneration buffer screening is illustrated in this paper using a lectin – glycoprotein interaction as an

example where multiple interactions between lectins and glycans need to be effectively broken and simple regeneration buffers are often not applicable.

Materials and methods

Materials and reagents

Soybean agglutinin (SBA) was purchased from Vector laboratories (Burlingame, California USA). Acetic acid, sodium hydroxide, urea, *ortho*-phosphoric acid, calcium chloride dihydrate, magnesium chloride, glycin, ethanol and hydrochloric acid were of analytical grade and purchased from Merck Millipore (Amsterdam, The Netherlands). Formic acid, Tween80, RBS neutral, manganese chloride, zinc chloride, ethanolamine, HEPES, sodium chloride, glycerol, fetuin, EDTA, sodium carbonate, ethylene glycol, SDS, CHAPS, Triton-X100, guanidine hydrochloride were of analytical grade and purchased from Sigma-Aldrich (Zwijndrecht, The Netherlands). Ultrapure water was produced in house using a Millipore Milli-Q system.

Easy2Spot SensEye sensors were supplied by IBIS Technologies (Enschede, The Netherlands). Experiments were performed on an IBIS MX96 (IBIS Technologies, Enschede, The Netherlands) and continuous flow microspotter (CFM) (Wasatch microfluidics, Salt Lake City, Utah, USA).

Buffer selection

A selection of 42 buffers for regeneration screening was made, based on the subclasses of regeneration buffers (A) acidic, (B) basic, (C) chelating, (D) detergents, (I) ionic and (U) non-polar water soluble solvents.[2,3] Buffers of choice were: 1% formic acid (A1-a); 10% formic acid (A1-b); 10 mM HCl (A2-a); 100 mM HCl (A2-b); 25 mM phosphoric acid (A3-a); 100 mM phosphoric acid (A3-b); 10 mM glycin-HCl pH 2.0 (AB1-a); 100 mM glycin-HCl pH 2.0 (AB1-b); 10 mM glycin-HCl pH 2.0 / 20 mM EDTA (ABC); 10 mM glycin-HCl pH 2.0 / 1% SDS (ABD); 10 mM glycin-HCl pH 2.0 / 1M NaCl (ABI); 10 mM glycin-HCl pH 2.0 / 1% ethanol (ABU); 10 mM HCl / 1% SDS (AD1); 25 mM phosphoric acid / 1% SDS (AD2); 25 mM phosphoric acid / 1% SDS / 20 mM EDTA (ADC); 10 mM HCl / 3 M $MgCl_2$ (AI1-a); 10 mM HCl / 1M NaCl (AI1-b); 25 mM phosphoric acid / 3 M $MgCl_2$ (AI2-a); 25 mM phosphoric acid / 1 M NaCl (AI2-b); 25 mM phosphoric acid / 1 M NaCl / 20 mM EDTA (AIC); 10 mM HCl / 1% ethanol (AU1); 25 mM phosphoric acid / 1% ethanol (AU2); 10 mM glycin-NaOH pH 10.0 (B1); 10 mM HEPES-NaOH pH 8.5 (B2); 10 mM NaOH (B3-a); 100 mM

NaOH (B3-b); 200 mM Na_2CO_3 pH 11 (B4); 10 mM HEPES / 20 mM EDTA (BC1); 10 mM HEPES / 20 mM EDTA / 1 M NaCl (BCI); 25% Ethylene glycol (D1-a); 50% Ethylene glycol (D1-b); 1% SDS (D2-a); 20% SDS (D2-b); 0.3% CHAPS (D3); 0.3% Triton-X100 (D4); 3 M guanidine chloride (I1); 3 M $MgCl_2$ (I2); 1 M NaCl (I3); 4 M urea (I4); 4 M KCl (I5); 10% ethanol (U1-a); 20% ethanol (U1-b).

Scouting protocol

An Easy2Spot SensEye was cover coupled with Soybean agglutinin (SBA) lectin. In cover coupling, the entire surface of a sensor is exposed to the same ligand solution, to create a homogeneously immobilized surface. A baseline of 1 minute was recorded on the pre-activated Easy2Spot sensor followed by an injection of 100 µL of a 4 µM SBA solution in 50 mM sodium acetate pH 4.5 / 0.05% Tween80. An association time of 10 minutes was programmed enabling covalent coupling of SBA lectin to the sensor surface. No dissociation, regeneration or wash steps were programmed. Next the sensor was deactivated with ethanolamine pH 8.5 for 8 minutes.

A 500 µg/mL fetuin solution in HEPES buffered saline pH 7.2 (20 mM HEPES, 150 mM NaCl, 0.05 w/v% Tween80, 1 mM $ZnCl_2$, 1 mM $CaCl_2$, 1 mM $MnCl_2$ and 1 mM $MgCl_2$) was injected onto the cover coupled SBA sensor. An injection volume of 100 µL was used. A baseline of 2 minutes was followed by an association phase of 15 minutes until sufficient binding of fetuin was measured (approximately 1000 RU). No dissociation, regeneration or wash steps were applied. Hereafter the sensor was directly transferred to the CFM for regeneration.

One of the selected regeneration buffers per well was pipetted into 48 wells of a 96-well plate, with a total volume of 150 µL per buffer. The SBA cover coupled sensor with fetuin bound to it was placed in the CFM printer, which was set-up to print 42 different regeneration buffers. Six channels of the CFM were used as reference and contained Milli-Q water. A pre-buffer gap of 25 µL between system buffer (Milli-Q) and regeneration buffers through each of the 48 channels was programmed. A print time of 5 minutes with regeneration buffers was used followed by a post-print wash of 2 minutes with Milli-Q water. Directly after regeneration the sensor was transferred to the IBIS MX96 instrument.

A baseline of 2 minutes, followed by an association time of 15 minutes with 500 µg/mL fetuin solution and 5 minutes dissociation was performed. The injection volume was 100 µL. A mild regeneration with 25 mM phosphoric acid in 2 steps was applied followed by a wash

step. The analysis cycle was finished with a calibration cycle according to the IBIS calibration method. In short, calibration is performed with mixtures of glycerol in running buffer and MQ water at different levels. The RU at each spot on the sensor is measured for all mixtures. All experiments on the MX96 were performed at a temperature of 25°C.

Data were acquired in iSPR software and data analysis was performed in SPRint (IBIS Technologies BV, Enschede, The Netherlands). Calculations were performed in GraphPad Prism 6.01 (GraphPad Software, La Jolla, California, USA).

Results and discussion

Scouting of regeneration buffers in multiplexed format is demonstrated with the interaction between soybean agglutinin (SBA) lectin as a ligand and the glycoprotein fetuin as the analyte, according to the workflow in Figure 2.1-a. The entire surface was covalently coupled with SBA lectin and activity of the surface was verified by binding with fetuin (Figure 2.1-b, sensorgram I). A total of 48 spots were regenerated with one of the buffers by exposing the SBA-fetuin complex to the buffers using the microfluidics of the continuous flow microspotter (CFM). Following multiplexed regeneration, fetuin was injected again to reestablish binding to SBA lectin (Figure 2.1-b, sensorgram II) for determination of regeneration efficiency. The entire surface was regenerated with a mild regeneration buffer (25 mM phosphoric acid) followed by another fetuin injection to determine surface activity (Figure 2.1-b, sensorgram III).

Regeneration efficiency and surface activity were calculated based on report points at 15 minutes association, rather than comparing baseline levels. Baseline levels are usually evaluated to determine regeneration efficiency, but due to transfer of the sensor from MX96 to CFM and vice versa the sensor cannot be replaced with millidegree resolution and baselines cannot be compared. Therefore we chose to determine regeneration parameters from report points after 15 minutes with the same analyte concentration after baselines were zeroed. Three scenarios were then observed: 1) high surface activity and proper regeneration; 2) high surface activity but insufficient regeneration and 3) poor surface activity (Figure 2.1-b).

A poor surface activity was measured when the third sensorgram (Figure 2.1-b (3)) did not reach a similar response level compared to responses on a new surface in the first sensorgram. The ligand was destroyed and hence the regeneration buffer was not a suitable candidate. Surface activity was calculated based on the signal after a two-fold regeneration.

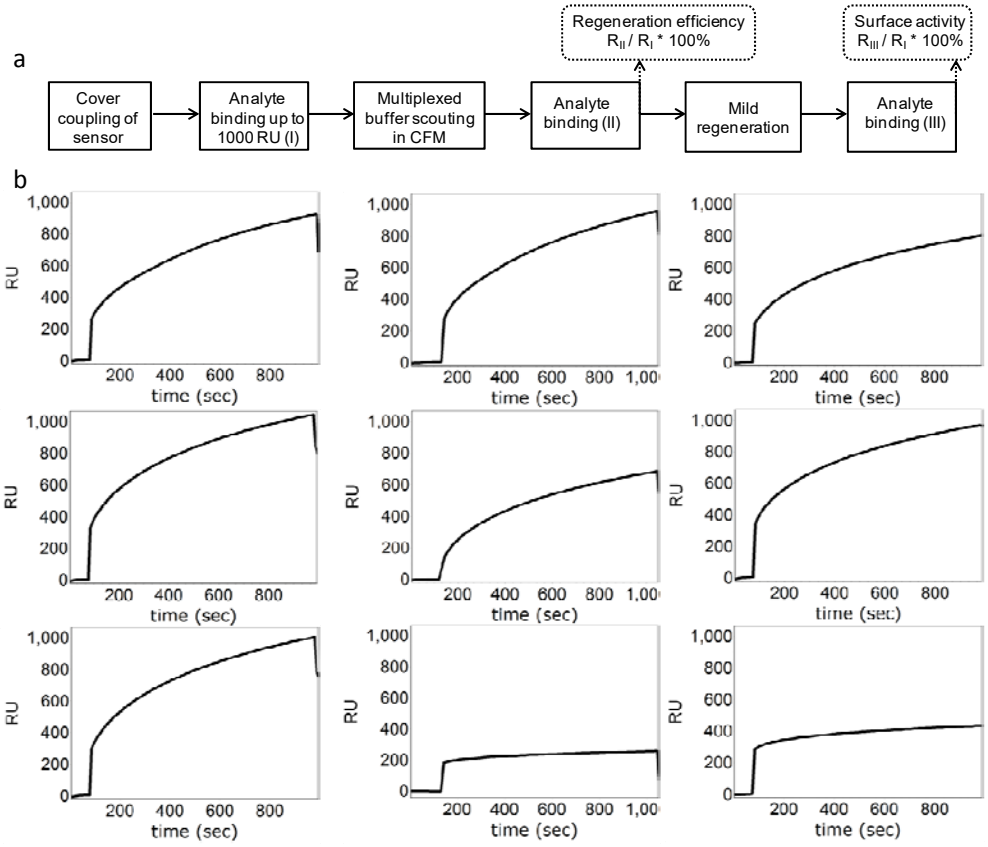

Figure 2.1 *a) Workflow of the multiplexed regeneration buffer scouting with continuous flow microspotter and SPR imaging. b) Sensorgrams of regeneration efficiency and surface activity in a multiplexed buffer screening. Sensorgram I: Binding of analyte (fetuin) to ligand (SBA lectin) on a newly prepared surface. Sensorgram II: Binding of analyte to ligand after regeneration with one of the buffers in the screening. Sensorgram III: Binding of analyte to ligand after mild regeneration of surface with 25 mM phosphoric acid. 1) High regeneration efficiency and high surface activity after regeneration with 25 mM phosphoric acid / 3M MgCl2. 2) Poor regeneration efficiency but high surface activity with 10 mM glycin-HCl pH2.0 / 1% ethanol. 3) Poor regeneration efficiency and poor surface activity with 10 mM HCl / 1% SDS (see text for further explanation).*

First a regeneration cycle was performed with one of the buffers in the CFM, followed by a mild regeneration with 25 mM phosphoric acid in the IBIS MX96. Responses at 15 minutes in measurement III (after mild regeneration) were divided by responses at 15 minutes in measurement I (new surface) (Figure 2.1-b) and expressed as percentages.

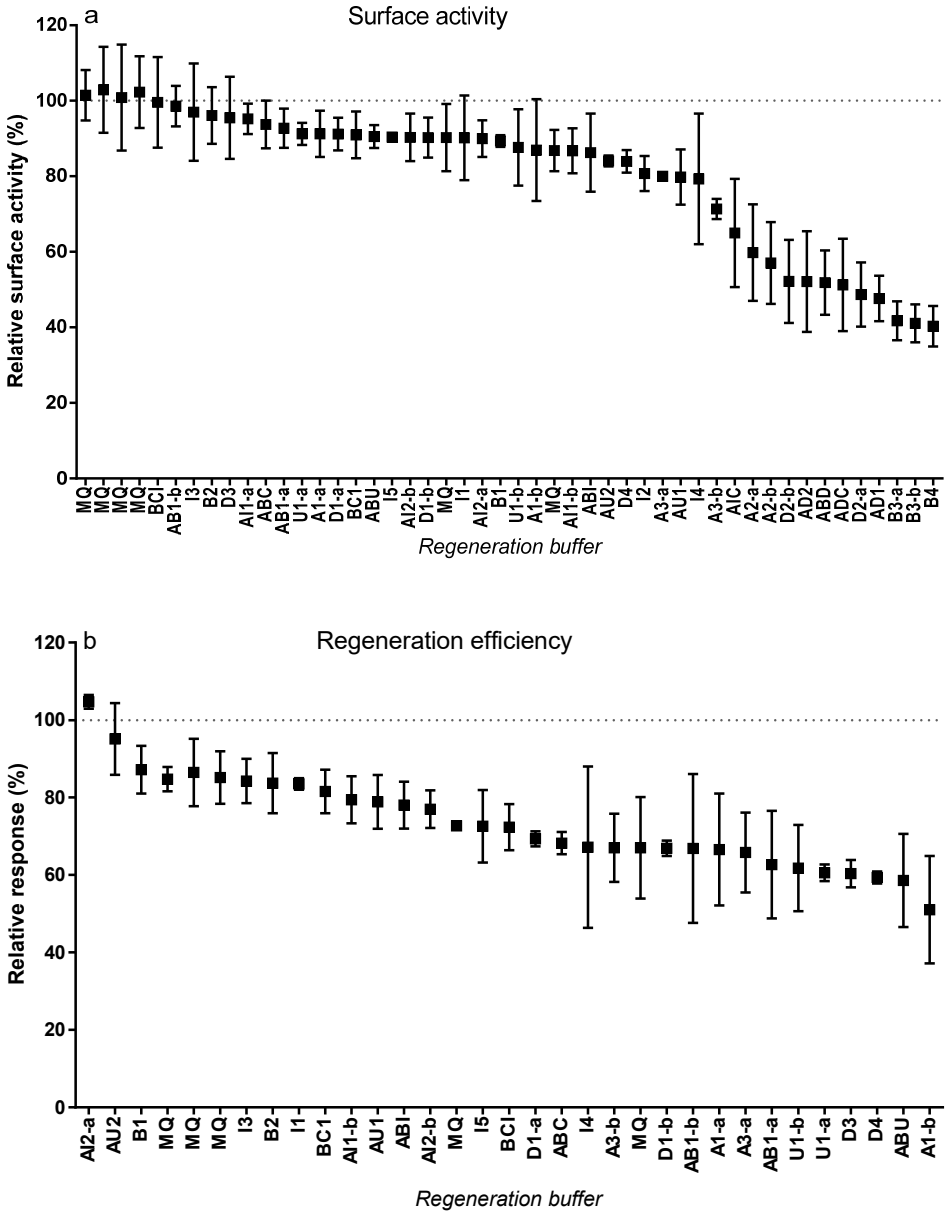

Figure 2.2 *Evaluation of multiplexed regeneration buffer screening. a) Remaining surface activity of ligand SBA towards binding of fetuin for 42 different regeneration buffers and six reference measurements (Milli-Q water. b) Regeneration efficiency of the buffers with a surface activity >70%. Dotted line indicates 100% level. Experiments were performed in triplicate.*

Surface activity of the ligand was determined for each of the tested regeneration buffers (Figure 2.2-a) and those buffers resulting in less than 70% active ligand were considered too harsh regeneration conditions. The ligand, SBA, was damaged too much by SDS-containing buffers (ABD, AD1, AD2, ADC, D2-a, D2-b), 10 mM and 100 mM glycin-HCl pH 2.0 (A2-a, A2-b), 10 mM and 100 mM NaOH (B3-a, B3-b) and 200 mM Na2CO3 pH 11 (B4). Elimination of regeneration buffers that destroy the ligand (i.e. surface activity below 70%) resulted in a subset of mild regeneration buffers.

Regeneration efficiency was then evaluated for the mild regeneration buffers. Regeneration efficiency was expressed as the level of binding which was measured after regeneration in the CFM relative to the level of binding on a newly prepared surface. Responses at 15 minutes in measurement II (after CFM regeneration) were divided by responses at 15 minutes in measurement I (new surface) (Figure 2.1-b) and expressed as percentages. Mild regeneration buffers were either too mild or were capable of sufficient removal of analyte. Too mild buffers removed insufficient amounts of bound analyte (Figure 2.1-b (2)) as indicated by sensorgram II which does not reach the same response level. Mild buffers that were capable of removing sufficient amounts of bound analyte (Figure 2.1-b (1)) resulted in similar responses in all three sensorgrams and were considered to be good regeneration conditions for the SBA – fetuin interaction. Regeneration efficiencies for all mild regeneration buffers were calculated and results of triplicate measurements are shown in Figure 2.2-b. Best regeneration efficiencies were measured with 25 mM phosphoric acid / 3 M MgCl2 (AI2-a) and 25 mM phosphoric acid / 1% ethanol (AU2) for the SBA-fetuin complex.

Summary

We have demonstrated a new regeneration scouting workflow capable of testing 48 different regeneration buffers simultaneously in affinity-based biosensor applications. The full experimental workflow can be performed within three hours and triplicate measurements within one working day. The continuous flow microspotter (CFM) is ideally suited for this buffer scouting, adding a novel application to the usage of the instrument. Furthermore the workflow is an economic alternative as it consumes minute amounts of ligand, analyte and buffers. Additionally all tests can be performed on a single sensor even when harsh regeneration conditions are to be tested.

Chapter 2

Acknowledgements

We thank EFRO Province of Gelderland and Overijssel, the Netherlands for financially supporting this research project.

References

1. Drake, A. W. and Klakamp, S. L. A strategic and systematic approach for the determination of biosensor regeneration conditions. J.Immunol.Methods 31-8-2011; 371(1-2): 165-169
2. Fischer, M. J. Amine coupling through EDC/NHS: a practical approach. Methods Mol.Biol. 2010; 627 55-73
3. Andersson, K., Hamalainen, M., and Malmqvist, M. Identification and optimization of regeneration conditions for affinity-based biosensor assays. A multivariate cocktail approach. Anal.Chem. 1-7-1999; 71(13): 2475-2481
4. Andersson, K., Areskoug, D., and Hardenborg, E. Exploring buffer space for molecular interactions. J.Mol.Recognit. 1999; 12(5): 310-315
5. Natarajan, S., Katsamba, P. S., Miles, A., Eckman, J., Papalia, G. A., Rich, R. L., Gale, B. K., and Myszka, D. G. Continuous-flow microfluidic printing of proteins for array-based applications including surface plasmon resonance imaging. Anal.Biochem. 1-2-2008; 373(1): 141-146

CHAPTER 3

Rapid buffer and ligand screening for affinity chromatography by multiplexed Surface Plasmon Resonance imaging

The contents of this chapter have been accepted as:

Karin P.M. Geuijen, Daniëlle E.J.W. van Wijk-Basten, David F. Egging, Richard B.M. Schasfoort, Michel H. Eppink

Rapid buffer and ligand screening for affinity chromatography by multiplexed Surface Plasmon Resonance imaging

Biotechnology Journal (2017)

Chapter 3

Abstract

Protein purifications are often based on the principle of affinity chromatography, where the protein of interest selectively binds to an immobilized ligand. The development of affinity purification requires selecting proper wash and elution conditions. In recent years, miniaturization of the purification process is applied to speed up the development (e.g. microtiterplates, robocolumns). We have studied the application of surface plasmon resonance imaging (SPRi) as a tool to simultaneously screen many buffer conditions for wash and elution steps in an affinity-based purification process. Additionally, the protein A ligand stability after exposure to harsh cleaning conditions often limits the reuse of resins and is determined at lab scale. We also used the SPRi technology to screen ligand life-time with respect to alkali stability and demonstrated that SPRi can successfully be applied in screening experiments for process developments in a miniaturized approach. The amount of resin, protein and buffer in these studies was reduced 30-300-fold compared to 1 mL column scale, and approximately 10-1000-fold compared to filter plate experiments. The overall development time can be decreased from several months towards days. The multiplexed SPRi can be applied in screening affinity chromatography conditions in early stage development for ligand development and recombinant protein production.

Introduction

Affinity chromatography is a highly selective capture step in the purification of many recombinant proteins, where the interaction is based on reversible binding.[1] Within the biopharmaceutical industry, protein A chromatography is often applied as the first unit operation to remove the majority of impurities, such as host cell proteins (HCPs), fragments, DNA and media components, from a cell culture harvest to purify mAbs.[2-5]

Recombinant protein A has been engineered to obtain a more stable protein[3] that can withstand harsh conditions on a purification column, such as high flow rates, different wash buffers and additives or cleaning conditions.[6] Many different engineered protein A-based resins are available nowadays for efficient IgG purification,[3,7] which have a longer resin life-time compared to their native counterparts, mainly due to an improved alkali stability. Affinity columns are generally rigorously cleaned after each purification cycle to prevent cross-contamination, often by dilute NaOH solutions. The applied cleaning-in-place (CIP) solution depends on resin type and on ligand stability, and therefore ligand life-time has to be studied during the development of new affinity ligands.[8-11]

Process development of a protein A purification step for IgGs involves the selection of wash and elution conditions. HCP levels can vary significantly in protein A pools amongst different mAbs and removal thereof is dependent on the selected wash conditions.[12] In recent years, wash conditions have been investigated to remove a larger fraction of HCPs[13-15] and aggregates[16] while maintaining high overall yield. A rapid screening of the various steps in the purification process enables a fast transfer to pilot-scale experiments where only a selection of conditions can be tested.[17] Especially with the development of newly engineered protein A ligands, or any other affinity ligand, there is a broad interest in miniaturized screening approaches to speed up the development process.[18,19]

Here we describe an alternative screening technology, based on multiplexed SPRi, to miniaturize process development using protein A and IgG as a model system. We screened elution and wash buffers in a simulated Protein A affinity chromatography step and we performed an alkali stability test of the protein A ligands at microgram scale. The use of a 48-channel continuous flow microspotter (CFM) to screen 48 different buffers for interaction analysis has been proven before[20] and we further optimized the experimental set-up to screen for protein A process development.

Chapter 3

Materials and methods

Elution buffer screening using SPRi

A G-COOH sensor (SSens BV, Enschede, the Netherlands) was activated with EDC/NHS in 50mM MES buffer according to manufacturer's instructions in the IBIS MX96 (IBIS Technologies BV, Enschede, the Netherlands). MabSelect SuRe (MSS) ligand (GE life sciences) was diluted to 1 µM in 50 mM sodium acetate pH 4.0 / 0.05% polysorbate 80 and immobilized on the entire surface of the sensor. The sensor was deactivated by 1 M ethanolamine pH 8.5 during 10 minutes in the IBIS MX96.

Recombinant human IgG (Synthon Biopharmaceuticals BV, Nijmegen, the Netherlands) was diluted to 1 µM in PBS buffer pH 7.4 / 0.05% polysorbate 80 and injected over the MSS sensor with a total association time of 10 minutes until equilibrium was reached ($R_{eq}1$), after a baseline of 1 minute. Subsequently, the sensor was transferred to the continuous flow microspotter (CFM, Wasatch, Salt Lake City, USA) where the surface was exposed to 48 different buffers simultaneously for 1 minute in a 4x12 array. Elution buffers that were screened were prepared from a 50 mM sodium acetate stock solution at pHs of 6.0; 5.5; 5.25; 5.0; 4.8; 4.5; 4.0; 3.5; 3.25; 3.0 or 2.7 and 2 M NaCl stock solution. Buffers were mixed in different ratios and diluted with MQ water to obtain 25 mM sodium acetate buffers at the indicated pH, with salt concentrations of 0, 250, 500 or 1000 mM NaCl. PBS pH 7.4 was included as a reference buffer for normalization of the results. The sensor surface was transferred back to the IBIS MX96 and a baseline of 1 minute was followed by association of 1 µM IgG solution for 10 minutes again ($R_{eq}2$), followed by a complete regeneration of the surface with 25 mM phosphoric acid pH 3.0. This entire procedure, except immobilization, was repeated four times.

Sensorgrams were calibrated, referenced and zeroed and the binding levels at equilibrium were determined. First the recovery for each condition was calculated and normalized against PBS buffer to correct for dissociation of IgG from MSS ligand during buffer flushes in the system.

Normalized recovery = $([1- (R_{eq}2/ R_{eq}1)]_{tested\ buffer} / [1- (R_{eq}2/ R_{eq}1)]_{PBS}) *100\%$. The normalized recovery was then translated into yield as follows: Yield = 100% - normalized recovery.

Elution buffer screening using PreDictor plates

PreDictor plates (GE life sciences) with 50 µL MabSelect SuRe media per well were prepared according to manufacturer's protocol. Equilibration and wash steps consisted of 3x 200 µL PBS buffer pH 7.4. Purified IgG sample (Synthon Biopharmaceuticals BV) at 5 mg/mL was loaded to each well in 200 µL after equilibration. The wells were washed followed by IgG elution using buffers of 25 mM sodium acetate at pH 3.0-5.75 in 0.25 increments. IgG concentrations in the eluates were determined by OD_{280} measurements with the Infinite M1000 reader (Tecan, Männedorf, Switzerland).

Wash buffer screening using SPRi

A pre-activated Easy2Spot G-type sensor (SSens BV) was immobilized with 12 spots of MabSelect SuRe ligand (GE life sciences), 12 spots of MabSelect ligand (GE life sciences) and 12 spots of KanCapA ligand (Kaneka, Tokyo, Japan) at concentrations between 50 and 1.6 µg/mL in 50 mM sodium acetate pH 4.5 / 0.05% polysorbate 80. Immobilization was performed in the continuous flow microspotter (CFM) with a 5-minute print time. The sensor was deactivated by 1 M ethanolamine pH 8.5 during 10 minutes in the IBIS MX96.

Association of 100 µL of an IgG CCF (Synthon Biopharmaceuticals BV) to the different ligands was performed for 3 minutes ($R_{eq}1$) after a baseline of 1 minute. This was followed by injections of wash buffer for 3 minutes and then again an injection of the same IgG CCF for 3 minutes ($R_{eq}2$). The sensor was regenerated with 25 mM phosphoric acid pH 3 for 30 seconds. This entire procedure was repeated three times for each wash buffer. A total of 48 different wash buffers were selected for this screening, and one per cycle was injected. The wash buffers consisted of 10, 25 or 100 mM Tris pH 8 or sodium acetate pH 5. The 25 mM buffers were used in combination with various additives at different concentrations. The tested additives in both buffers were: NaCl (0.5, 1 and 2 M), arginine (0.5, 1 and 2 M), $CaCl_2$ (0.5, 1 and 2 M), Na_2SO_4 (0.5, 1 and 1.5 M), isopropanol (5, 10 and 20%), ethanol (5, 10 and 20%) and urea (0.5, 1 and 2 M).

Sensorgrams were calibrated, referenced and zeroed and binding levels at equilibrium were determined. Recoveries were calculated and normalized against 10mM Tris pH8 buffer as follows:

Normalized recovery = $([1- (R_{eq}2/ R_{eq}1)]_{\text{tested buffer}} / [1- (R_{eq}2/ R_{eq}1)]_{\text{10mM Tris pH8}})*100\%$.

Wash buffer screening using filter plates

96-well filter plates (Whatman) were filled with 40 µL resin (MabSelect SuRe or KanCapA) and equilibrated with 3x 200 µL PBS buffer pH 7.4. Then 6x 300 µL of IgG CCF was added to the wells and subsequently washed with 2x 200 µL of the following buffers: PBS buffer pH 7.4; either 25 mM Tris pH 8 or 25 mM sodium acetate pH 5; each of the 48 selected wash buffers with additives (section 2.3) and at last 25 mM Tris pH 8 or 25 mM sodium acetate pH 5. The protein was eluted in 2x 200 µL 25 mM acetate pH 3.0. Recovery of IgG for the wash and elution steps was determined by OD280 nm with the Infinite M1000 reader (Tecan, Männedorf, Switzerland).

Alkali resistance testing using SPRi

A pre-activated Easy2Spot G-type sensor was prepared as described in the wash buffer screening. Association of 100 µL of an IgG CCF (Synthon Biopharmaceuticals BV) at approximately 1-2 mg/mL IgG was performed for 15 minutes after a baseline of 1 minute. The surface was regenerated with 25 mM sodium acetate pH 3 and then 10 cycles of 0.1 or 0.5 M NaOH were injected during 15 minutes. Each 10^{th} cycle, the initial IgG CCF was injected again. This entire procedure was repeated ten times to simulate a total of 100 NaOH cycles.

Sensorgrams were referenced and zeroed; responses at equilibrium were determined and expressed as binding capacity. Binding capacity of the first injection was set to 100% and binding capacity of subsequent cycles was calculated relative to the first cycle.

Alkali resistance testing using columns

Protein A columns of 1 mL with either MabSelect SuRe or KanCapA resin were used to determine the alkali resistance. First the dynamic binding capacity (DBC) was determined at 10% breakthrough using purified IgG, followed by a run with IgG CCF to determine product quality, followed by 8 runs of sanitization with 0.5 M NaOH. This sequence of 10 runs was repeated 10 times to simulate 100 sanitization steps in total. The purification run with CCF consisted of following steps with 10 column volumes (CV) each: equilibration with PBS pH 7.4 at 1 mL/min; sample load at 0.5 mL/min; wash in 4 steps with different wash buffers; IgG elution with 25 mM sodium acetate pH 3.0; regeneration with 0.5 M acetic acid (MSS) or 1 M acetic acid (KCA); wash with purified water; sanitization with 0.5 M NaOH during 15 minutes and wash with purified water.

The DBC of the initial run was set to 100% and every 10th cycle the DBC was calculated, followed by normalization relative to the initial value.

Statistical data analysis

Statistical analysis of the data was performed in GraphPad Prism 6. Correlation analysis was used in the elution buffer and wash buffer screening. Linear regression analysis was performed on the alkali stability, and slopes of the regression curves were compared with each other.

Results and discussion

Comparison of elution buffer screening using SPRi or filter plates

A screening of elution buffer conditions for the interaction between MabSelect SuRe (MSS) and IgG was performed on an SPRi sensor surface to prove the concept of the technology (Figure 3.A.1). An array of 48 elution buffers was simultaneously flushed over the surface, to determine the influence of the buffer on the IgG yield, similar to the set-up in Geuijen et al.[20] The yields obtained in SPRi experiments match closely to the yields that were obtained in filter plate experiments and to values reported in literature (Figure 3.1).[21] Correlation between the SPRi results and filter plate experiments was 0.94 with P=0.005 in the buffers without NaCl addition. Slightly lower correlation values, of 0.67, 0.84 and 0.84 for 1M NaCl, 0.5M NaCl and 0.25M NaCl respectively, were determined for the other elution buffer conditions.

Minor differences between the different techniques were measured at pH 3.3 and pH 3, and between pH 4 and pH 5 upon NaCl addition. The infliction point of the binding equilibrium between IgG and MSS is around these pH values, and this may impact the results. The interactions between MSS and IgG are partly based on electrostatic interactions[22,23] and addition of NaCl to the buffer reduces these interactions. This directly impacts the binding equilibrium, resulting in reduced affinity around pH 4-5, which is translated to increased elution in the SPRi experiments upon NaCl addition. At pH 3.3 and pH 3, the slightly higher recovery in filter plate experiments may be explained by the presence of an agarose backbone on the resin, which may stabilize the interaction between MSS and IgG.[23] In SPRi experiments the MSS ligand is directly immobilized onto the sensor surface and this may have an impact on the stability of the interaction around the infliction point of the equilibrium.

Furthermore the intrinsic binding capacity of the filter plates and the SPRi sensor may be different, which can impact the results. Columns or filter plates are often loaded up to saturation, whereas the maximum binding capacity of MSS on the SPRi sensor is not reached.

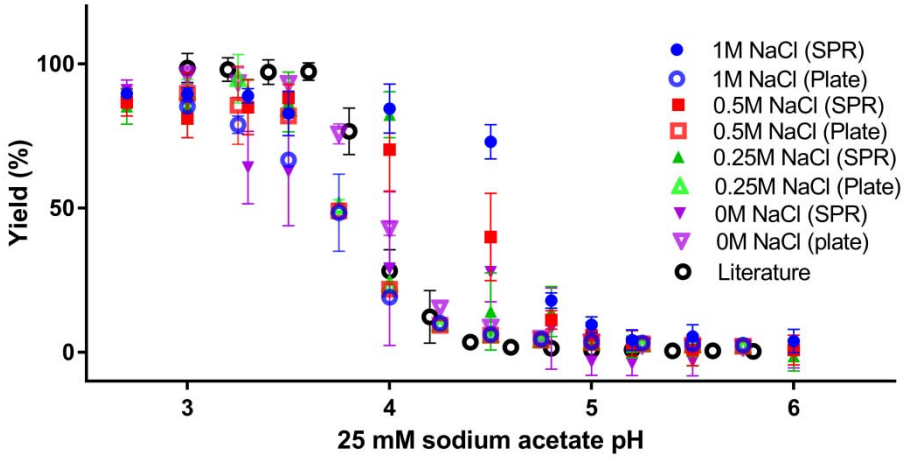

Figure 3.1 *Elution pH profiles of IgG on MabSelect SuRe determined by multiplexed surface plasmon resonance, PreDictor plate experiments and literature values of PreDictor plate experiments.*[21] *Each value of SPRi and filter plate experiments represents the IgG yield at indicated buffer pH of four replicates, with error bars indicating ± one standard deviation.*

Comparison of wash buffer screening using SPRi or filter plates

Wash buffers were screened on the SPRi platform with MabSelect (MS), MabSelect SuRe (MSS) and KanCapA (KCA) protein A ligand simultaneously on a single SPRi sensor (Figure 3.A.2). No filter plate experiments with MS were performed, so focus will be on the results of MSS and KCA. A total of 48 wash buffers were selected (see materials and methods section) and IgG recovery was determined. IgG recoveries of the different wash buffers between filter plate experiments and SPRi experiments were compared. Results between SPRi and filter plates correlate well to each other as determined by statistical correlation analysis ($r=0.57$ for pH8 and $r=0.83$ for pH5; both with $P<0.0001$).

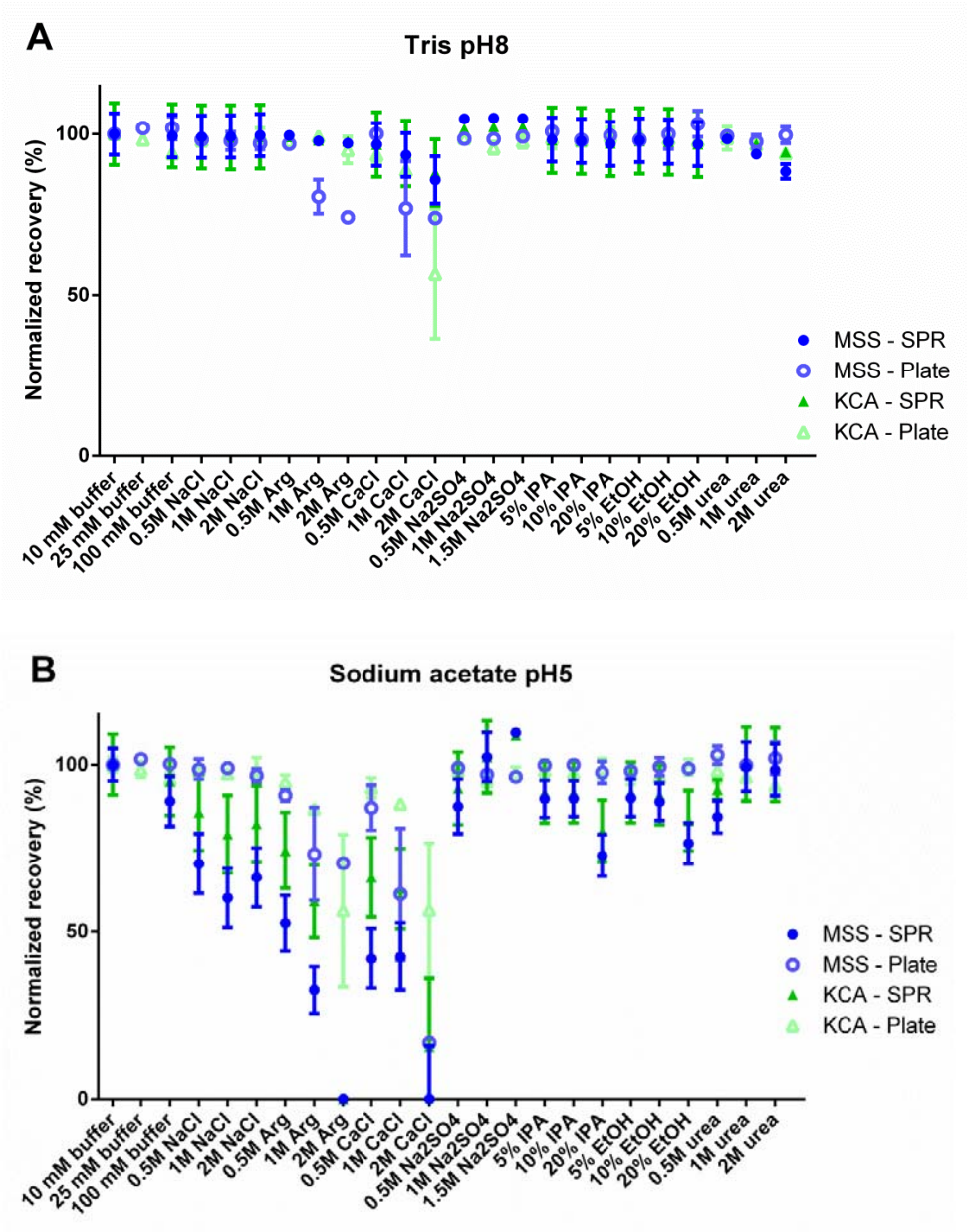

Figure 3.2 *Wash buffer screening on MabSelect SuRe (MSS) and KanCap A (KCA) protein A ligands determined by multiplexed surface plasmon resonance and in filter plates in A) 25 mM tris buffer pH8 and B) 25 mM sodium acetate pH5. Various additives at different concentrations were tested in both buffer systems. Values indicate the IgG recovery in % after the wash step by elution at pH 3 (filter plates, n=2), or by measurement of remaining IgG on the ligands (SPRi, n=3). Error bars represent ± one standard deviation.*

Recoveries of the wash buffer screening at pH 5 were comparable between SPRi and filter plates for four of the tested additives and in the sodium acetate buffer without additive (Figure 3.2-B). Two additives (1 and 2 M arginine or $CaCl_2$) had reduced recoveries in the filter plate experiments and even lower recoveries in the SPRi experiments for both ligands. Additionally, a reduced recovery in SPRi experiments was detected with NaCl as additive, which was not observed in filter plate experiments. Protein interactions are based on complex formation between the two binding partners, and this is influenced by the experimental conditions. Especially at pH 5, where the interaction between protein A and IgG is close to the infliction point of the equilibrium, the affinity is weaker compared to higher pH, and as a result dissociation will be faster. In SPRi experiments, the flow rate is relatively high compared to column chromatography (µL/seconds *vs* mL/minutes). This translates to residence times of 0.24 seconds in SPRi experiments, compared to 3x 1 minute in filter plate experiments. Since the interaction is based on equilibrium between association and dissociation, a higher flow rate or a shorter residence time may impact this equilibrium directly by preventing rebinding events and driving the equilibrium further towards dissociation, resulting in larger IgG loss (expressed as lower recovery).

The majority of wash buffers at pH 8 had recoveries of >95% (Figure 3.2-A), both in filter plates and SPRi experiments. Lower recoveries were determined in buffers with 1 or 2 M arginine (MSS and KCA) and 1 or 2 M $CaCl_2$ (MSS only) in filter plate experiments. In the SPRi experiments a similar trend in reduced recovery was observed with $CaCl_2$ as additive, although total recovery was higher as compared to filter plates. Both are strong basic additives, which may not be fully washed out upon start of elution. The lower recoveries are only observed using the buffers with higher molarities of either arginine or $CaCl_2$, which suggests that the pH during elution is possibly still too high to fully recover the IgG from the resin. Since flow rates in SPRi experiments are higher compared to filter plate experiments, and therefore residence times of the buffer are shorter, as explained earlier, those basic additives are washed more rapidly in the SPRi experiments, resulting in higher recoveries because of a proper elution pH.

Comparison of ligand alkali resistance using SPRi or small-scale columns

The resin life-time in chromatographic purifications is mainly affected by the cleaning-in-place procedure, which is often performed with 0.1 or 0.5 M NaOH solutions, especially for the engineered protein A ligands. CIP cycles were simulated on 1 mL columns and on

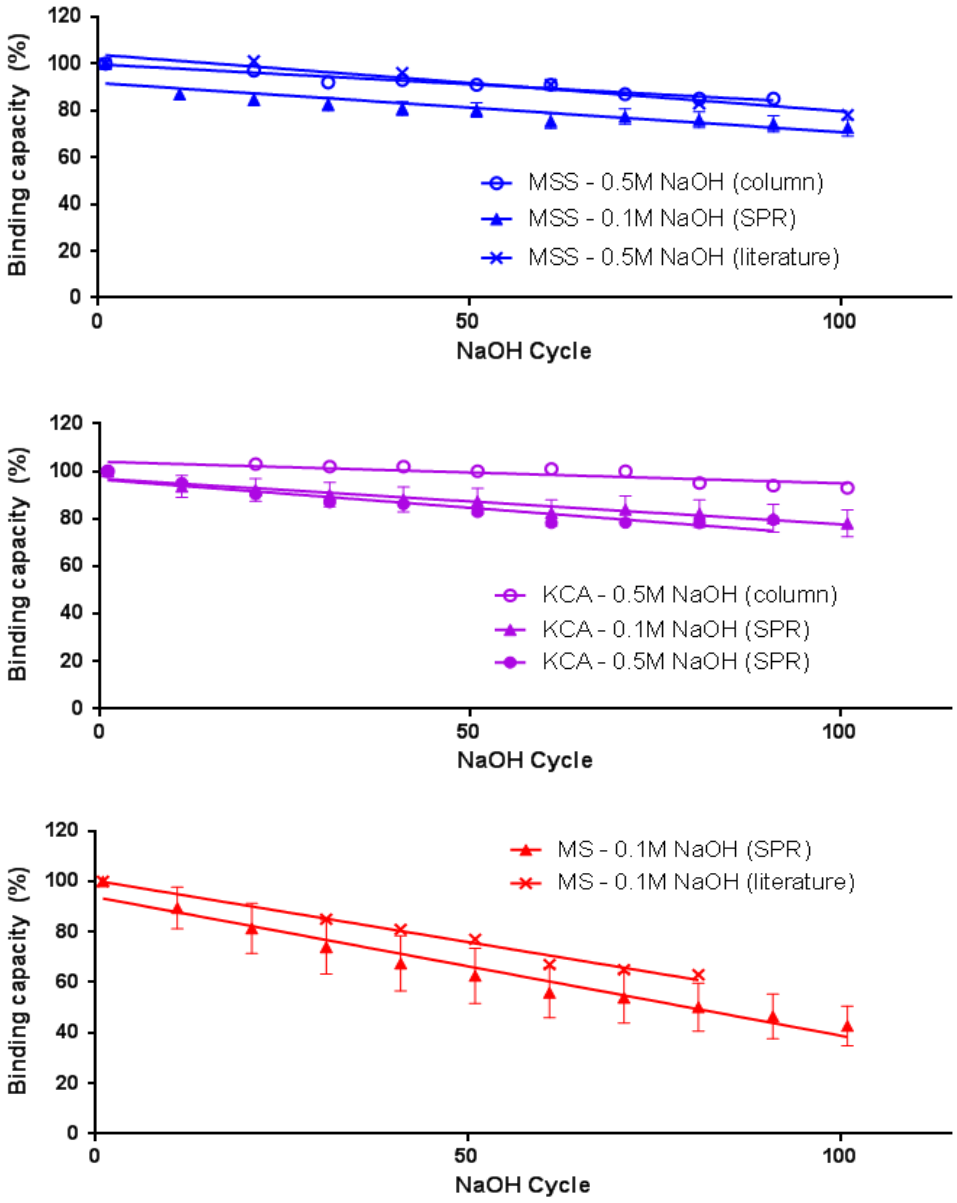

Figure 3.3 *Alkali resistance testing of three protein A ligands: (A) MabSelect SuRe [MSS], (B) KanCapA [KCA] and (C) MabSelect [MS]) determined by multiplexed surface plasmon resonance, on 1 mL chromatography columns and literature.[24,25] Values represent the binding capacity of the ligand, determined by dynamic binding capacity at 10% breakthrough in column experiments (n=1) and by IgG binding responses in SPRi (n=12). Twelve independent spots on a single SPRi sensor for each of the ligands were evaluated and error bars indicate ± one standard deviation.*

SPRi up to 100 cycles. Every 10th cycle, the binding capacity expressed as the fraction of IgG that still bound was determined (Sensorgrams are shown in Figure 3.A.3).

MS is not resistant to 0.5 M NaOH and therefore the SPRi experiments were performed with 0.1 M NaOH, since all three ligands were tested simultaneously. An initial experiment with only KCA ligand at the sensor surface was performed with 0.5 M NaOH. KCA and MSS have a binding capacity around 75-85% of the initial binding capacity after 100 cycles of NaOH, with an exposure time of 15 minutes per cycle (Figure 3.3). These results are comparable for the different methods that were applied. MS, which is less alkali-stable, had a binding capacity of only 50% after 80 cycles, which is in agreement with approximately 60% reported by the supplier.[24] Resin life-time of all three ligands (MSS, KCA and MS) is in agreement between column experiments, SPRi experiments and literature value.[24,25] A linear regression analysis on the slopes of the binding-capacity curves shows no significant differences between techniques for each ligand individually ($P = 0.85$ for MSS; $P = 0.17$ for KCA; $P = 0.30$ for MS).

Concluding remarks

The SPR imaging technology provides an attractive alternative for screening of process parameters, such as wash and elution buffers or alkali stability for affinity-based purification strategies as demonstrated here. We have proven the concept of this screening based on the interaction between protein A and IgG with results comparable to filter plate and column experiments. The SPRi screening is economically attractive compared to filter plate screening or column screening (Table 3.1), as consumption of all materials can be reduced nearly 20-fold up to >1000-fold. Especially reduction of IgG material needed for screening is an important benefit during early phase process development when often only limited material is available.

In a few experiments we found differences between the tested techniques, which were mostly found around pH 4 to 5, where the interaction equilibrium changes.[3] The combination of wash buffer pH5 and certain additives led to a lower recovery in the SPRi experiments, and the elution profile changed around pH 4 with the addition of NaCl. Differences in flow rate, chemical backbone and different spacer length in the SPRi technology compared to column resins may account for these deviations. For example, the higher flow rate in SPRi reduces rebinding effects, resulting in lower yields.[26] The agarose backbone of a resin may have a stabilizing effect on the interaction, as shown by molecular modeling of the protein A – IgG interaction by Salvalaglio et al.[23]

Table 3.1 *Calculation on required materials for filter plate or column and SPRi experiments in elution buffer screening, wash buffer screening and alkali resistance screening*

		Ligand or resin (mL)	IgG (mg)	Buffers (mL)	n	Reduction factor		
						Ligand	IgG	buffer
Elution buffer	Filter plate	4.80	4	690	4	1600	22	96
	SPR	0.003	0.18	7.2	4			
Wash buffer	Filter plate	5.76	104	375	3	576	18	17
	SPR	0.01	5.76	21.6	3			
Alkali resistance	Column	1	544.5	2000	1	33	330	60
	SPR	0.03	1.65	33.3	1			

Overall column and filter plate experiments correlate well with the SPRi results. The major benefits of the SPRi technology are miniaturization and significant decrease in development time. Each of the described screenings was performed within 1 working day, whereas alkali stability on columns took several weeks. Buffer screening with filter plates is comparable in time, however much less material is needed in the SPRi screening strategy (Table 3.1).

The SPRi screening as demonstrated here can be very useful in early-phase discovery. The proof of concept was based on protein A – IgG interaction, but any type of interaction for affinity chromatography can be analyzed in this set-up. The technology is especially useful for screening many different ligands simultaneously, for example in selecting new ligands for affinity chromatography.[27]

Acknowledgements

We would like to thank Sanne Wilmsen, Lonnie Joosten-Stoffels, Eefje Verhofstad and Thomas de Beijer for executing part of the experimental work. We thank Kaneka Corporation for providing their protein A ligand free of charge.

Appendix A Sensorgrams

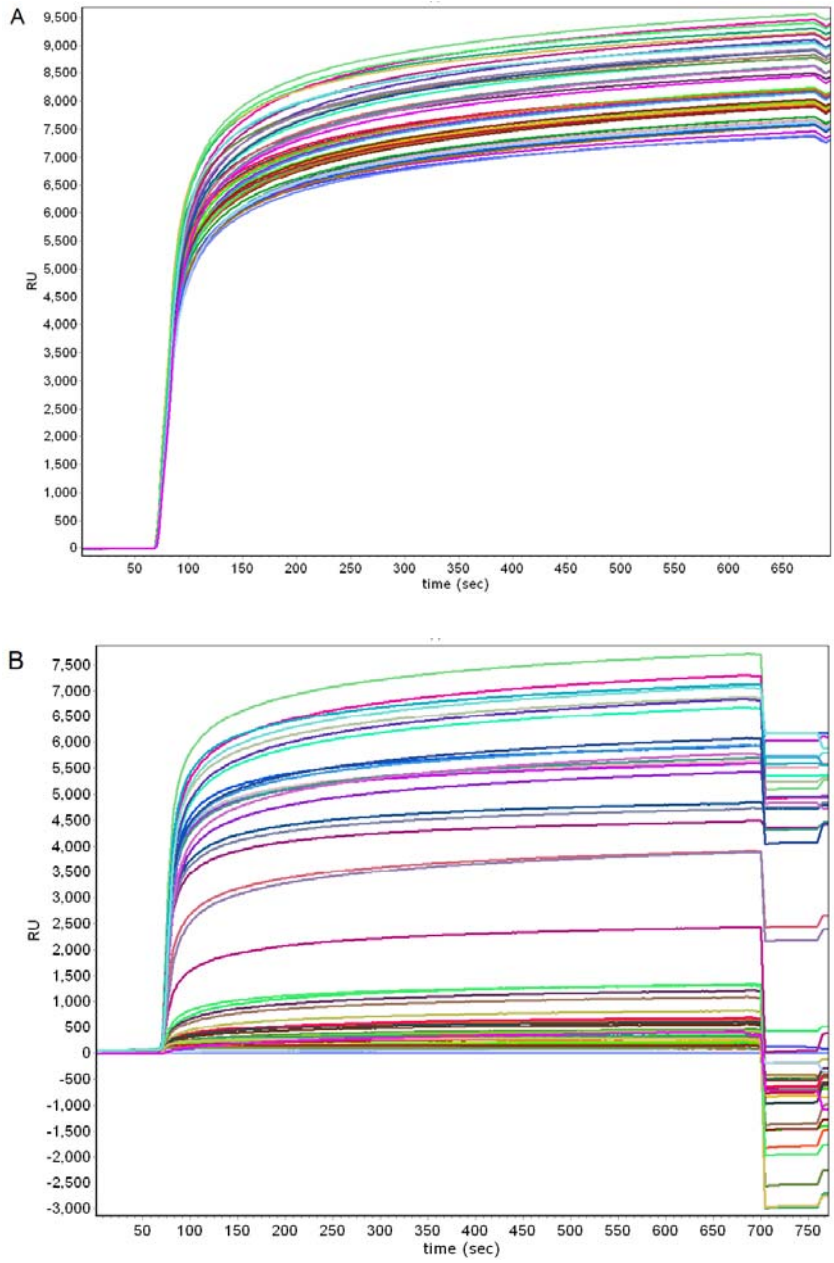

Figure 3.A.1 *Sensorgrams of elution buffer screening. IgG binding on 48 MSS spots before (A) and after (B) elution buffer application. Each coloured line represents one of the 48 MSS spots*.

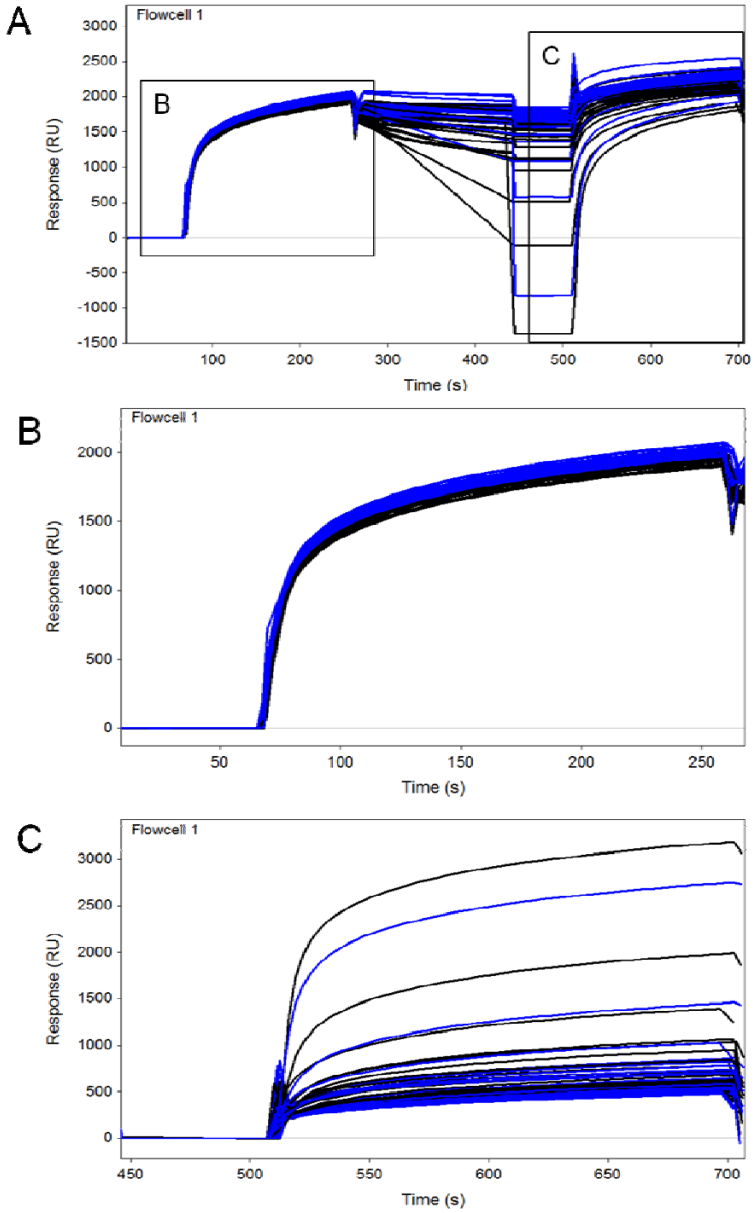

Figure 3.A.2 *Sensorgrams of wash buffer screening on MSS (black) and KCA (blue). Each line represents one of the selected wash buffers. A) Complete wash buffer cycle with IgG binding between 60 and 250 seconds, followed by different wash buffers between 250 and 450 seconds, followed by another IgG injection between 500 and 700 seconds. B) Close view of the initial IgG binding before wash buffer application. C) Close view of the IgG binding after wash buffer application, where baselines were zeroed to appropriately determine binding levels at equilibrium.*

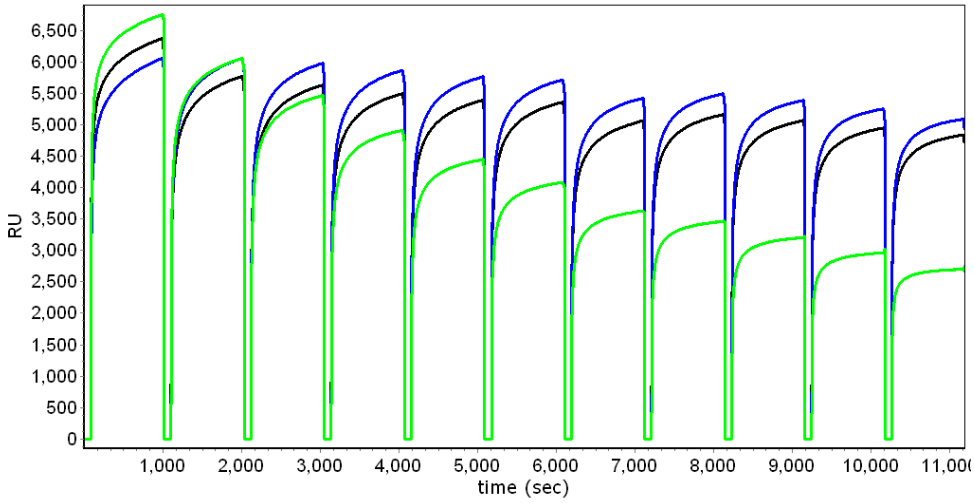

Figure 3.A.3 *Sensorgrams of alkali resistance screening on MSS (black), KCA (blue) and MS (green). IgG was injected each 10th NaOH cleaning cycle and these injections are shown.*

References

1. Cuatrecasas, P. Affinity chromatography. Annu.Rev.Biochem. 1971; 40 259-278
2. Huse, K., Bohme, H. J., and Scholz, G. H. Purification of antibodies by affinity chromatography. J.Biochem.Biophys.Methods 31-5-2002; 51(3): 217-231
3. Hober, S., Nord, K., and Linhult, M. Protein A chromatography for antibody purification. J.Chromatogr.B Analyt.Technol.Biomed.Life Sci. 15-3-2007; 848(1): 40-47
4. Liu, H. F., Ma, J., Winter, C., and Bayer, R. Recovery and purification process development for monoclonal antibody production. MAbs. 2010; 2(5): 480-499
5. Chollangi, S., Parker, R., Singh, N., Li, Y., Borys, M., and Li, Z. Development of robust antibody purification by optimizing protein-A chromatography in combination with precipitation methodologies. Biotechnol.Bioeng. 2015; 112(11): 2292-2304
6. Pabst, T. M., Palmgren, R., Forss, A., Vasic, J., Fonseca, M., Thompson, C., Wang, W. K., Wang, X., and Hunter, A. K. Engineering of novel Staphylococcal Protein A ligands to enable milder elution pH and high dynamic binding capacity. J.Chromatogr.A 3-10-2014; 1362 180-185
7. Hahn, R., Schlegel, R., and Jungbauer, A. Comparison of protein A affinity sorbents. J.Chromatogr.B Analyt.Technol.Biomed.Life Sci. 25-6-2003; 790(1-2): 35-51
8. Hahn, R., Shimahara, K., Steindl, F., and Jungbauer, A. Comparison of protein A affinity sorbents III. Life time study. J.Chromatogr.A 13-1-2006; 1102(1-2): 224-231
9. Jiang, C., Liu, J., Rubacha, M., and Shukla, A. A. A mechanistic study of Protein A chromatography resin lifetime. J.Chromatogr.A 31-7-2009; 1216(31): 5849-5855
10. Gronberg, A., Eriksson, M., Ersoy, M., and Johansson, H. J. A tool for increasing the lifetime of chromatography resins. MAbs. 2011; 3(2): 192-202
11. Rathore A, Pathak M, Ma G, and Bracewell D. Re-use of Protein A Resin: Fouling and Economics.BioPharm International 2015; 28: 28-33
12. Nogal, B., Chhiba, K., and Emery, J. C. Select host cell proteins coelute with monoclonal antibodies in protein A chromatography. Biotechnol.Prog. 2012; 28(2): 454-458
13. Ishihara, T. and Hosono, M. Improving impurities clearance by amino acids addition to buffer solutions for chromatographic purifications of monoclonal antibodies. J.Chromatogr.B Analyt.Technol.Biomed.Life Sci. 15-7-2015; 995-996 107-114
14. Shukla, A. A. and Hinckley, P. Host cell protein clearance during protein A chromatography: development of an improved column wash step. Biotechnol.Prog. 2008; 24(5): 1115-1121
15. Bolton, G. R., Selvitelli, K. R., Iliescu, I., and Cecchini, D. J. Inactivation of viruses using novel protein A wash buffers. Biotechnol.Prog. 2015; 31(2): 406-413
16. Yada, T., Nonaka, K., Yabuta, M., Yoshimoto, N., and Yamamoto, S. Choosing the right protein A affinity chromatography media can remove aggregates efficiently. Biotechnol.J. 23-9-2016; 1-8
17. Lye G, Hubbuch J, Schroeder T, and Williman E. Shrinking the costs of bioprocess development.BioProcess International 2009; 18-22
18. Fernandes, P., Carvalho, F., and Marques, M. P. Miniaturization in biotechnology: speeding up the development of bioprocesses. Recent Pat Biotechnol. 2011; 5(3): 160-173
19. Bergander, T., Nilsson-Valimaa, K., Oberg, K., and Lacki, K. M. High-throughput process development: determination of dynamic binding capacity using microtiter filter plates filled with chromatography resin. Biotechnol.Prog. 2008; 24(3): 632-639

20. Geuijen, K. P., Schasfoort, R. B., Wijffels, R. H., and Eppink, M. H. High-throughput and multiplexed regeneration buffer scouting for affinity-based interactions. Anal.Biochem. 1-6-2014; 454 38-40

21. High-throughput screening of elution pH for monoclonal antibodies on MabSelect SuRe using PreDictor plates.2008;

22. Gedig ET. Surface chemistry in SPR technology.2008; 173-220

23. Salvalaglio, M., Zamolo, L., Busini, V., Moscatelli, D., and Cavallotti, C. Molecular modeling of protein A affinity chromatography. J.Chromatogr.A 11-12-2009; 1216(50): 8678-8686

24. MabSelect SuRe affinity chromatography user instructions.2011;

25. Kaneka KanCapA Affinity Sorbent.2015;

26. Schuck, P. and Zhao, H. The role of mass transport limitation and surface heterogeneity in the biophysical characterization of macromolecular binding processes by SPR biosensing. Methods Mol.Biol. 2010; 627 15-54

27. Pabst, T. M., Wendeler, M., Wang, X., Bezemer, S., Hermans, P., and Hunter, A. K. Camelid VH H affinity ligands enable separation of closely related biopharmaceuticals. Biotechnol.J. 27-9-2016; 1-10

Chapter 3

CHAPTER 4

Label-free glycoprofiling with multiplex surface plasmon resonance: A tool to quantify sialylation of Erythropoietin

The contents of this chapter have been published as:

Karin P.M. Geuijen, Liem A. Halim, Huub Schellekens, Richard B. Schasfoort, René H. Wijffels, Michel H. Eppink

Label-free glycoprofiling with multiplex surface plasmon resonance: A tool to quantify sialylation of Erythropoietin

Analytical chemistry (2015) 87, pg 8115-8122

Chapter 4

Abstract

Protein glycosylation is among the most common and well defined post-translational modifications due to its vital role in protein function. Monitoring variation in glycosylation is necessary for producing more effective therapeutic proteins. Glycans attached to glycoproteins interact highly specific with lectins, natural carbohydrate-binding proteins, which property is used in the current label-free methodology. We have established a lectin micro-array for label-free detection of lectin-carbohydrate interactions allowing us to study protein glycosylation directly on unmodified glycoproteins. The method enables simultaneous measurement of up to 96 lectin-carbohydrate interactions on a multiplex surface plasmon resonance imaging platform within 20 minutes. Specificity determination of lectins succeeded by analysis of neoglycoproteins and enzymatically remodeled glycoproteins to verify carbohydrate binding. We demonstrated the possibilities for glycosylation fingerprinting by comparing different Erythropoietin sources without the need for any sample pretreatment and we were able to accurately quantify relative sialylation levels of Erythropoietin.

Introduction

Glycosylation is one of the most important and well-studied post-translational modifications on proteins. Glycans may affect the structure of glycoproteins, can stabilize the conformation of proteins and may influence the activity of the protein. Furthermore glycans are involved in protein-protein interactions and protein-cell communication. In biological samples, alterations in glycosylation are typical biomarkers of many diseases such as diabetes,[1,2] rheumatoid arthritis,[3] inflammatory bowel diseases,[4] or metastatic breast cancer.[5]

Additionally, from a therapeutic viewpoint protein glycosylation is important as it influences the function and efficacy of biopharmaceutical medicines.[6,7] For example, both secretion and efficacy of recombinant Erythropoietin (rhEPO) are largely dependent on glycosylation in general.[8] More specifically, half-life of circulating erythropoietin in the blood and in vivo bioactivity are affected by sialylation of the various glycans. [9,10] Erythropoietin is a glycosylated hormone that is produced in the kidneys and liver and regulates red blood cell (erythrocyte) production. Microheterogeneity of rhEPO products mainly originates from glycosylation variants at the three N-linked glycosylation and one O-linked glycosylation sites of the molecule. Glycosylation of rhEPO is one of the Critical Quality Attributes (CQA's) and many different analytical methods exist to characterize the glycans.[11,12]

Current analytical methods mainly study protein glycosylation based on detached glycans, requiring extensive sample preparation for release and labeling of the glycans followed by chromatographic or electrophoretic separation.[13,14] Other methods are based on mass spectrometric measurements and also require several sample preparation steps. [15-17] In the past decade glycan analysis, or glycoprofiling, has advanced to study intact glycoproteins by affinity-based methods. The majority of these affinity-based methods use lectins as ligands towards carbohydrates. Lectins are naturally occurring carbohydrate-binding proteins that are able to non-covalently bind sugars in a highly specific manner.[18]

Lectin-arrays are able to screen glycosylation profiles and detect differences in these profiles. A recent review by Hirabayashi et al.[19] emphasizes the opportunities for lectin microarrays in glycan analysis. Although current lectin microarrays have eliminated the time-consuming glycan release, fluorescent protein labeling reactions are still required in lectin arrays as described by Hsu et al.,[20] Tao et al.,[21] Wang et al., [22] Kuno et al., [23] Pilobello et al.,[24] Chen et al.,[25] and Rosenfeld et al.[26]

Label-free methods such as quartz crystal microbalance (QCM) or surface plasmon resonance (SPR) have been used to study carbohydrate-lectin interactions in real-time. The drawbacks of these methods include monitoring a limited number of lectin-carbohydrate interactions simultaneously[27,28] or using indirect coupling of lectins.[29] Karamanska et al.[30] have established a multiplex carbohydrate assay in order to analyze lectins, but glycan profiling of glycoproteins is not possible on such a microarray because the carbohydrates are immobilized.

We have developed a method that studies lectin-carbohydrate interactions on intact glycoproteins in a rapid, high-throughput, multiplex and label-free manner by surface plasmon resonance imaging. We are able to immobilize unmodified lectins on a sensor in multiplex format while they retain their active carbohydrate binding site. Lectin-glycoprotein interactions are measured without labeling glycoproteins before analysis. We examined the lectins on the array for the specific recognition of glycans and determined affinities / avidities of the selected lectins by means of neoglycoprotein analysis. Furthermore we used the lectin array to measure glycosylation fingerprints of differentially glycosylated proteins, such as enzymatically remodeled proteins and different sources of recombinant erythropoietin (rhEPO).

The method further demonstrated that sialylation of rhEPO could be accurately quantified. Relative quantitation of sialylation on rhEPO samples was performed with the lectin micro-array, based on the binding to *erythrina cristagalli* lectin (ECL) and Soybean agglutinin (SBA) lectins.

Materials and methods

Surface plasmon resonance method

Lectin – glycoprotein interactions were measured on an IBIS MX96 surface plasmon resonance (SPR) instrument (IBIS Technologies, Enschede, the Netherlands). Running buffer consisted of HEPES buffered saline (HBS; 20 mM HEPES and 150 mM NaCl) pH 7.2 with 0.05 wt/vol % Tween80 and 1 mM $ZnCl_2$, 1 mM $CaCl_2$, 1 mM $MnCl_2$ and 1 mM $MgCl_2$ added. After a baseline of 2 minutes, association times of 10 to 20 minutes and dissociation times of 5 to 20 minutes were programmed. These were followed by a regeneration of 1 minute in 2 steps and a wash step of 1 minute. Regeneration was performed with either 3M $MgCl_2$ or 25 mM phosphoric acid. Analyses were performed at 25°C and samples were also kept at 25°C. Samples were analyzed in duplicate or triplicate on sensor surfaces with at

least three independent spots of each lectin. All samples were buffer exchanged by 10 kD spin filters to running buffer or directly diluted in running buffer. All chemicals were of analytical grade and purchased from Sigma-Aldrich (Zwijndrecht, The Netherlands) or Merck (Darmstadt, Germany).

Lectin immobilization

Immobilization of lectins on a SensEye G-COOH (IBIS Technologies, Enschede, The Netherlands) was performed in 50 mM sodium formate or sodium acetate buffers pH 3.0, pH 3.5, pH 4.0 or pH 4.5 containing 0.05 wt/vol % Tween80. Lectins Con A and PA-I were purchased from Sigma-Aldrich (Zwijndrecht, The Netherlands) and all other lectins were purchased from Vector Laboratories (Burlingame CA, USA). Lectins were immobilized in series of 4 or 5 dilutions ranging from 0.01 – 1 µM. A continuous flow microspotter (CFM) (Wasatch microfluidics, Salt lake City, Utah, USA) was used to array the lectins on the sensor. Printing with the CFM was set up with a flow time of 15 minutes and a post-print rinse of 2 minutes. No pre-print buffer prime was used and an air gap of 25 µL was programmed. Printing was performed with the 4x12 printhead or with the 6x8 printhead. In a double print set-up, a printing time of 5 minutes was used in two sequential prints, resulting in 96 spots on the sensor. Before lectin printing the G-COOH sensors were activated with EDC/NHS activation in MES pH 5.4 buffer according to the manufacturer's protocol. Sensor surfaces were deactivated with 1M ethanolamine pH 8.5 after immobilization of the lectins according to the manufacturer's protocol.

Kinetic analysis of neoglycoproteins

Affinity measurements of lectins were performed with neoglycoproteins. Fucose-BSA, Mannose-BSA and Galactose-BSA (GlycoDiag, Orleans, France), N-acetyllactosamine-BSA (Dextra, Reading, U.K.), N-acetylglucosamine-BSA and Sialic acid-BSA (Vector laboratories, Burlingame) were the neoglycoproteins of choice. A kinetic titration set-up was used, in which thirteen dilutions from 0.5 nM to 2 µM (0.45 - 0.9 - 1.9 - 3.9 - 7.8 - 15.6 - 31.3 - 62.5 – 125 – 250 – 500 – 1000 - 2000 nM) of the neoglycoproteins were injected without regeneration between the injections. An association time of 5 minutes was followed by a dissociation time of 4 minutes. The sensor was regenerated with 25 mM phosphoric acid after an entire series of one neoglycoprotein for 0.5 minutes. Running buffer and temperature settings were as mentioned above. BSA was included as a control.

Data analysis was performed in Scrubber software (BioLogic, Campbell, Australia). A 1:1 binding model was used for curve fitting. A selection of the thirteen dilutions was made for each lectin-neoglycoprotein pair by selecting the lowest possible concentrations at which interaction was measured. KD, kd, ka and Rmax values were determined from 1:1 curve fitting models. At least three independent KD, kd or ka and Rmax values were calculated and plotted against each other. A KD, kd or ka at Rmax=100 RU was interpolated or extrapolated from a logarithmic curve for each combination to determine the affinity. No corrections for avidity effects have been made, as the same analyte was used for each lectin and the number of glycan moieties on the neoglycoproteins may vary and is an average.

Exoglycosidase treatments

Approximately 2.5 mg of fetuin was sequentially treated with exoglycosidases α-2-3,6,8,9-neuraminidase (12.5U), β-(1-4,6)-galactosidase (1U), β-N-acetylhexosaminidase (2U), α-mannosidase (0.5U) and β-mannosidase (0.5U). All exoglycosidases were purchased from Sigma-Aldrich (Zwijndrecht, The Netherlands) except β - (1-4,6)-galactosidase which was purchased from Prozyme (Hayward CA). Reaction volumes were 150-200 µL, and after each incubation step a fraction of the sample was removed. Remaining sample was buffer exchanged to the recommended buffer for each of the exoglycosidases with 10 kD cut-off filters. Sample concentrations were checked with Nanodrop after each buffer exchange.

Erythropoietin was desialylated with α-2-3,6,8,9-neuraminidase. Erythropoietin (100 µL of a 0.5 µg/µL solution) was incubated with 10 µL of α-2-3,6,8,9-neuraminidase (5U) at 37°C for 24 hrs. Sample was buffer exchanged to running buffer with 10 kD cut-off filters and concentration was determined with Nanodrop. The five rhEPO brands were a kind gift of Prof. H. Schellekens from University Utrecht, the Netherlands.

N-UHPLC analysis of 2-AB labeled glycans

Native and remodeled glycoproteins were deglycosylated and labeled with 2-AB label using the AssayMAP® GlykoPrep kit, according to standard procedure. After clean-up of labeled glycans they were separated on a Shimadzu Nexera UHPLC system (Kyoto, Japan) using a gradient with 100 mM ammonium formate pH 4.4 and acetonitrile as mobile phases on an Acquity UPLC BEH Glycan column (2.1 x 150 mm, dp 1.7 µm) from Waters (Milford, USA). Gradient separation was performed with 26% to 33.5% mobile phase B in the first 30

minutes, at a flow rate of 0.6 mL/min. Over the next 30 minutes the percentage of mobile phase B was increased to 36%, followed by a wash step to 100% B in 2 minutes with a flow rate of 0.25 mL/min and kept there for 1 minute. The gradient was changed to initial conditions in 1 minute after which the flow rate was increased to 0.6 mL/min and kept there for 5 minutes to condition for the next injection. Column temperature was set to 60°C and fluorescence was measured at 425 nm after excitation at 360 nm.

Quantitation of sialylation

Untreated and desialylated EPO (Calbiochem, Merck Millipore (Darmstadt, Germany)) were diluted to 7 µg/mL (200 nM) in running buffer. Sialylation levels of these standards were set to 100% and 0% respectively. Calibration standards at 50%, 60%, 70%, 80%, 90% and 100% sialylation were made by mixing the two standards. Binding to four independent spots of both SBA and ECL lectins was measured as the response in RU after 10 minutes association time and plotted against the theoretical sialylation level. Quadratic curve fitting was applied to the individual calibration curves. Unknown samples were interpolated from the calibration curve to determine sialylation levels.

HSA depletion of biosimilar EPO

HSA depletion of some Erythropoietin batches (Brand A, B and C) was performed using an HSA and IgG depletion kit (GE healthcare, Uppsala). Spin traps were equilibrated three times with HBS buffer and centrifugated at 800 g for 30 seconds. EPO samples were diluted 1:1 in HBS buffer and applied to the spin traps in fractions of 3 times 100 µL followed by a 5 minutes incubation step and centrifugation at 800 g for 30 seconds. Then up to 5 times 100 µL HBS was added to the spin traps for elution and centrifugated at 800 g for 30 seconds. All flow-through and elution fractions were collected separately and subjected to SDS-PAGE for purity analysis. None of the fractions contained HSA anymore so all fractions were pooled for a HSA-depleted EPO sample.

Deglycosylation of glycoproteins

Fetuin was deglycosylated in a native state with protein deglycosylation mix (New England Biolabs) with 30 µL of a 5 mg/mL fetuin solution, 5 µL 10X reaction buffer and 15 µL enzyme cocktail. Sample was incubated at 37°C for 6 hrs. Other proteins were deglycosylated with PNGase F. Mixtures containing 500 µg of glycoprotein (2 to 5 mg/mL) and 15 µL PNGase F enzyme were incubated at 37°C for 6 hrs. Full deglycosylation of the

samples was checked by CE-SDS analysis on a PA800 plus instrument (Beckman-Coulter, Brea California, USA). Samples were analyzed using the SDS molecular weight kit (Beckman-Coulter) in the default CE-SDS method according to supplier after incubation with SDS sample buffer for 5 minutes at 73°C.

Results and discussion

Immobilization and activity of lectins

A panel of lectins displaying recognition towards glycan epitopes on mammalian glycoproteins was selected based on their specificity indicated by the supplier (Table 4.1). Lectins were immobilized after optimization of the immobilization pH (Table 4.1) and ligand densities. A sensor with eighteen different lectins in five dilutions including six reference spots (blanks) was successfully applied using two sequential 48 spot prints, enabling monitoring of glycan binding to eighteen different lectins on a total of 96 spots simultaneously. The number of lectins to be studied can even be extended further using fewer dilutions or replicates per lectin.

Glycan-binding domains of the lectins could become inaccessible for interaction analysis when lectins are immobilized, especially when the binding site is positioned next to the reactive primary amine with which the lectin will be immobilized with EDC/NHS coupling. Activity of the lectins after covalent coupling to the sensor surface was checked using glycoproteins; Transferrin (Appendix A, Figure 4.A.1), Fetuin and RNAse B (data not shown) were checked for dose-dependent responses. Dose-dependency of glycoproteins was measured on each of the lectins, indicating that lectins can be immobilized using EDC/NHS coupling chemistry on carboxyl sensors without loss of the carbohydrate-binding function.

Specificity and apparent affinity determination by neoglycoproteins

Although the specific binding of certain monosaccharides or glycan epitopes by lectins is known, this specificity is not always consistent between different publications[18,19,23-25,31,32] and the specificity indicated by the supplier. To verify the specificity of the selected lectins, we examined neoglycoproteins as model compounds after immobilization of the lectins. After that, we used the SPR to determine apparent affinities for each lectin-neoglycoprotein pair. Neoglycoproteins are chemically glycosylated bovine serum albumin (BSA) proteins carrying 20-30 homogeneous glycan residues per molecule. Neoglycoproteins

modified with sialic acid, galactose, N-acetylglucosamine (GlcNAC), N-acetyllactosamine (LacNAc), mannose or fucose residues were chosen to determine apparent affinity and specificity of the immobilized lectins.

Table 4.1 *Lectins selected for immobilization, pI value, immobilization pH and their reported and determined specificity*

abbre-viation	lectin name	pI	immobili-zation pH	primary specificity [I]	others epitopes	binding in our study [II]
AAL	Aleuria aurantia lectin	9.0	4.5	Fuc	-	Fuc
LTA	Lotus tetragonolobus agglutinin	7.3 - 8.2	4.5	Fuc	-	Fuc
UEA	Ulex europaeus agglutinin	4.5 - 5.1	4.0	Fuc	-	Fuc
Con A	Concanavalin A	4.5 - 5.5	4.5	Man	Glu	Man
GNL	Galanthus nivalis lectin	3.5 - 4.0	3.5	Man	-	Man
HHL	Hippeastrum hybrid lectin	4.7 - 5.1	3.0	Man	-	*Man*
LCA	Lens culinaris agglutinin	7.6 - 8.4	4.5	Man	Glu, Fuc	Man
NPA	Narcissus pseudonarcissus agglutinin	4.2 - 4.6	3.5	Man	-	*Man*
PSA	Pisum sativum agglutinin	6.0 - 6.7	4.5	Man	Glu	Man
GSL II	Griffonia (Bandeiraa) simplicifolia lectin II	5.0 - 6.0	4.5	GlcNAc	-	GlcNAc, Man
WGA	Wheat germ agglutinin	> 9.0	4.5	GlcNAc	SA	GlcNAc (also LacNAc was bound via GlcNAc)
SBA	Soybean agglutinin	5.8 - 6.0	4.5	GalNAc	Gal	Gal (also LacNAc was bound via Gal)
PA-I	Pseudomonas aeruginosa lectin	- [III]	- [III]	Gal	-	*n.d.*
RCA I	Ricinus communis agglutinin	7.8	4.5	Gal	-	Gal, LacNAc, Man, Fuc
Ricin B	Ricinus communis agglutinin B chain	4.5	4.0	Gal	-	*n.d.*
ECL	Erythrina cristagalli lectin	6.3 - 6.5	4.5	LacNAc	-	Gal, LacNAc
MAL I	Maackia amurensis lectin I	4.7	4.0	LacNAc	-	LacNAc
ACL	Amaranthus caudatus lectin	6.7 - 7.7	4.5	Gal-GalNAc	SA	SA

Table 4.1 *continued*

abbre-viation	lectin name	pI	immobili-zation pH	primary specificity [I]	others epitopes	binding in our study [II]
MAL II	Maackia amurensis lectin II	4.7	4.0	SA (– gal – GalNAc)	-	SA, LacNAc
SNA	Sambucus nigra agglutinin	5.4 - 5.8	4.5	SA (– gal)	-	All tested glycan moieties
PHA-E	Phaseolus vulgaris Erythroagglutinin	6.0 - 8.0	4.5	LacNAc-man	-	SA, Gal, Man
PHA-L	Phaseolus vulgaris Leucoagglutinin	4.2 - 4.8	3.5	LacNAc-man in triantennary structures	-	*no binding with neoglycoproteins*

[I]Primary specificity according to suppliers' information (www.vectorlabs.com/data/brochure/VectorCatalogue2012.pdf) and Sigma-Aldrich website, and according to CFG website (www.functionalglycomics.org). Fuc: fucose; Man: mannose; Glu: glucsose; Gal: galactose; GlcNAc: N-acetylglucosamine; GalNAc: N-acetylgalactosamine; LacNAc: N-acetyllactosamine; SA: sialic acid

[II] n.d.: not determined

[III] No pI of PA-I lectin was specified by the supplier (Sigma-Aldrich); lectin was not immobilized in any of the tested buffers

We used a 20-plex lectin microarray with lectins in two dilutions to measure neoglycoprotein binding and apparent affinity or avidity. Neoglycoproteins were injected between 0.5 nM and 2 µM in a kinetic titration.[33] Apparent affinity, association rates and dissociation rates of each lectin-neoglycoprotein combination was determined by curve fitting with a 1:1 binding model and determination of lectin specificity was derived from the apparent affinity values (Figure 4.1-a) and compared to the indicated specificities.[23,24,31] At least three independent curve fittings were applied to each lectin-neoglycoprotein pair, from which K_D and Rmax values were determined.

Residual plots were visually checked for correct distribution of residuals (Figure 4.1-a). Apparent affinities at Rmax=100 RU were interpolated or extrapolated from plotting the individual K_D and Rmax determinations (Figure 4.1-b). The same interpolation or extrapolation was performed for association and dissociation rates (Appendix B, Figure 4.B.1 and Figure 4.B.2 respectively).

Many lectins have a highly defined primary specificity and our results are in accordance with the supplier's specificity. However, on a number of lectins also cross-reactivity with non-target neoglycoproteins was measured at lower apparent affinities. Apparent affinities

of the specific binders are in general in the low nM range (Figure 4.1-b). However, since the neoglycoproteins carry 20-30 glycan residues per molecule, the reported affinities reflect mostly the avidity of the interaction. The fucose-binding lectins AAL, LTA and UEA are all very specific and bind to fucose-BSA with high apparent affinity (1-10 nM). Only LTA shows cross-reactivity towards unmodified BSA with an apparent affinity around 200 nM. Also the mannose-binding lectins (Con A, GNL, HHL, LCA, NPA and PSA) are all very specific towards mannose, as no cross-reactivity could be measured. Con A has the highest apparent affinity of these lectins, at approximately 16 nM, while the other lectins bind mannose-BSA at apparent affinities between 66 and 230 nM. Specifity for GlcNAc-binding lectins WGA and GSL II can also be confirmed with these data, showing that WGA is the stronger binder of the two with an apparent affinity close to 2 nM. WGA also has a strong apparent affinity towards LacNAc-BSA (9 nM), which may be explained by the GlcNAc residue that is part of this LacNAc structure. Cross-reactivity of mannose-BSA was measured on GSL II, indicating that WGA is the favourable lectin for measuring GlcNAc binding based on stronger apparent affinity and no cross-reactivity. In addition to confirmation of lectin specificity (Table 4.1), many neoglycoproteins bound to RCA I and SNA. RCA I binds galactose-BSA and LacNAc-BSA with highest apparent affinities (1 nM) but cross-reactivity of unmodified BSA (10 nM), mannose-BSA and fucose-BSA (both 100 nM) was found. SNA lectin, selected for its sialic acid binding properties, is the least specific lectin of all lectins tested on our array. All of the analytes, including the BSA control, bind to SNA lectin at apparent affinities between 50 nM and 1 µM. The strongest binding is measured for non-modified BSA, while the binding of sialic acid is much weaker compared to unmodified BSA and apparent affinities of fucose-BSA and LacNAc-BSA.

SBA seems to be the lectin of choice for monitoring galactose-binding, with an apparent affinity of approximately 20 nM and only cross-reactivity towards LacNAc which contains a galactose residue in its structure. Lectins that were selected for their specific binding towards LacNAc (ECL and MAL I) are quite specific, but have rather low apparent affinities (30 –100 nM). ECL binds galactose-BSA at similar apparent affinity compared to LacNAc-BSA, which indicates that ECL does not only recognize the LacNAc moiety, but is able to bind a single galactose as well. ACL is the most specific lectin towards sialic acid, of the lectins that were included in this study. Both ACL and MAL II have apparent affinities for sialic acid in the 5-10 nM range. However, MAL II cross-reacts with unmodified BSA and LacNAc-BSA. As already discussed previously, SNA is the least specific lectin and is not recommended to use for sialic acid binding.

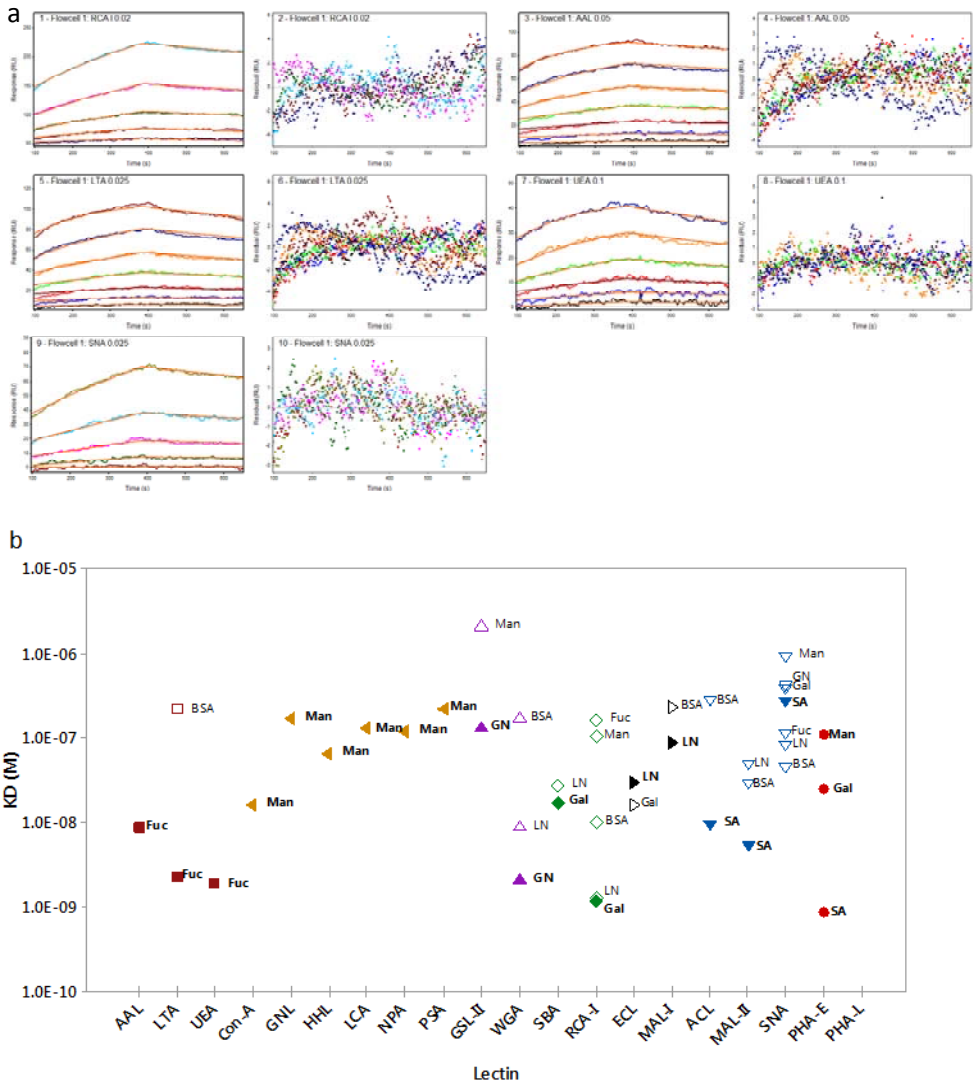

Figure 4.1 *Specificity measurements of 20 tested lectins. a) Sensorgrams from a kinetic titration of fucose-BSA binding to RCA I, AAL, LTA, UEA and SNA respectively including the results of 1:1 Langmuir model global fitting and the corresponding residuals for each global fit. The residuals indicate how closely the modeled curves match with the measured curves and should be randomly distributed over the time axis and over the various concentrations that are analyzed. b) Apparent affinity of neoglycoproteins at Rmax values of 100 RU after kinetic fitting are plotted for each lectin (n=4, measurements on two different arrayed sensors). Closed data points refer to specific binding, open data poins refer to cross-reactants. Data labels were added for clarity; Fuc: Fucose-BSA, Man: Mannose-BSA, GN: N-acetylglucosamine-BSA, LN: N-acetyllactosamine-BSA, Gal: Galactose-BSA, SA: Sialic acid-BSA, BSA: unmodified BSA.*

Furthermore PHA-E bound all neoglycoproteins, but we were only able to determine apparent affinities for sialic acid-BSA, galactose-BSA and mannose-BSA, which makes it non-specific for glycosylated BSA proteins (Figure 4.1-b). On the other hand, PHA-L bound none of the neoglycoproteins which may be explained by its specificity towards triantennary glycans carrying the gal-GlcNAc-man epitope. This epitope is not present at tested neoglycoproteins and therefore no binding could be measured with these models. All of the lectins that show specific binding do so in the nM range, which may be considered strong binding. Non-specific binding is generally not measured, and if measured it is in the µM range or the high nM range, which is relatively weak binding when compared to the specific binding.

Specificity determination by glycan remodeling

Specificity of the lectins was further investigated using enzymatically remodeled fetuin and transferrin. Both glycoproteins were sequentially treated with α -2-3,6,8,9-neuraminidase, β-(1-4,6)-galactosidase, β-N-acetylhexosaminidase and α-mannosidase to cleave the N-glycans (Figure 4.2). Fetuin also carries O-glycans that are cleaved off by exoglycosidases such as neuraminidase and β-N-acetylhexosaminidase. Full cleavage of monosaccharides by exoglycosidases was checked with N-UHPLC analysis after release and 2-AB labeling as a reference method (Appendix C, Figure 4.C.1). As a control, a fully deglycosylated sample was included in the analysis.

Remodeled fetuin (Appendix C, Figure 4.C.2) and transferrin (data not shown) were analyzed on the lectin microarray to measure differential binding related to the specificity of the lectins based on the exposed glycan moiety. Due to the complexity of the protein glycosylation compared to the neoglycoproteins, it was decided to only evaluate the specificity in a qualitative fashion by comparing binding intensities in equilibrium state. Overall the specificity measured with remodeled fetuin and transferrin confirmed the results of neoglycoprotein analysis and is in agreement with suppliers' information. Only for a minority of lectins we have found differences in lectin specificity. The deglycosylated control was used to determine background binding on each lectin as no specific glycan binding is expected in the fully deglycosylated samples. Signals of glycosylated samples that were at least three times the response level of the control sample were considered to be true glycan binding. We based this evaluation on the limit of detection qualification in the EMEA guidelines, where a signal-to-noise ratio of 3 is applied.[34]

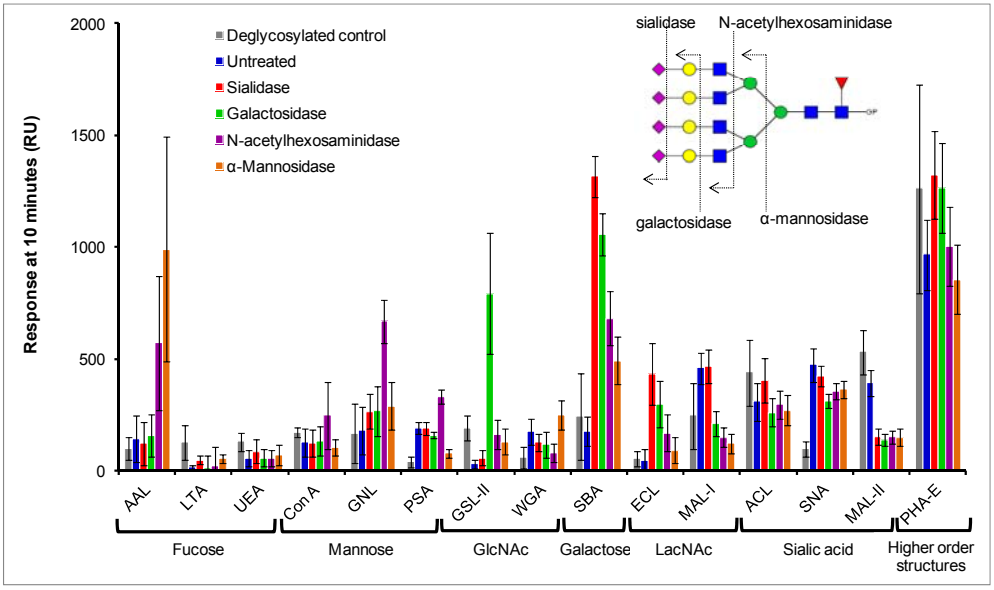

Figure 4.2 *Glycosylation fingerprints of remodeled fetuin samples expressed as SPR response units after 10 minutes association on fifteen different lectins. Treated samples (n=9) were analyzed three times on two different sensors containing triplicate spots of each lectin (n=6 on sensor 1, n=3 on sensor 2); the untreated sample (n=6) was analyzed once on two different sensor containing triplicate spots of each lectin (n=3 on sensor 1 and on sensor 2). The deglycosylated sample, where N- and O-glycans were removed, was analyzed on one sensor with triplicate spots of each lectin (n=3). The inset schematically shows the remodeling of a N-glycan.*

Clear elevated responses of sialidase-treated fetuin, exposing the galactose, were measured on SBA and ECL lectins (Figure 4.2). This binding decreased again in samples cleaved with galactosidase and N-acetylhexosaminidase which verifies its binding towards galactose and N-acetylgalactosamine. Signals did not decrease to zero because O-glycans of fetuin contain N-acetylgalactosamine which can also bind to SBA lectin. The binding measured after galactosidase treatment predominantly originates from N-acetylgalactosamine on O-glycans which are removed after N-acetylhexosaminidase treatment resulting in further decrease.

Increasing response on AAL lectin, a fucose-binder, was measured after N-acetylhexosaminidase and α-mannosidase treatment (Figure 4.2). Core fucose may be shielded or sterically hindered by sialic acids and galactoses on N-glycan structure and therefore may not be well recognized by AAL lectin. Upon exoglycosidase treatments the

glycan structure is reduced and the fucose residue may become more accessible for AAL to bind to.

Responses of fetuin after treatment with N-acetylhexosaminidase increased on mannose-specific lectins Con A, GNL and PSA lectins confirming mannose recognition as mannose becomes the terminal monosaccharide. A more pronounced increase in signal is measured with GNL and PSA lectins compared to Con A (Figure 4.2).

An increase in binding of fetuin on GSL II lectin was measured after treatment with galactosidase which decreased again after treatment with N-acetylhexosaminidase. These changes clearly verify the specificity towards GlcNAC. Specificity towards GlcNAC was assigned to WGA with neoglycoproteins (Figure 4.1-b), whereas in the remodeling experiments with fetuin hardly any binding to WGA was measured for the different treated samples (Figure 4.2). Possibly the cross-reaction of fetuin itself, demonstrated with deglycosylated fetuin (data not shown), prevents binding of exposed GlcNAc residues to WGA lectin.

Sialic acid binders ACL and SNA bound all variants of remodeled fetuin at similar levels compared to untreated, i.e. sialylated, fetuin and were not considered as sialic acid specific (Figure 4.2). In the neoglycoprotein experiments we already determined that SNA binds to all tested monosaccharides. On the other hand, MAL II lectin bound untreated, i.e. sialylated, fetuin at higher levels than the remodeled samples, although response of deglycosylated fetuin was comparable to sialylated fetuin again. Cross-reactivity of deglycosylated fetuin, where N- and O-glycans were enzymatically removed, was measured on each lectin. Certain lectins (e.g. PHA-E, MAL II) had a higher cross-reactivity towards deglycosylated protein than others. Potentially these lectins specifically bind to exposed glycan moieties, but are able to strongly cross-react with non-glycosylated fetuin, in absence of glycans, as well.

Binding of untreated and sialidase-treated fetuin, both of which display the LacNAc epitope, on MAL I lectin was measured whereas further cleaved samples displayed lower levels of binding (Figure 4.2). Upon cleavage with galactosidase, the LacNAc epitope is broken which caused the reduction in signals. Responses of fetuin samples after galactosidase treatment and further treatments were comparable to the response measured for deglycosylated fetuin and can thus be attributed to cross-reactivity of the protein.

Erythropoietin analysis with lectin micro-array

The developed lectin micro-array was validated on erythropoietin (rhEPO). Erythropoietin is a highly glycosylated protein. rhEPO N-glycosylation is mainly present as tri- and tetra-antennary glycans terminating with up to four sialic acids linked to the N-acetyllactosamine chains.[15,35] rhEPO O-glycosylation is of the mucin-type and carries up to two sialic acids connected to either galactose or N-acetylgalactosamine [15,35,36]. The relation between sialylation of rhEPO and its in vivo activity has been proven by Dubé et al.[8] and can therefore be an important critical quality attribute (CQA) of rhEPO therapeutics.

We measured five different brands of rhEPO and tested the lectin micro-array to discriminate between the batches based on a glycosylation fingerprint. Three of the batches contained HSA as a stabilizer, which caused a high background signal. The HSA was removed with a HSA depletion kit in less than 30 minutes (see materials and methods section). The glycosylation fingerprints of the five rhEPO batches were quite distinct from each other, especially on those lectins that bind to LacNAc (MAL I), sialic acid (ACL and MAL II) or higher order structures, i.e. tri- and tetra-antennary glycans (PHA-E) (Figure 4.3-a). None of the tested brands bound to fucose, mannose and N-acetylglucosamine specific lectins (not shown). rhEPO was desialylated in order to further characterize these differences. Binding of the sialylated (Figure 4.3-a) and desialylated (Figure 4.3-b) rhEPO batches to lectins specific towards terminating galactose and sialic acids indicates that there are differences in terms of glycosylation on these rhEPO batches. The rhEPO samples were all diluted to the same concentration in activity (IU/mL), since large differences in responses were measured when all brands were diluted to the same protein concentration in µg/mL.

Brands A and E have highly similar glycosylation fingerprints on the selected lectins. Sialylated samples of both brands only bind to MAL I and PHA-E lectins, whereas desialylated samples bind to SBA and ECL. Brand B has a different glycosylation fingerprint compared to the other four batches, especially with respect to binding to MAL I, SNA and PHA-E. It hardly binds to MAL I and PHA-E lectins and has the highest response on SNA lectin. However, desialylated brand B is highly comparable to the brands A, C and E, whereas brand D has a very distinct glycosylation fingerprint after desialylation. Binding to MAL II, SNA and MAL I remains only for batch D after desialylation. Although no complete identification of glycans on each of the batches can be performed with the current results, we can clearly demonstrate that the lectin sensor is capable of measuring differences between different rhEPO brands based on a glycan fingerprint. The relevance of these

differences should be demonstrated by comparison with an in vivo study. The method was further evaluated for relative quantitation of sialylation.

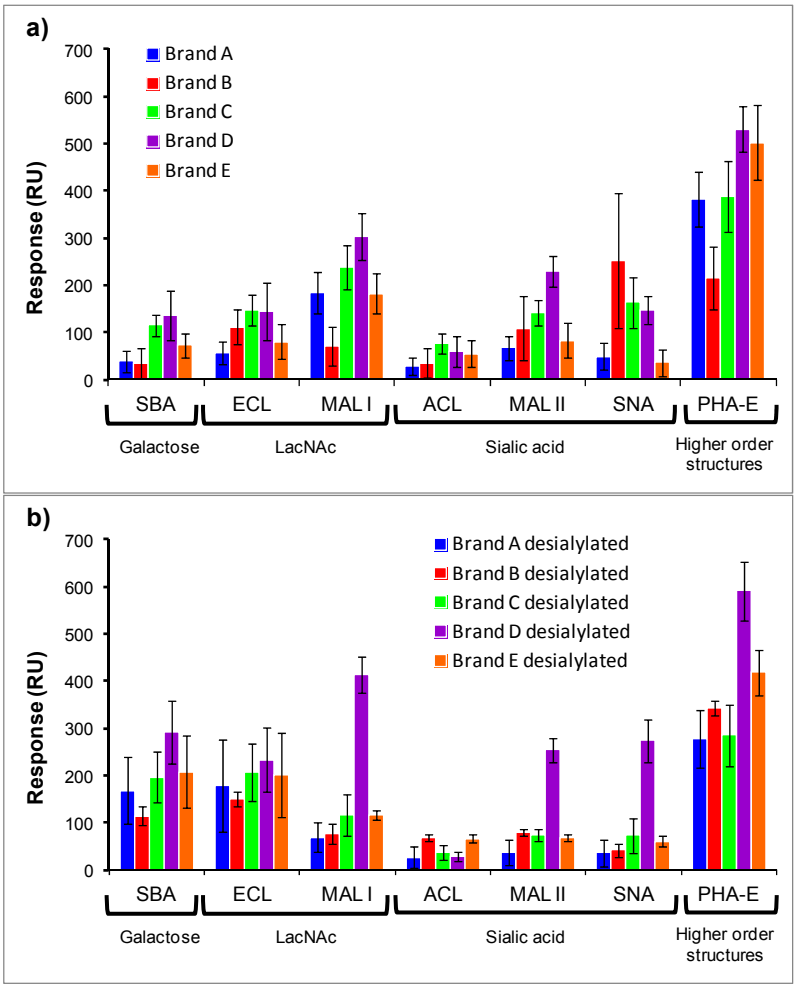

Figure 4.3 *Glycosylation fingerprints of five different EPO brands (1000 IU/mL) on a subset of lectins on the lectin micro-array of a) native EPO samples and b) desialylated EPO samples. Desialylated "Brand B" was analyzed at 733 IU/mL instead of 1000 IU/mL. Samples were analyzed on a sensor with three independent spots of each lectin and repeated on two days with independent sample dilutions (n=6).*

The quantitation was evaluated by comparing binding of desialylated rhEPO and untreated rhEPO to galactose-binding lectin SBA and LacNAc-binding lectin ECL, which both increased upon desialylation. Optimization of sample concentrations resulted in analysis of EPO

samples down to 1.4 µg/mL (Appendix D, Figure 4.D.1), which corresponds to a total EPO consumption of no more than 200 ng. At this concentration, both SBA and ECL lectin were still capable of measuring clear differences in untreated EPO and desialylated EPO. Higher sensitivity, i.e. larger differences in responses between desialylated EPO and untreated EPO, is obtained at higher sample concentrations and therefore 7 µg/mL was chosen for relative quantitation.

Table 4.2 *Relative quantification of EPO sialylation on SBA and ECL lectins* [a]

		SBA			ECL		
rhEPO sample	Theoretical % sialylation	avg % sialylation	%CV	Deviation (% sialylation)	avg % sialylation	%CV	Deviation (% sialylation)
1	66.7	70.0	1.1	3.3	70.1	3.2	3.4
2	98.3	97.0	0.8	-1.4	98.6	1.3	0.2
3	75.0	76.6	2.0	1.6	76.4	1.0	1.4
4	96.7	95.8	1.4	-0.9	96.7	1.3	0.0
5	88.7	88.3	0.8	-0.3	87.9	0.6	0.7

[a]EPO samples 1 to 5 are mixtures of untreated (100% sialylated) and sialidase-treated (0% sialylated) EPO to known relative sialylation levels.

Calibration standards from Calbiochem rhEPO at different sialylation levels were measured and responses at equilibrium were plotted against the theoretical sialylation level (Appendix D, Figure 4.D.2). We used a relative quantitation method to proof the quantitative capabilities of the lectin sensor. Next to the calibration standards, we prepared five samples by mixing untreated and desialylated rhEPO from the same brand in different ratios and determined the sialylation by interpolation of the calibration curves. Sialylation of five different rhEPO samples were accurately quantified (Table 4.2). Relative quantification on SBA lectin resulted in no more than 3.3% deviation between determined and theoretical level of sialylation, with a %CV of 2.0% or less on an average of four independent lectin spots. Slightly higher deviations between determined and theoretical level of sialylation were detected on ECL lectin, with a maximum deviation of 3.4%. Variation on ECL lectin was 3.2% CV or lower on an average of four independent lectin spots.

Conclusions

The broad diversity and general occurrence of glycans as post-translational modification on proteins requires rapid and sensitive methods to profile and monitor glycosylation. We demonstrated that surface plasmon resonance imaging can be employed to study lectin-carbohydrate interactions in a multiplexed manner. Glycan fingerprints are measured in a high-throughput set-up as up to 96 lectin-carbohydrate interactions are measured simultaneously generating a glycoprofile which can be used for comparative purposes. Screening of up to seventy samples can be performed within one day as each analysis only takes up to 20 minutes. Intact glycoproteins can be analyzed after diluting into the corresponding system buffer without any laborious sample pre-treatment steps. In case of the rhEPO analyses, we needed to remove HSA which is added as a stabilizer in certain rhEPO brands. The depletion step that we applied took less than 30 minutes. Multiple samples can be depleted simultaneously and are directly buffer exchanged to running buffer. Lectins can be directly immobilized on the SPR sensor while maintaining their carbohydrate-recognition properties. Different glycosylation patterns on a panel of fifteen lectins were measured for distinctly glycosylated proteins which could be related to the expected glycans. Glycan alterations on the proteins, deliberately applied by exoglycosidase cleavages, were effectively detected by the created lectin microarray. Binding to the lectins was enhanced or decreased after sequential cleavage of the glycan structure and was in accordance with the specificity of the lectins. Specificity of the lectins on the microarray was checked by neoglycoprotein analysis in this study and verified the reported specificities for nearly all studied lectins. Affinities of the lectins binding to defined carbohydrates on neoglycoproteins could easily be determined with the multiplex SPR method. We used these affinities to verify the specificity of the lectins and determine the strong and weak binders. Few lectins bound all neoglycoproteins or remodeled proteins regardless of the exposed glycan epitope and were considered rather non-specific. In many cases of high cross-reactivity also binding of non-glycosylated proteins was measured and these lectins were no further included on our array.

The presented method is able to measure lectin-carbohydrate interactions in real-time and label-free. The method has no prerequisites for labeling as SPR measures differences in refractive index at a sensor surface; both ligand and analyte can be successfully analyzed in their native state. Furthermore it is a true multiplex method since 96 interactions are studied simultaneously on a single sensor with sufficient possibilities to apply negative, positive

controls and controls for normalization of the responses, whereas in other SPR-based methods the number of different ligands is limited.

The power of the method was further proven by relative quantitation of EPO sialylation. We optimized measurements on two lectins specific towards galactose to quantify sialylation levels on EPO. Relative EPO sialylation can be accurately determined at levels between 50% and 100% with the developed lectin micro-array, consuming only 700 ng of EPO for a single measurement. The deviation between actual and measured sialylation levels is no more than 3.4%. Furthermore, a %CV of 3.2 or less was measured based on four independent lectin spots. Different brands of EPO were analyzed on the lectin micro-array and distinct glycosylation fingerprints were obtained. Especially large differences in both N- and O-sialylation were measured for the different batches. The relevance of these differences should be proven with in vivo data, which is currently on-going.

The combination of label-free, multiplex and real-time measurements opens up new prospects for rapid glycosylation fingerprinting. The lectin micro-array has many advantages over existing glycoprofiling methods, such as the ability to measure intact glycoproteins, the low sample consumption, the high accuracy, sensitivity and the possibility to quantitatively determine specific glycan moieties.

Acknowledgements

We thank EFRO Province of Gelderland and Overijssel, the Netherlands for giving us the opportunity to financially support the research project. We would like to thank J. Brouwer for most of the experiments with Erythropoietin.

Appendix A Transferrin analysis on lectin sensor

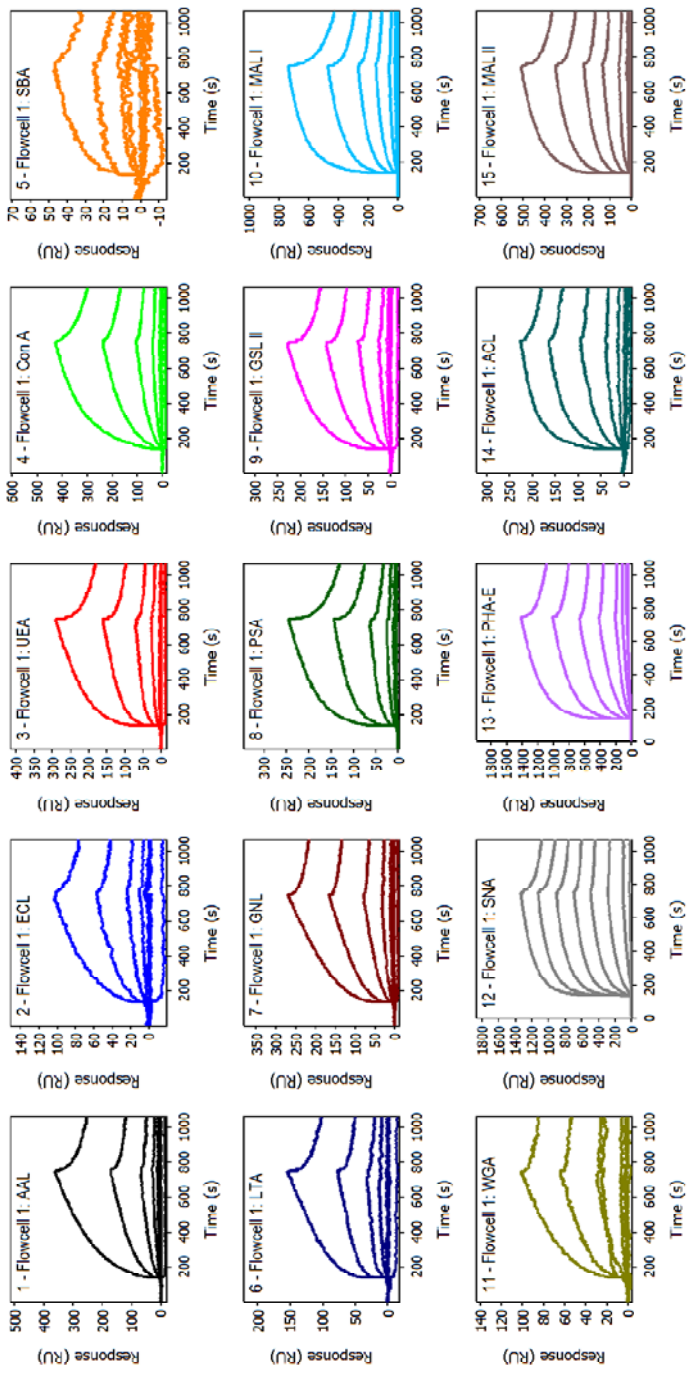

Figure 4.A.1 *Dose dependent binding of transferrin (concentrations 0.45 to 1000 µg/mL) on fifteen different immobilized lectins. Eight dilutions of transferrin on each of the lectin spots are shown. Dose dependency is proven as increasing transferrin concentrations result in higher intensity sensorgrams. Note that Y-axis of each sensorgram is different by scaling to the highest intensity signal*

Appendix B Kinetic data of neoglycoproteins

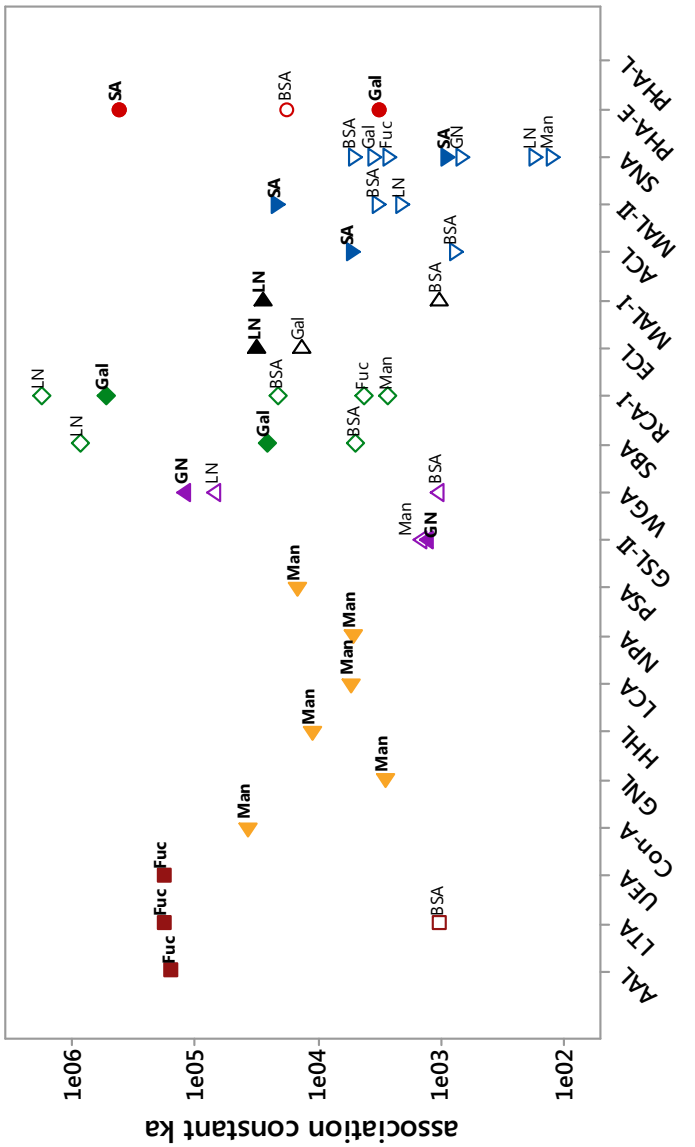

Figure 4.B.1 *Association constants of neoglycoproteins at Rmax values of 100 RU after kinetic fitting are plotted for each lectin (n=4, measurements on two different arrayed sensors). Closed data points refer to specific binding, open data poins refer to cross-reactants. Data labels were added for clarity; Fuc: Fucose-BSA, Man: Mannose-BSA, GN: N-acetylglucosamine-BSA, LN: N-acetyllactosamine-BSA, Gal: Galactose-BSA, SA: Sialic acid-BSA, BSA: unmodified BSA.*

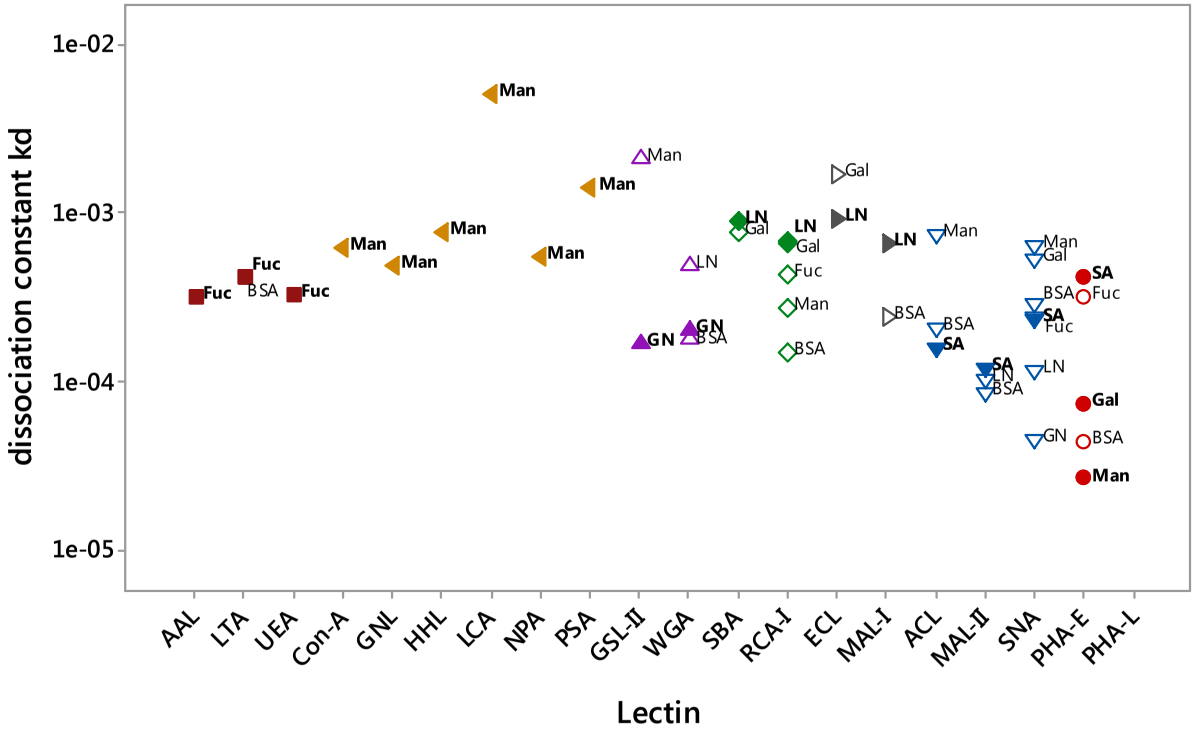

Figure 4.B.2 *Dissociation constants of neoglycoproteins at Rmax values of 100 RU after kinetic fitting are plotted for each lectin (n=4, measurements on two different arrayed sensors). Closed data points refer to specific binding, open data poins refer to cross-reactants. Data labels were added for clarity; Fuc: Fucose-BSA, Man: Mannose-BSA, GN: N-acetylglucosamine-BSA, LN: N-acetyllactosamine-BSA, Gal: Galactose-BSA, SA: Sialic acid-BSA, BSA: unmodified BSA.*

Appendix C Analysis of remodeled glycoproteins

Figure 4.C.1 *Analysis of remodeled fetuin glycoprotein. N-UHPLC chromatograms of untreated and treated fetuin samples to check full monosaccharide cleavage. Glycans elute off the column from smaller to larger; peaks at the end of the chromatograms represent higher glycan structures (e.g. sialylated glycans, tri- and tetra-antennary) than the ones in the front starting from core structure eluting around 4 minutes.*

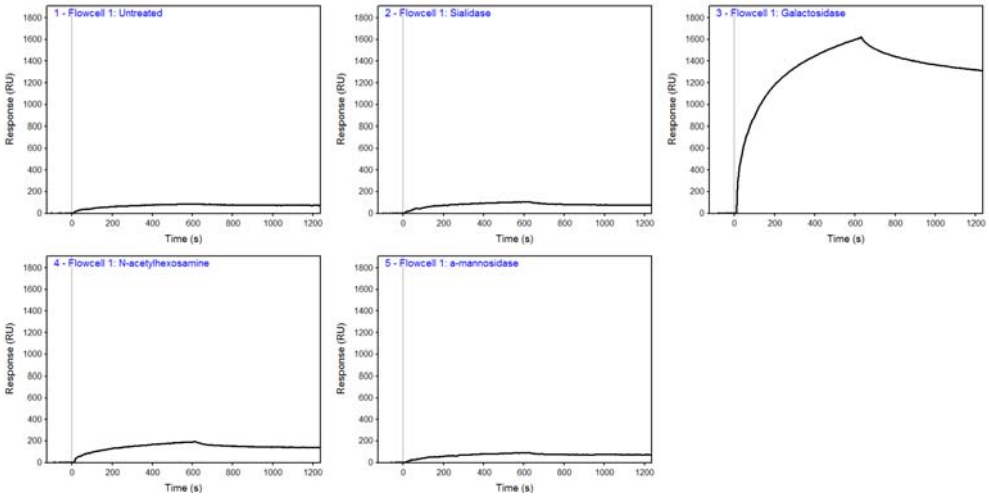

Figure 4.C.2 *Sensorgrams of fetuin samples (125 µg/mL) in the different steps of the remodeling expressed as binding on GSL II lectin immobilized at 0.56 µM.*

Appendix D EPO analysis on SBA and ECL lectins

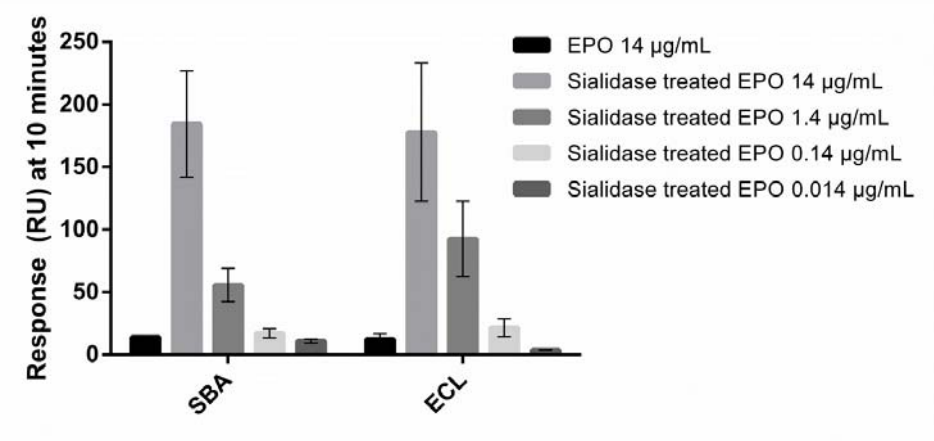

Figure 4.D.1 *Discriminatory power of the lectins SBA and ECL between untreated and sialidase-treated EPO at different concentrations (n=3). Concentrations down to 1.4 µg/mL can be used to measure differences in sialylation.*

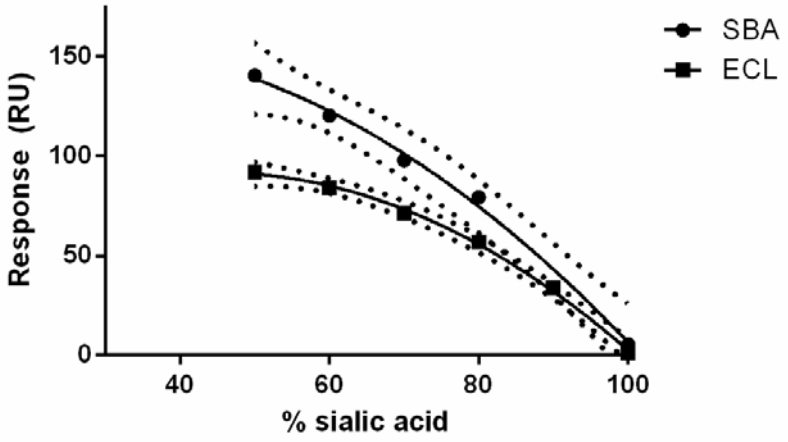

Figure 4.D.2 *Calibration curves of the response in RU after 10 minutes association plotted against the level of sialylation using quadratic curve fitting measured on (a) SBA lectin and (b) ECL lectin. EPO measurements at 7 µg/mL with sialylation levels between 50 and 100%. Measurements were performed at four individual spots of both SBA and ECL lectin; calibration curves of a single lectin spot is shown. R2 on SBA lectin was between 0.990 and 0.996; R2 on ECL lectin was between 0.990 and 0.998 on the independent calibration curves.*

References

1. Katahira, M., Hanakita, M., Ito, T., and Suzuki, M. The ratio of glycosylated albumin to glycosylated hemoglobin differs between type 2 diabetic patients with low normoalbuminuria and those with high normoalbuminuria or microalbuminuria. Diabetes Care 2013; 36(12): e207-e208
2. Bunn, H. F., Gabbay, K. H., and Gallop, P. M. The glycosylation of hemoglobin: relevance to diabetes mellitus. Science 7-4-1978; 200(4337): 21-27
3. Bertok, T., Klukova, L., Sediva, A., Kasak, P., Semak, V., Micusik, M., Omastova, M., Chovanova, L., Vlcek, M., Imrich, R., Vikartovska, A., and Tkac, J. Ultrasensitive impedimetric lectin biosensors with efficient antifouling properties applied in glycoprofiling of human serum samples. Anal.Chem. 6-8-2013; 85(15): 7324-7332
4. Shinzaki, S., Kuroki, E., Iijima, H., Tatsunaka, N., Ishii, M., Fujii, H., Kamada, Y., Kobayashi, T., Shibukawa, N., Inoue, T., Tsujii, M., Takeishi, S., Mizushima, T., Ogata, A., Naka, T., Plevy, S. E., Takehara, T., and Miyoshi, E. Lectin-based immunoassay for aberrant IgG glycosylation as the biomarker for Crohn's disease. Inflamm.Bowel.Dis. 2013; 19(2): 321-331
5. Fry, S. A., Afrough, B., Lomax-Browne, H. J., Timms, J. F., Velentzis, L. S., and Leathem, A. J. Lectin microarray profiling of metastatic breast cancers. Glycobiology 2011; 21(8): 1060-1070
6. Raju, T. S. Terminal sugars of Fc glycans influence antibody effector functions of IgGs. Curr.Opin.Immunol. 2008; 20(4): 471-478
7. Arnold, J. N., Wormald, M. R., Sim, R. B., Rudd, P. M., and Dwek, R. A. The impact of glycosylation on the biological function and structure of human immunoglobulins. Annu.Rev.Immunol. 2007; 25 21-50
8. Dube, S., Fisher, J. W., and Powell, J. S. Glycosylation at specific sites of erythropoietin is essential for biosynthesis, secretion, and biological function. J.Biol.Chem. 25-11-1988; 263(33): 17516-17521
9. Egrie, J. C. and Browne, J. K. Development and characterization of novel erythropoiesis stimulating protein (NESP). Br.J.Cancer 2001; 84 Suppl 1 3-10
10. Elliott, S., Egrie, J., Browne, J., Lorenzini, T., Busse, L., Rogers, N., and Ponting, I. Control of rHuEPO biological activity: the role of carbohydrate. Exp.Hematol. 2004; 32(12): 1146-1155
11. Schriebl, K., Trummer, E., Lattenmayer, C., Weik, R., Kunert, R., Muller, D., Katinger, H., and Vorauer-Uhl, K. Biochemical characterization of rhEpo-Fc fusion protein expressed in CHO cells. Protein Expr.Purif. 2006; 49(2): 265-275
12. Harazono, A., Hashii, N., Kuribayashi, R., Nakazawa, S., and Kawasaki, N. Mass spectrometric glycoform profiling of the innovator and biosimilar erythropoietin and darbepoetin by LC/ESI-MS. J.Pharm.Biomed.Anal. 2013; 83 65-74
13. Skibeli, V., Nissen-Lie, G., and Torjesen, P. Sugar profiling proves that human serum erythropoietin differs from recombinant human erythropoietin. Blood 15-12-2001; 98(13): 3626-3634
14. Le, Floch F., Tessier, B., Chenuet, S., Guillaume, J. M., Cans, P., Marc, A., and Goergen, J. L. HPCE monitoring of the N-glycosylation pattern and sialylation of murine erythropoietin produced by CHO cells in batch processes. Biotechnol.Prog. 2004; 20(3): 864-871
15. Jiang, J., Tian, F., Cai, Y., Qian, X., Costello, C. E., and Ying, W. Site-specific qualitative and quantitative analysis of the N- and O-glycoforms in recombinant human erythropoietin. Anal.Bioanal.Chem. 31-7-2014;-
16. Kawasaki, N., Ohta, M., Hyuga, S., Hyuga, M., and Hayakawa, T. Application of liquid chromatography/mass spectrometry and liquid chromatography with tandem mass spectrometry

to the analysis of the site-specific carbohydrate heterogeneity in erythropoietin. Anal.Biochem. 1-10-2000; 285(1): 82-91

17. Hashii, N., Harazono, A., Kuribayashi, R., Takakura, D., and Kawasaki, N. Characterization of N-glycan heterogeneities of erythropoietin products by liquid chromatography/mass spectrometry and multivariate analysis. Rapid Commun.Mass Spectrom. 30-4-2014; 28(8): 921-932

18. Ambrosi, M., Cameron, N. R., and Davis, B. G. Lectins: tools for the molecular understanding of the glycocode. Org.Biomol.Chem. 7-5-2005; 3(9): 1593-1608

19. Hirabayashi, J., Yamada, M., Kuno, A., and Tateno, H. Lectin microarrays: concept, principle and applications. Chem.Soc.Rev. 29-4-2013; 42(10): 4443-4458

20. Hsu, K. L., Pilobello, K. T., and Mahal, L. K. Analyzing the dynamic bacterial glycome with a lectin microarray approach. Nat.Chem.Biol. 2006; 2(3): 153-157

21. Tao, S. C., Li, Y., Zhou, J., Qian, J., Schnaar, R. L., Zhang, Y., Goldstein, I. J., Zhu, H., and Schneck, J. P. Lectin microarrays identify cell-specific and functionally significant cell surface glycan markers. Glycobiology 2008; 18(10): 761-769

22. Wang, H., Li, H., Zhang, W., Wei, L., Yu, H., and Yang, P. Multiplex profiling of glycoproteins using a novel bead-based lectin array. Proteomics. 2014; 14(1): 78-86

23. Kuno, A., Uchiyama, N., Koseki-Kuno, S., Ebe, Y., Takashima, S., Yamada, M., and Hirabayashi, J. Evanescent-field fluorescence-assisted lectin microarray: a new strategy for glycan profiling. Nat.Methods 2005; 2(11): 851-856

24. Pilobello, K. T., Krishnamoorthy, L., Slawek, D., and Mahal, L. K. Development of a lectin microarray for the rapid analysis of protein glycopatterns. Chembiochem. 2005; 6(6): 985-989

25. Chen, S., LaRoche, T., Hamelinck, D., Bergsma, D., Brenner, D., Simeone, D., Brand, R. E., and Haab, B. B. Multiplexed analysis of glycan variation on native proteins captured by antibody microarrays. Nat.Methods 2007; 4(5): 437-444

26. Rosenfeld, R., Bangio, H., Gerwig, G. J., Rosenberg, R., Aloni, R., Cohen, Y., Amor, Y., Plaschkes, I., Kamerling, J. P., and Maya, R. B. A lectin array-based methodology for the analysis of protein glycosylation. J.Biochem.Biophys.Methods 10-4-2007; 70(3): 415-426

27. Safina, G., Duran, IuB, Alasel, M., and Danielsson, B. Surface plasmon resonance for real-time study of lectin-carbohydrate interactions for the differentiation and identification of glycoproteins. Talanta 15-6-2011; 84(5): 1284-1290

28. Yakovleva, M. E., Safina, G. R., and Danielsson, B. A study of glycoprotein-lectin interactions using quartz crystal microbalance. Anal.Chim.Acta 23-5-2010; 668(1): 80-85

29. Foley, K. J., Forzani, E. S., Joshi, L., and Tao, N. Detection of lectin-glycan interaction using high resolution surface plasmon resonance. Analyst 2008; 133(6): 744-746

30. Karamanska, R., Clarke, J., Blixt, O., Macrae, J. I., Zhang, J. Q., Crocker, P. R., Laurent, N., Wright, A., Flitsch, S. L., Russell, D. A., and Field, R. A. Surface plasmon resonance imaging for real-time, label-free analysis of protein interactions with carbohydrate microarrays. Glycoconj.J. 2008; 25(1): 69-74

31. Safina, G. Application of surface plasmon resonance for the detection of carbohydrates, glycoconjugates, and measurement of the carbohydrate-specific interactions: a comparison with conventional analytical techniques. A critical review. Anal.Chim.Acta 27-1-2012; 712 9-29

32. Iskratsch, T., Braun, A., Paschinger, K., and Wilson, I. B. Specificity analysis of lectins and antibodies using remodeled glycoproteins. Anal.Biochem. 15-3-2009; 386(2): 133-146

33. Karlsson, R., Katsamba, P. S., Nordin, H., Pol, E., and Myszka, D. G. Analyzing a kinetic titration series using affinity biosensors. Anal.Biochem. 1-2-2006; 349(1): 136-147

34. ICH Topic Q2 (R1) Validation of Analytical Procedures: Text and Methodologies. ICH Topic Q2 (R1) Validation of Analytical Procedures: Text and Methodologies 2015;-

35. Nimtz, M., Martin, W., Wray, V., Kloppel, K. D., Augustin, J., and Conradt, H. S. Structures of sialylated oligosaccharides of human erythropoietin expressed in recombinant BHK-21 cells. Eur.J.Biochem. 1-4-1993; 213(1): 39-56

36. Tran, D. T. and Ten Hagen, K. G. Mucin-type O-glycosylation during development. J.Biol.Chem. 8-3-2013; 288(10): 6921-6929

CHAPTER 5

Characterization of low affinity Fcγ receptor biotinylation under controlled reaction conditions by mass spectrometry and ligand binding analysis

The contents of this chapter have been published as:

Karin P.M. Geuijen, David F. Egging, Stefanie Bartels, Jan Schouten, Richard B. Schasfoort, Michel H. Eppink

Characterization of low affinity Fcγ receptor biotinylation under controlled reaction conditions by mass spectrometry and ligand binding analysis

Protein Science (2016) 10, 1841-1852

Abstract

Chemical protein biotinylation and streptavidin or anti-biotin based capture is regularly used for proteins as a more controlled alternative to direct coupling of the protein on a biosensor surface. Upon biotinylation an interaction site of interest may be blocked by the biotin groups, diminishing apparent activity of the protein. Minimal biotinylation can circumvent the loss of apparent activity, but still a binding site of interest can be blocked when labeling an amino acid involved in the binding. Here we describe reaction condition optimization studies for minimal labeling. We have chosen low affinity Fcγ receptors as model compounds as these proteins contain many lysines in their active binding site and as such provide an interesting system for a minimal labeling approach. We were able to identify the most critical parameters (protein:biotin ratio and incubation pH) for a minimal labeling approach in which the proteins of choice remain most active towards analyte binding. Localization of biotinylation by mass spectrometric peptide mapping on minimally labeled material was correlated to protein activity in binding assays. We show that only aiming at minimal labeling is not sufficient to maintain an active protein. Careful fine-tuning of critical parameters is important to reduce biotinylation in a protein binding site.

Introduction

Protein binding analysis in biosensor experiments relies in many cases on appropriate immobilization or capture of one of the interaction partners on a solid surface. Many different approaches for protein immobilization are generally applied throughout ligand binding studies. However, a key requirement in such a study is that the immobilized or captured ligand remains active, in other words, the interaction site involved in binding should not be blocked or masked.[1]

A commonly used immobilization strategy is based on amine coupling of the ligand directly to the sensor surface.[2] Coupling through amine groups is considered to be a random process, hence orientation and cross-linking of the ligand on the sensor surface is less well controllable. For ligands that have many lysines in or around the interaction site of interest, this may result in a marginally active or inactive surface. Other direct coupling chemistries, such as thiol coupling, may face similar problems, as any amino acid that is directly coupled to a sensor surface may have an impact on the protein binding characteristics.

Alternative approaches are mainly based on protein capture, in which a protein can be captured to the surface in a highly selective manner. The orientation of the ligand to the surface will be more site-directed and when carefully constructed one can design the capture in such a way that the interaction site is not blocked. Capture approaches that are often used include the capture of his-tagged proteins by an anti-histidine antibody[3,4] or the capture of biotinylated proteins by a streptavidin surface.[2] A disadvantage of most capture approaches is that in general the ligand will be regenerated after interaction measurements, and ligand capture has to be repeated with each analysis. The regeneration and recapture of ligand is not necessary when the biotin-streptavidin capture is chosen, because the affinity of biotin to streptavidin is high[5,6] and virtually no dissociation takes place. Next to this high affinity, the capture is specific, therefore only biotinylated proteins will be captured in most well-defined buffer systems.

Biotinylation of proteins is most elegantly performed by incorporating an AviTag™ into the protein,[7] a peptide sequence that can then be specifically biotinylated by bacterial biotin ligase (BirA) *in vitro* or *in vivo*. However, when a protein is not expressed with such a tag, chemical biotinylation provides a robust alternative. Chemical biotinylation can generally be performed on primary amines, where similar considerations are applicable as in direct coupling on a sensor surface. A number of groups have shown that controlling the pH

during the coupling reaction may drive preference for reactions on α-amino groups or ε-amino groups.[8,9] Selo et al.[9] were able to selectively biotinylate α-amino groups over ε-amino groups, which then results in biotinylation at a peptide's N-terminus instead of randomly on various lysines in the peptide sequence. However, these experiments were performed on small peptides with a limited number of amine groups on lysines present and may therefore differ from reaction conditions in entire proteins with a large number of lysines. Papalia and Myszka[10] have reported a minimal labeling approach, in which they chose the reaction conditions in such a way that only a limited number of lysines in a protein is biotinylated, thereby reducing the chance of biotinylation in the binding site of interest in a protein. Furthermore, they concluded that low levels of biotinylation lead to less cross-linking of the ligand on the surface, resulting in high-density surfaces with optimal activity.

Here we describe the biotinylation of Fcγ receptors, a class of cell surface receptors that is important in the binding of IgG to effector cells in a human body.[11-13] Five different subclasses of Fcγ receptors are known, with different isoforms and natural variants,[14,15] all of which carry many lysines in or close to the IgG binding site.[16-22] As an alternative to amine groups (lysines), coupling may be performed on carbohydrates, however the presence of carbohydrates depends on the expression platform[23,24] and moreover Fcγ receptor glycosylation plays a crucial role in IgG binding.[25]

Hence these receptors provide an interesting group of proteins in which the impact of minimal biotin labeling may be studied. A minimal degree of biotinylation is defined here as a maximum of one biotin attached to a single protein molecule, which corresponds to a degree of labeling of approximately 1. A subset of Fcγ receptors was selected to explore the influence of the biotinylation reaction conditions on IgG binding, which included the factors protein:biotin ratio, reaction pH and reaction time based on previous publications.[9,10] Experimental setup and analyses of the data were executed under a statistical design of experiments (DoE). Furthermore, using FcγRIIb as a model system, we investigated whether certain reaction conditions could be correlated to remaining ligand binding activity, defined as binding to IgG and to biotinylation at certain lysine residues (ε-amines) or at the N-terminus (α-amine) within the protein. Therefore, surface plasmon resonance (SPR) binding assays and mass spectrometry (MS) analyses were performed respectively. Results of the different SPR and MS analysis were used to identify the most critical parameters in chemical biotinylation impacting Fcγ receptor activity after minimal labeling.

Materials and methods

Expression and purification of Fcγ receptors

Fcγ receptors were expressed and purified at Synthon Biopharmaceuticals BV (Nijmegen, the Netherlands). The amino acid sequences of the extracellular domains of the human Fcγ receptors were derived from Uniprot: FcγRIIIa (FCGR3A) from entry P08637 amino acids 17-208, FcγRIIIb (FCGR3B) from entry O75015 amino acids 20-208, FcγRIIa (FCGR2A) from entry P12318 amino acids 36-218 and FcγRIIb (FCGR2B) from entry P31994 amino acids 46-217. A leader sequence and a hexa-histidine-tag were included at the N-terminus and C-terminus respectively. DNA synthesis was performed by GeneArt (part of Thermo Fisher Scientific (Waltham, MA USA)). The synthesized DNA fragments were cloned into a pcDNA3.1 (Life Technologies, part of Thermo Fisher Scientific) based vector. Plasmid preparations were made using the EndoFree Plasmid Maxi Kit (QIAGEN (Hilden, Germany)). The Fcγ receptors were expressed using the Expi293 Expression System (Life Technologies). Transient transfections were performed according to the manufacturer's protocol.

Histidine-tagged Fcγ receptors were purified from cell cultures by Immobilized Metal Affinity Chromatography (IMAC) on a 5 mL Chelating Sepharose Fast Flow column on an ÄKTA explorer 100 system (GE life sciences (Eindhoven, the Netherlands)). The column was charged with 100 mM copper(II)sulfate after which the supernatants were loaded. The column was washed with PBS pH 7.4 / 20 mM imidazole after which the target protein was eluted in a gradient elution with PBS pH 7.4 / 20mM imidazole to PBS pH 7.4 / 500 mM imidazole.

Biotinylation

Biotinylation reactions were performed with EZ-link Sulfo-NHS-LC biotin (Thermo Scientific (Waltham, MA USA)) which was dissolved in MQ water. Multiple factor levels of incubation time (30, 135 and 240 minutes), incubation pH (pH 6.5, pH 7.0 and pH 7.5 in case of FcγRIIa and FcγRIIb; pH 6.5, pH 7.5 and pH 8.5 in case of FcγRIIIa and FcγRIIIb) and protein:biotin ratios (1:0.5; 1:1.25 and 1:2) were applied as per DoE based setup (Table 5.1). Fcγ receptors were diluted to 1 mg/mL in PBS buffer at the indicated pH. The reaction volumes were kept constant at 200 µL and 10 µL biotin stock solution was added to the desired protein:biotin ratio. Biotinylation reactions were performed on ice and after incubation free biotin was removed using PD G-25 minitraps (GE life sciences) according to

manufacturer's instructions. The degree of labeling was determined by FluoReporter Biotin quantitation kit (Invitrogen (Waltham, MA USA)) according to manufacturer's protocol.

Surface Plasmon Resonance analysis

Biotinylated Fcγ receptors were immobilized on G-Strep SensEye® sensors (Ssens BV (Enschede, The Netherlands)) in the continuous flow microspotter (CFM) (Wasatch Microfluidics, Salt Lake City, UT, USA) using a print time of 5 minutes and a 50 mM sodium acetate buffer pH 4.5/0.05 w/v% Tween 80. Interaction measurements between Fcγ receptors and monoclonal antibody (Synthon Biopharmaceuticals BV, Nijmegen, The Netherlands) were performed on an IBIS MX96 SPRi instrument (IBIS Technologies BV, Enschede, The Netherlands) in HBS buffer pH7.2 / 0.05 w/v% Tween 80. A baseline of 1 minute was followed by an association time of 5 to 20 minutes and dissociation at 1 µL/second in 1 step for 4 minutes. Regeneration was performed with 25 mM phosphoric acid pH 3.0 in a single step of 30 seconds.

Mass spectrometry analysis

An UPLC-ESI-qTOF (Waters, Milford USA) was used to analyze intact proteins and for peptide mapping. Intact mass analysis was performed on a polymeric reversed phase column (PLRP-S, 50x4.6mm, 5µm (Agilent, Santa Clara, CA, USA) operated at 60°C and a flow rate of 400 µL/min was used. Mobile phase A and B consisted of 0.05% TFA in Milli-Q and 0.05% TFA in 50% acetonitrile respectively. A linear gradient from 60% A to 1% A in 35 minutes after a baseline of 2 minutes at 60% A was followed by 1% A for 3 minutes and an equilibration step at 60% A for 2 minutes. Online UV detection was measured at 280 nm. Online MS detection with an MS scan method was used from 400 to 4500 m/z with a scan time of 0.98 seconds and an interscan time of 0.02 seconds. The following conditions were used for the MS: capillary voltage of 3 kV, sample cone of 25 V, source temperature of 120°C, desolvation temperature of 200°C and a desolvation gas flow of 600L/hr. Intact mass analysis was performed on Fcγ receptors, that were deglycosylated by overnight incubation with PNGase F at 37°C.

A reversed phase C18 column (Shim-pack XR-ODS II, 150 x 2.1 mm, 2.2 µm (Shimadzu, Kyoto, Japan)) at 30°C and a flow rate of 250 µL/min was used for the peptide mapping analysis. Trypsin digestion of Fcγ receptors was performed at 37°C overnight and chymotrypsin digestion of Fcγ receptors was performed in the presence of $CaCl_2$ at 35°C for 4 hrs after deglycosylation, reduction and alkylation of the protein. The separation was

performed with a baseline at 96% A for 2 minutes followed by a linear gradient from 96% A to 30% A in 30 minutes. Then the %A decreased to 1% in 2 minutes and was kept at 1% for 5 minutes, followed by returning to 96% A in 3 minutes and equilibration for 3 minutes. Online UV detection was measured at 214 nm and 280 nm. Online MS detection with an MSE method was used from 100 to 1700 m/z mass scan and a scan time of 0.5 seconds and interscan time of 0.1 seconds. The second mass scan was from 100 to 2000 m/z with a scan time of 0.5 seconds and interscan time of 0.1 seconds using a collision energy ramp from 19 to 30 eV for peptide fragmentation. The same MS settings as described before were used for the peptide mapping analysis. Data acquisition and data analysis was performed in MassLynx software (version 4.1) (Waters, Milford, MA, USA).

Statistical analysis

A 2-level full factorial Design of Experiments (DoE) was created in Minitab v17 (Minitab Ltd, Coventry, UK) which consisted of three factors at 2 levels and three replicates of center points (Table 5.1). In total the DoE consisted of eleven independent runs (a run is defined as a biotinylation reaction on one Fcγ receptor) for each Fcγ receptor (a total of 44 runs). Statistical analysis of data for output variables was performed in Minitab. Output variables included the degree of labeling, ligand density on the sensor surface, IgG binding to immobilized Fcγ receptor and in addition for FcγRIIb, biotin distribution and relative amount of biotinylated residues from peptide mapping quantification.

Results and discussion

IgG binding studies to biotinylated Fcγ receptors

The Fcγ receptors were biotinylated under controlled conditions (Table 5.1) to be used as ligands in IgG binding studies. Our previous experiences showed that direct immobilization of the Fcγ receptors minimizes their activity for IgG binding and only a limited stability on the surface is obtained (data not shown). The IgG binding sites of Fcγ receptors contain a number of lysines,[16-22] hence, upon amine coupling on a sensor surface the interaction with IgG will be affected. In our experiments degrees of labeling of the different samples were determined at values between 0.36 and 1.78 indicating that on average a minimal amount of biotins had been attached to the proteins.

Immobilization of all samples to a streptavidin SensEye® sensor surface was performed, followed by analysis of IgG binding to the Fcγ receptors. The ligand density on

Table 5.1 *Experimental conditions for biotinylation*

Run no	Protein:biotin ratio	Incubation pH [I]	Incubation time (min)
1	1:2	6.5	240
2	1:2	6.5	30
3	1:0.5	6.5	30
4	1:0.5	6.5	240
5	1:2	7.5 / 8.5	30
6	1:1.25	7.0 / 7.5	135
7	1:1.25	7.0 / 7.5	135
8	1:0.5	7.5 / 8.5	30
9	1:2	7.5 / 8.5	240
10	1:1.25	7.0 / 7.5	135
11	1:0.5	7.5 / 8.5	240

[I] pH 6.5-7.0-7.5 in case of FcγRIIa and FcγRIIb; pH 6.5-7.5-8.5 in case of FcγRIIIa and FcγRIIIb
The "Run no" column shows the order of experiments after randomization by Minitab software

the sensor surface expressed in resonance units (RU) was plotted against the degree of labeling (Figure 5.1-a). The amount of ligand that was immobilized on the sensor surface is independent of the degree of biotinylation indicated by the apparent random distribution of points in this plot. This was verified by a regression analysis of the ligand density versus the degree of labeling where no significant effect on the slope of the regression was found (P=0.58, P=0.12, P=0.63 and P=0.19 for FcγRIIIa, FcγRIIIb, FcγRIIa and FcγRIIb respectively). As a control, non-labeled proteins were also applied to the surface under the same conditions resulting in no immobilization of ligand with FcγRIIIa. In case of the other three ligands, the RU determination from the camera image calculated 36 to 60 RU of ligand, which is too low for proper functional ligand coupling. This was confirmed by injecting IgG samples over these spots which resulted in no measurable interaction (Figure 5.1-b). This indicates that no relevant amount of functional ligand adheres non-specifically to the surface. The immobilization levels in each of the biotinylated samples are higher compared to the control samples, except for 1 sample which was present in a blocked flowchannel.

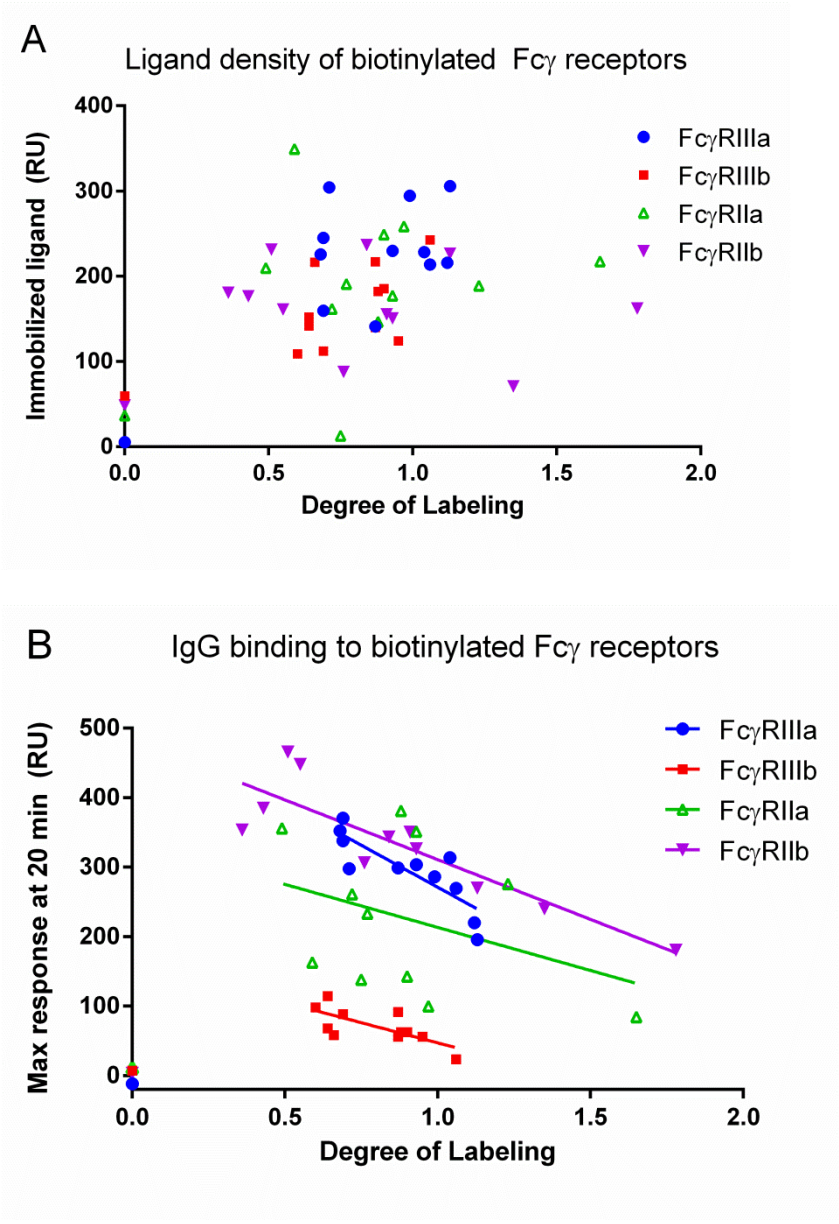

Figure 5.1 *Effect of biotinylation on ligand immobilization and remaining activity for four Fcγ receptors. a) Ligand density in resonance units (RU) is plotted against the level of biotinylation expressed as degree of labeling. b) Maximum IgG binding response in RU plotted against the level of biotinylation expressed as degree of labeling.*

Papalia and Myszka[10] have shown that similar surface densities are reached at different degrees of labeling, but that the chance of cross-linking at the surface becomes higher at higher labeling degrees. We were interested to see whether possible cross-linking at the surface could have an influence on the remaining activity of the receptors on the surface. Binding of IgG to immobilized Fcγ receptors at similar ligand densities was measured in an SPR measurement (Appendix A; Figure 5.A.1). The binding of IgG is expressed as the maximum response after 20 minutes association time and this value is plotted against the degree of labeling (Figure 5.1-b). An actual steady state is not reached in any of the sensorgrams which is related to the biphasic binding of IgG to Fcγ receptors.[25,26] Hence, for comparison of the remaining activity under different biotinylation conditions the maximum response at 20 minutes post injection was chosen as measure for binding.

Higher responses are measured on those receptors with a lower degree of labeling and lower responses are measured at higher degrees of labeling (Figure 5.1-b). No IgG binding is measured on the spots where we immobilized non-labeled control samples. It must be noted that non-labeled protein contributes to the calculated degree of labeling, yet is not immobilized and henceforth does not contribute to either immobilized ligand response or IgG binding response. The significant factors contributing to this trend were found in a statistical analysis of the IgG binding as an output in the DoE analysis (example of FcγRIIb shown in Figure 5.2). The statistical analysis indicated that significant factors on the IgG binding response are the protein:biotin ratio during biotinylation ($P<0.0005$), the interaction between the protein:biotin ratio with the incubation pH ($P=0.001$) and the interaction between protein:biotin ratio with the incubation time ($P=0.015$). The main driver for significant differences in remaining ligand activity is the protein:biotin ratio. Within each of the different protein:biotin ratio conditions that were tested, also the combination with either of the two other input variables has a significant influence. However, the incubation pH and incubation time on its own do not have a significant influence on the IgG binding to biotinylated Fcγ receptors. The adjusted model where non-significant interactions of factors were excluded has a predictive R2 of 98%. Appropriateness of the statistical model was evaluated by analysis of the normalized residuals (Appendix B, Figure 5.B.1).

These data suggest that either cross-linking of the ligand at the surface may occur, as proposed by Papalia and Myszka[10] or that the biotins are present at lysines in or near the interaction site involved in IgG binding.

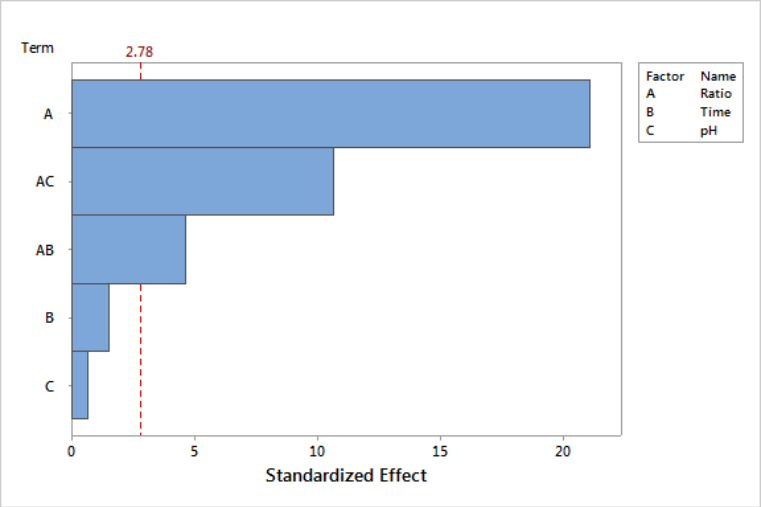

Figure 5.2 *Pareto chart of the factors used in the design of experiments (DoE) for IgG binding activity to FcγRIIb as output variable. Significant factors for the IgG binding response are identified.*

Biotin distribution by mass spectrometry

In the paper by Papalia and Myszka[10] high degrees of labeling are related to more ligand cross-linking at the sensor surface. For cross-linking at the surface, the biotin loading on a single protein molecule should be at least two or more. To determine whether more cross-linking may occur under certain biotinylation conditions, we determined the biotin distribution on the protein molecules by intact mass spectrometry analysis. An average degree of labeling of 1 can be obtained when exactly each protein carries a single biotin, however in theory it may as well be possible that a percentage of the proteins carry two or more biotins and the other percentage is not labeled at all. On average, both samples may give a degree of labeling of 1. Subsequently, unlabeled protein molecules will not be immobilized on a streptavidin sensor and only the proteins with multiple biotins will be immobilized in the latter case, which may be prone to cross-linking in contrast to a protein that only carries a single biotin. FcγRIIb was taken as a model system for further investigation.

In the intact mass analysis of FcγRIIb after deglycosylation we could distinguish peaks that correspond to the mass of the intact protein (Figure 5.3-a) and to masses of the intact protein with one, two or three biotins attached (the peak with three biotins attached not being visible in the mass spectra that are shown). The calculations of biotin distribution on

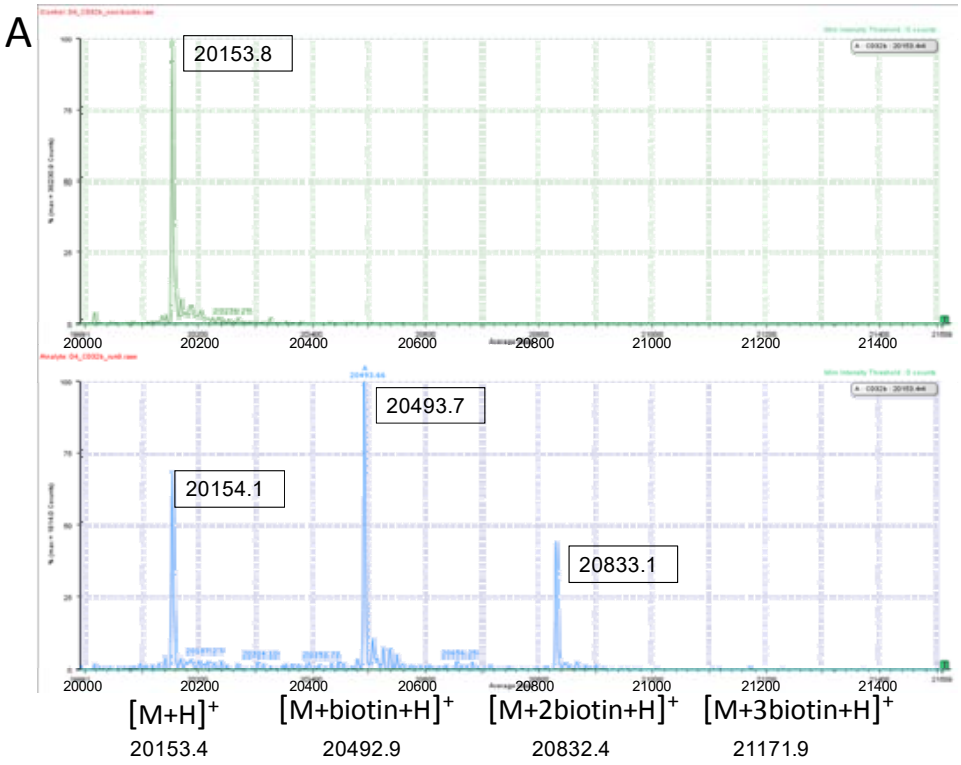
A
20153.8
20493.7
20154.1
20833.1
20000
20200
20400
20600
20800
21000
21200
21400
[M+H]+
20153.4
[M+biotin+H]+
20492.9
[M+2biotin+H]+
20832.4
[M+3biotin+H]+
21171.9

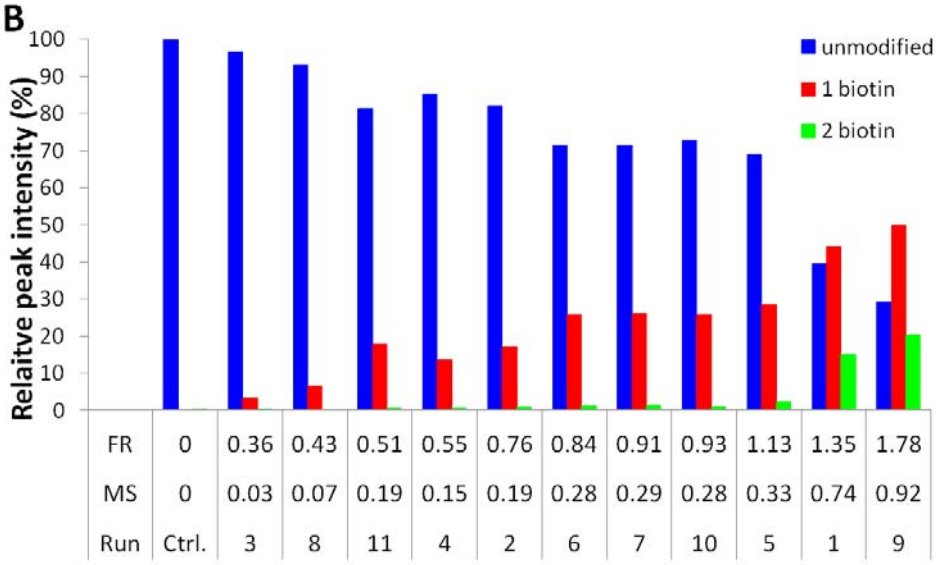
B
Relaitve peak intensity (%)
100
90
80
70
60
50
40
30
20
10
0
unmodified
1 biotin
2 biotin
FR 0 0.36 0.43 0.51 0.55 0.76 0.84 0.91 0.93 1.13 1.35 1.78
MS 0 0.03 0.07 0.19 0.15 0.19 0.28 0.29 0.28 0.33 0.74 0.92
Run Ctrl. 3 8 11 4 2 6 7 10 5 1 9

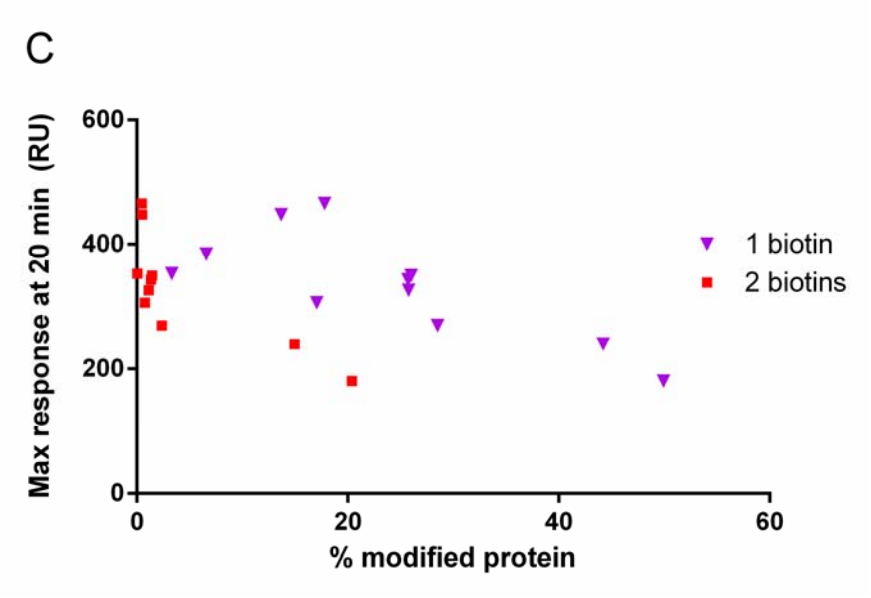

Figure 5.3 *Biotin distribution under various biotinylation conditions. a) Deconvoluted mass spectra of the control sample (unlabeled FcγRIIb; top) and one of the biotinylated samples (pH 7.5, 240 minutes, 1:2 protein:biotin ratio; bottom). b) Relative intensities of the peaks in the mass spectra corresponding with the number of biotins on the protein. The X-axis represents the degree of labeling (DOL) as determined in the fluorescence assay (FR) and as determined by mass spectrometry (MS) and the run number of the DoE (Run). C) Correlation between the percentage of modified protein and the IgG binding response in SPR binding assay for species with 1 or 2 biotin molecules attached.*

FcγRIIb were based on the ion intensities of the corresponding peaks in the mass spectra which were then used for a relative quantitation (Figure 5.3-b). Similar experiments were performed on the other three Fcγ receptors and data are shown in supporting information (Appendix C, Figure 5.C.1, Figure 5.C.2 and Figure 5.C.3). The ion intensities of the unmodified proteins may be overestimated compared to the biotinylated proteins due to differences in ionization efficiency between the different species. This leads to lower degrees of labeling based on the MS data compared to the fluorescent biotin quantitation kit (both values are indicated inFigure 5.3-b). Although the percentage of unmodified protein may be overestimated, the distribution of the peaks among the different samples can be compared to each other from species to species as all samples were analyzed with the same settings and in a single analysis. The degrees of labeling from fluorescent determination by the

FluoReporter kit are used for quantitation purposes and MS data are only used for comparison of biotin distribution on the proteins.

The distribution of biotins on the protein molecules is different between the eleven biotinylation conditions (Figure 5.3-b). Highest biotin loading is reached in the samples with the highest protein:biotin ratio. Only under these conditions a substantial percentage of protein with two biotins attached is formed and only very limited protein with 3 or more biotins are found overall (<0.5%). The distribution of protein species with only a single biotin and without biotin modification varies between the applied reaction conditions and only a minor difference in IgG binding is measured in these samples (Figure 5.3-c) whereas lowest IgG binding is measured for the samples with double-biotinylated species. Together these data suggest that a decrease in IgG binding is most likely not dependent on ligand cross-linking at the surface, or at best plays a minor role under the investigated conditions.

Biotin localization by peptide mass mapping

Our second hypothesis for the reduced ligand activity considered biotinylation of lysines that are present in or near the interaction site involved in IgG binding. The Fcγ receptors have many lysines in their IgG binding site[19,20] (Figure 5.4), and consequently we were interested to identify the actual positions that are biotinylated to determine whether this IgG binding site is influenced upon biotinylation. As the four low affinity Fcγ receptors are relatively similar proteins we chose FcγRIIb as a model to identify the biotinylated residues by peptide mass mapping analysis.

The biotinylated samples and a non-modified sample of FcγRIIb were subjected to deglycosylation, reduction, alkylation and trypsin or chymotrypsin digestion to generate short peptides of the proteins. We chose a chymotrypsin digestion over a trypsin digestion for quantitation, because the biotin modification is expected on lysines. The more commonly used trypsin enzyme cleaves at lysines, but does not recognize biotinylated lysines[27] which would complicate the calculation of modified residues. Chymotrypsin on the other hand cleaves a protein into relatively small peptides because it cleaves at several different amino acids (Tyr, Trp, Phe, Met, Leu and His[28]). The use of chymotrypsin prevents the presence of lysines at the C-terminus of the peptide which simplifies the data analysis for quantitation compared to a tryptic digestion. Chymotryptic peptides on the other hand are less facile to fragment in MS/MS analysis, which is necessary to identify the exact location of the biotins. A trypsin digestion for the localization at specific residues was therefore included.

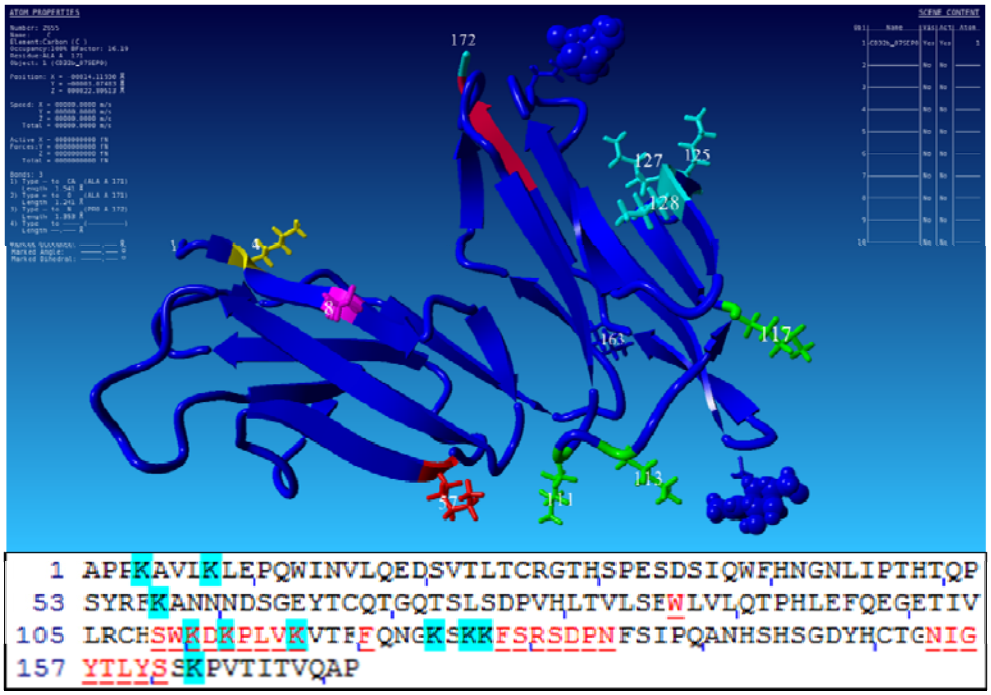

Figure 5.4 *Three-dimensional protein model of FcγRIIb with lysine residues indicated as colored amino acids. Below is the amino acid sequence of FcγRIIb with the IgG binding site from Hulett et al21 in red and underlined and the lysine residues in blue.*

First of all we used MS/MS fragmentation data of the tryptic digests to determine which lysines were biotinylated and whether the N-terminal alanine was biotinylated as well (Appendix D). The tryptic peptides T112-117 (DKPLVK) and T112-125 (DKPLVKVTFFQNGK), which contain the lysines that are present in one of the active binding sites of FcγRIIb, are modified at Lys^{113} and Lys^{117} (Appendix D, Figure 5.D.1 to Figure 5.D.7). In the MS/MS fragmentation spectra we could localize the biotin at Lys^{113} in peptide T112-117 and at Lys^{117} in peptide T112-125. The latter one explains the missed trypsin cleavage of this peptide, as trypsin does not recognize the lysine upon biotinylation and cannot cleave at this lysine.[27] The MS/MS fragmentation spectra of biotinylated peptides T1-4 and T1-8 were used to determine whether the lysine or the N-terminal alanine was biotinylated (Appendix D, Figure 5.D.8 and Figure 5.D.9). MS/MS fragmentation of biotinylated T1-4 proves that the N-terminal alanine of this peptide is biotinylated and trypsin cleaves at the non-modified lysine (Lys^4) (Appendix D, Figure 5.D.8). Fragmentation of biotinylated peptide T1-8, which contains a missed trypsin cleavage site, matches with the expected fragment ions of the

peptide with the biotin conjugated to the lysine at position 4. In this peptide the N-terminal alanine is not biotinylated as expected fragment ions for this modification are absent (Appendix D, Figure 5.D.9).

After we confirmed that the N-terminal alanine and each of the lysines in the amino acid sequence were biotinylated, we quantified the percentage of biotinylation at each position from the chymotrypsin digestion. A short cleavage time was used for chymotrypsin to maintain moderately sized peptides which are generally well ionized in mass spectrometry analysis (Appendix E, Table 5.E.1). A few peptides contained more than one lysine in the amino acid sequence of the chymotryptic peptides. Quantitation of these peptides was performed on the masses corresponding to peptides with one, two or three biotins attached. The exact location of biotin on a particular lysine could not be determined in these chymotryptic peptides, but trypsin data proved that all of the lysines and the N-terminal alanine in FcγRIIb were biotinylated, only not all to the same extent. Quantitation was based on the peak area in extracted ion chromatograms of the unmodified and modified peptides in the chymotrypsin digestion. Ionization efficiencies of non-modified peptides and of biotinylated peptides are most likely different, due to the modification. The calculated percentages of modification should therefore only be used to compare the reaction conditions among each other, rather than as absolute numbers. The extracted ion chromatograms of peptides C1-7 (APPKAVL) and C111-120 (KDKPLVKVTF) in the non-modified sample and one of the biotinylated samples are used to illustrate the quantitation (Appendix E, Figure 5.E.1 and Figure 5.E.2).

Peak area percentages of biotinylated peptides were calculated for each of the eleven DoE runs (Figure 5.5-a). Two peptides, C1-7 and C111-120, have the highest levels of biotinylation irrespective of the labeling conditions that were applied, as the highest percentage of modification is detected at both peptides in each of the eleven samples that have been analyzed. In DoE runs 1 and 9 (lowest IgG binding), these peptides are modified at levels over 30%. These peptides contain residues Ala^{1} and Lys^{4} and residues Lys^{111}, Lys^{113} and Lys^{117} respectively. All other lysines that are present in the amino acid sequence are modified with biotin to some extent, but modification levels are below 10% in each of the reaction conditions. To quantify biotinylation levels at Ala^{1} we used the trypsin digestion. Only for this position the tryptic peptide mapping could be used, as we measured both the non-modified tryptic peptide T1-4 and the biotinylated peptide T1-4, which was biotinylated at Ala^{1} as previously shown in the MS/MS fragmentation spectrum. We expected a higher level of biotinylation at Ala^{1} in

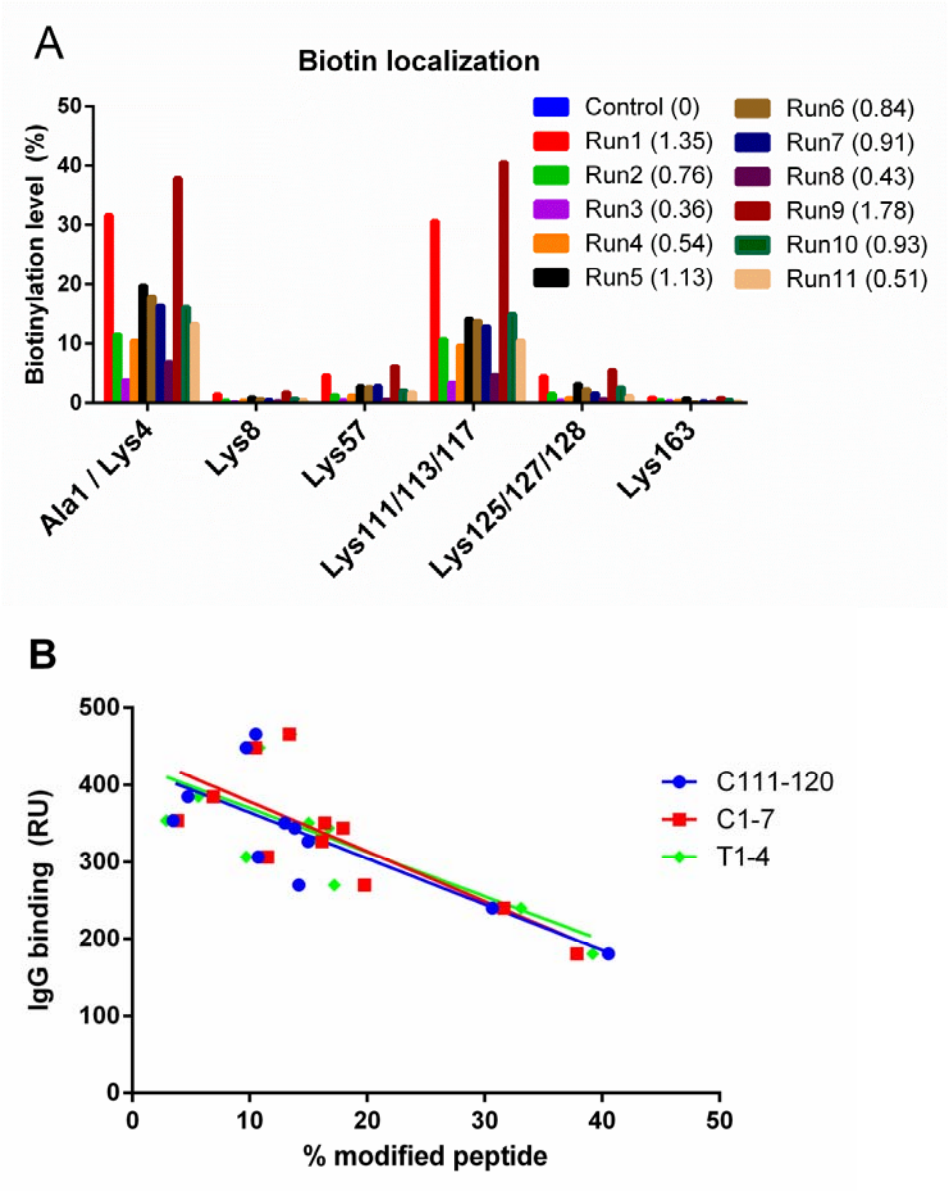

Figure 5.5 *a) Biotinylation levels on the different modified residues. Extracted ion chromatograms from peptide mass mapping chromatograms were integrated. The peak area of the modified peptide relative to the total peak area of a particular peptide was used to calculate the percentage of biotinylation at each position. Run numbers correspond to the different DoE samples and reaction conditions areas indicated in Table 1 and the degrees of labeling are indicated between brackets. b) Correlation between IgG binding in the SPR assay and % of modified peptides C1-7 and ,C111-120 and T1-4 (representing total biotin modifications, i.e. 1 and 2 biotins per peptide relative to total peptide).*

the DoE runs incubated at pH 6.5 since other groups[8,9] have published that incubation at lower pH (e.g. pH 6.5) would preferentially incorporate the biotins at α-amines (i.e. the N-terminus). If the reaction would shift to the α-amine at pH 6.5, we would expect an increase in biotinylation levels at peptide T1-4 (Ala^1) or peptide C1-7 (Ala^1/Lys^4) and a decrease in biotinylation levels at any of the other peptides when incubated at pH 6.5. However, we do not see a shift of biotinylation at ε-amines (i.e. lysines) towards biotinylation at the α-amine when incubating at lower pH. The biotinylation levels at peptides T1-4, C1-7 and C111-120 are similar when compared between each of the tested conditions (Figure 5.5-a). Runs 1 to 4 have been incubated at pH 6.5 and no increase in biotinylation level at peptide C1-7 or peptide T1-4 compared to e.g. peptide C111-120 is observed in one of these runs. Both groups[8,9] have performed the experiments on short peptides rather than on intact proteins, which may explain the apparent discrepancies with our results as the environment of the biotinylation site is different.

Lysines at positions 111, 113 and 117 in the protein are present in one of the interaction sites known for IgG binding (Figure 5.4).[19,20] The samples with highest biotinylation levels on Lys^{111}, Lys^{113} and Lys^{117} have a higher degree of labeling and lowest responses in the IgG binding assay on SPR. We hypothesized that the lysines that are more prone towards biotinylation may be easier accessible, for example because they are more surface exposed. The three dimensional model of FcγRIIb (Figure 5.4) displays all lysine residues which are all present on the outside of the protein model, making all of them easily accessible for modifications. This does not explain the preference of biotinylation at certain residues. Possibly the local electrostatic environment around Lys^{111}, Lys^{113} and Lys^{117} is preferred for the biotinylation reaction.

The percentage of biotinylation at peptide C111-120 (KDKPLVKVTF), containing Lys^{111}, Lys^{113} and Lys^{117}, was used as an output in a statistical analysis of the DoE. Both protein:biotin ratio ($P<0.0005$) and the incubation pH ($P<0.0005$) have a significant impact on the level of biotinylation at this specific position, as well as the interaction between the two parameters ($P=0.004$) (Figure 5.6). Appropriateness of the statistical model was evaluated by analysis of the normalized residuals (Appendix B, Figure 5.B.2). However, similar significance in these factors was observed for the other peptides e.g. C1-7 ($P<0.0005$ for ratio and for incubation time, $P=0.002$ for the interaction between both). The same factors that have significant influence on the degree of labeling at individual peptide level drive the total degree of labeling (Figure 5.6).

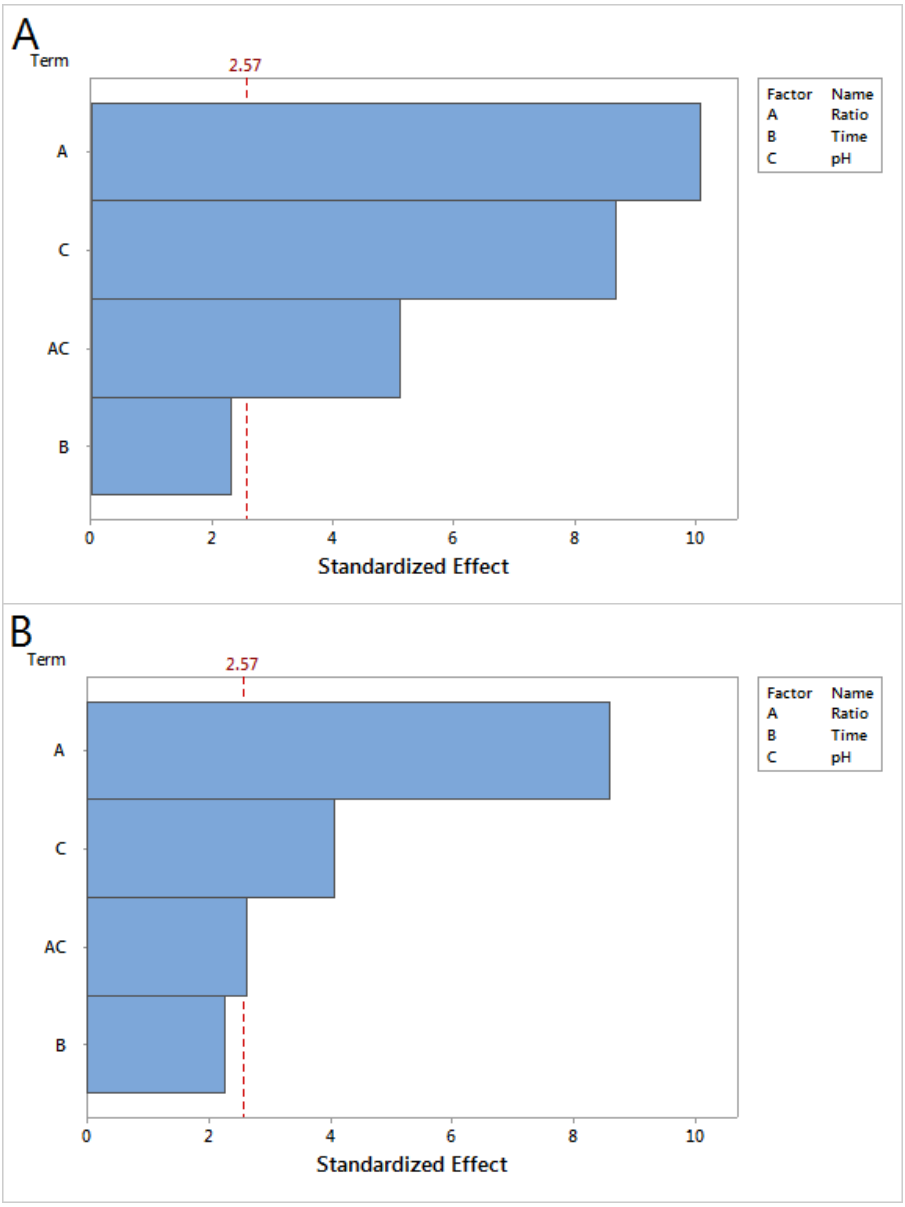

Figure 5.6 *Pareto chart of the factors used in the DoE based on the percentage of modified peptide C111-120 (a) and total degree of labeling (b).*

This suggests that these factors relate to the degree of labeling, in other words the pattern of labeled peptides is the same for each of the tested conditions (Figure 5.5-a). This is also illustrated by the co-linearity of the IgG binding and % modified peptide (Figure 5.5-

b) of peptides C1-7, C111-120 and T1-4. All three peptides show similar correlation between IgG binding and the percentage of modification which is in line with the correlation found in the degree of labeling and IgG binding presented in Figure 5.1. Linear regression analysis of percentage of modified peptides versus IgG binding (Figure 5.5-b) shows that there is a significant deviation from zero, i.e. correlation between the two variables (P=0.048, P=0.051 and P=0.0093 for C111-120, C1-7 and T1-4 respectively). However, when we exclude the two highest levels of modification, then the linear regression is not significantly different from zero (P=0.35, P=0.31 and P=0.53 respectively). These highest two points originate from the only two reaction conditions where a substantial amount of double-biotinylated species are formed (Figure 5.3-b). These results suggests that reaction conditions that lead to a substantial percentage of FcγRIIb protein with 2 biotin molecules attached most likely have a reduced binding activity.

Steady state equilibrium affinity determination

Minimally labeled material for each of the four low-affinity Fcγ receptors was taken for further assay development. The receptors were biotinylated at a protein:biotin ratio of 1:0.75, incubation time of 30 minutes and an incubation pH of 6.5. Degrees of labeling were determined between 0.38 and 0.59. No mass spectrometry analyses were performed on these newly prepared ligands, but based on results in Figure 5.3-b we assumed that there are no substantial amount of double-biotinylated species present in these preparations. IgG1 samples between 9 nM and 20 µM were injected for steady state equilibrium (SSE) affinity determination (Figure 5.7). Affinities determined from these minimally labeled samples were compared with values from literature[15,29] (Table 5.2) determined at 25°C. The paper of Bruhns et al.[15] reports K_A values which were converted to K_D values for our comparison ($K_D=1/K_A$). Both references used the steady state equilibrium determination for affinity. Bruhns et al.[15] directly immobilized the Fcγ receptors with an amine coupling; Patel et al.[29] immobilized the IgG on the sensor surface by amine coupling and used the Fcγ receptors as analyte.

Affinities that we determined with the minimally labeled material are highly similar compared to the two references; all three values are of the same order of magnitude (Table 5.2). These results indicate that a minimal labeling of ligands provides a robust alternative for routine use of ligands that are problematic to immobilize by direct coupling.

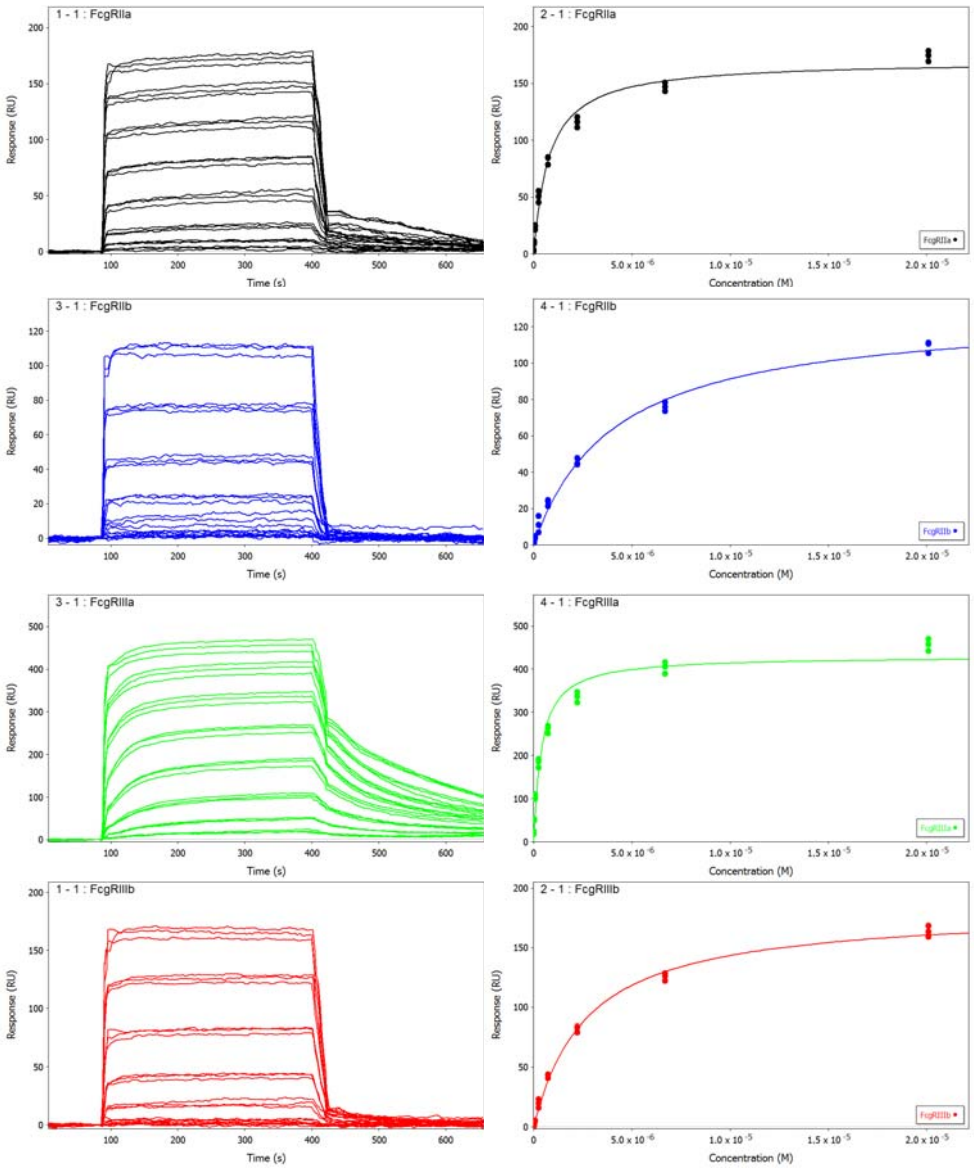

Figure 5.7 *Steady state equilibrium (SSE) affinity determination of IgG1 on four low affinity Fcγ receptors immobilized on a streptavidin sensor after minimal biotinylation. FcγRIIa in black, FγRIIb in blue, FcγRIIIa in green and FcγRIIIb in red. Sensorgrams of a triplicate concentration series between 9 nM and 20 µM are shown on the left side, concentration vs response curves for SSE affinity determination are shown on the right side. Analyses were performed at 25°C for comparison with values from literature.*

Table 5.2 *Steady state equilibrium affinity determinations*

Receptor	K_D (μM) (this paper)	K_D (μM)[29]	K_D (μM)[15]
FcγRIIa	0.79 ± 0.11	0.80	0.19
FcγRIIb	4.07 ± 0.21	3.10	8.33
FcγRIIIa	0.38 ± 0.03	0.85	0.85
FcγRIIIb	2.70 ± 0.17	1.90	4.55

Conclusions

Protein biotinylation is applied in many cases where a protein needs to be immobilized on a sensor surface for protein interaction measurements. In certain cases, direct immobilization is not preferred because the protein becomes partially inactive or the protein conformation changes upon direct coupling. One of the possibilities to overcome these issues is by capturing a protein by the high affinity biotin-streptavidin interaction. However, chemical biotinylation of one of the interaction partners may be required, which may interfere with the binding site and reduce activity. Here we have shown that aiming at a minimal protein labeling is successful to maintain protein activity. In the examples of Fcγ receptors that we showed here, we were able to obtain low levels of biotinylation while similar ligand densities were obtained on the sensor surface. Statistical evaluation of a design of experiments revealed that a very low protein:biotin ratio is a key parameter to obtain the most active protein on the surface while still sufficient amounts of protein are labeled in order to immobilize these.

However, even when low levels of biotinylation (between 0.3 and 1.8) were obtained under various conditions, differences in protein binding were measured while similar ligand densities were obtained. This is likely due to partial inactivity of the captured ligand. Further characterization of biotinylated Fcγ receptors by mass spectrometry showed that proteins that have two or more biotins attached on a relatively large fraction of the total protein resulted in less active proteins on the sensor surface. This may be due to ligand cross-linking at the surface, however, the highest biotin loading that we found was two biotins on a protein and only very little cross-linking is expected. On the other hand, localization of the biotins in the protein sequence of FcγRIIb by peptide mapping mass spectrometry showed that under all of the tested reaction conditions one of the lysine containing peptides is preferentially biotinylated. The lysines at positions 111, 113 and 117 in the protein sequence (peptide C111-120), which are present at one of the IgG binding sites of FcγRIIb, were

most prone towards biotinylation. We have shown here that biotinylation of these residues has a direct impact on the remaining activity of the protein on the sensor surface.

The level of biotinylation at these positions can be minimized, most notably by choosing conditions in which limited proteins with two coupled biotins are formed. Although the reaction cannot be directed to the α-amine at the N-terminus, biotinylation at the IgG binding site can be minimized by selection of reaction conditions that will mainly result in a single biotin on each protein, simply by reducing the chance of attaching a biotin in the IgG binding site. The aim should be to have the lowest amount of double-biotinylated species to have the most active ligand, while at the same time the highest amount of proteins is labeled with a single molecule to keep an efficient labeling procedure. In our example with FcγRIIb, the level of biotinylation is mainly driven by protein:biotin ratio and incubation pH. Most active ligand is mainly achieved by protein:biotin ratios of 1:0.5 and to a lesser extent at protein:biotin ratios of 1:1.25. However, this only impacts the total level of biotinylation and not the position of the coupled biotin. This supports the finding that minimizing the amount of proteins with two biotins attached is key in retaining activity. In addition, although pH was found to influence the degree of labeling, it was not found to be a significant factor in IgG binding. These conditions may vary from protein to protein, and therefore it is recommended to perform a small design of experiments study on other proteins.

In the end we tested whether the minimally labeled material will give us reliable affinity data in an IgG binding experiment. Steady state affinity measurement on minimally labeled Fcγ receptors matched with values that have been reported in literature. This finding strengthens our conclusion that a very minimal labeling of protein is recommended to retain the most active ligand on a sensor surface and excludes random immobilization by a direct amine coupling method.

Acknowledgments

We thank George Ye for the purification of Fcγ receptors and performing the DoE on biotinylation on all samples. We would also like to thank Dr. Mark Eggink for the critical review of the manuscript, especially the mass spectrometry part, and Dr. Siem Heisterkamp for the helpful discussions on the statistical data analysis and interpretation. We thank EFRO Province of Gelderland and Overijssel, the Netherlands for giving us the opportunity to financially support the research project.

Appendix A IgG binding to biotinylated Fcγ receptors

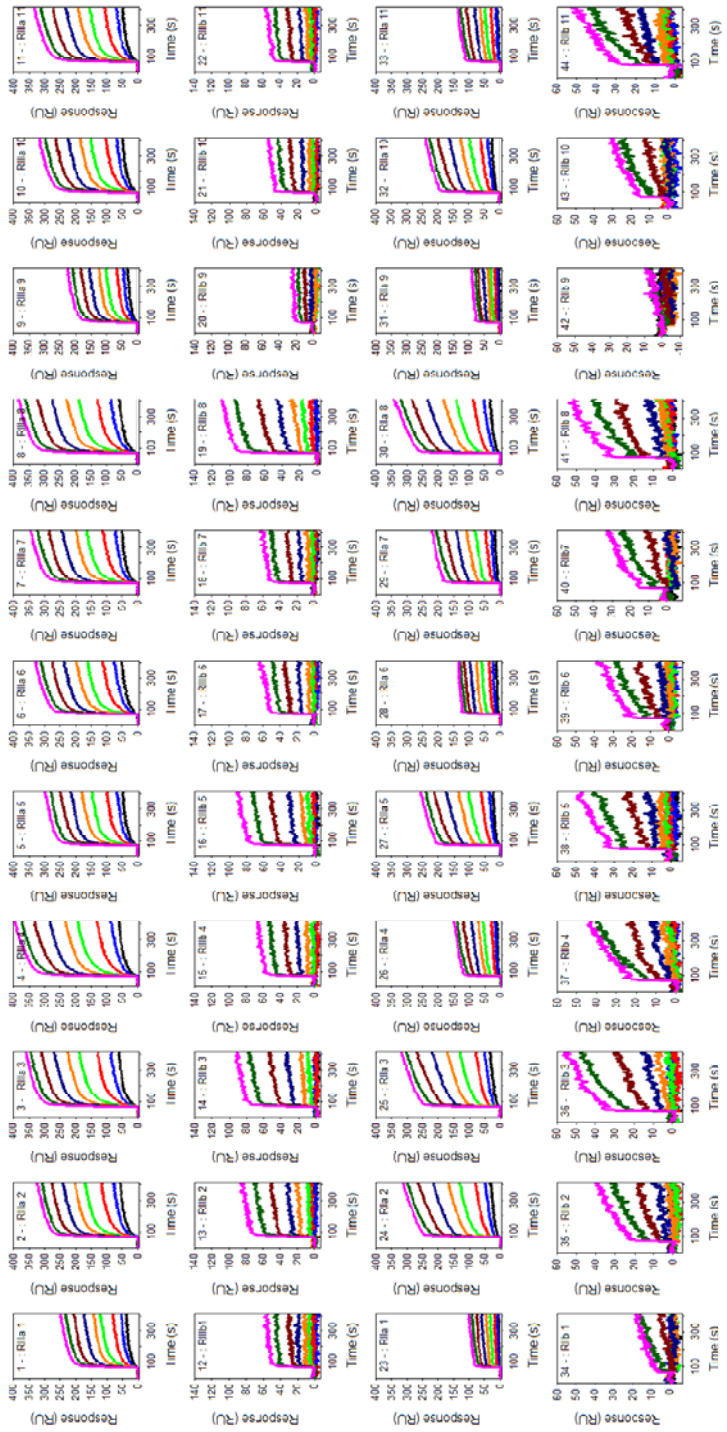

Figure 5.A.1 *Sensorgrams of IgG binding to immobilized biotinylated Fcγ receptors. Dilution series of IgG between 25 nM and 6.65 µM were injected on each of the Fcγ receptors. Samples that were biotinylated in eleven different biotinylation conditions of FcγRIIIa (row 1), FcγRIIIb (row 2), FcγRIIa (row 3) and FcγRIIb (row 4) were immobilized on a streptavidin sensor at similar ligand densities. X-axis displays the time in seconds; response in resonance units (RU) is displayed at Y-axes where per row the axis is at the same scale. Intensities after 20 minutes were compared between biotinylation conditions, although no steady state was reached at that point.*

Appendix B Statistical data analysis

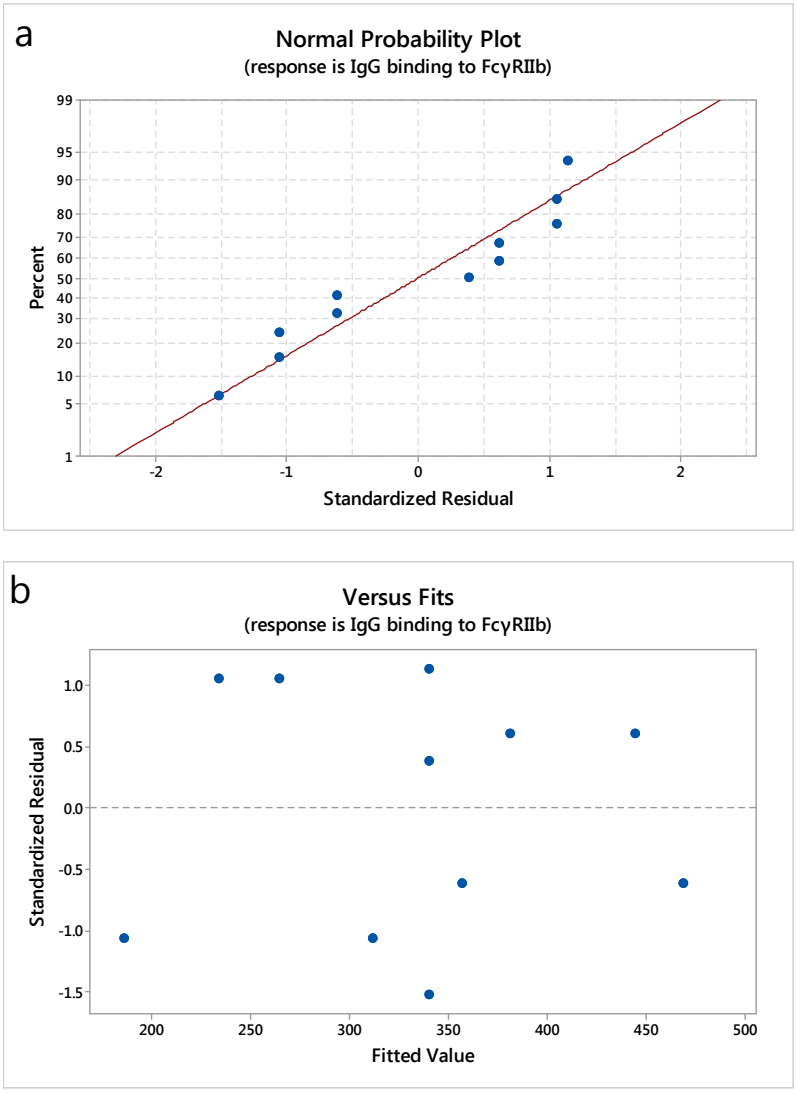

Figure 5.B.1 *Normal probability plot (a) and plot of standardized residuals versus fits (b) are shown to support the appropriateness of the statistical analysis of the DoE for IgG binding to FcγRIIb. The standardized residuals in the normal probability plot (a) are linearly distributed and the standardized residuals plotted against the fitted values are randomly distributed (b). Both graphs indicate a proper statistical evaluation of the peptide biotinylation*

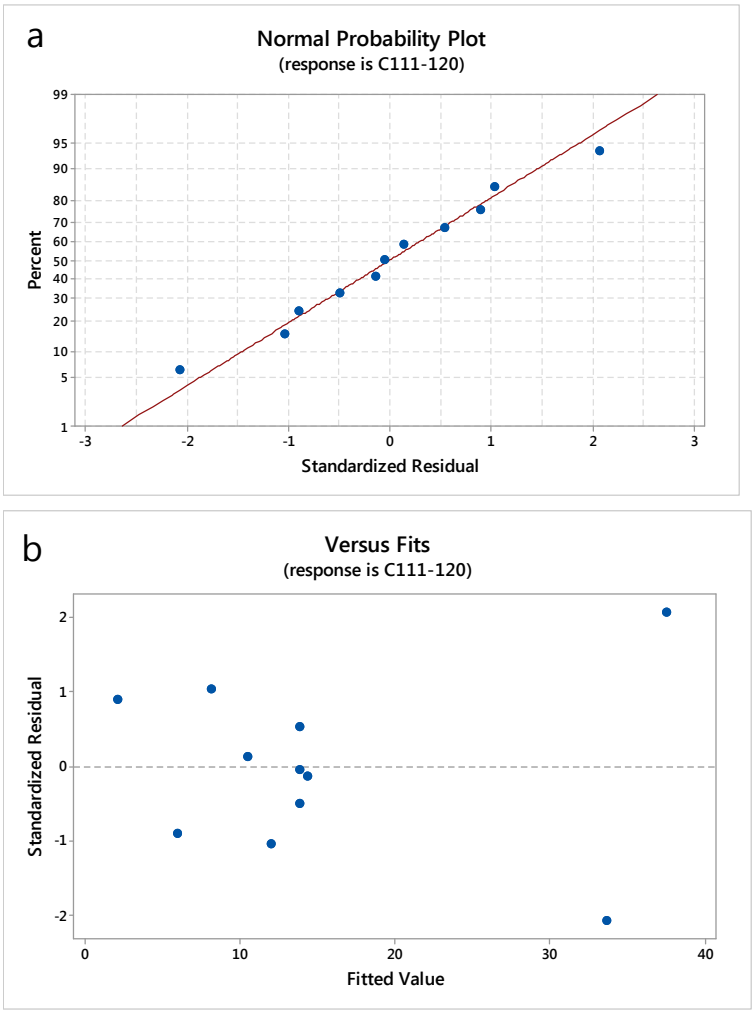

Figure 5.B.2 *Normal probability plot (a) and plot of standardized residuals versus fits (b) are shown to support the statistical analysis of the DoE for peptide biotinylation on C111-120. The standardized residuals in the normal probability plot (a) are linearly distributed and the standardized residuals plotted against the fitted values are randomly distributed (b). Both graphs indicate a proper statistical evaluation of the peptide biotinylation*

Appendix C Biotin distribution results

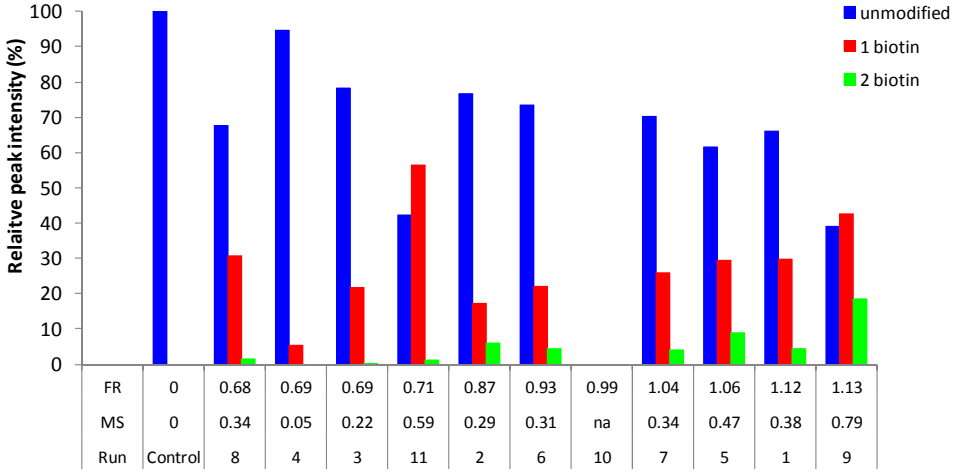

Figure 5.C.1 *Biotin distribution on FcγRIIIa expressed as relative intensities of the peaks in the mass spectra corresponding with the number of biotins on the protein. The X-axis represents the degree of labeling (DOL) as determined in the fluorescence assay (FR) and as determined by mass spectrometry (MS) and the run number of the DoE.*

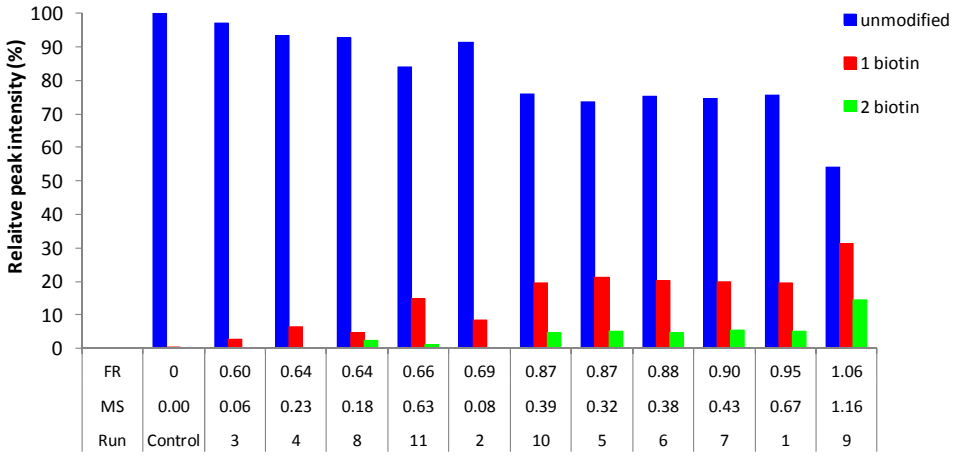

Figure 5.C.2 *Biotin distribution on FcγRIIIb expressed as relative intensities of the peaks in the mass spectra corresponding with the number of biotins on the protein. The X-axis represents the degree of labeling (DOL) as determined in the fluorescence assay (FR) and as determined by mass spectrometry (MS) and the run number of the DoE.*

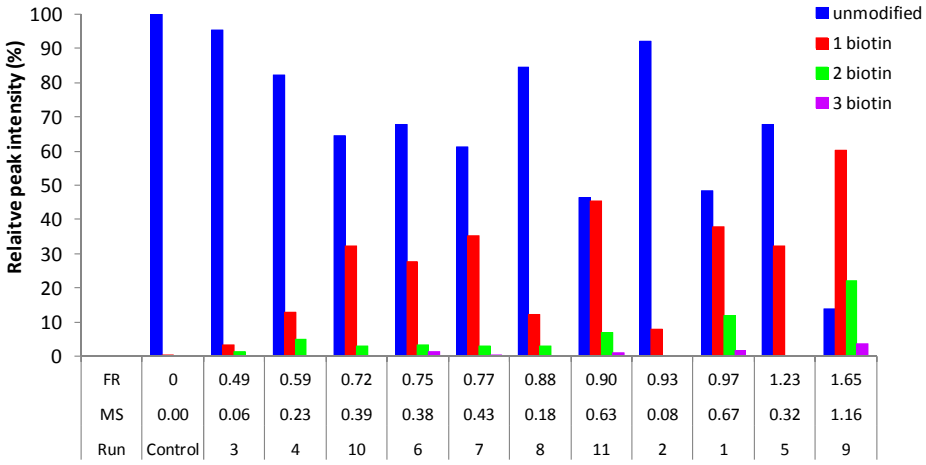

Figure 5.C.3 *Biotin distribution on FcγRIIa expressed as relative intensities of the peaks in the mass spectra corresponding with the number of biotins on the protein. The X-axis represents the degree of labeling (DOL) as determined in the fluorescence assay (FR) and as determined by mass spectrometry (MS) and the run number of the DoE.*

Appendix D MS and MS/MS results

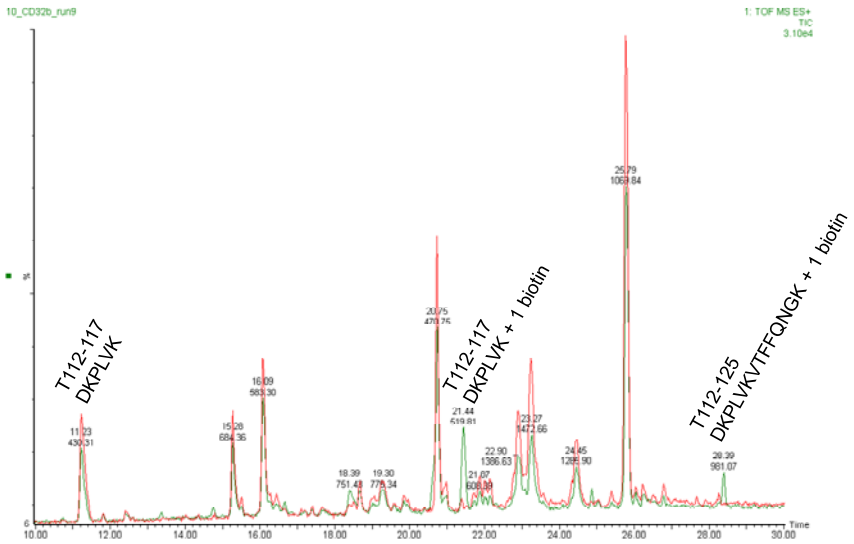

Figure 5.D.1 *Part of the tryptic peptide mapping chromatogram (10-30 minutes) of the control sample (red) and a biotinylated sample (green) showing the same peptide T112-117 without biotin (11.2 minutes), T112-117 with a biotin (21.4 minutes) and in a missed cleavage site T112-125 with a biotin (28.4 minutes).*

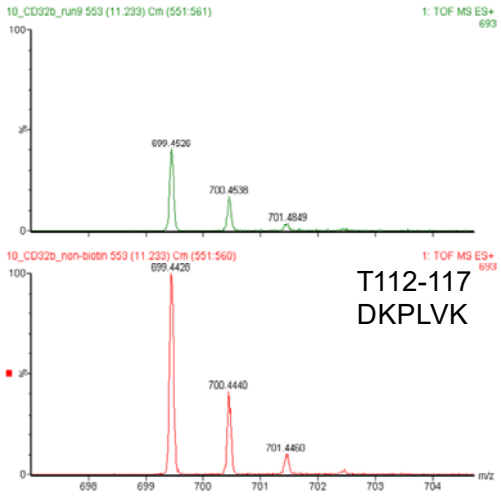

Figure 5.D.2 *Mass spectrum corresponding to the peaks at 11.2 minutes of the control sample (red) and the biotinylated sample (green), showing a decrease in peak intensity of the unmodified peptide T112-117 in the biotinylated sample, and no peaks of the biotinylated peptides T112-117 and T112-125 in the control sample.*

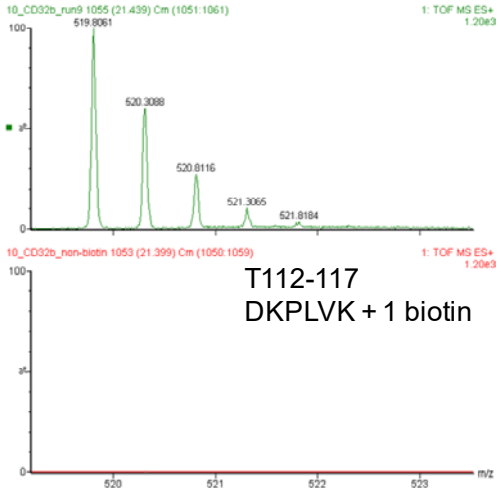

Figure 5.D.3 *Mass spectra corresponding to the peaks at 21.4 minutes of the control sample (red) and the biotinylated sample (green), showing no peaks of the biotinylated peptide T112-117 in the control sample.*

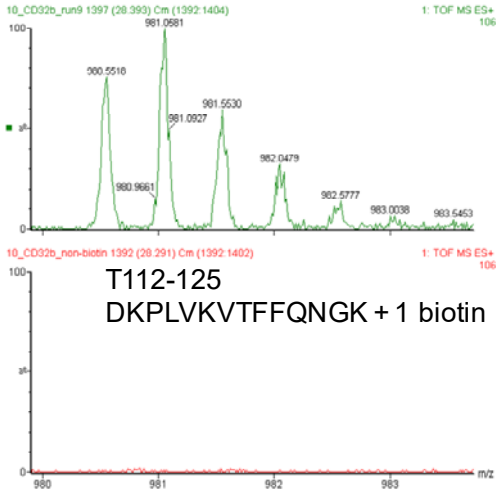

Figure 5.D.4 *Mass spectra corresponding to the peaks at 28.4 minutes of the control sample (red) and the biotinylated sample (green), showing no peaks of the biotinylated peptide T112-125 in the control sample.*

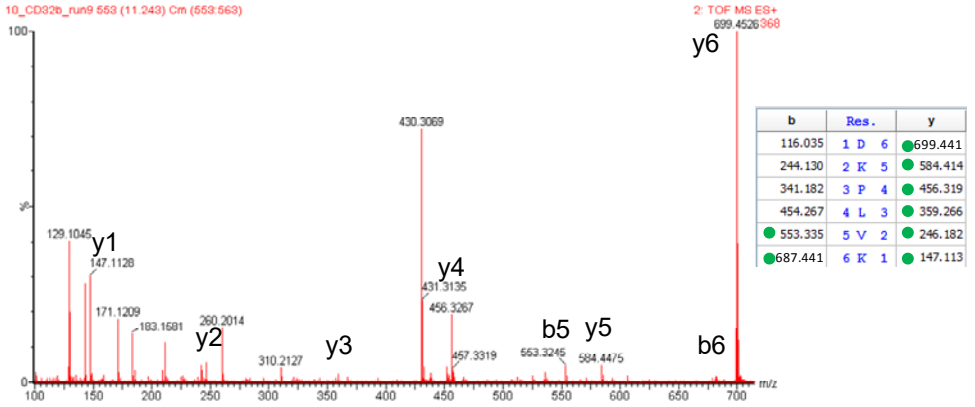

Figure 5.D.5 *MS/MS fragmentation spectrum of the unmodified peptide T112-117 including the expected fragment table with b- and y- ions for this peptide are shown at the right side. Green bullets indicate the fragment ions that are detected. The unmodified peptide T112-117 is confirmed by the full y-series that is detected.*

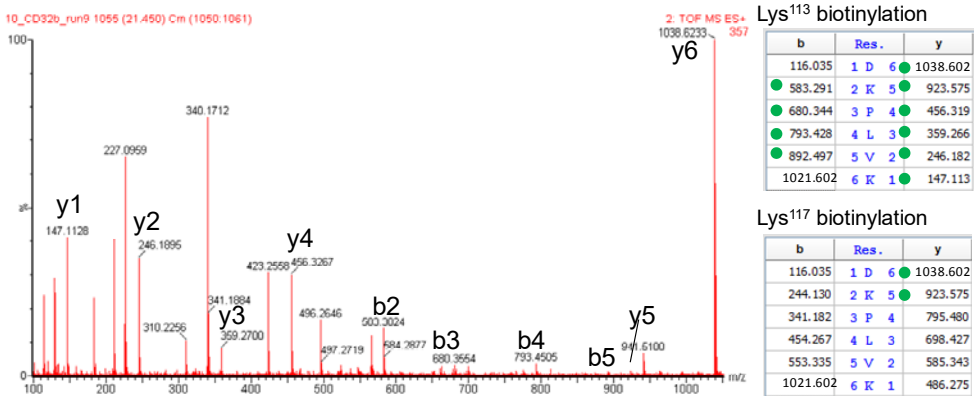

Figure 5.D.6 *MS/MS fragmentation spectrum of the biotinylated peptide T112-117 including the expected fragment tables with b- and y- ions for the different potential biotinylation sites are shown at the right side. Green bullets indicate the fragment ions that are detected. Biotinylation in peptide T112-117 is confirmed at Lys113 by the full y-series and 4 out of 6 b-series ions. The alternative biotinylation site (Lys117) can be eliminated as only 2 y-ions are detected, which are equal to the Lys113 biotinylation.*

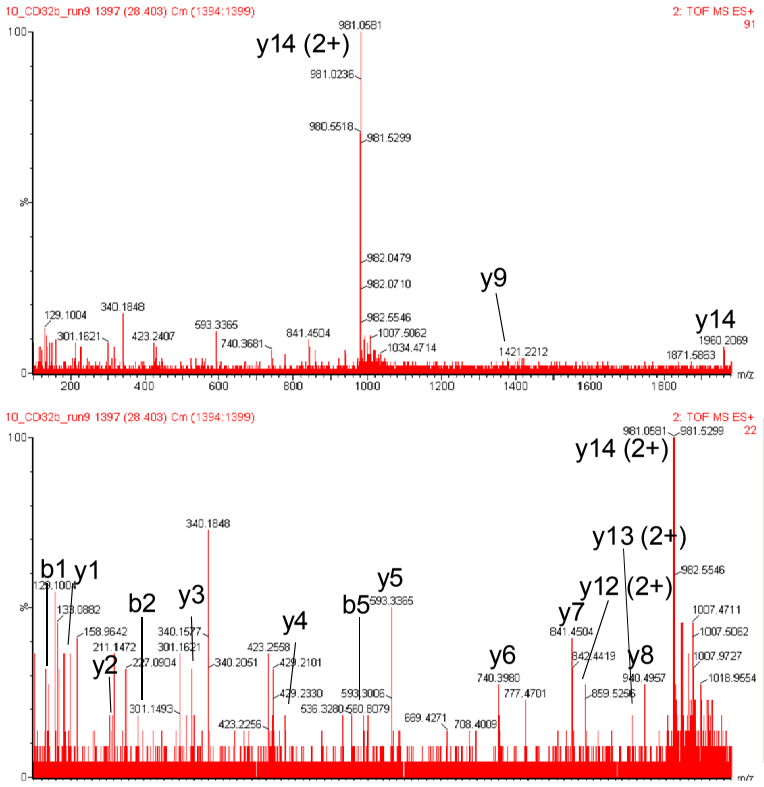

Lys^{113} biotinylation

b	Res.	y
116.035	1 D 14	1960.073
583.291	2 K 13	1845.046
680.344	3 P 12	1377.789
793.428	4 L 11	1280.737
892.497	5 V 10	1167.653
1020.592	6 K 9	1068.584
1119.660	7 V 8	940.489
1220.708	8 T 7	841.421
1367.776	9 F 6	740.373
1514.845	10 F 5	593.305
1642.903	11 Q 4	446.236
1756.946	12 N 3	318.178
1813.967	13 G 2	204.135
1943.073	14 K 1	147.113

Lys^{117} biotinylation

b	Res.	y
116.035	1 D 14	1960.073
244.130	2 K 13	1845.046
341.182	3 P 12	1716.951
454.267	4 L 11	1619.898
553.335	5 V 10	1506.814
1020.592	6 K 9	1407.746
1119.660	7 V 8	940.489
1220.708	8 T 7	841.421
1367.776	9 F 6	740.373
1514.845	10 F 5	593.305
1642.903	11 Q 4	446.236
1756.946	12 N 3	318.178
1813.967	13 G 2	204.135
1943.073	14 K 1	147.113

Lys^{125} biotinylation

b	Res.	y
116.035	1 D 14	1960.073
244.130	2 K 13	1845.046
341.182	3 P 12	1716.951
454.267	4 L 11	1619.898
553.335	5 V 10	1506.814
681.430	6 K 9	1407.746
780.498	7 V 8	1279.651
881.546	8 T 7	1180.582
1028.614	9 F 6	1079.535
1175.683	10 F 5	932.466
1303.741	11 Q 4	785.398
1417.784	12 N 3	657.339
1474.806	13 G 2	543.296
1943.073	14 K 1	486.275

Figure 5.D.7 *MS/MS fragmentation spectra of the biotinylated peptide T112-125 including the expected fragment tables with b- and y- ions for the different potential biotinylation sites are shown at the right side. Green bullets indicate the fragment ions that are detected. Biotinylation in peptide T112-125 is confirmed at position Lys117 by the nearly complete y-series. Both Lys113 and Lys125 biotinylation sites can be eliminated for this peptide due to the poor coverage of ions in the fragmentation spectrum.*

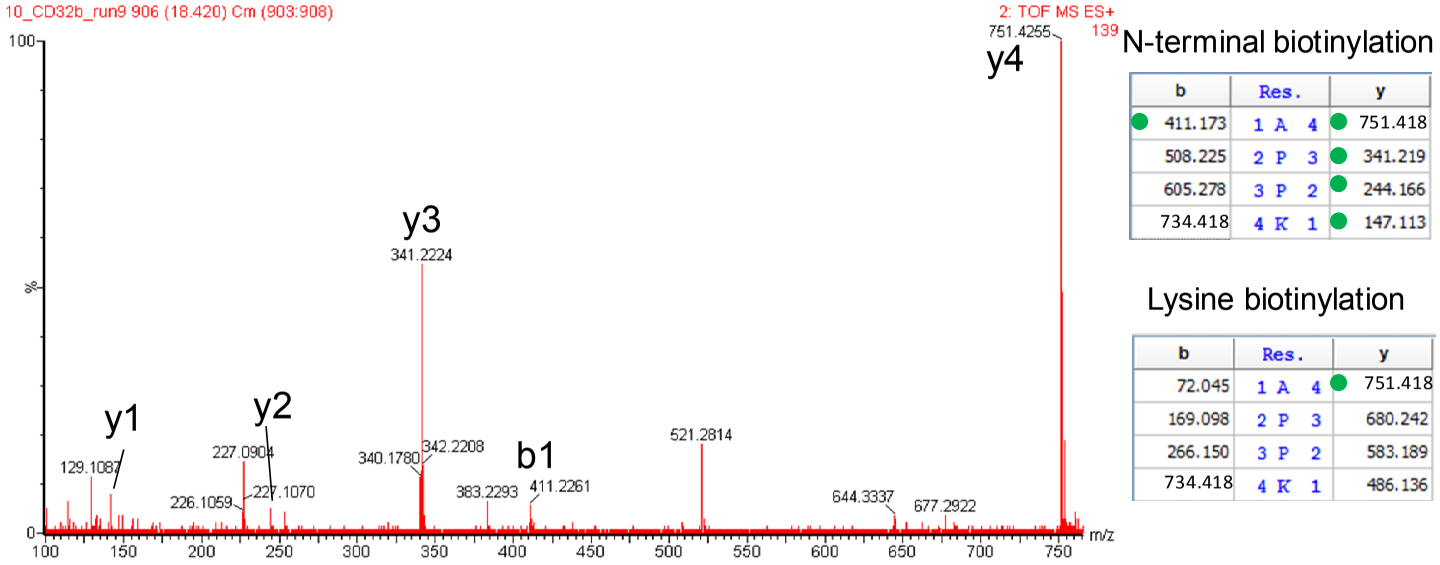

Figure 5.D.8 *MS/MS fragmentation spectra of peptide T1-4 modified with biotin. Fragmentation tables based on N-terminal biotinylation or lysine biotinylation are shown at the right side. The green bullets indicate which ions are found in the MS/MS spectrum, showing that the N-terminal alanine is biotinylated at peptide T1-4 as all y-ions can be assigned in the MS/MS spectrum.*

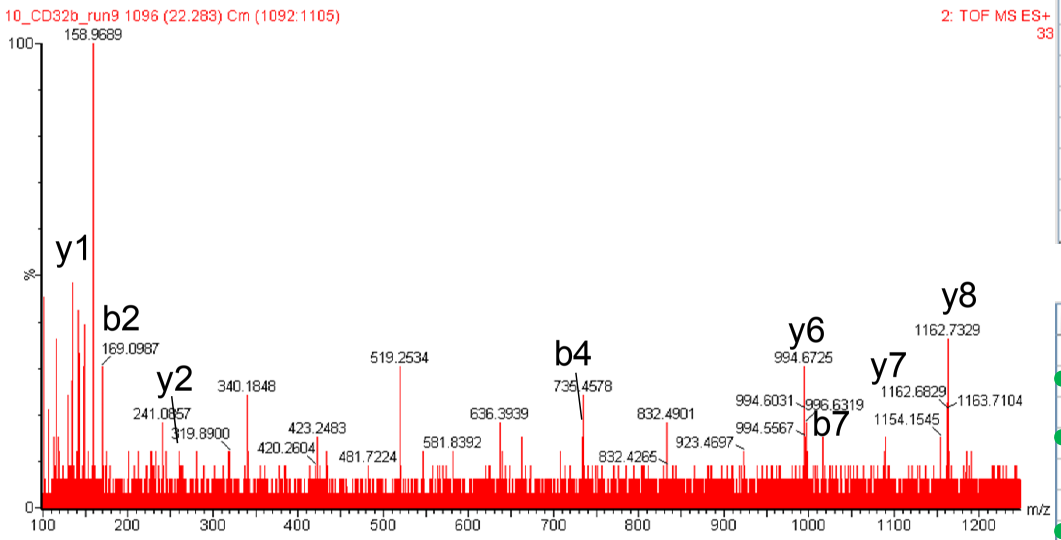

N-terminal biotinylation

b	Res.	y
411.174	1 A 8	1162.702
508.227	2 P 7	752.503
605.280	3 P 6	655.451
733.375	4 K 5	558.398
804.412	5 A 4	430.303
903.480	6 V 3	359.266
1016.564	7 L 2	260.197
1145.702	8 K 1	147.113

Lysine biotinylation

b	Res.	y
72.045	1 A 8	1162.702
169.098	2 P 7	1091.631
266.150	3 P 6	994.578
733.373	4 K 5	897.526
804.410	5 A 4	430.303
903.479	6 V 3	359.266
1016.563	7 L 2	260.197
1145.702	8 K 1	147.113

Figure 5.D.9 *MS/MS fragmentation spectra of peptide T1-8 modified with biotin . Fragmentation tables based on N-terminal biotinylation or lysine biotinylation are shown at the right side. The green bullets indicate which ions are found in the MS/MS spectrum, showing that Lys[4] is biotinylated in peptide T1-8 because of ions y6, y7 and b2 that can be assigned in this fragmentation spectrum only.*

Appendix E Chymotrypsin digestion

Table 5.E.1 *Chymotryptic peptides of FcγRIIb which are modified with biotin, the corresponding masses and retention time in the EIC chromatograms*

Peptide	Amino acid sequence	Residue(s)	Modifi-cation	$[M+H]^+$	m/z	charge	t_R (min)
C1-7	APPKAVL	Ala^1 Lys^4	-	695.4	695.4	1	16.4
			1 biotin	1034.6	517.8	2	23.5
C8-24	KLEPQWINVLQED SVTL	Lys^8	-	2012.0	1006.5	2	29.8
			1 biotin	2351.2	1176.1	2	32.7
C57-66	KANNNDSGEY	Lys^{57}	-	1112.4	556.7	2	10.1
			1 biotin	1451.6	726.3	2	17.4
C111-120	KDKPLVKVTF	Lys^{111} Lys^{113} Lys^{117}	-	1174.8	587.9	2	20.0
			1 biotin	1513.8	757.4	2	23.7
			1 biotin	1513.8	757.4	2	24.3
			1 biotin	1513.8	757.4	2	24.6
			2 biotin	1853.0	927.0	2	27.3
			2 biotin	1853.0	927.0	2	27.9
			2 biotin	1853.0	927.0	2	28.3
C121-129	FQNGKSKKF	Lys^{125} Lys^{127} Lys^{128}	-	1083.6	542.3	2	12.3
			1 biotin	1422.8	711.9	2	18.7
			1 biotin	1422.8	711.9	2	19.6
C161-173	SSKPVTITVQAPH	Lys^{163}	-	1364.8	682.9	2	16.6
			1 biotin	1704.0	852.5	2	21.5

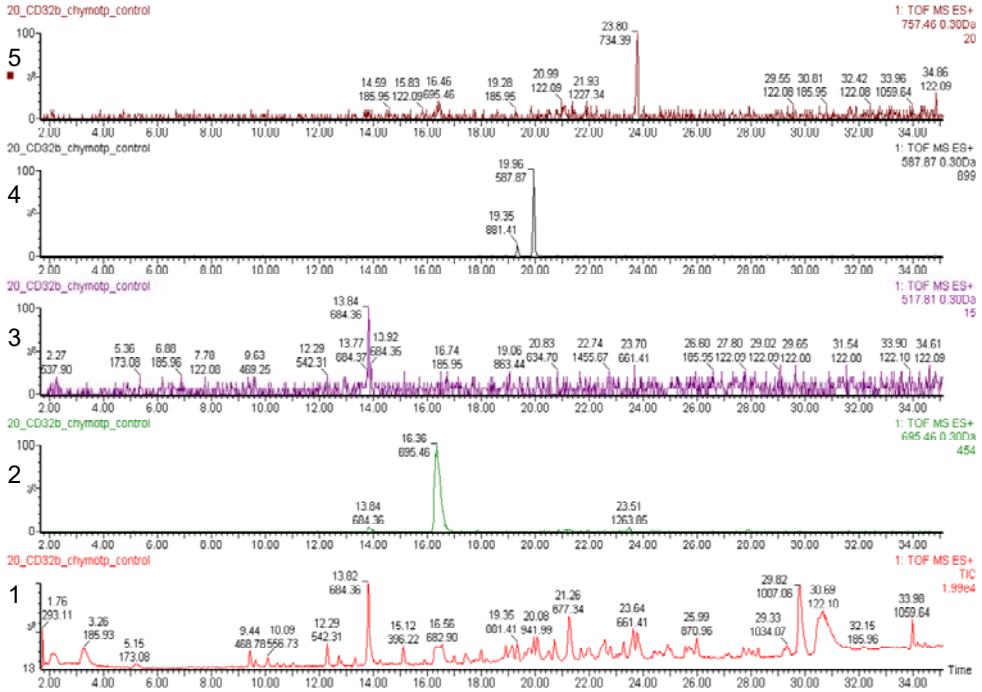

Figure 5.E.1 *Chymotryptic digestion of FcγRIIb control sample. Total ion current chromatogram (1) and extracted ion chromatograms of peptide C1-7 without biotin (2) at 16.4 minutes and C1-7+biotin (3) where no peak with the correct mass is detected, peptide C111-120 without biotin (4) at 19.9 minutes and C111-120+biotin (5) where no peak with the correct mass is detected.*

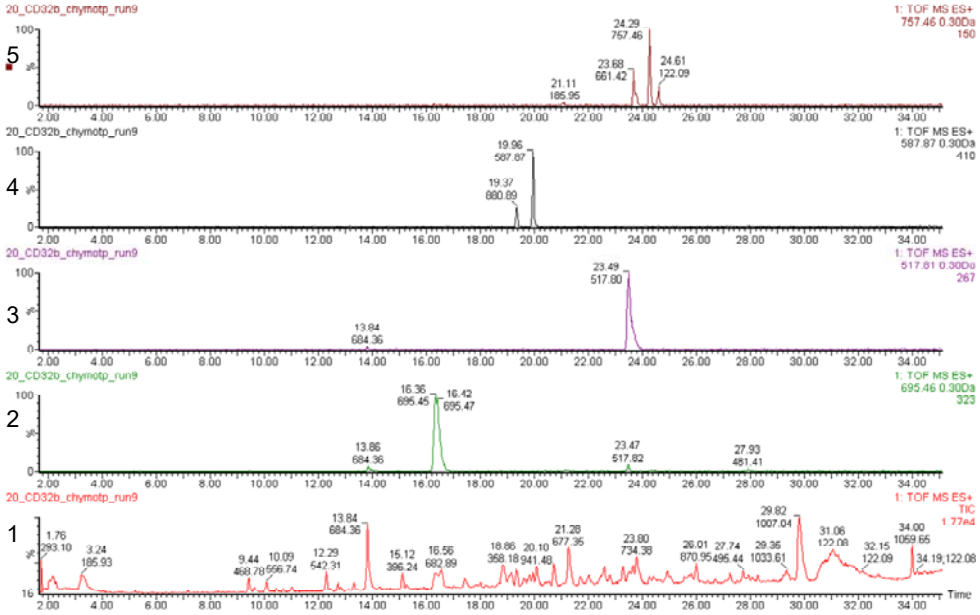

Figure 5.E.2 *Chymotryptic digestion of FcγRIIb biotinylated sample. Total ion current chromatogram (1) and extracted ion chromatograms of peptide C1-7 without biotin (2) at 16.4 minutes and C1-7+biotin (3) at 23.5 minutes, peptide C111-120 without biotin (4) at 19.9 minutes and C111-120+biotin (5) at 23.9, 24.3 and 24.6 minutes. Peptide C111-120 contains three lysines that can possibly be biotinylated and these can be resolved on the reversed phase C18 column, appearing as three separate peaks with the same mass.*

References

1. Zhen, G., Eggli, V., Voros, J., Zammaretti, P., Textor, M., Glockshuber, R., and Kuennemann, E. Immobilization of the enzyme beta-lactamase on biotin-derivatized poly(L-lysine)-g-poly(ethylene glycol)-coated sensor chips: a study on oriented attachment and surface activity by enzyme kinetics and in situ optical sensing. Langmuir 23-11-2004; 20(24): 10464-10473

2. Rich, R. L., Papalia, G. A., Flynn, P. J., Furneisen, J., Quinn, J., Klein, J. S., Katsamba, P. S., Waddell, M. B., Scott, M., Thompson, J., Berlier, J., Corry, S., Baltzinger, M., Zeder-Lutz, G., Schoenemann, A., Clabbers, A., Wieckowski, S., Murphy, M. M., Page, P., Ryan, T. E., Duffner, J., Ganguly, T., Corbin, J., Gautam, S., Anderluh, G., Bavdek, A., Reichmann, D., Yadav, S. P., Hommema, E., Pol, E., Drake, A., Klakamp, S., Chapman, T., Kernaghan, D., Miller, K., Schuman, J., Lindquist, K., Herlihy, K., Murphy, M. B., Bohnsack, R., Andrien, B., Brandani, P., Terwey, D., Millican, R., Darling, R. J., Wang, L., Carter, Q., Dotzlaf, J., Lopez-Sagaseta, J., Campbell, I., Torreri, P., Hoos, S., England, P., Liu, Y., Abdiche, Y., Malashock, D., Pinkerton, A., Wong, M., Lafer, E., Hinck, C., Thompson, K., Primo, C. D., Joyce, A., Brooks, J., Torta, F., Bagge Hagel, A. B., Krarup, J., Pass, J., Ferreira, M., Shikov, S., Mikolajczyk, M., Abe, Y., Barbato, G., Giannetti, A. M., Krishnamoorthy, G., Beusink, B., Satpaev, D., Tsang, T., Fang, E., Partridge, J., Brohawn, S., Horn, J., Pritsch, O., Obal, G., Nilapwar, S., Busby, B., Gutierrez-Sanchez, G., Gupta, R. D., Canepa, S., Witte, K., Nikolovska-Coleska, Z., Cho, Y. H., D'Agata, R., Schlick, K., Calvert, R., Munoz, E. M., Hernaiz, M. J., Bravman, T., Dines, M., Yang, M. H., Puskas, A., Boni, E., Li, J., Wear, M., Grinberg, A., Baardsnes, J., Dolezal, O., Gainey, M., Anderson, H., Peng, J., Lewis, M., Spies, P., Trinh, Q., Bibikov, S., Raymond, J., Yousef, M., Chandrasekaran, V., Feng, Y., Emerick, A., Mundodo, S., Guimaraes, R., McGirr, K., Li, Y. J., Hughes, H., Mantz, H., Skrabana, R., Witmer, M., Ballard, J., Martin, L., Skladal, P., Korza, G., Laird-Offringa, I., Lee, C. S., Khadir, A., Podlaski, F., Neuner, P., Rothacker, J., Rafique, A., Dankbar, N., Kainz, P., Gedig, E., Vuyisich, M., Boozer, C., Ly, N., Toews, M., Uren, A., Kalyuzhniy, O., Lewis, K., Chomey, E., Pak, B. J., and Myszka, D. G. A global benchmark study using affinity-based biosensors. Anal.Biochem. 15-3-2009; 386(2): 194-216

3. Harrison, A., Liu, Z., Makweche, S., Maskell, K., Qi, H., and Hale, G. Methods to measure the binding of therapeutic monoclonal antibodies to the human Fc receptor FcgammaRIII (CD16) using real time kinetic analysis and flow cytometry. J.Pharm.Biomed.Anal. 7-4-2012; 63 23-28

4. Dorion-Thibaudeau, J., Raymond, C., Lattova, E., Perreault, H., Durocher, Y., and De, Crescenzo G. Towards the development of a surface plasmon resonance assay to evaluate the glycosylation pattern of monoclonal antibodies using the extracellular domains of CD16a and CD64. J.Immunol.Methods 2014; 408 24-34

5. Chaiet, L. and Wolf, F. J. THE PROPERTIES OF STREPTAVIDIN, A BIOTIN-BINDING PROTEIN PRODUCED BY STREPTOMYCETES. Arch.Biochem.Biophys. 20-7-1964; 106 1-5

6. Weber, P. C., Ohlendorf, D. H., Wendoloski, J. J., and Salemme, F. R. Structural origins of high-affinity biotin binding to streptavidin. Science 6-1-1989; 243(4887): 85-88

7. Smelyanski, L. and Gershoni, J. M. Site directed biotinylation of filamentous phage structural proteins. Virol.J. 2011; 8 495-

8. Gaudriault, G. and Vincent, J. P. Selective labeling of alpha- or epsilon-amino groups in peptides by the Bolton-Hunter reagent. Peptides 1992; 13(6): 1187-1192

9. Selo, I., Negroni, L., Creminon, C., Grassi, J., and Wal, J. M. Preferential labeling of alpha-amino N-terminal groups in peptides by biotin: application to the detection of specific anti-peptide antibodies by enzyme immunoassays. J.Immunol.Methods 15-12-1996; 199(2): 127-138

10. Papalia, G. and Myszka, D. Exploring minimal biotinylation conditions for biosensor analysis using capture chips. Anal.Biochem. 2010; 403(1-2): 30-35

11. Nimmerjahn, F. and Ravetch, J. V. Fcgamma receptors as regulators of immune responses. Nat.Rev.Immunol. 2008; 8(1): 34-47

12. Vidarsson, G., Dekkers, G., and Rispens, T. IgG subclasses and allotypes: from structure to effector functions. Front Immunol. 2014; 5 520-

13. van Sorge, N. M., van der Pol, W. L., and van de Winkel, J. G. FcgammaR polymorphisms: Implications for function, disease susceptibility and immunotherapy. Tissue Antigens 2003; 61(3): 189-202

14. Mellor, J. D., Brown, M. P., Irving, H. R., Zalcberg, J. R., and Dobrovic, A. A critical review of the role of Fc gamma receptor polymorphisms in the response to monoclonal antibodies in cancer. J.Hematol.Oncol. 2013; 6 1-

15. Bruhns, P., Iannascoli, B., England, P., Mancardi, D. A., Fernandez, N., Jorieux, S., and Daeron, M. Specificity and affinity of human Fcgamma receptors and their polymorphic variants for human IgG subclasses. Blood 16-4-2009; 113(16): 3716-3725

16. Lu, J., Ellsworth, J. L., Hamacher, N., Oak, S. W., and Sun, P. D. Crystal structure of Fcgamma receptor I and its implication in high affinity gamma-immunoglobulin binding. J.Biol.Chem. 25-11-2011; 286(47): 40608-40613

17. Ramsland, P. A., Farrugia, W., Bradford, T. M., Sardjono, C. T., Esparon, S., Trist, H. M., Powell, M. S., Tan, P. S., Cendron, A. C., Wines, B. D., Scott, A. M., and Hogarth, P. M. Structural basis for Fc gammaRIIa recognition of human IgG and formation of inflammatory signaling complexes. J.Immunol. 15-9-2011; 187(6): 3208-3217

18. Sondermann, P., Huber, R., Oosthuizen, V., and Jacob, U. The 3.2-A crystal structure of the human IgG1 Fc fragment-Fc gammaRIII complex. Nature 20-7-2000; 406(6793): 267-273

19. Sondermann, P., Huber, R., and Jacob, U. Crystal structure of the soluble form of the human fcgamma-receptor IIb: a new member of the immunoglobulin superfamily at 1.7 A resolution. EMBO J. 1-3-1999; 18(5): 1095-1103

20. Hulett, M. D., Witort, E., Brinkworth, R. I., McKenzie, I. F., and Hogarth, P. M. Identification of the IgG binding site of the human low affinity receptor for IgG Fc gamma RII. Enhancement and ablation of binding by site-directed mutagenesis. J.Biol.Chem. 27-5-1994; 269(21): 15287-15293

21. Hulett, M. D., Witort, E., Brinkworth, R. I., McKenzie, I. F., and Hogarth, P. M. Multiple regions of human Fc gamma RII (CD32) contribute to the binding of IgG. J.Biol.Chem. 8-9-1995; 270(36): 21188-21194

22. Zhang, Y., Boesen, C. C., Radaev, S., Brooks, A. G., Fridman, W. H., Sautes-Fridman, C., and Sun, P. D. Crystal structure of the extracellular domain of a human Fc gamma RIII. Immunity. 2000; 13(3): 387-395

23. Sondermann, P., Jacob, U., Kutscher, C., and Frey, J. Characterization and crystallization of soluble human Fc gamma receptor II (CD32) isoforms produced in insect cells. Biochemistry 29-6-1999; 38(26): 8469-8477

24. Jung, S. T., Kang, T. H., and Georgiou, G. Efficient expression and purification of human aglycosylated Fcgamma receptors in Escherichia coli. Biotechnol.Bioeng. 1-9-2010; 107(1): 21-30

25. Hayes, J. M., Frostell, A., Cosgrave, E. F., Struwe, W. B., Potter, O., Davey, G. P., Karlsson, R., Anneren, C., and Rudd, P. M. Fc gamma receptor glycosylation modulates the binding of IgG glycoforms: a requirement for stable antibody interactions. J.Proteome.Res. 5-12-2014; 13(12): 5471-5485

26. Champion, T. and Beck, A. Capture of the human IgG1 antibodies by protein A for the kinetic study of h-IgG/FcgammaR interaction using SPR-based biosensor technology. Methods Mol.Biol. 2013; 988 331-343

27. Azim-Zadeh, O., Hillebrecht, A., Linne, U., Marahiel, M. A., Klebe, G., Lingelbach, K., and Nyalwidhe, J. Use of biotin derivatives to probe conformational changes in proteins. J.Biol.Chem. 27-7-2007; 282(30): 21609-21617

28. Appel, W. Chymotrypsin: molecular and catalytic properties. Clin.Biochem. 1986; 19(6): 317-322

29. Patel, R. and Andrien, B. A., Jr. Kinetic analysis of a monoclonal therapeutic antibody and its single-chain homolog by surface plasmon resonance. Anal.Biochem. 1-1-2010; 396(1): 59-68

Chapter 5

CHAPTER 6

Rapid screening of IgG quality attributes: effects on Fc receptor binding

The contents of this chapter have been submitted as:

Karin P.M. Geuijen, Cindy Oppers-Tiemissen, David F. Egging, Peter J. Simons, Louis Boon, Richard B.M. Schasfoort, Michel H.M. Eppink

Rapid screening of IgG quality attributes: effects on Fc receptor binding

Abstract

Fcγ receptor and neonatal Fc receptor (FcRn) interactions of therapeutic antibodies are measured *in vitro* as indicators of antibody functional performance. The Fc tail interactions are important for the efficacy and safety of therapeutic antibodies. High-throughput binding studies on each of the human Fcγ receptor classes (FcγRI, FcγRIIa, FcγRIIb, FcγRIIIa and FcγRIIIb) as well as FcRn have been developed and performed with human IgG after stress-induced modifications to identify potential impact *in vivo*. Interestingly we found that asparagine deamidation reduced the binding to the low affinity Fcγ receptors (FcγRIIa, FcγRIIb, FcγRIIIa and FcγRIIIb), while FcγRI and FcRn binding were not impacted. Deglycosylation completely abolished the binding to all Fcγ receptors, but showed no impact on the binding to FcRn. On the other hand, afucosylation only impacted the binding to FcγRIIIa and FcγRIIIb. Methionine oxidation at levels below 7%, multiple freeze-thaw cycles and short-term thermal/shake stress did not influence binding to any of the Fc receptors. The presence of high molecular weight species, or aggregates, disturbed measurements in these binding assays, i.e. a few percent (up to 5%) of aggregates in IgG samples changed the binding and kinetics to each of the Fc receptors. Overall, the screening assays as designed in this manuscript prove that rapid and multiplexed binding assays may be a valuable tool for lead optimization, process development, in-process controls and for biosimilarity assessment of IgGs during development and manufacturing of therapeutic IgGs.

Introduction

Therapeutic antibodies, like IgGs, are one of the largest classes of modern biopharmaceuticals and the market for these products continues to grow year by year.[1] Interactions of IgGs with effector cells through Fcγ receptors are often considered a mode of action of therapeutic antibodies.[2-4] Fcγ receptors are cell surface receptors that can be found on innate immune effector cells such as natural killer cells and macrophages. A therapeutic IgG binds to a membrane-bound antigen on target cells by its complementary determining regions (CDRs) in the variable domain, while the Fc region in the constant domain of that same IgG can bind to various Fcγ receptors on effector cells, which could lead to effector function, like antibody-dependent cellular cytotoxicity (ADCC) or phagocytosis (ADCP). Therefore, binding of therapeutic antibodies to Fcγ receptors should be evaluated as part of the critical quality attribute assessment.[2]

Different Fcγ receptor subclasses are known to be present on human effector cells: the high affinity FcγRI (CD64) and the low affinity receptors FcγRIIa (CD32a), FcγRIIb (CD32b), FcγRIIIa (CD16a) and FcγRIIIb (CD16b).[5,6] Within these five subclasses different polymorphic variants exist, which, in some cases, influence binding of IgG to these receptors.[7] Furthermore, the neonatal Fc receptor (FcRn) determines the half-life of IgGs in the bloodstream. Binding of FcRn to IgG takes place in the endosome at acidic pH, and the IgG is then recycled back into plasma at neutral pH, thereby preventing lysosomal degradation. Recent studies have investigated the correlation between the *in vitro* binding of IgGs to FcRn and their corresponding serum half-life.[8,9] Datta-Mannan et al.[10] suggest that the *in vitro – in vivo* correlation of the FcRn binding cannot always directly be made, since IgG target binding may influence elimination of the IgG from the system as well. FcRn does not belong to the Fcγ receptor subclasses and binds to a different region in the IgG [11] than IgG regions recognized by Fcγ receptors. We will refer to Fc interactions as a general term, which includes both the Fcγ interactions and FcRn interactions.

Therapeutic IgGs are prone to many different post-translational modifications during production and processing, which may have an impact on the Fc tail functionality. Monitoring the levels of modifications throughout the entire development, production and marketing of IgGs are required from a regulatory perspective. Several modifications on IgGs are known to affect the binding to Fc receptors, such as aglycosylation [12-16], differential glycosylation (i.e. galactosylation [12,14,15], sialylation [12] and fucosylation [13,16-19], methionine oxidation [20-23] and aggregation [15,23-27]. We investigated the effects of these modifications,

and additionally looked into effects of asparagine deamidation, heat/shake stress and repeated freeze-thaw cycles on IgGs to Fc receptor binding. Stress studies were performed to accelerate modifications on an IgG1 and these were measured on all Fc receptors and quantified by HPLC, CE or mass spectrometry as a reference method. Modifications that were introduced were kept at levels that are likely to be expected during actual in-process measurements or shelf-life studies. i.e. generally not higher than 10% modification.

The aim of our study is to develop a screening assay that would rapidly measure IgG binding to the different Fcγ receptors and FcRn as part of critical quality attribute (CQA) assessments during lead optimization studies and in-process control. However, the biological differences in binding properties between Fc receptors prevented the development of a single screening sensor. Affinity ranges of FcRn and FcγRI (nM) compared to FcγRIIIa, FcγRIIIb, FcγRIIa and FcγRIIb (μM) limited the analysis of IgGs in proper concentration ranges for each of the Fc receptor in a single measurement. On top of that, kinetics of IgG binding to FcRn follow a completely different profile (association at pH 6, dissociation at both pH 6 and pH 7.4) compared to the other Fcγ receptors (association and dissociation at pH 7.4) and this could not be combined into a single assay. Therefore, Fcγ receptor interactions of FcγRIIa, FcγRIIb, FcγRIIIa and FcγRIIIb were simultaneously measured in an SPR imaging set-up, while a separate SPR method for FcγRI binding and a BLI method for FcRn binding were developed, all aimed at rapid measurements of IgG samples for high throughput screening purposes.

Two possible assay set-ups were considered: Fc receptor or IgG immobilization as ligand at the sensor surface. Preferably the Fc receptors are used as ligand at the sensor surface, as this may best reflect the binding of Fc receptor to IgG *in vivo*, with Fc receptors present at cell surfaces. However, limited receptor stability of Fcγ receptors at the sensor surface (unpublished results) is most likely the reason why most literature about SPR-based or BLI-based Fcγ receptor binding studies is based on either capture approaches where fresh ligand is captured each cycle [12,15,16,24,25] or where IgG is immobilized at the sensor surface followed by Fcγ receptor injections.[12,28] We have developed a rapid multiplexed SPR sensor with the Fcγ receptors captured by biotin-streptavidin capture where ligand instability was mitigated. This method was qualified for proper performance, followed by analysis of stressed IgG samples to investigate the effects of IgG degradation on previously mentioned stress conditions on Fcγ receptor binding. The same stressed IgG samples were furthermore analyzed on the screening assays for FcγRI and FcRn. We found effects of

deamidation on Fc receptor binding that, to the author's knowledge, have not been described previously in literature.

Materials and methods

Recombinant proteins

The monoclonal antibody, a human IgG1, was produced and purified by Synthon Biopharmaceuticals BV. IgG1 samples with aberrant fucosylation profiles were a kind gift from Bioceros BV. The IgG samples from both sources have the same amino acid sequence and were produced in CHO cells.

Human Fcγ receptors FcγRIIIa, FcγRIIIb, FcγRIIa and FcγRIIb were produced in a HEK293 expression system at Synthon Biopharmaceuticals BV. Receptors were expressed with a C-terminal His-tag followed by IMAC purification as previously described [29]. Human FcRn (Human FCGRT & B2M heterodimer) and human FcγRI with a C-terminal AVI-tag and C-terminal His-tag were purchased from Sino Biological.

Preparation of stressed human IgG samples

IgG1 samples were exposed to accelerated oxidation by mixing 200 µL of 25 mg/mL IgG1 with 4 µL (0.1%); 10 µL (0.25%) or 20 µL (0.5%) 5% H_2O_2 (Sigma-Aldrich) and kept at room temperature for 10 minutes. Then, 5 µL catalase (4 U) (Sigma-Aldrich) was added and kept at room temperature for 5 minutes. Accelerated deamidation was induced on the IgG1 by keeping the protein in 50 mM sodium phosphate buffer pH 8 at 20 mg/mL for 48, 72 or 96 hours at 40°C. Samples were neutralized to pH 7.2 after incubation. As a control, samples were placed at the same temperature and time in neutral pH (HEPES-buffered saline (HBS) buffer pH 7.2).

Thermal/shake stress was performed on the IgG1 samples by placing them at 40°C at 1000 rpm in HBS buffer pH 7.2 for 1, 4, 24, 32, 48 or 72 hours. Another thermal/shake stress was applied by placing the IgG1 samples at 70°C or 75°C for 15 minutes at 300 rpm.

Freeze-thaw stress was applied by placing 250 µL of IgG1 at 25 mg/mL in HBS pH 7.2 buffer at -80°C. Samples were thawed and frozen again from 1 up to 10 freeze-thaw cycles in total.

The IgG1 sample was deglycosylated by mixing 50 µL sample (25 mg/mL) with 130 µL 200 mM sodium phosphate buffer pH 6.8. Then, 20 µL PNGase F solution was added and the solution was incubated at 37°C for 24 hours.

Characterization of stressed samples

The levels of methionine oxidation and asparagine deamidation in the stressed samples were determined using a tryptic peptide mapping followed by separation on a reversed phase C18 column and either UV or MS detection was used for quantitation.

Aggregation levels were determined based on a SEC-HPLC separation. The deglycosylated sample was checked for complete removal of glycans using CE-SDS under non-reducing conditions.

Antigen target binding was verified on a Biacore T200 instrument (GE Life Sciences). Recombinant human antigen (R&D systems) was immobilized on a CM5 chip (GE life sciences) at 2.5 µg/mL in sodium acetate pH 4.0. MabSelectSure (GE Life Sciences) was immobilized on the same sensor at 40 µg/mL in sodium acetate pH 4.5 for total IgG1 determination. A contact time of 1200 seconds and 360 seconds were applied respectively and immobilization was performed at 25°C. IgG1 binding to antigen target and MabSelectSure were determined at 37°C with an association time of 42 seconds and dissociation time of 30 seconds and a flow rate of 10 µL/min. Regeneration was performed with 10 mM glycin-HCl pH 1.5 with a contact time of 30 seconds and flow rate of 30 µL/min. Antigen target binding was expressed as binding relative to a reference sample which was set at 100% binding. Data of the MabSelectSure surface were only included to verify appropriate IgG concentrations in case of reduced antigen target binding. All sensorgrams were referenced and zeroed during data analysis.

Antigen target binding of the aberrant fucosylated samples were measured in an ELISA format. The antigen was coated in flat-bottom half-area 96-well clear polystyrene plates at 0.75 µg/mL in PBS pH 7.2. After blocking with 1% w/v BSA, serially diluted IgG samples and references were added followed by a detection step with 1:5000-diluted HRP-labeled goat anti-human IgG Fcγ-specific antibodies. Optical densities were read at 450 nm after development with a ready-to-use tetramethylbenzidine solution according manufacturer's instructions (Thermo Fisher Scientific Inc) using an ELISA reader (BioRad Laboratories). All binding reactions were performed at room temperature in the presence of 1% w/v BSA and 0.05% v/v Tween-20 detergent.

Fucosylation levels of aberrantly fucosylated samples were determined by mass spectrometry. Samples were partially reduced with 100 mM dithiotreitol in 100 mM Tris-HCl pH 8.0 at a concentration of 0.21 mg/mL. Samples were desalted online using a reversed-phase cartridge prior to injection into the MS system (Agilent 6540 Q-ToF equipped with

Jetstream ESI source). Approximately 945 ng of each sample was loaded onto the column. The mass spectra of light and heavy chains were deconvoluted using maximum entropy algorithm.

Covalent aggregates

An IgG1 sample after protein A purification was taken for the preparation of covalent aggregates. Five milliliter of IgG1 sample at 4 mg/mL was placed at pH 3 for 1 hour to create additional aggregates, followed by neutralization to pH 5 and a pre-concentration on 30 kD spin filters to > 100 mg/mL and a final volume of approximately 75 µL. Fifty microliters of this high concentration sample was mixed with 2 µL 100 mM DSS stock solution (Thermo Scientific) and incubated at room temperature for 15 minutes. The reaction was quenched with 2 µL 1M Tris pH 7.8 and kept at room temperature for 15 minutes. Samples were diluted with 500 µL MQ water to a concentration of approximately 9 mg/mL. This sample was separated into fractions by preparative size exclusion chromatography (SEC).

Preparative SEC purification

A preparative SEC purification was performed on the covalent aggregate sample and on the deamidated sample with elevated aggregate levels. A Superdex 200 10/30 column (24 ml) column was equilibrated with PBS pH 7.4 buffer using an ÄKTA explorer 100 system (GE life sciences) at a flow rate of 1 mL/min. An isocratic run in PBS pH 7.4 was performed on 0.5 mL of each sample and fractions were collected based on UV280 nm signal. Collected fractions were analyzed on SDS-PAGE to determine the monomer, dimer and higher oligomeric species in each fraction. Fractions with similar SDS-PAGE profiles were pooled for further analysis.

Low affinity Fcγ receptors relative binding determination

Recombinant human FcγRIIa, FcγRIIb, FcγRIIIa and FcγRIIIb were biotinylated as previously reported.[29] Fcγ receptors were then immobilized on a G-Strep SensEye® sensor (Ssens BV) at 5 µg/mL or 10 µg/mL in 50 mM sodium acetate pH 4.5 / 0.05% Tween80 with a print time of 5 minutes.

Samples were analyzed in a relative binding approach on IBIS MX96 SPRi (IBIS Technologies BV) with HBS buffer pH 7.2 / 0.05% Tween80 as running buffer. A baseline of 1 minute was followed by an association time of 2 minutes and a dissociation time of 1

minute. Then the sensor surface was regenerated with 25 mM phosphoric acid pH 3.0 in a single step of 30 seconds. Sensorgrams were referenced and zeroed. Binding levels at equilibrium (2 minutes) were used to determine relative binding levels. Relative binding was defined as the level of binding with respect to a reference sample which is set to 100% binding activity. Relative binding was determined at 50 µg/mL IgG1 and 250 µg/mL IgG1 (FcγRIIa and FcγRIIIa) or 250 µg/mL IgG1 and 1000 µg/mL IgG1 (FcγRIIb and FcγRIIIb). Activity of Fcγ receptors at the sensor surface reduced over time and we corrected for the decaying surface by applying a correction factor. Four calibration curves were injected distributed over the sample sequence. The decay in binding of these calibration curves was used to determine the correction factor for each sample, depending on the injection cycle number.

FcγRI kinetic determination

Single cycle kinetics of IgG1 on FcγRI was performed on a CAPchip (GE life sciences) with HBS-EP+ as running buffer on a Biacore T200 instrument (GE Life Sciences). The CAPchip was used according to manufacturers' protocol. Recombinant FcγRI was captured on a CAPchip at 0.5 µg/mL for 60 seconds at 2 µL/min. Five increasing sample concentrations of IgG1 were injected (0.06, 0.19, 0.56, 1.67 and 5 nM). The association time was set at 120 seconds, the dissociation time at 900 s (flow rate 30 µl/min). Regeneration was performed for 60 seconds (flow rate 5 µl/min) according to CAPchip protocol. Analyses were performed at 37°C. Data analysis was performed in the BiaEvaluation software (GE life sciences) and fitted to a 1:1 kinetic model to determined k_a, k_d and K_D observed.

FcRn kinetic determination

Multi-cycle kinetics of IgG1 on FcRn was performed on AR2G sensor tips in an Octet Red384 (Pall ForteBio). AR2G sensor tips were activated by EDC/NHS according to manufacturers' protocol, followed by immobilization of 6 µg/mL recombinant human neonatal Fc receptor (FcRn) in sodium acetate pH 5.0. After immobilization the sensor tips were deactivated by ethanolamine pH 8 according to manufacturers' protocol.

IgG1s were analyzed in 50 mM phosphate / 150 mM NaCl buffer / 0.1% Tween 20 pH 6 at concentrations of 320 nM and 80 nM down to 2.5 nM. The samples at 320 nM were dissociated in 50 mM phosphate buffer / 150 mM NaCl / 0.1% Tween 20 pH 7.2, while dissociation for the remaining dilutions was performed in 50 mM phosphate / 150 mM NaCl

buffer / 0.1% Tween 20 buffer pH 6. Regeneration of the sensor tips was performed with 100 mM Tris / 200 mM NaCl / 0.1% Tween 20 buffer pH 8. Data analysis was performed in corresponding software (Pall ForteBio) and sensorgrams were referenced and zeroed, followed by fitting to a heterogeneous ligand model to determine k_a, k_d and K_D observed at pH 6. Additionally, the highest IgG concentration, dissociated at pH 7.2, was analyzed for k_d and fraction bound at 5 seconds after start of dissociation. Fraction bound was determined at 5 seconds after the start of dissociation, with the response at t=0 seconds after start of dissociation was normalized to 100%.

Fcγ receptor analysis on immobilized IgG1

Stressed IgG1 samples and reference samples were immobilized on a G-COOH SensEye® sensor (Ssens BV) after activation with EDC/NHS according to manufacturers' protocol. Immobilization of the samples at 1 µg/mL dilutions in 10 mM sodium acetate pH 4.5 / 0.05% Tween80 was performed in the continuous flow microspotter (CFM) (Wasatch Microfluidics) using a print time of 5 minutes. Next, the sensor was deactivated with 1M ethanolamine pH 8.5 to manufacturers' protocol.

Interaction measurements between monoclonal antibody and various recombinant human Fcγ receptors (FcγRI from R&D systems, Minneapolis, MN, USA, others from Synthon Biopharmaceuticals BV) were performed on an IBIS MX96 SPRi instrument (IBIS Technologies BV). Fcγ receptors were diluted into HBS buffer pH 7.2 / 0.05 w/v% Tween80 running buffer. The following start concentrations were used: FcγRI: 40 nM, FcγRIIa: 20 µM, FcγRIIb: 25 µM, FcγRIIIa: 20 µM, FcγRIIIb: 24 µM and for each eight 2-fold dilutions were made. A baseline of 2 minutes was followed by an association time of 5 minutes and dissociation at 1 µL/second in 1 step for 4 minutes. The instrument was kept at 37°C during analysis. Regeneration was performed with 25 mM phosphoric acid pH 3.0 in a single step of 30 seconds. Sensorgrams were referenced and zeroed, followed by steady state equilibrium affinity determination in Scrubber (BioLogic).

Statistical data analysis

The results for each of the binding assays were statistically evaluated in Minitab. Duplicate or triplicate measurements were performed for each of the samples and methods. The relation between binding or affinity and the percentage of modification was performed with regression analysis.

Chapter 6

Results and discussion

Assay development and method performance

Low affinity Fcγ receptors were minimally biotinylated [29] followed by immobilization on a single streptavidin sensor. Degrees of labeling were between 0.3 and 0.5 for the different Fcγ receptors and proper IgG binding was measured on each of the Fcγ receptors. Decay in IgG binding responses, indicative of receptor instability at the sensor surface, was measured. A 30-60% reduction in Rmax values was determined during 60 regeneration cycles. A regeneration buffer scouting as described in Geuijen et al. [30] showed that a regeneration buffer of 25 mM phosphoric acid adjusted to pH 3.0 was most suitable., Use of this regeneration buffer improved receptor stability, although still decay in binding was observed (Figure 6.1). The fast on and off-rate of the receptors at the surface prevented the use of kinetic data. As the method was intended as a fast screening method, a relative binding approach was chosen.

The decay in IgG binding response to the receptor may be described by a logarithmic function (Figure 6.1) which was used to correct for reduced binding. In an analytical run four separate calibration curves of reference standard were injected distributed throughout the run, which were used to determine the values of the logarithmic function, with which the concentration of a sample at any cycle may be calculated. The validity of such a mathematical correction for the decay in response was verified in a method qualification, where range, accuracy, precision, specificity (Table 6.1) and model fit were assessed. Model fits to a logarithmic function had a $R^2 > 0.995$ in all experiments, and residuals were randomly distributed over the fitted curve. Specificity was assessed by injecting two different batches of IgA molecules, which should not bind to Fcγ receptors. Relative binding compared to an IgG reference was measured and was acceptable, although slightly higher values were measured on FcγRIIIb. Accuracy and precision data were analyzed in a general linear model in an ANOVA analysis, and none of the parameters that were included (operator, run number, spot number) were significant factors that contributed to the variance. Intermediate precision of test samples from the qualification were 12% or lower (Table 6.1), which is comparable to or below variability in binding studies based on kinetics (e.g. Katsamba et al.[31], Navratilova et al.[32] and Rich et al.[33]) and therefore variability was found acceptable for the intended purpose of the method.

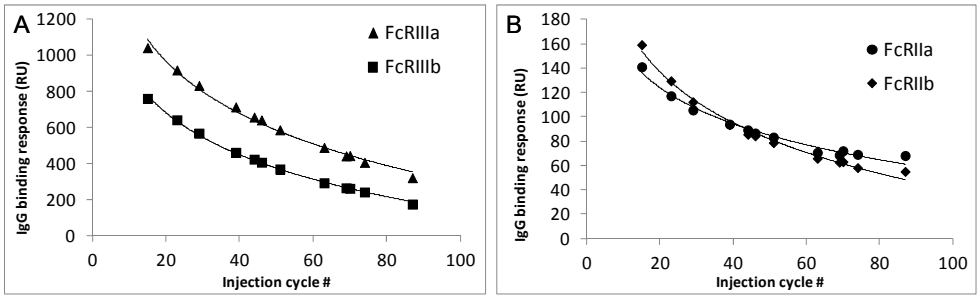

Figure 6.1 *IgG binding response at 500 µg/mL to the four low affinity Fcγ receptors (A: FcγRIIIa and FcγRIIIb; B: FcγRIIa and FcγRIIb) during 90 sequential analyses. Each curve followed a logarithmic decay, which was used to correct for decay according to injection cycle number.*

As previously mentioned, separate assays for FcγRI and FcRn were used. FcγRI interactions were measured in a single cycle kinetics measurement where five dilutions of IgG were injected on captured biotinylated FcγRI with an intermediate precision in K_D of 9.6%. A multi-cycle kinetics measurement based on BLI was developed for FcRn, where association was performed at pH 6 and dissociation of the highest IgG concentration was performed at pH 7.4 and dissociation of the other IgG concentrations measured at pH 6. Intermediate precision of 11.0% on K_D and 14.0% on fraction bound at neutral pH were determined. Method performance of both methods was found acceptable. Sample throughput of the FcγRIIa/b / FcγRIIIa/b and FcRn methods was high, with only 5 minutes analysis time per sample. Unfortunately, the throughput of the FcγRI method was somewhat lower compared to the other two methods, with 45 minutes per sample but still acceptable for the high-throughput screening purpose of this study. In the end, three separate screening methods for full Fc tail functionality of IgGs were available which all passed the set qualification criteria.

Characterization of stressed samples

A selection of the most common degradations in IgGs was made to measure the impact on Fc effector function, by studying binding to Fc receptors on the three screening assays. IgG1 samples were subjected to accelerated oxidation, accelerated deamidation, thermal/shake stress, freeze-thaw cycles and deglycosylation. Additionally, a few IgG samples with aberrant/different fucosylation levels were available for Fc effector binding, induced by applying variations in bioreactor process parameters. The stressed IgG samples were modified at the level of oxidation (mainly H:Met^{252}), asparagine deamidation (three

main sites in this IgG1), aggregation levels and the percentages of deglycosylation. These IgG samples were analyzed for antigen target binding by SPR or ELISA in case of aberrantly fucosylated samples (Table 6.2). Peptide mapping-based methods were used to quantify the levels of oxidation and deamidation and HP-SEC to determine the aggregate levels (Table 6.2). Next, the IgG samples were analyzed on SPR and BLI to measure the binding to Fc receptors (Table 6.3).

Table 6.1 *Range, accuracy, intermediate precision and specificity of relative binding assay*

Fcγ receptor	Range (µM)	Test sample	Nominal value [IgG] (µM)	Accuracy (%)	Intermediate precision (%)	Specificity: % binding of IgA
FcγRIIIa	0.104 – 3.33	LLOQ	0.11	96.6	7.75	
		LQC	0.20	97.6	5.59	0.5
		MQC	0.89	106.0	5.33	1.8
		HQC	2.67	84.4	8.08	
		ULOQ	3.11	93.8	5.13	
FcγRIIIb	0.832 – 26.67	LLOQ	0.89	110.6	4.48	
		LQC	3.11	87.1	2.70	9.9
		MQC	6.67	91.5	5.79	13.2
		HQC	20.00	104.4	7.12	
		ULOQ	22.22	104.3	11.99	
FcγRIIa	0.104 – 3.33	LLOQ	0.11	111.4	7.99	
		LQC	0.20	90.6	4.09	1.4
		MQC	0.89	92.0	7.50	3.3
		HQC	2.67	101.5	12.11	
		ULOQ	3.11	101.4	7.33	
FcγRIIb	0.832 – 26.67	LLOQ	0.89	106.2	5.93	
		LQC	3.11	90.3	3.64	14.3
		MQC	6.67	96.1	4.45	27.9
		HQC	20.00	101.5	6.81	
		ULOQ*	22.22	101.0	6.83	

* One sample was excluded due to an air bubble in the injection; n=17. All other results are based on n=18.

LLOQ: lower limit of quantitation, LQC: low quality control, MQC: middle quality control, HQC: high quality control, ULOQ: upper limit of quantitation

Asparagine deamidation was measured on all potential deamidation sites, and three major sites were detected. Two deamidation sites are present in the CDR of the antibody (referred to as HC-CDR and LC-CDR) and one site is present in the Fc region of the antibody (referred to as HC-Fc). Deamidation levels increased up to approximately 15% and 40% for the two sites in the CDR respectively. In the Fc region, asparagine deamidation increased up to 10%. High molecular weight (HMW) species increased during forced deamidation for 96

hours to 4.5% which may influence the measurements and this was further investigated by separating HMW species from monomer (see below).

Table 6.2 *Results of reference analyses to determine stress levels and antigen target binding*

Stress condition*	Ox Met^{255}	D-N HC CDR	D-N LC CDR	D-N HC Fc	% HMW	% insoluble HMW	% Deglycosylation	% Afucosylation	Antigen target binding (%)
Reference	2.5	9.8	9.7	3.8	1.3	n.d.	n.d.	11	100.0
H_2O_2_0.1%	3.7	9.6	9.6	n.d.	1.2	n.d.	n.d.	11	100.9
H_2O_2_0.25%	5.1	9.6	9.7	n.d.	1.3	n.d.	n.d.	11	100.7
H_2O_2_0.5%	7.1	9.6	9.6	n.d.	1.3	n.d.	n.d.	11	99.3
pH7.2_48h	2.8	10.1	13.5	5.7	1.7	n.d.	n.d.	11	97.6
pH7.2_72h	2.9	10.0	15.3	5.3	2.1	n.d.	n.d.	11	96.5
pH7.2_96h	2.9	10.4	17.4	5.1	2.3	n.d.	n.d.	11	94.9
pH8.0_48h	3.2	12.5	27.5	9.4	2.3	n.d.	n.d.	11	85.3
pH8.0_72h	3.4	13.7	34.6	10.1	2.2	n.d.	n.d.	11	80.9
pH8.0_96h	3.7	15.7	40.6	10.6	4.5	n.d.	n.d.	11	75.5
40C-24h	n.d.	n.d.	n.d.	n.d.	1.6	n.d.	n.d.	11	96.4
40C-48h	n.d.	n.d.	n.d.	n.d.	2.0	n.d.	n.d.	11	95.2
40C-72h	n.d.	n.d.	n.d.	n.d.	2.0	n.d.	n.d.	11	94.1
70C_15m	n.d.	n.d.	n.d.	n.d.	1.7	1.15	n.d.	11	103.0
75C_15m	n.d.	n.d.	n.d.	n.d.	1.5	51.4	n.d.	11	61.9
F-T 1	n.d.	n.d.	n.d.	n.d.	1.2	n.d.	n.d.	11	101.9
F-T 5	n.d.	n.d.	n.d.	n.d.	1.2	n.d.	n.d.	11	100.4
F-T 10	n.d.	n.d.	n.d.	n.d.	1.3	n.d.	n.d.	11	101.6
DG 0	n.d.	n.d.	n.d.	n.d.	n.d.	n.d.	0	11	92.2
DG 100	n.d.	n.d.	n.d.	n.d.	n.d.	n.d.	100	11	95.9
AF 3	n.d.	n.d.	n.d.	n.d.	n.d.	n.d.	n.d.	3	103.1
AF 8	n.d.	n.d.	n.d.	n.d.	n.d.	n.d.	n.d.	8	100.8
AF 70	n.d.	n.d.	n.d.	n.d.	n.d.	n.d.	n.d.	70	115.6

*Ox: oxidation; D-N: aspargine deamidation; F-T: freeze-thaw cycles; DG: deglycosylation; AF: afucosylation

HC: heavy chain; LC: light chain; CDR: Complementarity-determining region; Fc: fragment crystallizable; HMW: high molecular weight species. n.d.: Not determined

Increased HMW species were also detected in the samples that were heated to 70ºC and 75ºC. In all other stressed IgG samples the levels of HMW species remained similar to the

references. Oxidation levels in IgG samples that were exposed to H_2O_2 increased to approximately 7%. Antigen target binding remained unaffected under the applied stress conditions, except for (1) the deamidated IgG samples due to two deamidation sites that are present in the CDR, and (2) thermal/shake stressed IgG samples at 75˚C/300 rpm for 15 minutes. No altered binding to any of the Fc receptors was measured for the IgG samples that were subjected to thermal/shake stress and freeze-thaw cycles (Table 6.3), and therefore these results are not further discussed.

Low affinity Fc receptors screening

Binding to the low affinity Fcγ receptors (FcγRIIIa, FcγRIIIb, FcγRIIa and FcγRIIb) was measured in a relative binding set-up, where a reference standard was set to 100% activity and stressed IgG samples were measured relative to this standard.

Asparagine deamidation reduced binding to the low affinity Fcγ receptors to approximately 50-80% binding relative to the reference (Table 6.3 and Figure 6.2). A regression analysis of the percentage of deamidation against relative binding showed that these differences are statistically significant ($P < 0.0005$ for each of the Fcγ receptors). An increase in HMW species was observed in the deamidated samples next to increased deamidation levels. The lower relative binding on the low affinity Fcγ receptors of these samples may therefore also be induced by aggregates. The deamidated sample (72 hrs) was separated into a monomer and aggregated fraction by preparative SEC. The monomeric deamidated peak was analyzed on analytical SEC and was found to be pure monomer directly after separation. After short term overnight storage, the sample contained approximately 0.5% HMW species which cannot be avoided due to the intrinsic property of IgGs to form a small fraction of aggregates (Figure 6.A.1). However, this low aggregate level is comparable to the reference sample and therefore this sample was considered a representative sample to study the effect of deamidation only. Measurement of relative binding to FcγRIIIa/b and FcγRIIa/b resulted in approximately 50-80% relative binding of the monomeric deamidated sample, compared to approximately 60% of the non-purified sample (Figure 6.B.1). These data indicate that deamidation alone reduces binding to Fcγ receptors.

No difference in binding was observed after oxidative stress (Table 6.3), which is generally found in literature as well.[14,20] Only Bertolotti-Ciarlet et al.[20] found a decrease in binding (roughly 20% decrease) on FcγRIIa with IgG oxidized on Met^{252} to 80%. However,

the methionine oxidation levels in our stressed samples did not exceed 7% of oxidation, which may explain this difference in results.

Table 6.3 *Summarized results of stressed IgG1 samples on Fc receptor binding*

	Relative binding (%)				Affinity (nM)		Fraction bound (%)
Stress condition*	**FcγRIIIa**	**FcγRIIIb**	**FcγRIIa**	**FcγRIIb**	**FcγRI**	**FcRn**	**FcRn**
Reference	100.0	100.0	100.0	100.0	0.56	5.7	8.3
H_2O_2_0.1%	103.6	93.1	103.9	107.4	0.93	n.d.	n.d.
H_2O_2_0.25%	102.8	101.1	104.5	103.5	0.53	6.2	6.4
H_2O_2_0.5%	97.4	94.9	100.1	100.1	0.42	6.2	7.7
pH7.2_48h	97.4	89.6	140.3	92.9	0.59	5.5	7.6
pH7.2_72h	92.7	86.5	143.9	92.9	0.48	6.1	8.3
pH7.2_96h	96.9	88.3	132.1	94.7	0.58	5.6	7.9
pH8.0_48h	59.5	52.5	76.6	54.4	0.52	6.0	7.8
pH8.0_72h	53.2	53.8	64.5	53.6	0.55	5.5	6.5
pH8.0_96h	61.8	65.9	78.2	61.8	0.55	5.3	10.0
40C-24h	96.8	106.1	92.5	101.1	0.53	5.5	7.9
40C-48h	101.8	105.9	91.8	100.1	0.45	5.0	7.3
40C-72h	102.9	107.1	97.5	103.1	0.53	5.4	8.6
70C_15m	72.7	126.7	62.5	93.4	n.d.	34.2 #	n.d. #
75C_15m	388.7	> 1000	> 1000	> 1000	n.d.	0.4 #	n.d. #
F-T 1	80.1	106.5	102.2	102.3	0.52	5.7	8.4
F-T 5	103.0	104.7	92.3	97.2	0.42	5.7	8.1
F-T 10	98.7	102.0	85.9	95.9	0.48	5.2	7.4
DG 0	106.2	104.9	99.5	105.3	0.52	4.9	8.5
DG 100	6.5	10.5	10.3	15.3	No fit	6.3	4.1
AF 3	79.7	83.9	101.5	90.6	0.44	3.7	14.3
AF 8	87.7	93.0	97.6	84.2	0.43	3.7	14.1
AF 70	158.6	186.3	103.5	110.5	0.33	3.8	15.7

* F-T = freeze-thaw cycles; DG = deglycosylation; AF = afucosylation. n.d.: not determined

Non-specific binding to reference channels was measured; kinetics on FcRn could not be determined

Lack of binding of deglycosylated IgG to the low affinity Fcγ receptors has been described extensively [12-16] and was confirmed in our study. Fully deglycosylated IgG1 had a maximum of 15% binding response relative to the reference ($P < 0.0005$ for all low affinity

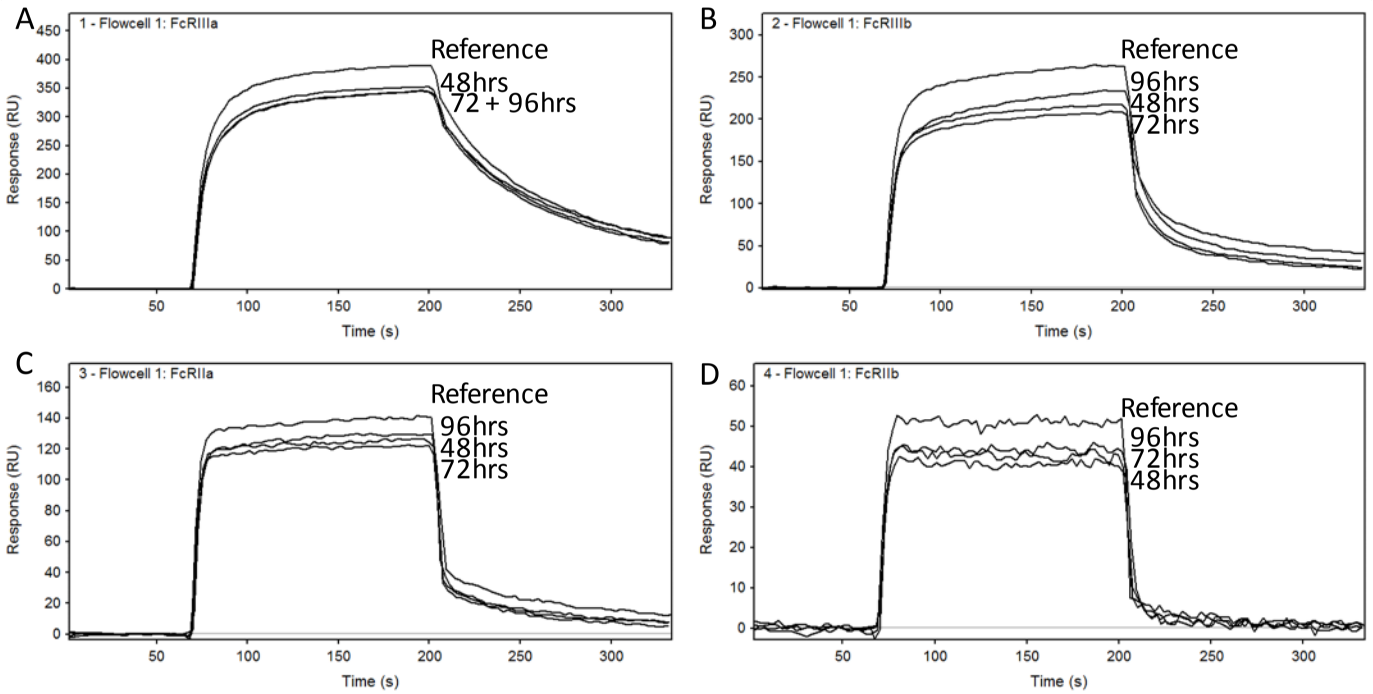

Figure 6.2 *Sensorgrams of a reference IgG sample and the deamidated IgG samples at pH 8 at different time points. Injections at 250 µg/mL IgG are shown on (A) FcγRIIIa, (B) FcγRIIIb, (C) FcγRIIa and (D) FcγRIIb, respectively.*

Fcγ receptors). The glycans in the Fc region of an antibody have a stabilizing (i.e. IgG folding) effect and are required for a proper interaction with these Fcγ receptors.[34]

Apart from full deglycosylation of the IgG1, we analyzed IgG1s with aberrant/different fucosylation levels. A different feed strategy in the bioreactor was applied, which resulted in IgGs with afucosylation levels of 3, 8 and 70% respectively. Variation of afucosylation only affected binding to FcγRIIIa and FcγRIIIb; a significant difference in relative binding between the three samples is measured from low to high corresponding to the afucosylation levels ($P < 0.0005$ in regression analysis for both receptors). A binding of 158-186% on FcγRIIIa and FcγRIIIb of the sample that was afucosylated for 70% was measured relative to the reference. The 3% and 8% afucosylated samples had a relative binding of 80-93%, which is due to the slightly lower afucosylation level compared to the reference sample (11% afucosylation). Binding to FcγRIIa and FcγRIIb was unaffected by the lower afucosylation levels (Table 6.3).

FcγRI

The high affinity interactions on FcγRI were measured in a single cycle kinetic determination at pH 7.4. To our knowledge, no literature is available that describes the effect of IgG deamidation and FcγRI binding. We found no effect of deamidation of IgG1 on binding to FcγRI as shown in Figure 6.3. No effect of oxidation or fucosylation degree of IgG was measured on FcγRI binding, confirming earlier results in literature on FcγRI binding for oxidized IgG1 [20] and fucosylation.[17,18]

Deglycosylated IgG almost completely prevented binding to FcγRI (Figure 6.4), as shown by the maximum response of approximately 5 RU compared to 80 RU of the reference sample. A 1:1 kinetic fit was applied to the sensorgrams, which resulted in poor fits of the fully deglycosylated sample. The resulting kinetic parameters cannot be reliably determined and are not reported. Our results do not fully confirm earlier findings in literature, as approximately 60% binding to FcγRI remained in earlier studies.[12,13]

Hence we investigated binding of FcγRI to deglycosylated IgG1 by inverting the experimental set-up. Deglycosylated and glycosylated IgG1 were immobilized on the sensor surface and their binding to FcγRI in solution was analyzed. Virtually no binding to FcγRI was found (Figure 6.C.1-E), confirming our results as presented in Figure 6.4.

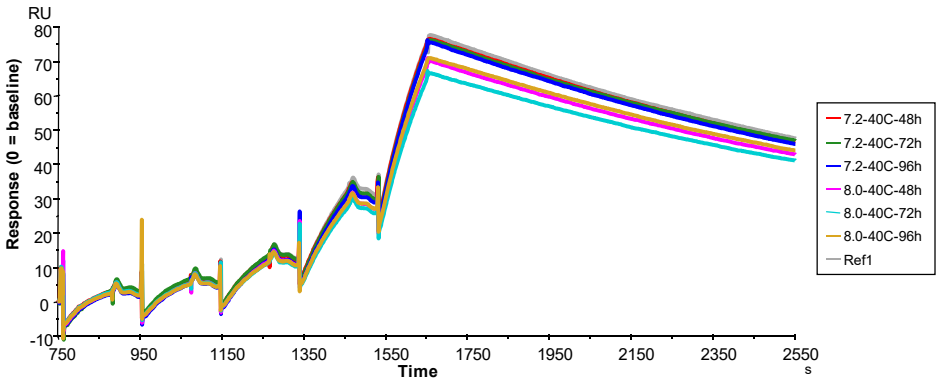

Figure 6.3 *Overlay of single cycle kinetics sensorgrams of deamidated and control IgG samples on FcγRI binding*

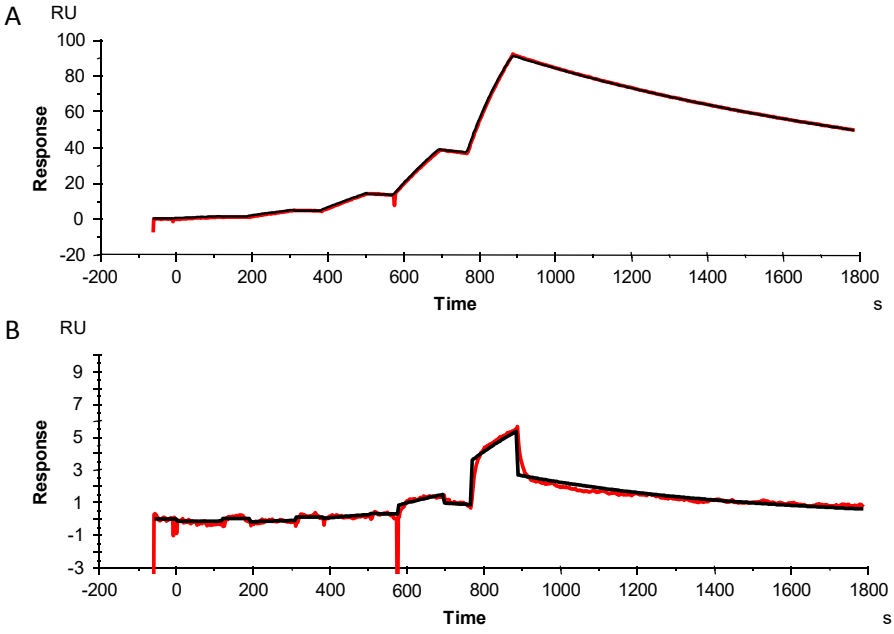

Figure 6.4 *Single cycle kinetics sensorgrams of glycosylated (A) and deglycosylated (B) IgG samples on FcγRI binding. Measured sensorgrams shown in red and fitted curves shown in black.*

FcRn

The mechanism of FcRn mediated IgG recycling is complex and encompasses IgG association at pH 6 and dissociation at pH 6 and pH 7.4. Most cited references only studied kinetics on FcRn at pH 6. Here, FcRn interactions were measured in a multi-cycle kinetics experiment of eight IgG1 dilutions. The lowest seven dilutions were used for kinetics determination at pH 6 by fitting both the association and dissociation phase to a heterogeneous ligand model, as proposed by Vaughn and Bjorkman.[35] The highest IgG dilution was associated at pH 6 and dissociation was measured at neutral pH. The dissociation rate and fraction bound at neutral pH were determined from this injection only.

No effect of IgG on FcRn binding at pH 6 was measured after deamidation in our assay and no differences in dissociation and fraction bound at neutral pH were measured (Figure 6.5). FcRn affinity and the fraction bound at neutral pH did not change depending on the fucosylation levels (Table 6.3). Deglycosylation resulted in a minor reduction in FcRn binding in a linear regression analysis (P=0.005). Additionally, measurements at neutral pH indicate a significantly lower fraction bound and a faster dissociation rate after deglycosylation (Figure 6.6 and Table 6.3). Deglycosylated IgG is still able to bind to FcRn, but dissociation at neutral pH is faster compared to the glycosylated counterpart, which may be important for the serum half-life.

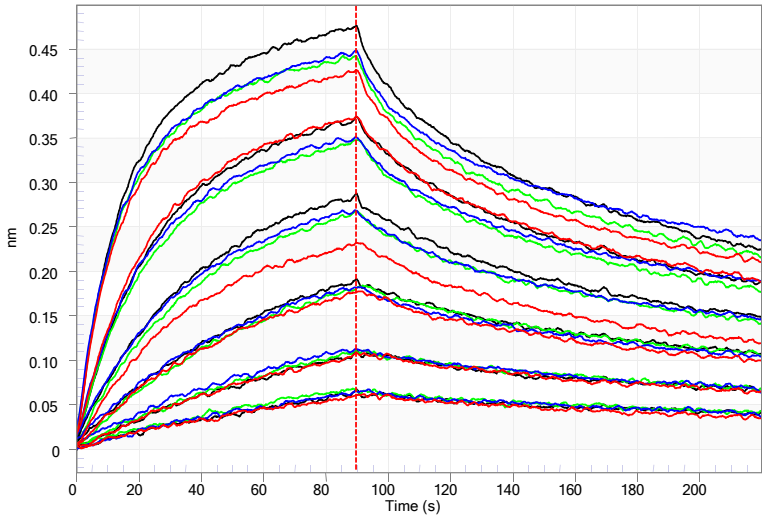

Figure 6.5 *Overlay of sensorgrams of deamidated samples on FcRn binding (reference in black; t=48 hours / pH 8 in green; t=72 hours / pH 8 in red and t=96 hours / pH 8 in blue). IgG concentrations between 2.5 and 10 nM.*

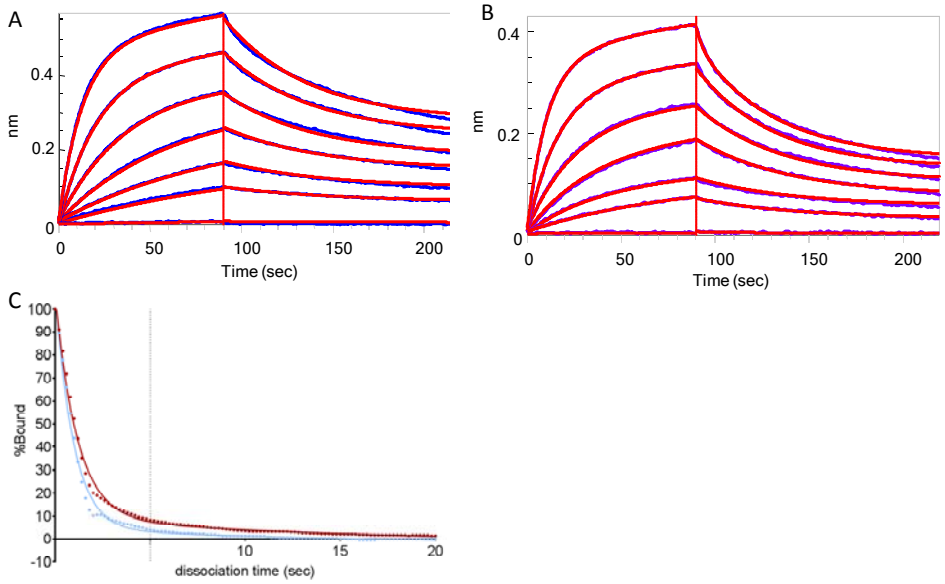

Figure 6.6 *Sensorgrams of IgG1 binding to FcRn of glycosylated (A) and deglycosylated (B) IgG1. Fitted curves are shown in red. C) The fraction bound at neutral pH of glycosylated (red) and deglycosylated (blue) IgG.*

We did not measure a significant decrease in affinity at pH 6 or in fraction bound at neutral pH on FcRn after methionine oxidation, whereas other publications [20-23] indicate that FcRn binding is reduced upon methionine oxidation (only studied at pH 6). However, highest oxidation levels that we induced were around 7%, whereas other groups report differences in FcRn binding at levels close to 80% of methionine oxidation. Stracke et al.[21] found that only one of the two heavy chains is oxidized when oxidation levels are around 50% or lower, and the other heavy chain of the antibody is still able to bind to FcRn. This agrees well with our results as no impact is measured at 7% oxidation.

Presence of HMW species

As mentioned above, the presence of aggregates in our stressed IgG samples could impact the binding to the Fcγ receptors and FcRn. Previous studies have already emphasized the importance to control the level of aggregates during these types of binding studies [15,15,24,25]. This was observed in deamidated IgG samples where the fraction of HMW

species increased with a few percent. Additionally, samples were heated to 70°C and 75°C to induce larger fractions of HMW species. HMW species impact binding to all of the Fc receptors. IgG samples were heated for 15 minutes at temperatures close to the first T_m (melting temperature) of the IgG1, which resulted in differential binding to the low affinity Fcγ receptors (Figure 6.7). Heating to 70°C, which is just below the T_m, decreased the relative binding to the low affinity receptors, except for FcγRIIIb where an increase was observed. However, heating to 75°C resulted in at least 4x more binding (relative binding 400% or higher), likely due to avidity effects of large aggregates that were present in these samples (Figure 6.7).

Heating of the IgG samples, especially to 75°C, resulted in a large fraction of insoluble aggregates, which behave completely different from monomers in our binding assay. A more controlled approach for aggregate preparation was performed by covalent coupling of IgG1s to each other using a chemical linker. Preparative SEC was used to separate the monomer from dimers, trimers and higher aggregates (Figure 6.A.2). The covalent dimers and oligomers that were separated by SEC showed similar behavior in the relative binding measurement on low affinity Fcγ receptors compared to the heated samples (results not shown). Relative binding up to 400-800% on each of the low affinity Fcγ receptors was measured.

Furthermore, the covalent dimers were analyzed in the FcγRI and FcRn binding assays. FcγRI binding with dimeric samples resulted in an apparent slower off-rate (Figure 6.D.1) and as a consequence an apparent higher affinity is measured with the covalent aggregate samples (Table 6.4). In case of FcRn, kinetic evaluation of the binding curves results in a 1:1 binding model at pH 6 for the dimer/oligomer sample, whereas the monomeric samples were fitted with a heterogenous ligand model (Figure 6.D.2). The dimeric sample could be equally well fitted with a 1:1 binding model and a heterogeneous ligand model. We have chosen to fit the 1:1 binding model for this sample. A difference in observed K_D and fraction bound at neutral pH was measured between monomer and dimer or oligomer samples (Table 6.4). However, the curve fitting was not corrected for a difference in molecular weight of the complex, because these were a mixture of monomers, dimers and trimers and no actual molecular mass could be determined. Assuming a molecular weight of 300 kDa for dimers instead of 150 kDa still resulted in an equally good fit with the 1:1 binding model and the heterogeneous ligand fit, still with different kinetic parameters compared to the monomeric reference.

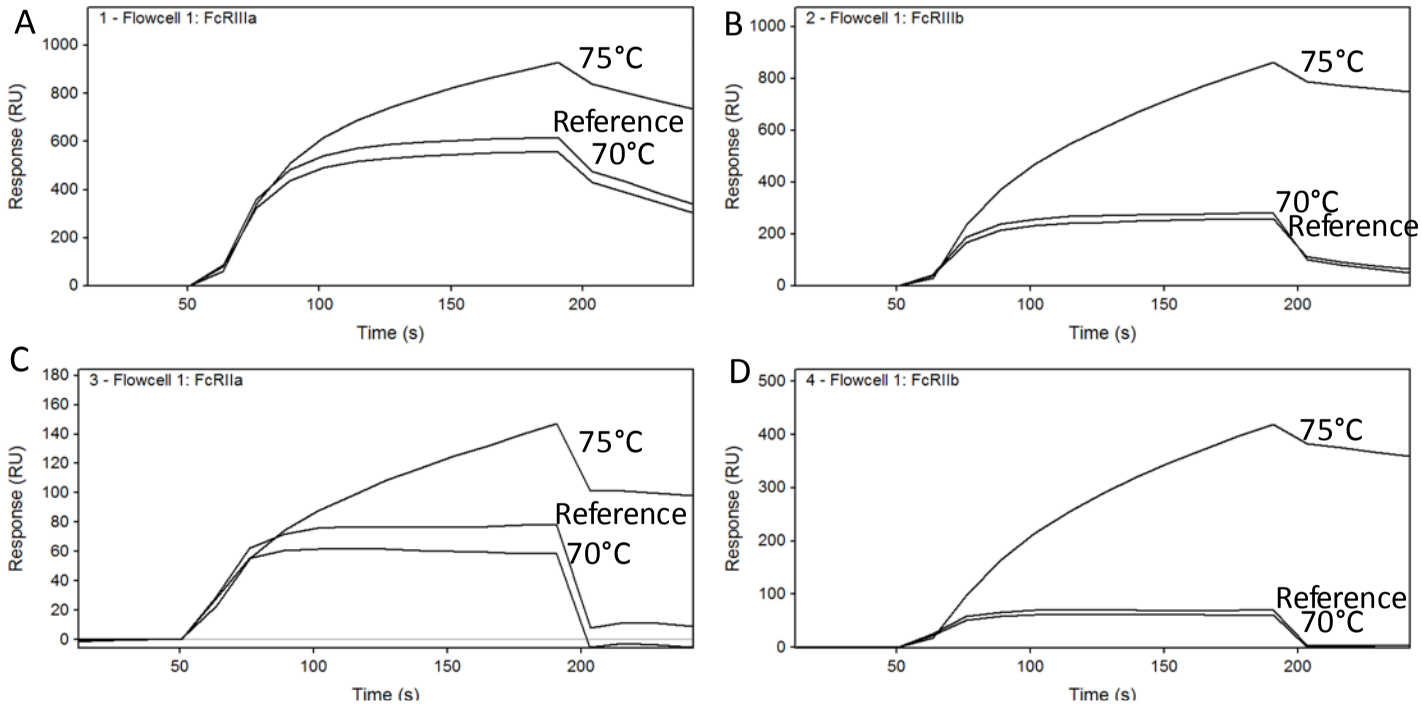

Figure 6.7 *Sensorgrams (measured at 250 µg/mL) of reference and aggregated IgG samples heated to 70°C and 75°C for 15 minutes on FcγRIIIa (A), FcγRIIIb (B), FcγRIIa (C) and FcγRIIb (D), respectively.*

The purified covalent aggregates contained approximately 73-77% dimers and 5-14% trimers and higher oligomers, which resulted in a 6 to 8-fold increase in apparent affinity on FcγRI and 2-fold increase in apparent affinity and fraction bound on FcRn. The increased apparent affinity is most likely an avidity effect than a true difference in affinity.

As an additional verification of the results, we measured all FcR interactions in the opposite set-up, where we immobilized the various stressed samples on a single SPR sensor and analyzed the binding to the different Fcγ receptors subsequently. In this set-up no differences in aggregated samples compared to the references was measured (Figure 6.C.1). Affinities that were determined on FcγRI in the opposite set-up matched closely to affinities that were measured for the aggregated samples in solution (0.2 nM for immobilized IgG vs 0.08 nM for dimeric IgG in solution), whereas the monomeric IgG in solution has an affinity of approximately 0.56 nM under tested conditions. Upon immobilization of the IgGs onto the sensor surface, pseudo-aggregates are created when the IgG molecules are immobilized in close proximity to each other, and this may mask the differences that are caused by actual aggregates.

Table 6.4 *Comparison of the effect of aggregate levels in IgG1 samples with respect to FcγRI and FcRn binding*

	% dimers	% trimers and higher	KD (nM) FcγRI	KD (nM) FcRn	Fraction bound (%) FcRn
IgG1 reference	1.2	n.d.	0.66	6.3	7.5
Monomer IgG1	1.8	n.d.	0.52	7.0	8.9
Dimer IgG1	76.7	5.1	0.08	3.1 *	17.3
Oligomer IgG1	73.4	14.0	0.07	3.0 *	17.7

* 1:1 binding model applied instead of heterogeneous ligand model. N.d. = not detected

Discussion

We assessed Fc tail functionality of IgG1 after exposure to various stress conditions using binding assays. Stress conditions that were applied and that did impact Fc tail functionality, included asparagine deamidation, deglycosylation, aberrant fucosylation or aggregation (Table 6.5). Importantly, no effects were measured after methionine oxidation, thermal/shake stress or repeated freeze-thaw cycles. Furthermore, we determined FcRn binding at pH 6 (kinetics) and at neutral pH (dissociation rate and fraction bound). Dissociation at neutral pH may be an important predictor for serum half-life of

antibodies,[9,36] however, most publications described the binding to FcRn at pH 6 alone. Instead, dissociation at pH 7.4 after association at pH 6 was analyzed here, resulting in a faster dissociation and lower fraction bound at pH 7.4 for a deglycosylated IgG sample. Other stress conditions did not influence FcRn dissociation at pH 7.4.

The impact of asparagine deamidation of IgG on FcRn binding was previously reported by Gandhi et al.[27], and no impact of deamidation on FcRn binding at pH 6 was found. Here, no impact of deamidation on FcγRI (pH 7.4) and FcRn (both pH 6 and pH 7.4) was measured. On the other hand, relative binding on the low affinity Fcγ receptors was reduced after asparagine deamidation (50-70% of reference). Upon deamidation, also the percentage of high molecular weight species increased and therefore the deamidated sample was purified into a monomeric fraction. In the purified monomeric deamidated sample, reduced binding was still measured on the low affinity Fcγ receptors, which could only be attributed to asparagine deamidation. The main deamidation site of this IgG is present in the CDR at the light chain (up to 40% modified), which is positioned relatively far away from the Fc interaction site (lower hinge, upper CH2 domain [37,38]). Deamidation at this position is not likely to change the folding of the protein in such a way that it would have a large impact on Fc receptor binding. 3D models of both structures do not point in the direction of altered Fc binding induced by CDR deamidation (Figure 6.E.1). In the lower hinge and upper CH2 domain no potential deamidation sites are present. In the Fc region (CH2 and CH3 domains) other deamidation sites are present, which are less vulnerable towards deamidation, but are affected after stress conditions. The major deamidation site in the Fc region of the heavy chain (amino acid sequence SNGQPENNY) was deamidated at levels around 10%. Shields et al. [11] have studied binding behavior on all Fc receptors by point mutation of amino acids in the Fc region and did not find any influence of the amino acids in this deamidation site (altered binding defined as reduction of 40% or more). Here, the reduced binding of the deamidated samples was 30-50%. After all three incubations (48, 72 and 96 hours), relatively similar binding levels and deamidation levels (around 10%) were found, whereas deamidation levels on the other two main deamidation sites in the CDR steadily increased over time. Collectively, this suggests that the HC-Fc deamidation is most likely responsible for reduced binding to low affinity Fcγ receptors after deamidation. Asparagine residues sensitive towards deamidation may differ between different IgGs as these may be present in the CDR region and can therefore be specific towards the studied antibody. However, our results suggest that the major deamidation site which affects Fc receptor binding is present in the conserved residues of the Fc region (SNGQPENNY). These

results indicate, together with data from Shields et al.[11], that the effects of deamidation on Fc receptor binding are not IgG dependent.

Table 6.5 *Summary of Fc tail interactions to monitor for changes in product characteristics*

IgG modification	FcγRIIIa	FcγRIIIb	FcγRIIa	FcγRIIb	FcγRI	FcRn
Deamidation (10-50%)	**Reduced relative binding***	**Reduced relative binding***	**Reduced relative binding***	**Reduced relative binding***	**No impact***	**No impact***
Deglycosylation (100%)	Hardly any binding	Hardly any binding	Hardly any binding	Hardly any binding	Hardly any binding	**Slightly faster off-rate. Lower fraction bound at neutral pH***
Aberrant fucosylation (3-70%)	Increased binding with lower fucosy-lation	Increased binding with lower fucosy-lation	No impact	No impact	No impact	**No impact***
Aggregation (5-75%)	Higher relative binding (>400%)	Higher relative binding (>400%)	Higher relative binding (>400%)	**Higher relative binding (>400%)***	Slower off-rate, increase K_D	Slower off-rate, increased K_D, 1:1 binding model
Oxidation (<7% on Met^{252})	No impact	No impact	No impact	No impact	No impact	No impact
Thermal/shake stress	**No impact***	**No impact***	**No impact***	**No impact***	**No impact***	**No impact***
Freeze-thaw cycles	**No impact***	**No impact***	**No impact***	**No impact***	**No impact***	**No impact***

* Results marked with an asterisk and in bold indicate results that have not been reported in literature to authors' knowledge

The structure of an IgG, with two heavy chains that both can potentially bind to Fc receptors complicates analysis of these molecules. Fc tail interactions are not necessarily impacted by modifications on one of the heavy chains alone. If only one heavy chain is involved in an interaction and one heavy chain remains unaffected, this does not necessarily impact Fc effector binding, as shown for methionine oxidation. In the Fc region of an IgG two main oxidation sites (H^{252} and H^{428}) are present, of which H^{252} is the most vulnerable oxidation site. Houde et al.[14] found that the conformation of IgGs is changed upon methionine oxidation, although this is not reflected in an altered binding to FcγRIIIa, which may be a result of one Fc tail that can still bind to the Fcγ receptor. No difference in relative binding of IgG on FcγRIIIa, neither on any of the other low affinity Fcγ receptors was measured with oxidation levels up to 7% after H_2O_2 stress in our study. Furthermore, no differences in affinity and kinetics of oxidized IgG to FcγRI or FcRn (pH 6 and pH 7.4) were detected. This is in agreement with results published by Bertolotti-Ciarlet et al.[20] who studied the interaction of IgGs to each of the Fcγ receptors. A few publications described the effect of methionine oxidation on FcRn binding measured at pH 6 [21,39]. In these studies, it was demonstrated that a single Met^{252} oxidation (i.e. one heavy chain modified) has no impact on FcRn binding kinetics. IgG with both heavy chains oxidized alter the binding kinetics to FcRn significantly, resulting in faster plasma clearance. However, these measurements were only performed at pH 6. Therefore we additionally measured dissociation rate and fraction bound at neutral pH and no differences in FcRn binding with oxidation levels up to 7% were shown. The average methionine oxidation of the studied IgG during production and processing did not exceed 2-3%. Hence, no impact on Fc tail functionality was expected. Wang et al.[39] analyzed IgG samples with a shelf-life of three years under refrigerated or frozen conditions. Even then, IgG oxidation levels did not exceed 13% and no effect on FcRn binding at pH 6 was detected. In summary, we postulate that both heavy chains should be oxidized in order to affect Fc tail functionality.

Hardly any IgG binding to the low affinity Fcγ receptors and FcγRI was measured after deglycosylation, which is in agreement with results from others.[12,13,15,40] The binding to FcRn receptor is not or only moderately influenced by the glycan occupancy, as similar affinity at pH 6 was measured using deglycosylated IgG1 compared to the glycosylated reference IgG However, dissociation at neutral pH was impacted by glycan occupancy, as the fraction bound at neutral pH significantly decreased after deglycosylation. Furthermore, fucosylation levels of the antibody have an impact on the binding to FcγRIIIa and FcγRIIIb, whereas no differences in binding were measured on any of the other Fc receptors. These

results are in agreement with literature.[13,16-19] None of the cited references studied the effect of deglycosylation on fraction bound at neutral pH, and we have demonstrated that there is a significant impact. A decrease in fucosylation induces stronger binding to FcγRIIIa and as such increases the antibody-dependent cellular cytotoxicity of the antibody. This increased affinity is caused by carbohydrate-carbohydrate interactions of both the IgG and the Fcγ receptor.[19] IgG glycosylation is important as it adds to the stability of the protein[41] and to maintain its effector binding characteristics[12], both in glycan site occupancy as well as glycosylation pattern differences (e.g. fucosylation levels). IgGs are more prone to aggregation when glycans are absent, which in turn has an effect on Fc effector functions. Furthermore glycans stabilize IgGs against proteases that may cleave the protein during harvesting or purification and as such proper glycan occupancy is critical for the quality of a therapeutic antibody, especially when effector function of the immune system are involved in the mode of action.[40,42]

The results for each of the Fcγ receptors indicate that dimers and oligomers, or aggregates, of IgGs bind stronger to the various types of Fc receptors and can therefore have a significant impact on affinity determinations. The binding of dimeric and oligomeric IgGs to low affinity Fcγ receptors changes, due to avidity effects and is reflected in an increase in relative binding to 400% or higher. Comparable increased affinities have been measured by Luo et al.[24] Similarly, Bajardi-Taccioli et al.[23] demonstrated an increase in relative activity on an FcRn binding assay when aggregates were spiked into the measured samples. A slower off-rate was measured with samples that contained up to 86% of aggregation. These results were all obtained with samples that contained a significant amount of aggregates (more than 80%). On the other hand, samples that contain no more than 2.5% of aggregates have no altered relative binding in our study, whereas Dorion-Thibaudeau et al. [15] found that HMW levels of only 2% already affected the binding to FcγRIIIa in their assay. Due to the avidity effects of aggregates, the impact of a small fraction of dimers and higher oligomers in samples can alter binding to Fc receptors and can therefore not be neglected. Protein aggregates may consist of reversible and irreversible aggregates[43]. Aggregates that are artificially created (heating or chemically coupling) can generally be well characterized by other analytical assays,[26,43,44] whereas reversible aggregates of IgGs which naturally occur, may fall apart upon dilution[43] and are therefore difficult to characterize. The nature of aggregates in stressed IgG samples may be different compared to naturally occurring aggregates, which complicates the assignment of the impact these have in binding assays. Still, we strongly recommend controlling the aggregate

level of samples when assessing Fc interactions in binding assays such as those described here.

No difference in binding was observed when aggregates were immobilized on the sensor surface. Most likely, the effects of aggregation are masked upon immobilization of IgGs in close proximity to each other. The immobilization of IgGs on the surface can cause the IgGs to behave as aggregates rather than monomeric molecules as they are covalently linked to the sensor surface in close proximity to each other, and therefore the differences between monomer and aggregate are no longer measured.

High-throughput analytical screening technologies are used more and more to rapidly identify critical process parameters and to monitor critical product quality attributes. Here we have shown that Fc binding assays can be applied for a rapid screening of product quality. Understanding the effects of process variation on Fc tail functionality early in the development can be beneficial for further process development, in lead optimization studies and in process characterization studies. Although ideally the Fc receptors screening should be performed on a single SPR assay, the differences in binding characteristics between the various receptors prevented such a multiplexed measurement. However, three separate high-throughput screening methods were developed and used to explore the total Fc region binding of stressed IgGs. Low affinity Fcγ receptors and FcRn binding were measured in only 5 minutes per sample, whereas the FcγRI assay takes 45 minutes per sample. Especially the screening of multiple Fcγ receptors in a single assay with only 5 minutes per sample dramatically increases sample throughput, and therefore such multiplexed methods are highly recommended to use.

Although the various stress-induced modifications are considered to be crucial for product quality, we here show that surprisingly most of those factors had only minor effects on Fc receptor binding within the range that is often found during development. This is relevant for the development of novel antibodies but has even more impact on the development of biosimilar antibodies. During the development of biosimilars, due to process difference with the innovator, small differences occur in e.g. level of oxidation or deamidation, for which the question always remains whether they are relevant for product quality. Biosimilarity assessment can be rapidly performed using such high-throughput screening assays. Here we show that only significant differences in these parameters impacted Fc receptor binding and minute changes had no impact at all, except for minor differences in the presence of HMW species.

Acknowledgments

The authors would like to thank Wendy Pluk, Jozefi Hortulanus and Eline van den Berg for characterization of stressed material by various analytical methods. We thank Myrthe Rouwette for the development of the FcγRI kinetic assay and Bram Nillessen and Sanne Wilmsen for their assistance in the preparation and separation of covalent aggregates.

We thank EFRO Province of Gelderland and Overijssel, the Netherlands for giving us the financial support for the research project.

Appendix A Chromatograms

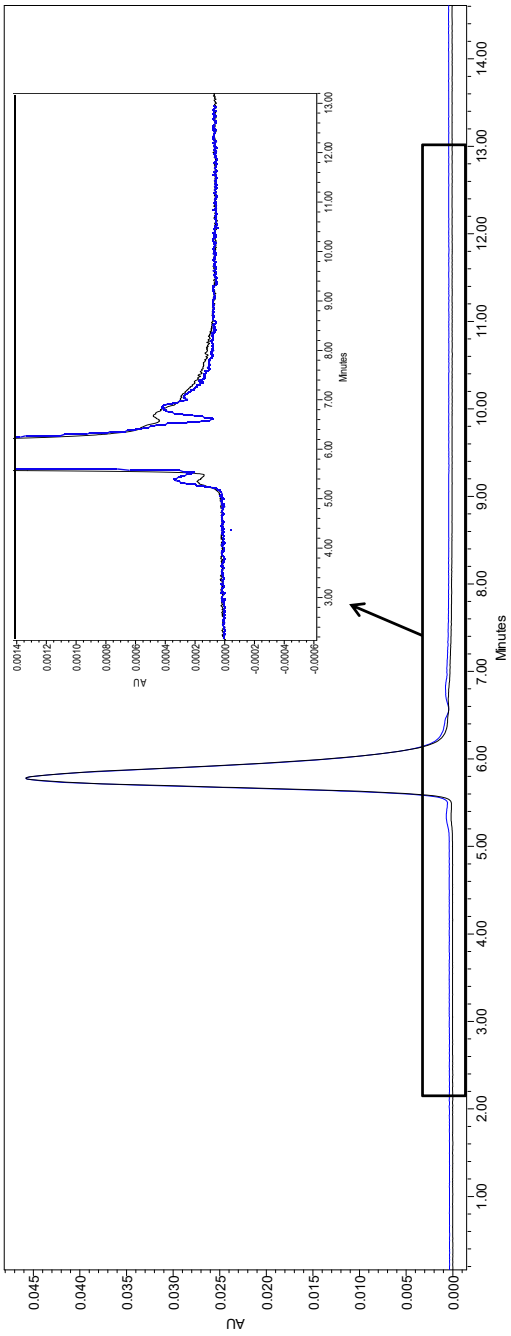

Figure 6.A.1 *Overlaid 280 nm chromatograms of purified monomeric deamidated sample, directly after preparative SEC (black) and after one freeze-thaw cycle overnight (blue). The small peak in front of the main peak corresponds to HMW species.*

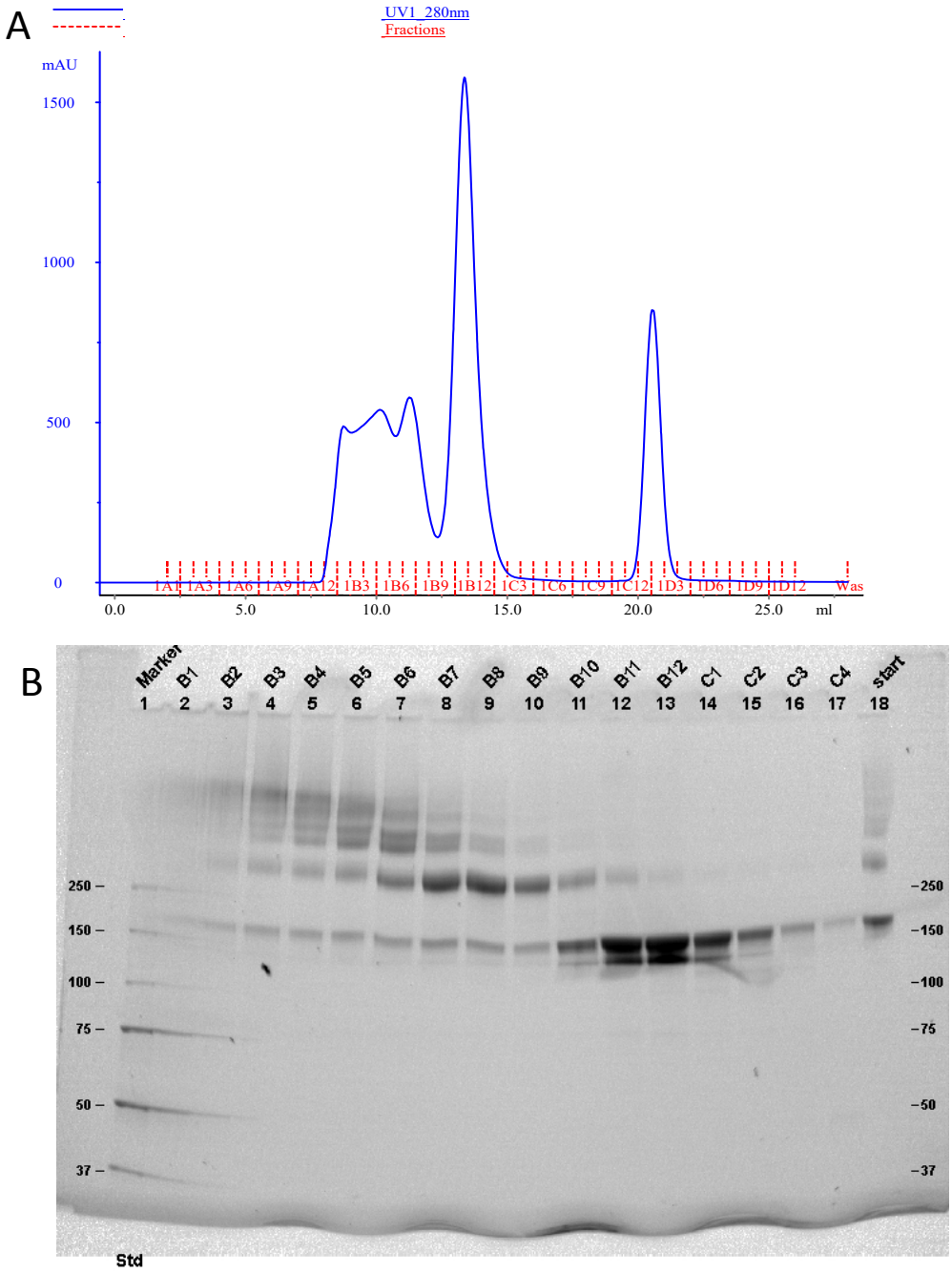

Figure 6.A.2 *Preparative SEC chromatogram at 280 nm of collected fractions (A) and corresponding SDS-PAGE analysis of the collected fractions (B). The fractions from B1 to C4, indicated in the chromatogram, were collected and analyzed.*

Appendix B Low affinity Fcγ receptor binding

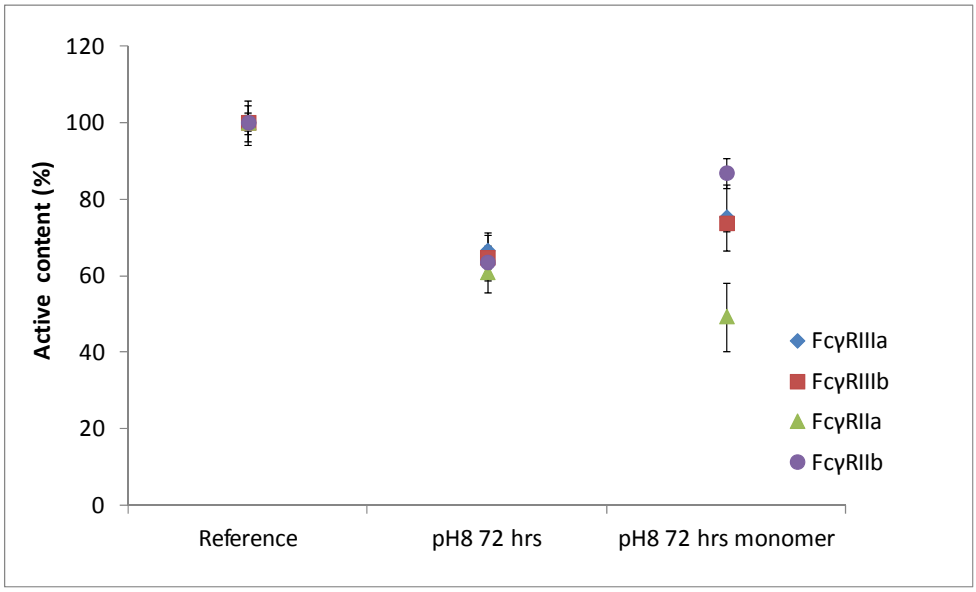

Figure 6.B.1 *Relative binding on the four low affinity Fcγ receptors with the deamidated sample before and after SEC purification*

Appendix C Statistical results

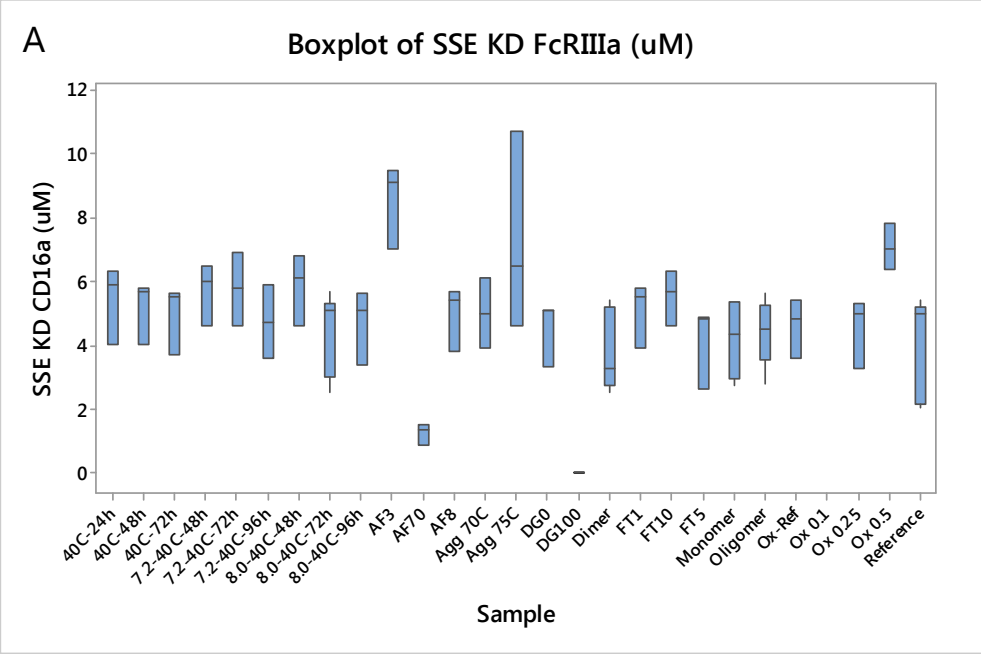

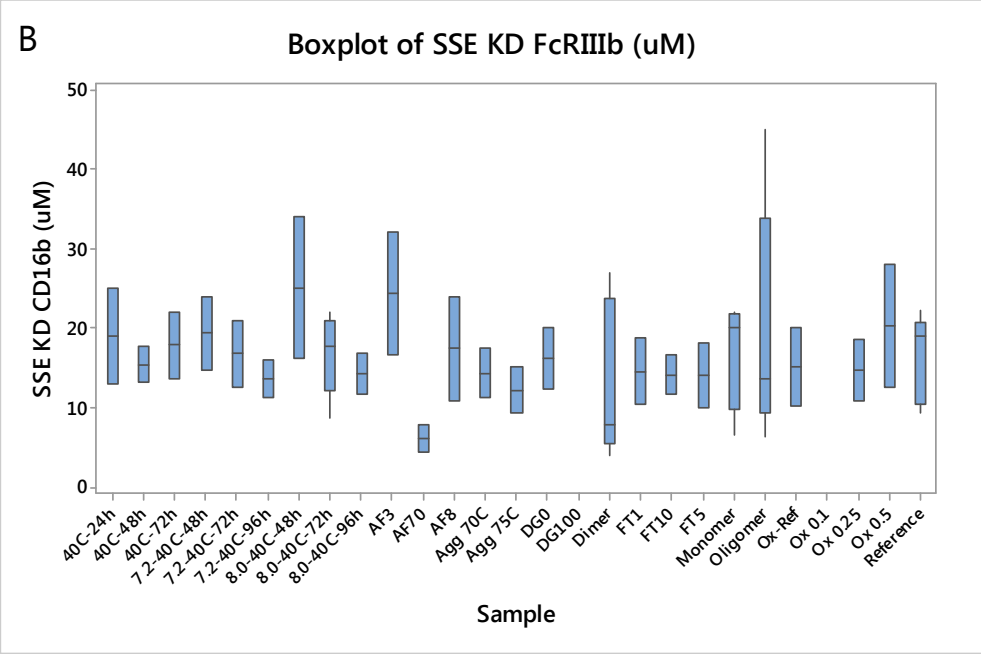

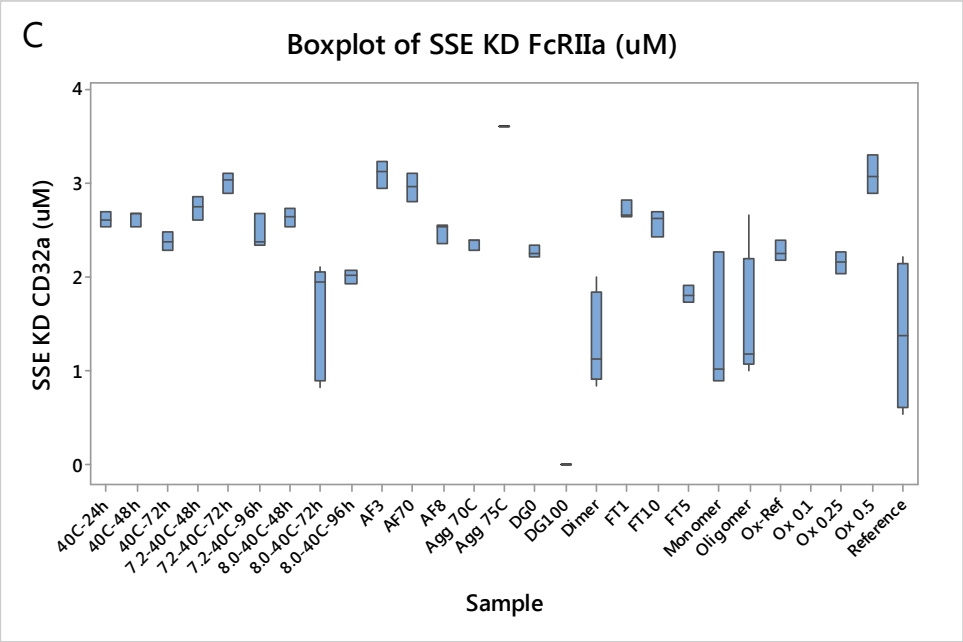
C
Boxplot of SSE KD FcRIIa (uM)
SSE KD CD32a (uM)
0
1
2
3
4
40C-24h
40C-48h
40C-72h
7.2-40C-48h
7.2-40C-72h
7.2-40C-96h
8.0-40C-48h
8.0-40C-72h
8.0-40C-96h
AF3
AF70
AF8
Agg 70C
Agg 75C
DG0
DG100
Dimer
FT1
FT10
FT5
Monomer
Oligomer
Ox-Ref
Ox 0.1
Ox 0.25
Ox 0.5
Reference
Sample

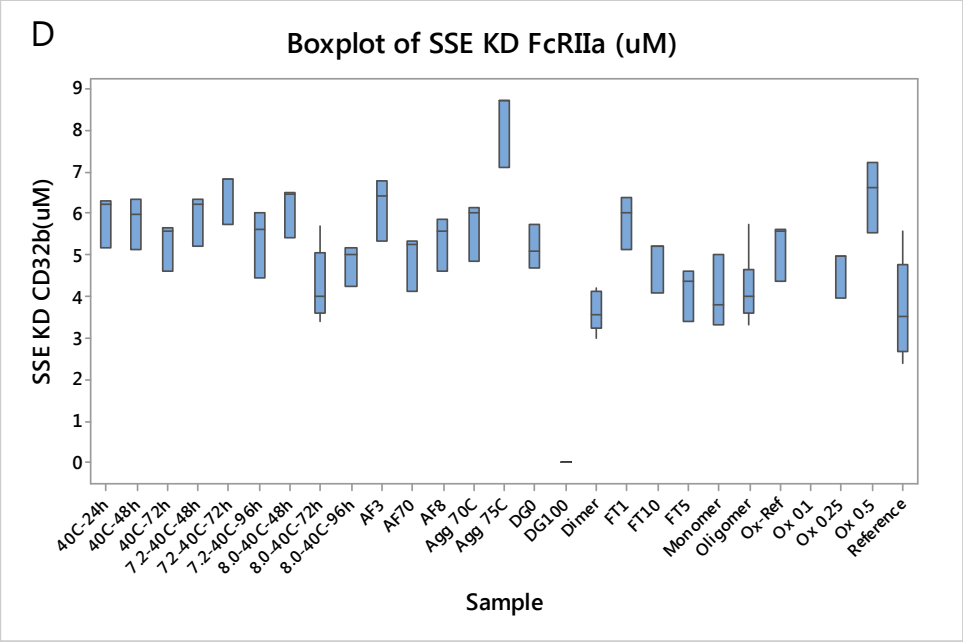
D
Boxplot of SSE KD FcRIIa (uM)
SSE KD CD32b(uM)
0
1
2
3
4
5
6
7
8
9
40C-24h
40C-48h
40C-72h
7.2-40C-48h
7.2-40C-72h
7.2-40C-96h
8.0-40C-48h
8.0-40C-72h
8.0-40C-96h
AF3
AF70
AF8
Agg 70C
Agg 75C
DG0
DG100
Dimer
FT1
FT10
FT5
Monomer
Oligomer
Ox-Ref
Ox 0.1
Ox 0.25
Ox 0.5
Reference
Sample

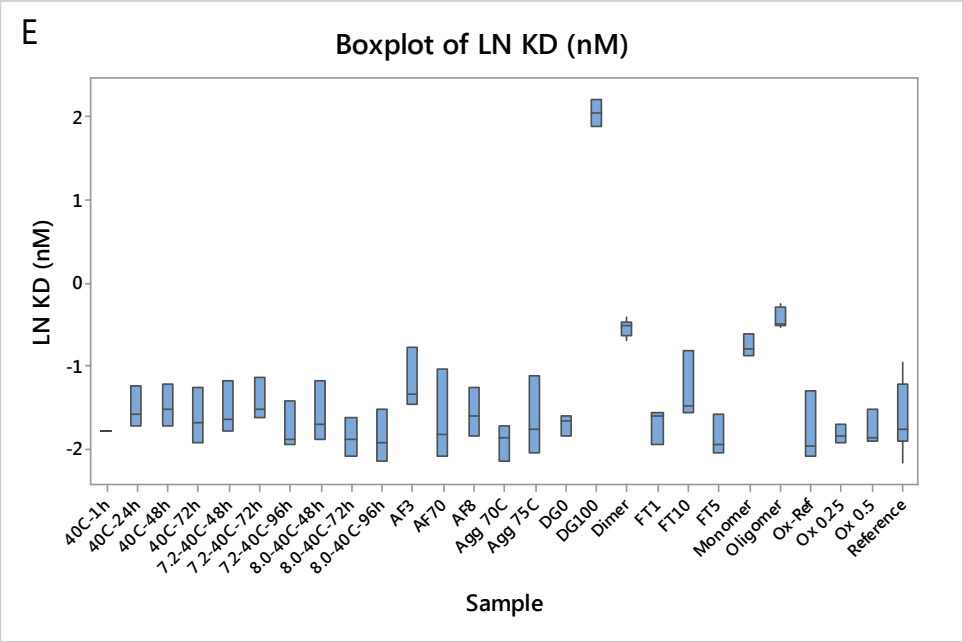

Figure 6.C.1 *Boxplots of apparent affinity of stressed samples immobilized on the sensor surface and Fcγ receptors injected as analytes. Steady state equilibrium affinity determined for (A) FcγRIIIa, (B), FcγRIIIb, (C) FcγRIIa, (D) FcγRIIb. Kinetic 1:1 fit to determine affinity for (E) FcγRI. Note that the Y-axis for graph E, FcγRI, is on logarithmic scale.*

Appendix D Additional sensorgrams

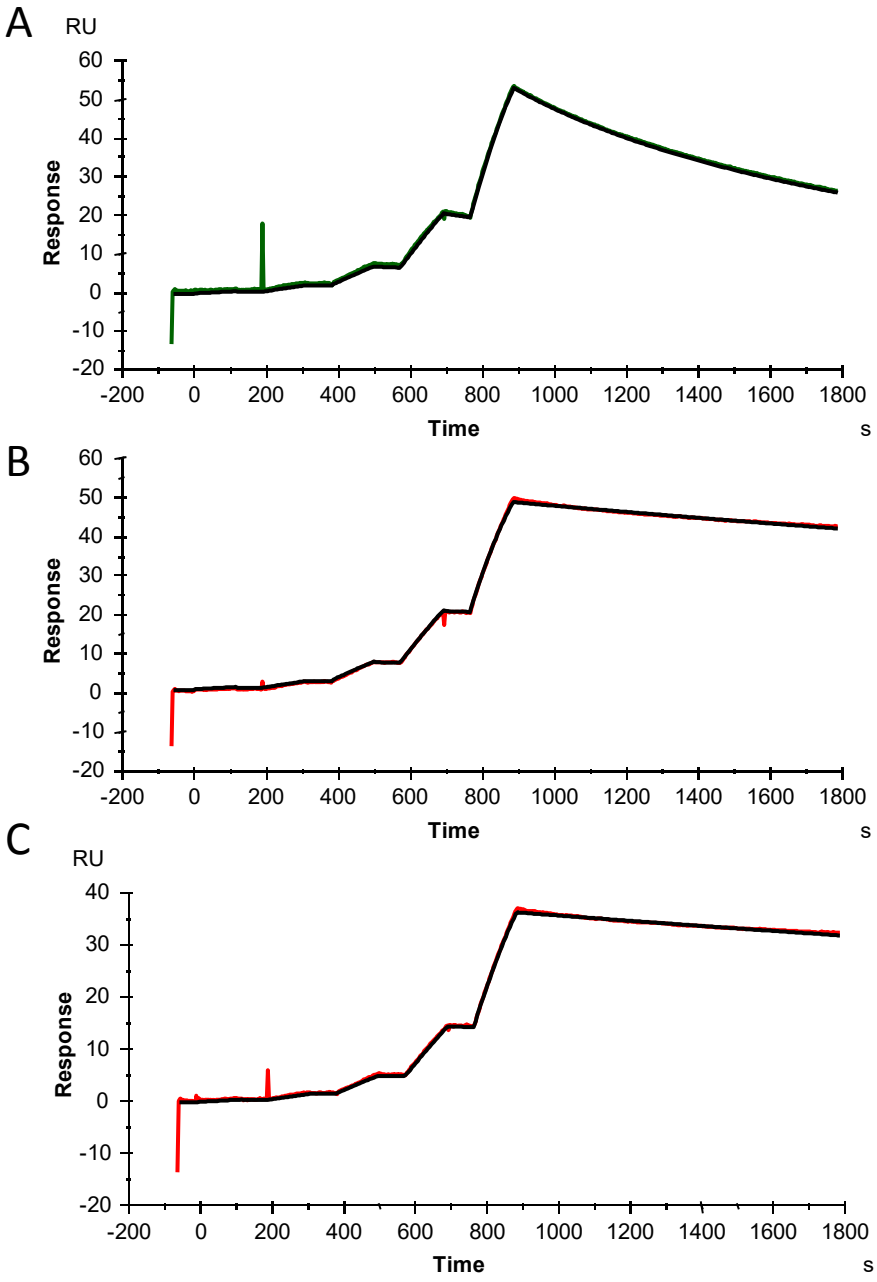

Figure 6.D.1 *Single cycle kinetics sensorgrams of purified monomer (A), dimer (B) and oligomer (C) fractions on FcγRI binding. Measured curves in green or red, fitted curves in black.*

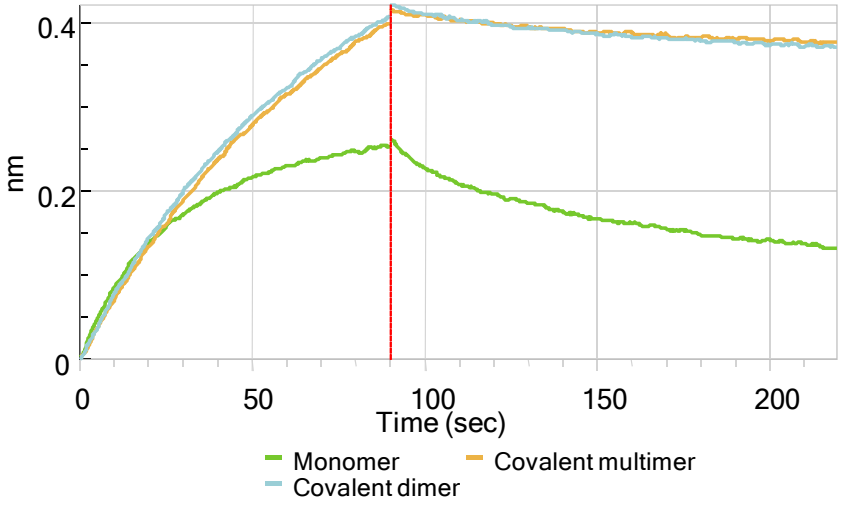

Figure 6.D.2 *Sensorgrams of a monomeric IgG1 sample (40 nM) in overlay with covalent dimer and multimer samples on FcRn binding*

Appendix E Three-dimensional model of IgG

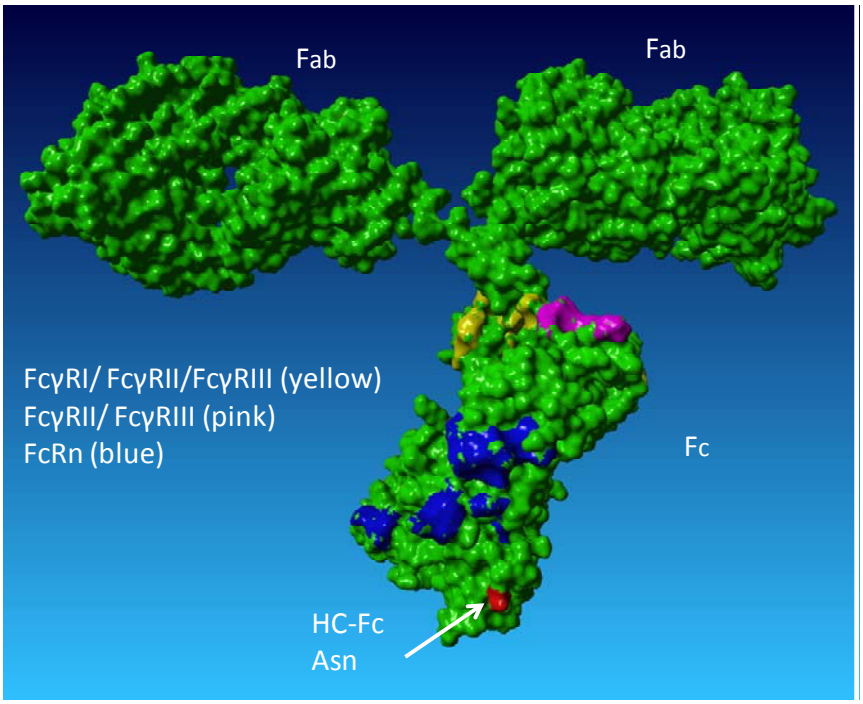

Figure 6.E.1 *Three-dimensional model of an IgG1 with the residues that are involved in Fc interactions indicated in yellow, pink and blue. The asparagine in the Fc region of the IgG that is most prone towards deamidation is indicated in red.*

References

1. Ecker, D. M., Jones, S. D., and Levine, H. L. The therapeutic monoclonal antibody market. MAbs. 2015; 7(1): 9-14
2. Jiang, X. R., Song, A., Bergelson, S., Arroll, T., Parekh, B., May, K., Chung, S., Strouse, R., Mire-Sluis, A., and Schenerman, M. Advances in the assessment and control of the effector functions of therapeutic antibodies. Nat.Rev.Drug Discov. 2011; 10(2): 101-111
3. Hogarth, P. M. and Pietersz, G. A. Fc receptor-targeted therapies for the treatment of inflammation, cancer and beyond. Nat.Rev.Drug Discov. 2012; 11(4): 311-331
4. Mellor, J. D., Brown, M. P., Irving, H. R., Zalcberg, J. R., and Dobrovic, A. A critical review of the role of Fc gamma receptor polymorphisms in the response to monoclonal antibodies in cancer. J.Hematol.Oncol. 2013; 6 1-
5. Nimmerjahn, F. and Ravetch, J. V. Fcgamma receptors as regulators of immune responses. Nat.Rev.Immunol. 2008; 8(1): 34-47
6. Vidarsson, G., Dekkers, G., and Rispens, T. IgG subclasses and allotypes: from structure to effector functions. Front Immunol. 2014; 5 520-
7. Koene, H. R., Kleijer, M., Algra, J., Roos, D., von dem Borne, A. E., and de, Haas M. Fc gammaRIIIa-158V/F polymorphism influences the binding of IgG by natural killer cell Fc gammaRIIIa, independently of the Fc gammaRIIIa-48L/R/H phenotype. Blood 1-8-1997; 90(3): 1109-1114
8. Suzuki, T., Ishii-Watabe, A., Tada, M., Kobayashi, T., Kanayasu-Toyoda, T., Kawanishi, T., and Yamaguchi, T. Importance of neonatal FcR in regulating the serum half-life of therapeutic proteins containing the Fc domain of human IgG1: a comparative study of the affinity of monoclonal antibodies and Fc-fusion proteins to human neonatal FcR. J.Immunol. 15-2-2010; 184(4): 1968-1976
9. Wang, W., Lu, P., Fang, Y., Hamuro, L., Pittman, T., Carr, B., Hochman, J., and Prueksaritanont, T. Monoclonal antibodies with identical Fc sequences can bind to FcRn differentially with pharmacokinetic consequences. Drug Metab Dispos. 2011; 39(9): 1469-1477
10. Datta-Mannan, A. and Wroblewski, V. J. Application of FcRn binding assays to guide mAb development. Drug Metab Dispos. 2014; 42(11): 1867-1872
11. Shields, R. L., Namenuk, A. K., Hong, K., Meng, Y. G., Rae, J., Briggs, J., Xie, D., Lai, J., Stadlen, A., Li, B., Fox, J. A., and Presta, L. G. High resolution mapping of the binding site on human IgG1 for Fc gamma RI, Fc gamma RII, Fc gamma RIII, and FcRn and design of IgG1 variants with improved binding to the Fc gamma R. J.Biol.Chem. 2-3-2001; 276(9): 6591-6604
12. Dashivets, T., Thomann, M., Rueger, P., Knaupp, A., Buchner, J., and Schlothauer, T. Multi-Angle Effector Function Analysis of Human Monoclonal IgG Glycovariants. PLoS.One. 2015; 10(12): e0143520-
13. Boesch, A. W., Brown, E. P., Cheng, H. D., Ofori, M. O., Normandin, E., Nigrovic, P. A., Alter, G., and Ackerman, M. E. Highly parallel characterization of IgG Fc binding interactions. MAbs 2014; 6(4): 915-927
14. Houde, D., Peng, Y., Berkowitz, S. A., and Engen, J. R. Post-translational modifications differentially affect IgG1 conformation and receptor binding. Mol.Cell Proteomics. 2010; 9(8): 1716-1728
15. Dorion-Thibaudeau, J., Raymond, C., Lattova, E., Perreault, H., Durocher, Y., and De, Crescenzo G. Towards the development of a surface plasmon resonance assay to evaluate the glycosylation pattern of monoclonal antibodies using the extracellular domains of CD16a and CD64. J.Immunol.Methods 2014; 408 24-34

16. Harrison, A., Liu, Z., Makweche, S., Maskell, K., Qi, H., and Hale, G. Methods to measure the binding of therapeutic monoclonal antibodies to the human Fc receptor FcgammaRIII (CD16) using real time kinetic analysis and flow cytometry. J.Pharm.Biomed.Anal. 7-4-2012; 63 23-28

17. Lu, Y., Vernes, J. M., Chiang, N., Ou, Q., Ding, J., Adams, C., Hong, K., Truong, B. T., Ng, D., Shen, A., Nakamura, G., Gong, Q., Presta, L. G., Beresini, M., Kelley, B., Lowman, H., Wong, W. L., and Meng, Y. G. Identification of IgG(1) variants with increased affinity to FcgammaRIIIa and unaltered affinity to FcgammaRI and FcRn: comparison of soluble receptor-based and cell-based binding assays. J.Immunol.Methods 28-2-2011; 365(1-2): 132-141

18. Junttila, T. T., Parsons, K., Olsson, C., Lu, Y., Xin, Y., Theriault, J., Crocker, L., Pabonan, O., Baginski, T., Meng, G., Totpal, K., Kelley, R. F., and Sliwkowski, M. X. Superior in vivo efficacy of afucosylated trastuzumab in the treatment of HER2-amplified breast cancer. Cancer Res. 1-6-2010; 70(11): 4481-4489

19. Ferrara, C., Grau, S., Jager, C., Sondermann, P., Brunker, P., Waldhauer, I., Hennig, M., Ruf, A., Rufer, A. C., Stihle, M., Umana, P., and Benz, J. Unique carbohydrate-carbohydrate interactions are required for high affinity binding between FcgammaRIII and antibodies lacking core fucose. Proc.Natl.Acad.Sci.U.S.A 2-8-2011; 108(31): 12669-12674

20. Bertolotti-Ciarlet, A., Wang, W., Lownes, R., Pristatsky, P., Fang, Y., McKelvey, T., Li, Y., Li, Y., Drummond, J., Prueksaritanont, T., and Vlasak, J. Impact of methionine oxidation on the binding of human IgG1 to Fc Rn and Fc gamma receptors. Mol.Immunol. 2009; 46(8-9): 1878-1882

21. Stracke, J., Emrich, T., Rueger, P., Schlothauer, T., Kling, L., Knaupp, A., Hertenberger, H., Wolfert, A., Spick, C., Lau, W., Drabner, G., Reiff, U., Koll, H., and Papadimitriou, A. A novel approach to investigate the effect of methionine oxidation on pharmacokinetic properties of therapeutic antibodies. MAbs. 2014; 6(5): 1229-1242

22. Neuber, T., Frese, K., Jaehrling, J., Jager, S., Daubert, D., Felderer, K., Linnemann, M., Hohne, A., Kaden, S., Kolln, J., Tiller, T., Brocks, B., Ostendorp, R., and Pabst, S. Characterization and screening of IgG binding to the neonatal Fc receptor. MAbs. 2014; 6(4): 928-942

23. Bajardi-Taccioli, A., Blum, A., Xu, C., Sosic, Z., Bergelson, S., and Feschenko, M. Effect of protein aggregates on characterization of FcRn binding of Fc-fusion therapeutics. Mol.Immunol. 2015; 67(2 Pt B): 616-624

24. Luo, Y., Lu, Z., Raso, S. W., Entrican, C., and Tangarone, B. Dimers and multimers of monoclonal IgG1 exhibit higher in vitro binding affinities to Fcgamma receptors. MAbs 2009; 1(5): 491-504

25. Li, P., Jiang, N., Nagarajan, S., Wohlhueter, R., Selvaraj, P., and Zhu, C. Affinity and kinetic analysis of Fcgamma receptor IIIa (CD16a) binding to IgG ligands. J.Biol.Chem. 2-3-2007; 282(9): 6210-6221

26. Paul, R., Graff-Meyer, A., Stahlberg, H., Lauer, M. E., Rufer, A. C., Beck, H., Briguet, A., Schnaible, V., Buckel, T., and Boeckle, S. Structure and function of purified monoclonal antibody dimers induced by different stress conditions. Pharm.Res. 2012; 29(8): 2047-2059

27. Gandhi, S., Ren, D., Xiao, G., Bondarenko, P., Sloey, C., Ricci, M. S., and Krishnan, S. Elucidation of degradants in acidic peak of cation exchange chromatography in an IgG1 monoclonal antibody formed on long-term storage in a liquid formulation. Pharm.Res. 2012; 29(1): 209-224

28. Patel, R, Johnson KK, Andrien B A, and Tamburini P P. IgG subclass variation of a monoclonal antibody binding to human Fc-gamma receptors. American Journal of Biochemistry and Biotechnology 17-7-2013; 9(3): 206-218

29. Geuijen, K. P., Egging, D. F., Bartels, S., Schouten, J., Schasfoort, R. B., and Eppink, M. H. Characterization of low affinity Fcgamma receptor biotinylation under controlled reaction conditions by mass spectrometry and ligand binding analysis. Protein Sci. 2016; 25(10): 1841-1852

30. Geuijen, K. P., Schasfoort, R. B., Wijffels, R. H., and Eppink, M. H. High-throughput and multiplexed regeneration buffer scouting for affinity-based interactions. Anal.Biochem. 1-6-2014; 454 38-40

31. Katsamba, P. S., Navratilova, I., Calderon-Cacia, M., Fan, L., Thornton, K., Zhu, M., Bos, T. V., Forte, C., Friend, D., Laird-Offringa, I., Tavares, G., Whatley, J., Shi, E., Widom, A., Lindquist, K. C., Klakamp, S., Drake, A., Bohmann, D., Roell, M., Rose, L., Dorocke, J., Roth, B., Luginbuhl, B., and Myszka, D. G. Kinetic analysis of a high-affinity antibody/antigen interaction performed by multiple Biacore users. Anal.Biochem. 15-5-2006; 352(2): 208-221

32. Navratilova, I., Papalia, G. A., Rich, R. L., Bedinger, D., Brophy, S., Condon, B., Deng, T., Emerick, A. W., Guan, H. W., Hayden, T., Heutmekers, T., Hoorelbeke, B., McCroskey, M. C., Murphy, M. M., Nakagawa, T., Parmeggiani, F., Qin, X., Rebe, S., Tomasevic, N., Tsang, T., Waddell, M. B., Zhang, F. F., Leavitt, S., and Myszka, D. G. Thermodynamic benchmark study using Biacore technology. Anal.Biochem. 1-5-2007; 364(1): 67-77

33. Rich, R. L., Papalia, G. A., Flynn, P. J., Furneisen, J., Quinn, J., Klein, J. S., Katsamba, P. S., Waddell, M. B., Scott, M., Thompson, J., Berlier, J., Corry, S., Baltzinger, M., Zeder-Lutz, G., Schoenemann, A., Clabbers, A., Wieckowski, S., Murphy, M. M., Page, P., Ryan, T. E., Duffner, J., Ganguly, T., Corbin, J., Gautam, S., Anderluh, G., Bavdek, A., Reichmann, D., Yadav, S. P., Hommema, E., Pol, E., Drake, A., Klakamp, S., Chapman, T., Kernaghan, D., Miller, K., Schuman, J., Lindquist, K., Herlihy, K., Murphy, M. B., Bohnsack, R., Andrien, B., Brandani, P., Terwey, D., Millican, R., Darling, R. J., Wang, L., Carter, Q., Dotzlaf, J., Lopez-Sagaseta, J., Campbell, I., Torreri, P., Hoos, S., England, P., Liu, Y., Abdiche, Y., Malashock, D., Pinkerton, A., Wong, M., Lafer, E., Hinck, C., Thompson, K., Primo, C. D., Joyce, A., Brooks, J., Torta, F., Bagge Hagel, A. B., Krarup, J., Pass, J., Ferreira, M., Shikov, S., Mikolajczyk, M., Abe, Y., Barbato, G., Giannetti, A. M., Krishnamoorthy, G., Beusink, B., Satpaev, D., Tsang, T., Fang, E., Partridge, J., Brohawn, S., Horn, J., Pritsch, O., Obal, G., Nilapwar, S., Busby, B., Gutierrez-Sanchez, G., Gupta, R. D., Canepa, S., Witte, K., Nikolovska-Coleska, Z., Cho, Y. H., D'Agata, R., Schlick, K., Calvert, R., Munoz, E. M., Hernaiz, M. J., Bravman, T., Dines, M., Yang, M. H., Puskas, A., Boni, E., Li, J., Wear, M., Grinberg, A., Baardsnes, J., Dolezal, O., Gainey, M., Anderson, H., Peng, J., Lewis, M., Spies, P., Trinh, Q., Bibikov, S., Raymond, J., Yousef, M., Chandrasekaran, V., Feng, Y., Emerick, A., Mundodo, S., Guimaraes, R., McGirr, K., Li, Y. J., Hughes, H., Mantz, H., Skrabana, R., Witmer, M., Ballard, J., Martin, L., Skladal, P., Korza, G., Laird-Offringa, I., Lee, C. S., Khadir, A., Podlaski, F., Neuner, P., Rothacker, J., Rafique, A., Dankbar, N., Kainz, P., Gedig, E., Vuyisich, M., Boozer, C., Ly, N., Toews, M., Uren, A., Kalyuzhniy, O., Lewis, K., Chomey, E., Pak, B. J., and Myszka, D. G. A global benchmark study using affinity-based biosensors. Anal.Biochem. 15-3-2009; 386(2): 194-216

34. Arnold, J. N., Wormald, M. R., Sim, R. B., Rudd, P. M., and Dwek, R. A. The impact of glycosylation on the biological function and structure of human immunoglobulins. Annu.Rev.Immunol. 2007; 25 21-50

35. Vaughn, D. E. and Bjorkman, P. J. High-affinity binding of the neonatal Fc receptor to its IgG ligand requires receptor immobilization. Biochemistry 5-8-1997; 36(31): 9374-9380

36. Yeung, Y. A., Leabman, M. K., Marvin, J. S., Qiu, J., Adams, C. W., Lien, S., Starovasnik, M. A., and Lowman, H. B. Engineering human IgG1 affinity to human neonatal Fc receptor: impact of affinity improvement on pharmacokinetics in primates. J Immunol. 15-6-2009; 182(12): 7663-7671

37. Ramsland, P. A., Farrugia, W., Bradford, T. M., Sardjono, C. T., Esparon, S., Trist, H. M., Powell, M. S., Tan, P. S., Cendron, A. C., Wines, B. D., Scott, A. M., and Hogarth, P. M. Structural basis for Fc gammaRIIa recognition of human IgG and formation of inflammatory signaling complexes. J.Immunol. 15-9-2011; 187(6): 3208-3217

38. Sondermann, P., Huber, R., Oosthuizen, V., and Jacob, U. The 3.2-A crystal structure of the human IgG1 Fc fragment-Fc gammaRIII complex. Nature 20-7-2000; 406(6793): 267-273

39. Wang, W., Vlasak, J., Li, Y., Pristatsky, P., Fang, Y., Pittman, T., Roman, J., Wang, Y., Prueksaritanont, T., and Ionescu, R. Impact of methionine oxidation in human IgG1 Fc on serum half-life of monoclonal antibodies. Mol.Immunol. 2011; 48(6-7): 860-866

40. Tao, M. H. and Morrison, S. L. Studies of aglycosylated chimeric mouse-human IgG. Role of carbohydrate in the structure and effector functions mediated by the human IgG constant region. J.Immunol. 15-10-1989; 143(8): 2595-2601

41. Zheng, K., Bantog, C., and Bayer, R. The impact of glycosylation on monoclonal antibody conformation and stability. MAbs. 2011; 3(6): 568-576

42. Sola, R. J. and Griebenow, K. Effects of glycosylation on the stability of protein pharmaceuticals. J.Pharm.Sci. 2009; 98(4): 1223-1245

43. Zhang, A., Singh, S. K., Shirts, M. R., Kumar, S., and Fernandez, E. J. Distinct aggregation mechanisms of monoclonal antibody under thermal and freeze-thaw stresses revealed by hydrogen exchange. Pharm.Res. 2012; 29(1): 236-250

44. Plath, F., Ringler, P., Graff-Meyer, A., Stahlberg, H., Lauer, M. E., Rufer, A. C., Graewert, M. A., Svergun, D., Gellermann, G., Finkler, C., Stracke, J. O., Koulov, A., and Schnaible, V. Characterization of mAb dimers reveals predominant dimer forms common in therapeutic mAbs. MAbs. 2016; 8(5): 928-940

Chapter 6

CHAPTER 7

General discussion

Chapter 7

Abstract

In the preceding chapters applications of multiplexed surface plasmon resonance imaging during the process development and product characterization of biopharmaceuticals have been highlighted.

Two different buffer screening applications have been developed for process development and described: screening for most optimal regeneration conditions for SPR-based applications and a similar approach where SPRi was used to optimize affinity chromatography conditions during process development.

Product characterization applications that have been developed included a glycoprofiling method of erythropoietin, which was applied to quantify sialylation levels of rhEPO. Additionally, a multiplexed method for characterization of Fcγ receptor binding of monoclonal antibodies was described, which is used to support in-process control measurements by rapidly screening product quality. This latter method could only be established after exploring the optimal conditions for minimal biotinylation. These were determined in a design of experiments, and labeling positions were identified by mass spectrometry methods.

In this chapter the general findings of how the SPRi platform is beneficial for process and product characterization during biopharmaceutical development are being discussed. We will also highlight a few applications that have been investigated but did not meet requirements for high-throughput screening. An outlook on SPRi applications and SPR-like technologies that have potential for future applications will further be discussed.

Introduction

Surface plasmon resonance (SPR) has emerged as a powerful analytical tool in food, environmental and pharmaceutical research over the past three decades. The technique is now generally accepted in research and development as well as in quality control analyses. More recently SPR imaging, or SPRi, has been developed and used in a number of applications, such as antibody affinity ranking,[1] epitope binning [2] or biomarker identification, [3-5] among many others.

In this work we have applied the SPRi platform to several process support and product characterization steps of biopharmaceutical proteins as outlined in previous chapters. The main findings from these studies will be further discussed including examples of a few applications that were not further developed after initial evaluation. In Figure 7.1 an overview of a general process for biopharmaceutical development is shown and the major opportunities for SPRi application are indicated, of which several have been tested and demonstrated in this work. Furthermore, an outlook to future applications of SPRi is provided, as well as an overview of other potential techniques that may be used for characterization of therapeutic proteins.

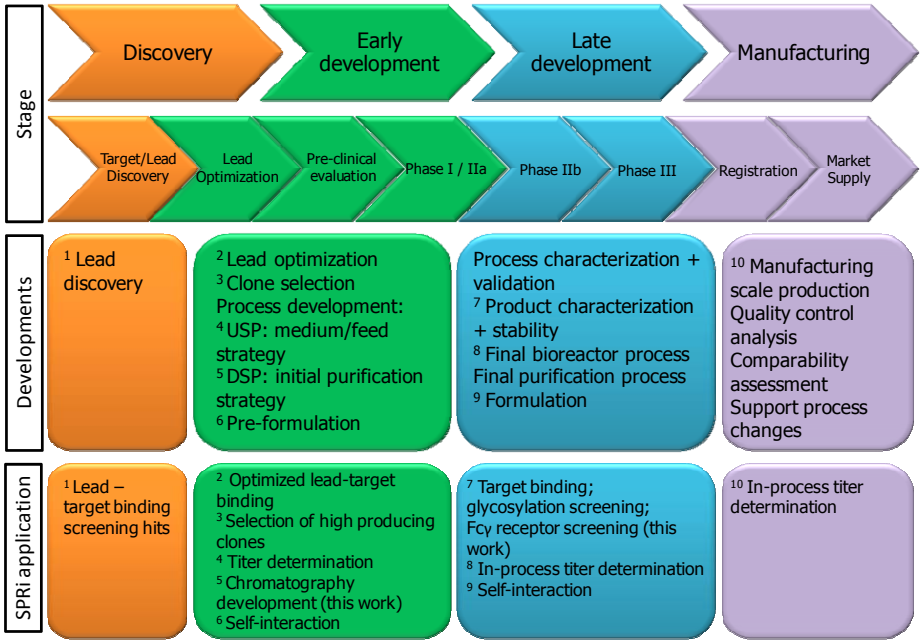

Figure 7.1 *Overview of biopharmaceutical development process including the different developments and indications where SPRi can be applied*

Chapter 7

Process development

Upstream processing

During the upstream process, the protein titer in the bioreactor is monitored to verify the production. Often, samples are taken daily to be measured off-line, but novel at-line methods using SPR have been developed in recent years to quantify the protein titer directly from the bioreactor (indicated in step 4, 8 and 10 in Figure 7.1).[6,7] Additionally, one aspect of the bioactivity of the proteins can directly be measured based on target binding (step 7 in Figure 7.1), whereas off-line measurements only provide the protein titer but cannot guarantee if this is functional product. Protein expression monitoring from crude cell lysates in biological samples has been determined by multiplexed SPR in other research as well.[8,9]

A similar titer determination assay was developed on the SPRi platform, using different experimental set-ups. The instrumental set-up of the IBIS MX96 system does not allow multiple samples to be analyzed simultaneously, unless these are immobilized or captured on the sensor surface in the CFM printer. Therefore, the following experimental set-up was investigated first: 1) immobilization of protein A / MabSelectSure (MSS) on the entire sensor surface (cover coupling), 2) 48-plex application of IgG to the MSS surface in the CFM printer, 3) read-out in the IBIS MX96 instrument (Figure 7.2-A). The read-out was based on the measurement of baseline levels before and after IgG application, or by ligand density measurement, which is an optical determination of surface spot intensity in the software. In both cases, the sensor was taken out of the instrument and placed back after IgG application, which introduced too much variation in the results. The regions of interest (ROIs) define the exact position of a sample, which is used for quantification. The ROIs that were placed before IgG application were not always at exactly the same position as after IgG application in the CFM, resulting in analytical variation.

A second approach used the same set-up, but instead of measuring baseline elevation, a secondary kappa-Fab fragment (KappaSelect) was used to measure the amount of IgG that was captured on each spot (Figure 7.2-B). This approach was successfully applied, although the amounts of KappaSelect needed to obtain quantitative data were too high to be economically feasible. The alternative of using an anti-kappa antibody is not feasible, as this antibody will also bind to the initial protein A surface and cannot be used quantitatively.

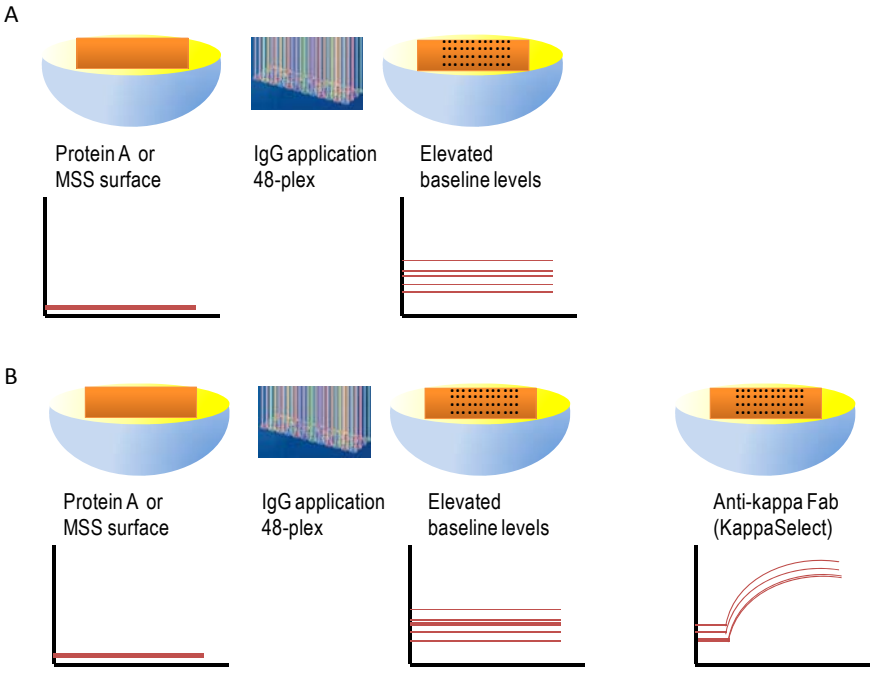

Figure 7.2 *Experimental set-up for IgG titer determination using the IBIS MX96 system and CFM printer. A) direct approach, measuring elevated baselines after IgG application. B) Use of secondary anti-kappa Fab fragment as read-out*

Other alternative approaches may be available, but have not been investigated further, since it would never lead to a direct approach and a secondary reagent will be necessary. In conclusion, the instrumental set-up of the IBIS system in combination with the CFM limited the use of a multiplexed titer determination. The sensor has to be transferred from IBIS to CFM and back, which is performed manually and is therefore not preferred in a rapid measurement. Direct measurements were not accurate enough due to variation in sensor position after transfer. If only a method for titer determination is required, other instruments or techniques (e.g. BLI / Octet, protein-A UPLC) are easily applied and are preferred. Titer determination in combination with bioactivity as described by Chavane et al.[6] and Jacquemart et al.[7] is feasible at the IBIS MX96 when antigen target and protein A are immobilized on the same sensor, although the multiplexing capabilities of the instrument are not fully utilized since only two of the 96 available ligand spots will be used. Any SPR instrument can as well be used for such an approach, and therefore such application is not a unique opportunity for SPRi instrumentation.

Downstream processing

In addition to support during the upstream process, the SPRi platform is an attractive alternative for high-throughput screening during downstream processing, mainly in the development of affinity chromatography. In case of process development for IgGs, protein A affinity chromatography is the method of choice as the primary purification step. Since SPR measures the affinity between two proteins based on their interaction, this technique is well suited for process simulation at a miniaturized scale.

In **Chapter 3** we have proven that SPRi can be used to simulate an affinity chromatography process. Finding optimal wash or elution buffer conditions is easily performed within a few hours to days. The screening technology is further interesting to ligand developers that want to test the stability of new ligands including the optimal buffer conditions for using those new ligands. In this protein A chromatography simulation several different instrumental set-ups have been applied for the elution buffer screening (Figure 7.3), wash buffer screening and ligand reusability screening (Figure 7.4). The wash buffer screening was performed using a similar approach as for the ligand reusability, but instead of injecting the buffer 10 times between two IgG injections, a new IgG injection was performed after each buffer injection. The elution buffer screening was performed in a similar set-up as the regeneration buffer scouting described in **Chapter 2**. The instrumental design of the IBIS MX96 in combination with the CFM requires manual transfer of the sensor from one instrument to the other as demonstrated in Figure 7.3, which introduces additional analytical variation because the sensor cannot be placed back at exactly the same position after transfer, as already discussed earlier.

The direct approach that was used for the wash buffer screening and ligand reusability (Figure 7.4) results in much less analytical variation because all measurements are performed in the IBIS MX96, without transfer of the sensor in between measurements. The drawback of this approach is that all buffers have to be tested sequentially in the SPR system, which increases experimental time compared to the indirect approach because the multiplexing capabilities are not fully utilized (Table 7.1). However, this can be automatically performed overnight or over a weekend without the need for an analyst to be present at the lab, whereas the indirect set-up requires an operator to manually transfer the sensor in between each measurement. Another benefit is that the wash buffer screening can then be performed on up to 96 different ligands at the same time for the number of wash buffer conditions or reusability cycles to be tested, to virtually unlimited numbers of test

conditions. This is often not necessary in a biopharmaceutical setting, as the choice of ligands for a chromatographic step is limited and often only one particular resin has to be screened. On the other hand, for ligand developers to test multiple new ligands the proposed screening approach is a valuable technology, which requires only minute amounts of material.

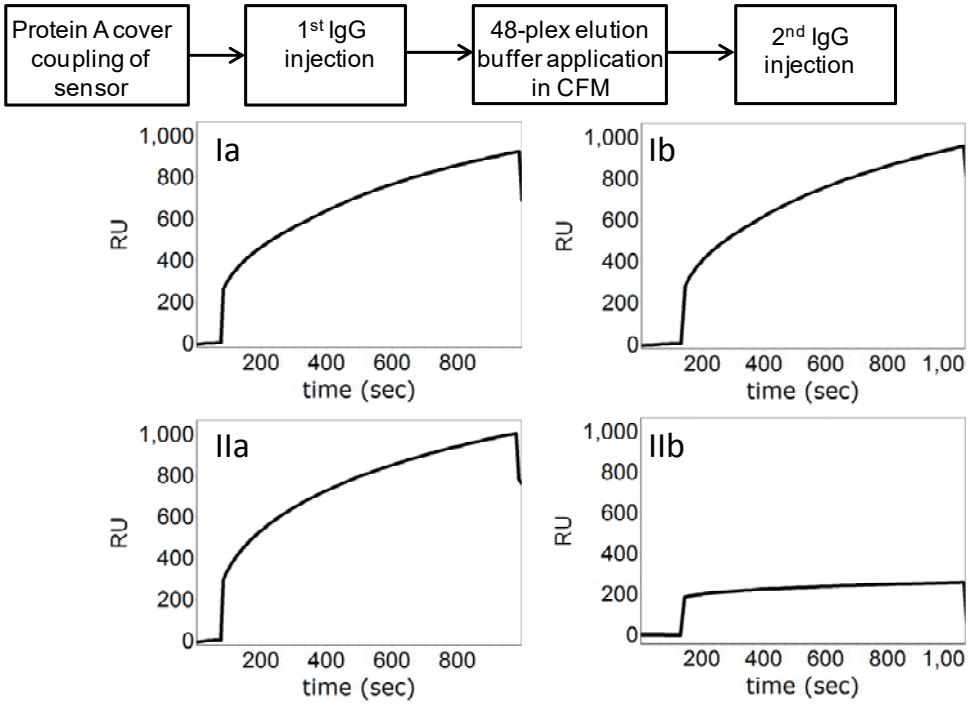

Figure 7.3 *Examples of elution buffer screening as performed in **Chapter 3**. In case of full elution of IgG from the surface, a similar response is measured in the second injection (example I), while in case of no elution of IgG, the surface is still saturated and no binding is measured in the 2nd injection of IgG (example II)*

Although there are some limitations to both the direct and indirect approach, as indicated in Table 7.1, the screening approach on SPRi consumes less amounts of ligand, proteins and buffers, while experimental time is in the same order of hours compared to other screening techniques that are often used (e.g. filter plates or robo-columns).[10-12] The direct approach is preferred over the indirect approach, because of the unattended operation and the smaller analytical variation in the results because there is no need for sensor transfer between instruments, despite the fact that the experiments will take more

time and consume somewhat more ligand, analyte and buffers in comparison to the indirect approach.

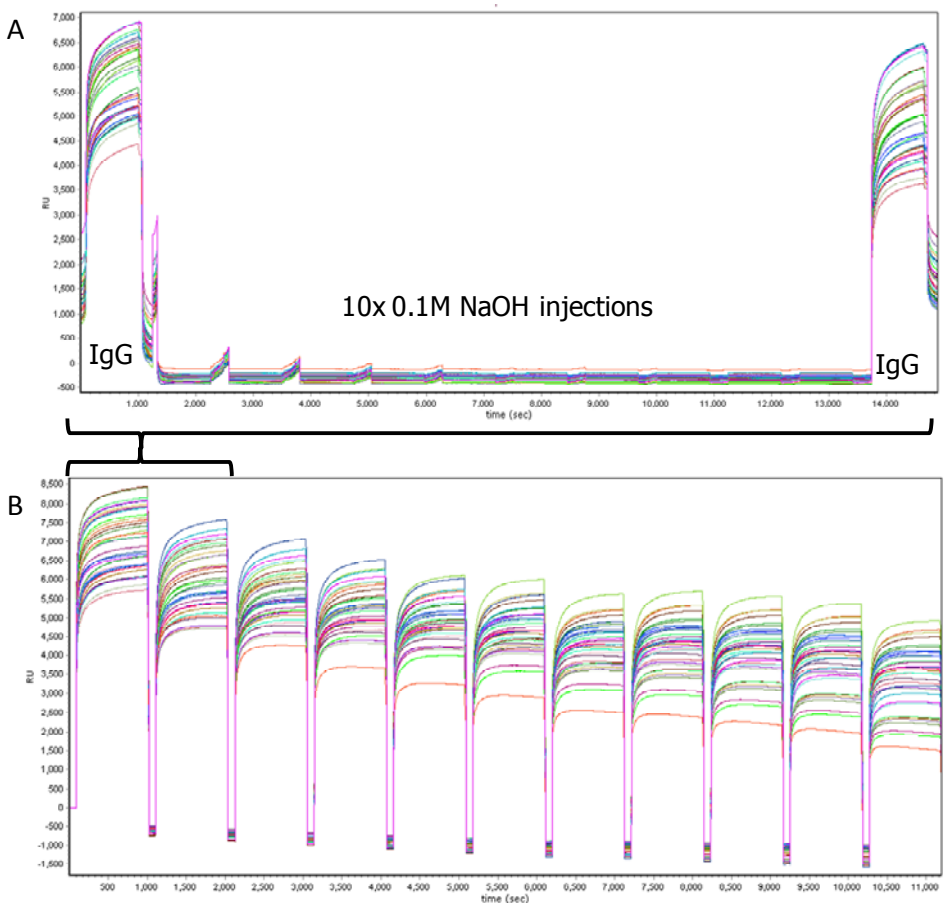

Figure 7.4 *Ligand reusability simulation on the SPRi platform, with 10 sequential NaOH injections (B) between each of the 10 IgG injections (A) to simulate in total 100 steps of NaOH cleaning on 36 individual ligand spots simultaneously*

Another part of the downstream process, or at least after protein purification, is the development of a formulation in which the protein is stable over prolonged time periods. One of the characteristics to determine during formulation development is the likelihood of a protein to interact with itself, because high levels of self-interactions may induce aggregates, which in turn lead to a lower product stability and may cause immunogenic reactions. Self-interaction chromatography is generally used to determine the self-

interaction of proteins in buffer of interest, and has in recent year already been miniaturized to microchip self-interaction studies.[13,14] Since self-interaction is based on protein-protein interactions, between the same protein, it can be studied in SPR methods. Self-interaction measurements on the SPRi platform have been investigated but with limited success. The low tendency of self-interaction of the studied IgG could not be measured with the SPR method, similar as self-interaction determinations by Patel et al.[15] Furthermore, in SPR measurements, often NaCl is added to the running buffer, which to some extent may prevent certain levels of non-specific binding to the sensor surface. No NaCl is present in most potential formulation buffers, which lead to relatively high levels of non-specific binding to the sensor surface. Other sensor types, which are developed to reduce non-specific binding, have been tested as well, but still no self-interaction could be measured. If present at all, the self-interaction is likely relatively weak and may therefore not be measurable under the investigated conditions.

Table 7.1 *Consumables for two approaches for buffer screening and ligand lifetime studies based on SPRi and the filter plate screening technology in comparison to conventional column screening*

Approach	Indirect	Direct	Filter plate*	Column (1 mL)
Applied in	Regeneration buffer (Chapter 2) Elution buffer (Chapter 3)	Wash buffer (Chapter 3) Ligand reusability (Chapter 3)	n.a.	n.a
Experiment time (n=1)	3 hours	24 - 48 hours	2-8 hours	Days - weeks
Amount of ligand/resin	3 µL	10 – 30 µL	2 – 4 mL	1 mL
Amount of sample	50 µg	1 – 2 mg	2 – 30 mg	> 500 mg
Amount of buffers	2 mL	5 – 40 mL	125-175 mL	2000 mL
Advantage	Very fast results Dynamic binding is measured; continuous flow	Automated performance Less analytical variation Dynamic binding is measured; continuous flow	Can be automated on pipetting robots	Dynamic binding is measured; continuous flow
Drawback	Manual sensor transfer; operator must be present. Analytical variation due to sensor transfer from IBIS to CFM	Test conditions must be sequentially injected; additional experiment time required	Static approach; no flow measurements	Takes many manual steps

* Based on a single 96-well plate

Chapter 7

Product characterization

Glycosylation fingerprinting

The characterization of protein glycosylation of biotherapeutics is of importance for the quality of the product, because it may determine the efficacy, half-life, stability and biological function of that protein. As already emphasized in the introduction, several methods to determine protein glycosylation are regularly used and are based on monosaccharide or glycan analysis, or more globally on the glycosylation fingerprint of a protein. The glycosylation fingerprint is a rough indication of the type of glycans that are present and the level of each, in a semi-quantitative measure, whereas full monosaccharide or glycan analyses provide accurate quantitative data on the carbohydrate compositions of glycoproteins.

Glycoprofiling or glycofingerprinting has been mainly determined on lectin arrays, by defining a panel of lectins to which the glycoprotein can specifically bind based on the glycan moieties that are present. Most of these lectin arrays are based on fluorescence detection, which requires the glycoprotein to be fluorescently labeled.[16-20] A similar glycoprofiling on a lectin array based on SPRi has been developed (**Chapter 4**), which prevents elaborate fluorescent labeling preparation. The described SPRi-based lectin array was able to measure glycofingerprints of different rhEPO biosimilar brands and showed differences between the brands.

The specificity of lectins is not always as high as needed for a proper glycoprofiling, as demonstrated by analyses of neoglycoproteins (**Chapter 4** and Figure 7.5, derived from Figure 4.1-B). Cross-reactivity with different glycan moieties or with non-glycosylated proteins, although at lower apparent affinities, may lead to difficulties in interpretation of the data. The high specificity that would be desired for such a profiling method would likely only be achieved by anti-glycan or anti-monosaccharide antibodies, because antibodies have a high specificity to the target against which they were raised. Additionally, high-affinity antibodies are easily selected from a pool of antibodies. However, antibodies against a specific glycan moiety are not readily available or not available at all. The natural occurrence of N-linked glycosylation in most animals that are generally used to raise antibodies limits the immunogenic potential of these glycan moieties.[21] Furthermore, the structural homology between the different N-glycan structures complicates a selective recognition for certain moieties even more.[21] A few anti-glycan antibodies have appeared in publications,

but the quality of these proteins is often lacking, which is another limitation for their widespread use, at least in case of N-glycosylation studies.[21] Last but not least, the costs for antibody generation against specific targets are high, while lectins can be relatively easy purified.

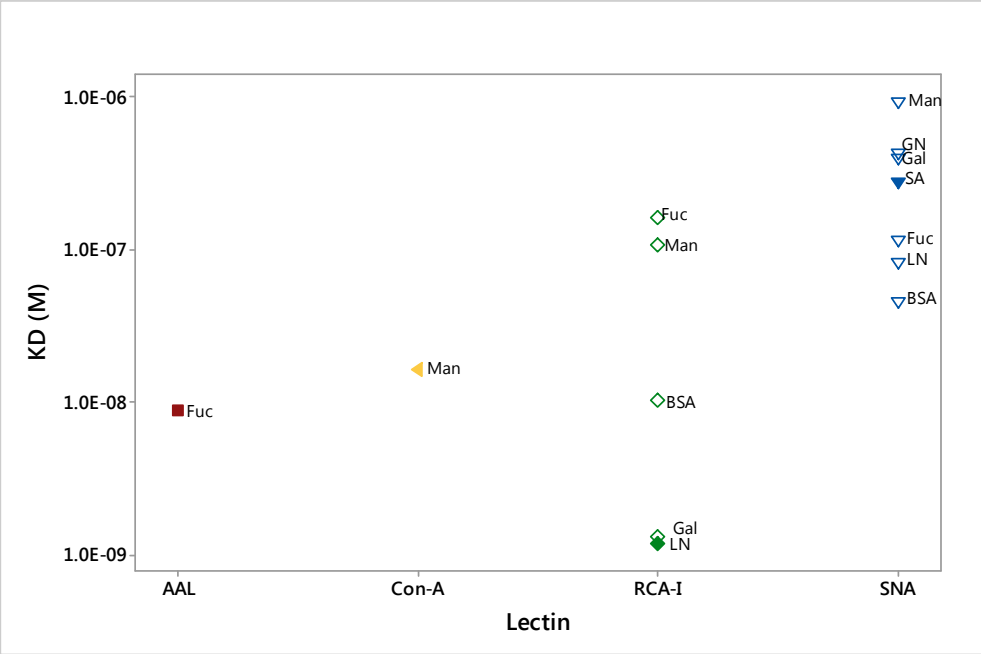

Figure 7.5 *Specificity of four selected lectins as demonstrated by neoglycoproteins (**Chapter 4**)*

These drawbacks of anti-glycan antibodies, and the natural occurrence of glycan-binding lectins, probably have led to the preference for lectins in fingerprinting methods, despite the cross-reactivity of some lectins. The glycoprofiling method on SPRi is an attractive tool in comparability studies for example in biosimilar assessments, or as an assay for in-process control. Fingerprint-like methods and orthogonal methods are becoming more important in biosimilarity assessments as indicated by the FDA, even though these methods are not necessarily validated.[22]

Fcγ receptor screening

Functionality of monoclonal antibodies partially depends on the binding of the Fc tail to various Fcγ receptors and serum half-life of IgGs is related to neonatal Fc receptor (FcRn) binding. The Fab region binds to the antigen target, and then effector cells which exhibit

one or more Fcγ receptors are responsible for clearance of pathogens or tumor cells, for example by antibody-dependent cell-mediated cytotoxicity (ADCC). The occurrence of various Fcγ receptors on human cells was used to design a screening tool based on SPRi to measure various Fcγ interactions simultaneously as part of critical quality attribute (CQA) assessment of antibodies, which was demonstrated in **Chapter 6**.

However, the broad range of affinities of the different Fcγ receptors (nM range for FcγRI and µm range for FcγRIIa/b and FcγRIIIa/b) prevented the application of all Fcγ receptors on the same multiplexed sensor surface. In addition to that, the FcRn could not be included in the same measurement, due to the different affinity range (nM range) and the interaction mechanism, which occurs at different pH compared to the Fcγ receptors. Therefore, separate methods were used to measure FcγRI and FcRn binding, whereas the different low affinity Fcγ receptors were immobilized on a single sensor surface, all with the aim for rapid characterization. Three different platforms were used to screen IgG binding to the various Fc receptors after stress-induced modifications on the IgGs in **Chapter 6**.

The developed screening method consisted of a sensor with four different immobilized Fcγ receptors, which is not the most optimal multiplexing capability that is possible on the IBIS MX96 instrument. However, different polymorphisms of these Fcγ receptors exist, which can have different affinity and binding properties for IgG compared to the natural variants.[23] For example, FcγRIIIa has a phenylalanine at position 158 (F158) in the natural, canonical sequence (Uniprot entry P08637), which has a weaker IgG binding than the allelic variant with valine at position 158 (V158).[24]

Another abundant, well-known mutation in the FcγRIIIa sequence is the presence of histidine or arginine at position 48, which replaces the leucine at position 48 in the canonical sequence and which is related to the allelic variant at position 158. Many more examples of amino acid mutations in the different Fcγ receptors have been identified (Table 7.2). The multiplexing capabilities of the IBIS MX96 can be fully exploited when the entire range of polymorphic variants is immobilized at the sensor surface, which is beneficial to screen IgG products for differential binding to each of these. This can be relevant for therapeutic antibodies, since different patients can have one or more of the different allelic variants expressed at their cells, which may affect the efficacy of the product and therefore it is important to chart possible effects on the different allelic variants.[25-29]

Table 7.2 *Known isoforms and polymorphic variants of the different Fcγ receptors from uniprot entrances*

Fcγ receptor	Isoform / mutation	Known effects on IgG binding
FcγRIIIa / CD16a (Uniprot P08637)	L48H	
	L48R	
	G139D	
	Y140H	
	F158V	Higher binding of hIgG1, hIgG3 and hIgG4.[24]
	F185S	
FcγRIIIb / CD16b (Uniprot O75015)	NA1	Similar binding for the three allelic variants [31,32]
	NA2	Similar binding for the three allelic variants [31]
	SH	Similar binding for the three allelic variants [31,33]
FcγRIIa / CD32a (Uniprot P12318)	AA35 missing	
	Q27R	
	M104V	
	Q127K	Clear interaction with hIgG2 [34]
	H131R	Minimal binding of IgG2 [31,35]
	I182V	
FcγRIIb / CD32b (Uniprot P31994)	AA 39-45 missing	
	AA 46 missing	
	AA 254-272 missing	
	Q83P	
	Y205F	
	I232T	
	Y258D	
FcγRI / CD64a (Uniprot P12314)	AA333-374 different	
	L105P	

The multiplexed Fcγ receptor screening sensor can furthermore be extended with receptors from various species, such as mouse, rabbit or monkey; species that are often used in preclinical tox studies and xenograft studies. Including receptors from these species on a single sensor would facilitate the translation or extrapolation of preclinical data from animal studies to human Fcγ receptor binding in clinical studies. Since up to 96 ligands can be immobilized onto a single sensor surface, and all these Fcγ receptors are structurally comparable, this should be feasible, but has not been performed in this work so far.

Cell applications

Recently several researchers published results on cell-based and cellular analyses using SPRi. Successful applications of living cell sensing have been proven. The following set-ups / applications of cell-based SPRi were published:

- Cell binding to specific capture ligands (cell receptor – ligand interactions), for example as a diagnostic tool,[36-39] among others
- Cellular responses to stimulation or inhibition of agents[40-43]
- Molecule secretion of captured cells[39,44,45]
- Blood group typing[46,47]

An attempt to implement the SPRi technique for high-throughput characterization of IgGs, in a similar way as the Fcγ receptor screening in **Chapter 6**, was investigated, but with limited success. HEK293F cells that were modified to express the different Fcγ receptors and FcRn individually on their cell surface were available. Fc receptor – IgG interactions can be studied in a more natural environment on whole cells using SPRi, with the Fc receptors attached to a cell surface followed by IgG injections.

The size of HEK293 cells is roughly 13-20 µm (determined by cell counting on Countess), whereas macrophages for example have a size of 20-30 µm,[48] which was considered an acceptable comparable cell size for these types of experiments. HEK293F cells (wild type or with any of the Fc receptors) could be captured on the sensor surface by anti-HLA antibodies. HLA, human leukocyte antigen, is present on the HEK293F cells and as such this capture was successful. The cells could also be regenerated from the sensor surface again, using 5 mM CHAPS as a regeneration agent, which eventually would lead to a re-usable sensor surface.

However, IgG binding to the Fc receptors on the captured cells could not be measured with the proposed set-up. Blank injections of buffer resulted in an increasing SPR signal

(Figure 7.6), which even continued during the dissociation phase (indicated by dotted line in Figure 7.6) on both WT and FcγRI cells. The signal that was measured with an injection of 250 nM IgG was lower compared to the blank (Figure 7.6-B).

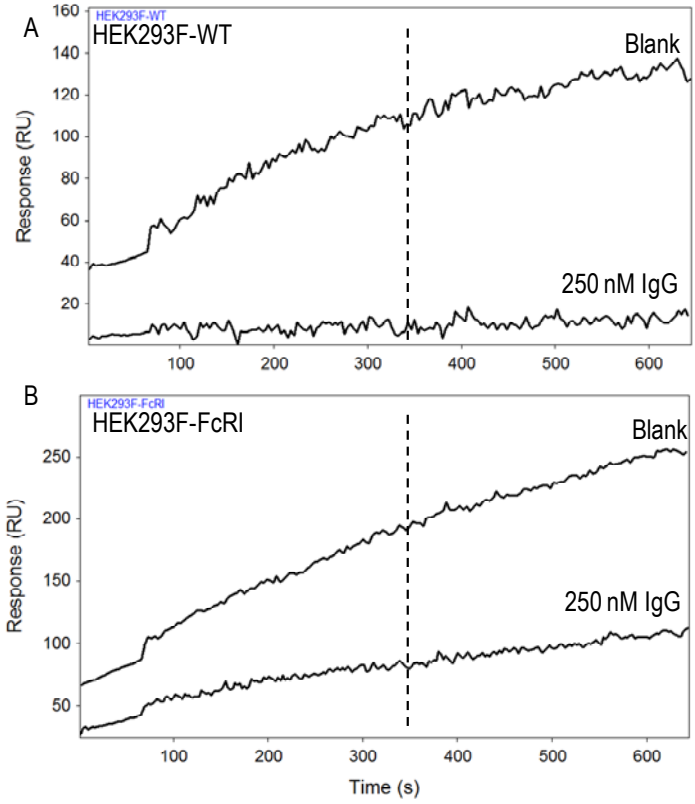

Figure 7.6 *Sensorgrams of blank and 250 nM IgG injections on captured HEK293F-WT cells (a) and HEK293F-CD64 cells (b). Dotted line indicates start of dissociation phase.*

The signal increment was possibly a result of cell movement on the sensor surface, since in blanks the signal steadily increases even during dissociation. Most likely the movements will be reduced after a long settling time (for example 30-60 minutes). Even then, after three blank injections, still no IgG binding to the HEK293F cells could be measured by SPR. Hypotheses for the lack of IgG binding measurements are:

1) IgG binding to the cells is outside of the evanescent field due to the large cell size (Figure 7.7); IgGs cannot reach the bottom of the flow cell / sensor surface due to

the presence of cells. The evanescent field determines where the SPR signal is most sensitive, which is approximately up to 400 nm from the surface.

2) Upon sedimentation the cell may spread out on the sensor surface, thereby blocking the accessibility of the Fcγ receptors at the cell close to the sensor surface (Figure 7.7-B). Experiments have been performed on a P-type SensEye sensor (SSens, Enschede), which consist of a planar, 2D-like sensor surface. Theoretically, cells will be captured closer to the sensor surface in comparison to more 3D-like sensor structures. Similar experiments on the G-type SensEye sensors did not improve the results, as still no IgG binding to captured cells was measured.

The proposed experimental set-up may be feasible using SPRi, although some improvements or changes are necessary. First, the number of receptors at a single cell may be reduced to overcome crowding effects at the top of the cell and force the IgG molecules further down the flow cell, closer to the sensor surface. The number of Fcγ receptors on each HEK293F cell is relatively large (approximately 170000 FcγRI receptors/cell, determined by FACS), while Richards et al.[49] determined approximately 50000 FcγRI receptors on macrophages, which is significantly lower. Macrophages and dendritic cells carry the highest number of FcγRI receptors on human effector cells;[50,51] for example 6-fold lower expression of FcγRI on monocytes was found by Jungi et al.[52] The HEK293F cells have much higher receptor densities compared to those naturally occurring effector cells, which may influence the IgG binding that can be measured.

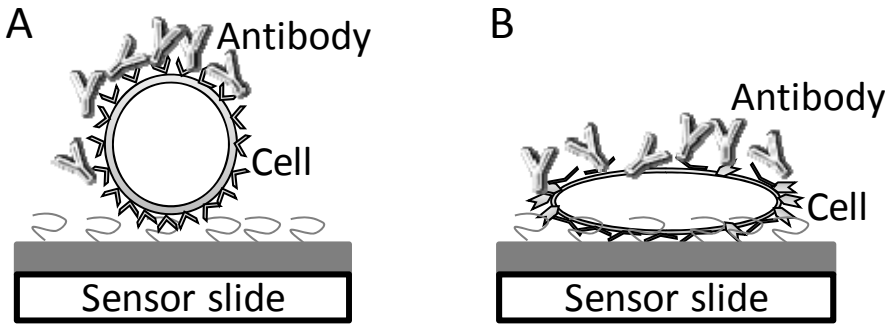

Figure 7.7 *Visualization of cell capture on the sensor surface. A) IgG mainly bind outside of the evanescent field due to the large cell size. B) Cell is spread out during sedimentation, thereby blocking the receptor accessibility at the cell – flow cell interface*

Secondly, the use of long-range SPR (LRSPR) may solve some of the issues with the sensitivity as the evanescent field is enlarged. LRSPR uses a sensor surface that is extended with 650 nm teflon layer,[53] 1200 nm teflon layer[54] or 950 nm Cytop fluoropolymer[41] between the glass and gold layer. This additional layer in the sensor enhances the penetration depth of the evanescent wave from approximately 200-400 nm in conventional SPR to 1–1.5 µm in LRSPR. The sensitivity of LRSPR is increased as a much sharper SPR reflectance angle is achieved. The combination of sensitive measurements further down the evanescent field may improve measurements of IgG binding to captured cells.

Another approach would be to fixate the cells onto the sensor surface to reduce cellular movements which possibly disturb SPR measurements. However, this limits the flexibility of the method, and hampers the development of a high-throughput screening. Lastly, it would be possible to immobilize or capture the cell membranes with Fc receptors instead of whole cells. In this approach, the problem with measuring outside of the evanescent field should be overcome, at least partially, and the Fcγ receptors would still be in a more native state in the lipid bilayer of the cell membrane compared to immobilization of only the extracellular part of the receptors which is now applied in SPR measurements.

SPRi equipment design

Surface plasmon resonance is relatively straightforward: interactions between two molecules of interest are measured in real-time and kinetics of the interaction can be determined. However, several practical aspects for the design of an experiment should be taken into consideration, in order to obtain high quality data. Most of these practical aspects are generally known and described in literature, but when developing multiplexed SPR methods these aspects can become challenging due to the fact that multiple, different ligands are used on a single sensor surface. We will briefly highlight a few of the most important aspects that should be taken into account for SPRi developments, including examples from the experiments that have been performed.

Ligand immobilization

A major benefit of SPR is the real-time measurement of protein binding, which is used to determine kinetic constants of protein interactions. Even though SPR is essentially label-free, still one of the proteins needs to be immobilized to the sensor surface, which may lead to similar limitations as in labeling methods, such as blocking the active binding site or changing the affinity of the ligand.[55] The choice of which of the two interaction partners

will be immobilized, depends on the purpose of the assay, the ease of immobilization of the intended ligand, and the remaining activity after immobilization. Generally, there are two options for immobilizing one of the proteins: covalent coupling or capture. Either way, the chance to inactivate the ligand is inherent to ligand immobilization, regardless of which immobilization strategy is chosen. Therefore, a proper immobilization strategy needs to be chosen and evaluated carefully.

Covalent coupling is stable, robust, easy to apply and a wide range of chemistries are available for coupling ligands to the surface (e.g. amine, thiol, aldehyde, carboxyl, hydroxyl).[56] Drawbacks of covalent coupling include the possibility of blocking the active binding site, similar to labeling approaches. Furthermore, proteins may be inactivated or become unstable or denaturate at the surface or can lose their natural conformation.[55,57] In addition, shielding effects or steric hindrance of ligands for analyte binding may occur if too many proteins are coupled close to each other. Particularly in multiplexed assays, it can be challenging to couple all ligands with the same chemistry, because all of the intended ligands must have the same reactive groups available for coupling, without affecting any of the binding properties.

Amine coupling is most widely applied in SPR, and was used to couple protein A to the sensor surface (**Chapter 3**) and to couple lectins to the sensor surface (**Chapters 2** and **Chapter 4**). In the protein A coupling, the entire sensor surface was covered with protein A to create binding sites for IgG without prerequisites for ligand density, other than sufficiently amount of protein A that had to be captured. In the lectin array on the other hand (**Chapter 4**), the surface densities and immobilization pH for each lectin was optimized in order to create an active surface for glycoprotein binding. Not all lectins could be preconcentrated to the sensor surface at the same pH, which resulted in a total of four different immobilization buffer pHs. Glycoprotein binding was verified with several model proteins (transferrin, ovalbumin, fetuin) and by neoglycoproteins for kinetic determinations. These experiments proved that the covalent amine coupling of lectins could be applied without major activity losses or protein inactivation. In case of the Fcγ receptor assay (**Chapter 6**), a direct covalent coupling was not suitable, as the active binding sites in the Fcγ receptors were partially blocked and resulted in a low active surface. A capture approach was chosen for the Fcγ receptor assay.

In capture approaches the immobilization can be more uniformly applied, as most capture approaches can be site-directed when properly designed. The most common capture approaches include biotin-streptavidin, His-tag capture on Ni-NTA surface or

antibody-based capture.[56] Drawbacks of capture approaches are the loss of ligand during wash or regeneration conditions if the affinity is too weak[57] and then re-usability of the sensor may become an issue. In case of biotin-streptavidin this is not an issue, since the strong affinity between these two is virtually as strong as a covalent bond. Capture by tags ideally results in uniform presentation of the ligand on the sensor surface, which may add in kinetic evaluation as surface heterogeneity is low. All ligands are similarly oriented to the sensor surface when inclusion of a tag is carefully designed.[56]

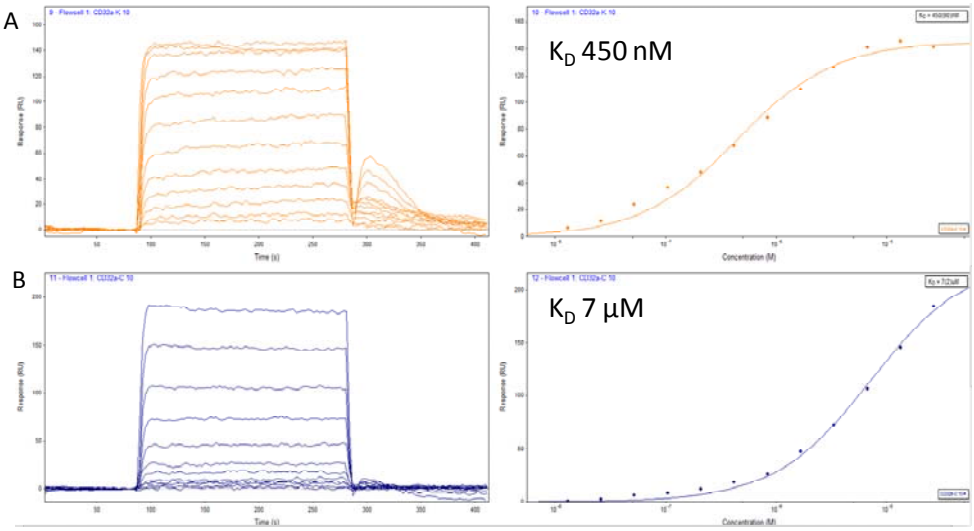

Figure 7.8 *Sensorgrams of IgG binding on FcγRIIa (left panels), biotinylated at lysines under minimal labeling approach (A) and biotinylated at carbohydrates (B), and the corresponding steady state equilibrium affinity determination (right panels)*

The lysines in the active binding site of Fcγ receptors that are involved in covalent coupling were also used to biotinylate the proteins. Initially a carbohydrate biotinylation was tested, however, this approach was even less successful than covalent coupling since the glycans of Fcγ receptors are a major contributor to the interaction with IgGs (Figure 7.8, Table 7.3).[58,59] Therefore, lysine biotinylation was chosen, and the biotinylation reactions were optimized to achieve a minimal labeling on the Fcγ receptors. We were able to minimize the number of biotins on a single Fcγ receptor protein and elucidated the major biotinylation sites by mass spectrometry (**Chapter 5**). Two lysines in the Fcγ receptor amino acid sequences were preferentially biotinylated, of which one is present in the active binding sites for IgG binding. Active ligands could be generated by minimizing the labeling

to maximum one biotin per protein, which was on either of these two preferred sites. The activity of the Fcγ receptors could be maintained to a certain extent, and affinity values close to reported values in literature were obtained (Table 7.3).

Table 7.3 *Affinity values of lysine biotinylation and carbohydrate biotinylation of Fcγ receptors*

Fcγ receptor	Lysine biotinylation		Carbohydrate biotinylation		Literature	
	K_D (μM)	Rmax (RU)	K_D (μM)	Rmax (RU)	K_D(μM)[15]	K_D (μM)[31]
FcγRIIIa	0.36	793	0.55	489	0.80	0.19
FcγRIIIb	2.21	1450	n.d.*	n.d.*	3.10	8.33
FcγRIIa	0.45	145	7.0	230	0.85	0.85
FcγRIIb	2.5	230	0.89	359	1.90	4.55

* n.d.: not determined: no binding of IgG could be measured on immobilized Fcγ receptor

An even more elegant biotinylation approach would be the use of an AVI-tag,[60] which is a small amino acid sequence that is added to the N-terminal or C-terminal of the protein of interest upon expression, followed by *in vivo* or *in vitro* biotinylation specifically at this position. This approach will generate a biotinylated ligand which is not affected in terms of binding properties, and allows for a site-directed immobilization on the sensor surface. However, the inclusion of this AVI-tag requires the development of a different expression vector, which was not available for the Fcγ receptors that were used during these studies.

In general, amine coupling is the most widely applied immobilization strategy, and can be applied in multiplexed SPR experiments as well. However, differences in immobilization properties of a wide variety of ligands may hamper the general applicability of this immobilization. Since streptavidin-biotin capture is nearly as strong as covalent coupling, and nowadays various elegant ways of incorporating biotins into proteins exist, this would be an attractive approach in ligand immobilization for multiplexed assays.

Regeneration conditions

Regeneration of the sensor surface is often applied to reuse the same ligands for multiple sequential analyses. Regeneration conditions should be mild, such that the binding capacity of the ligand is not destroyed, while capable of removing all bound analyte from the ligand. In most cases the immobilized ligands are proteins, that may be vulnerable to

harsh regeneration conditions, and therefore it is key to develop a mild, yet efficient regeneration strategy. Multiplexed SPR adds another difficulty, since finding regeneration conditions for tens to hundreds of ligands without destroying any of these may be quite challenging. Binding characteristics may be based on completely different types of interaction, which complicates finding the optimal yet simplest regeneration buffer. The protein-protein interactions that are studied are often a combination of electrostatic interactions, hydrophobic interactions and Van der Waals interactions, which are not necessarily broken under the same conditions. This was encountered on the lectin array (**Chapter 4**), where most default regeneration solutions (e.g. 10 mM glycin-HCl) were able to regenerate a few of the lectins, although none of the investigated solutions was able to regenerate all lectins sufficiently. The regeneration buffer scouting approach (**Chapter 2**) offered are an elegant way to screen many different buffers simultaneously, which eventually lead to a regeneration buffer cocktail (25 mM phosphoric acid / 3M $MgCl_2$) that was able to regenerate all lectins without destroying their binding properties. In **Chapter 2** only the initial steps of the screening are described, where a single ligand is coupled to the entire surface and a panel of 48 different regeneration buffer conditions was investigated. Then a new sensor was prepared where 8 ligands were immobilized in six replicate spots (48 spots in total), followed by screening the 12 most effective regeneration buffers from the first screening, in two sequential analyses. In case more ligands have to be investigated, less replicates per ligand can be spotted and only the most effective buffers can then be included in subsequent experiments. Overall, this may result in a single regeneration buffer for tens of ligands in only 2 experiments.

The regeneration buffer screening approach was also applied to the Fcγ receptor assay in **Chapter 6** (although not described in detail), as these receptors are vulnerable proteins that are easily destroyed at the sensor surface. The regeneration buffer screening for that assay resulted in 25 mM phosphoric acid pH 3 as a regeneration buffer. A 25 mM phosphoric acid buffer with a pH of 2.4 (by default) reduced the binding capacity of the receptors at the surface after each cycle, while only a slight pH increase to 3.0 was sufficient to efficiently remove the bound analytes and improved receptor stability at the sensor surface. This regeneration buffer was found after a single experiment performed in triplicate, using the multiplexed regeneration buffer scouting.

Non-specific binding and bulk effects

Non-specific binding and cross-reactivity can be an issue in protein interaction measurements.[56] Non-specific binding is mainly an issue in complex biological matrices, such as bioreactor harvest, urine, blood or plasma samples. Non-specific binding refers to compounds in the complex matrix interacting with the sensor surface or the chemistry at the sensor surface. The screening assays that were developed (**Chapter 4** and **Chapter 6**) were mainly based on purified sample material, where the chances for non-specific binding are marginal. The buffer screening approach for affinity chromatography (**Chapter 3**) used bioreactor harvest material and was carefully evaluated for non-specific binding. No harvest material bound to the reference spots, which are non-modified sensor surface areas, indicating that non-specific binding was not an issue during these experiments. However, bulk effects of harvest material were observed. Bulk effects appear when there is a mismatch in refractive index of the running buffer and the sample matrix or buffer. The refractive index of bioreactor harvest is different from the running buffer, resulting in bulk shifts, which could be corrected by reference subtraction.

Concluding remarks and future perspectives

Multiplexed high-throughput screening

Several multiplexed and label-free instruments are available nowadays (Table 7.4), of which the IBIS MX96 is one. Each of these systems has its own advantages and limitations, based on the instrumental design, such as, but not limited to: flexibility, sensitivity, temperature-control and ease-of-use.

High-throughput screening is often applied in areas where multiple samples need to be screened for several characteristics, or during process developments, as outlined throughout preceding chapters. SPRi can be applied in high-throughput profiling or fingerprinting methods, and as such can be an added value to those fields of research where many different samples or targets need to be screened. The choice for an array system (Figure 7.9) or a 'multiple-injector' system (Figure 7.10) depends on the requirements for the application that is developed.

In case of the lectin array screening (**Chapter 4**) an array system works best, since the large number of ligands is immobilized on a single sensor and samples are analyzed sequentially. However, the Fcγ receptor screening method in its current state (**Chapter 6**)

Table 7.4 *Overview of several commercial SPR instruments with multiplexing capabilities*

System	Vendor	Multiplexing #	Remarks
Array systems / imaging systems			
SPRimager II	GWCtechnologies	25 ROIs*	Many manual handling required
IBIS MX96	IBIS / Wasatch	96 ROIs	Off-line ligand spotting
OpenPlex	Horiba Scientific	400 ROIs	Direct coupling to MALDI-MS Off-line ligand spotting
XelPlex	Horiba Scientific	400 ROIs	Direct coupling to MALDI-MS Up to 6 running buffers Off-line ligand spotting
PlexArray	Plexera	5000 ROIs	Off-line ligand spotting
Multiple injector / flowchannel systems			
404pi	BiOptix	4 flow channels	Simultaneous injection of up to 4 different analytes Only 2 or 3 detection channels available when referencing is needed
NanoSPR8	NanoSPR	8 flow channels	Very small, portable instrument Can be coupled to electrochemical detection Many manual handling when running experiments
MASS-1	Sierra Sensors	8: 8 flow channels with 2 spots, of which 1 is reference	Automated switching between 5 running buffers Only single running buffer possible
8k	Biacore	8: 8 flow channels with 2 spots of which 1 is reference	
4000	Biacore	16: 4 flow channels with 5 spots, of which 1 is reference	
MASS-2	Sierra Sensors	16: 8 flow channels with 4 spots, of which 1 is reference	Up to 4 different running buffers
Proteon XPR36	BioRad	36: 6 flow channels with 6 spots + 42 reference spots	

#Criteria for multiplexing: at least 4 independent interactions have to be measured simultaneously in a single interaction; either by multiplexing the ligand, or by injecting multiple analytes simultaneously

* No specifications by vendor could be found; number of ROIs based on publications

would possibly be more efficiently performed on one of the "multiple-injector" systems, due to the limited number of receptors that are screened (only 6 receptors, 5 Fcγ receptors and FcRn), while the sample concentration and buffer requirements would allow simultaneous injection in different concentrations and buffer pH by a "multiple-injector" system in a single run such as the MASS-2 instrument. In the end, most applications can be designed on any

of the multiplexed instruments, since all rely on the same principle of multiplexing protein-protein interaction measurements although the highest possible throughput of the systems may not be fully utilized.

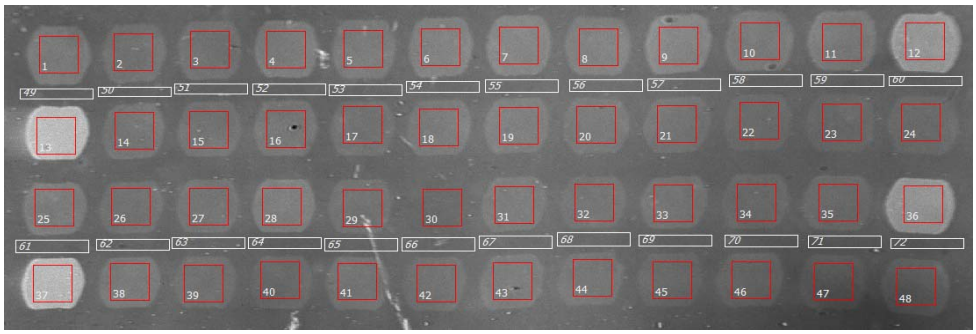

Figure 7.9 *Camera image of IBIS MX96 array with 4x12 immobilized spots. Red squares indicate the 'region of interest' (ROI) in which measurements are recorded. White squares indicate the reference ROIs used for correction*

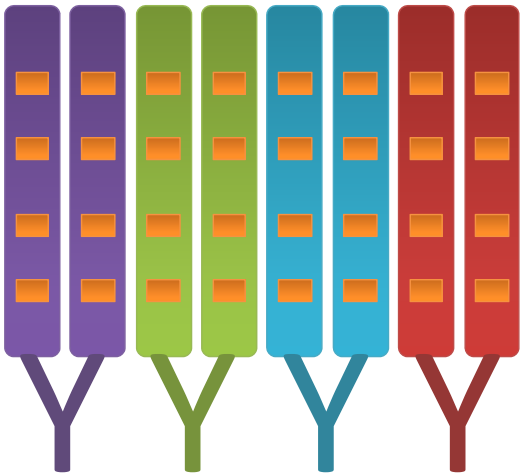

Figure 7.10 *Example of multiple injector/flow channel system with 8 flow channels and 4 detection spots per channel*

On the IBIS MX96 platform, a straightforward approach for comparability assessments would be to immobilize up to 96 samples onto a single sensor, and use the receptor or antigen (or any intended ligand) as analyte. Reversing the experimental set-up can significantly increase the throughput on the IBIS MX96 instrument, although it should be carefully assessed how representative the data from a reversed set-up are. Some of the

other array systems allow immobilization of even more ligands compared to the IBIS MX96 system (400 up to 5000). However, for applications such as those described here, a larger number of ligand spots is often not required and the available spots in the IBIS MX96 system already allows for screening many ligands simultaneously.

Future applications

Ideally, a multiplexed high-throughput screening method capable of simultaneously studying different characteristics of a biopharmaceutical would dramatically increase sample throughput. A combinatorial assay which directly links glycoprofiling to target-binding is a valuable addition. No further efforts in EPO receptor binding together with EPO glycoprofiling have further been, but it could be interesting for a multi-parameter profiling. The lectin array was not functional for glycoprofiling of IgGs and as such no target binding of IgGs has been included.

Looking one step further ahead would result in a combined glyco-profiling, target binding, titer determination and Fcγ receptor binding (only for IgGs) assay, measured all together on a single SPR sensor. However, combining multiple different protein-protein interaction measurements onto a single sensor surface brings along some other practical difficulties that need to be addressed. Practical aspects like differences in affinity between various ligands, differences in preferred running buffer and optimal regeneration conditions for a broad range of ligands should be aligned. It will be challenging to find optimal conditions for tens to hundreds of different ligands, such as buffer pH, optimal salt concentration or which additives to use (e.g. metal ions or surfactants) or regeneration conditions.[57] In the lectin array method (**Chapter 4**) already four different metal ions were added to the running buffer, since some lectins are only binding glycoproteins under influence of one or more of those metal ions.

Measurements of ligands that have a different affinity for the tested analyte will add another difficulty to assay development, as other requirements in minimum and maximum sample concentrations are expected. This was one of the issues for the Fc receptor screening, where the high affinity FcγRI and FcRn could not be included on a single biosensor with the low affinity Fcγ receptors (**Chapter 6**). The IgG concentrations that are needed for the low affinity receptors exceed the maximum level of analyte for the high affinity receptors; hence these receptors would become saturated. Furthermore, interactions with FcRn have a different mechanism for binding which requires a different buffer pH. Possible solutions to overcome the problem of a broad affinity range is by analyzing low

concentrations of analyte, which fall in the range of the high affinity interactions, followed by high concentration injections to measure the other interactions. However, the benefit of multiplexed analysis is no longer utilized and two separate methods would be able to generate similar data in equal analysis time. Another approach would be to use signal enhancers for the low-affinity interactions on that particular sensor surface.[57] However, label-enhanced measurements require other experimental optimization again and add complexity to the assay. The benefits of direct and label-free measurements are then no longer valid.

SPRi measurements on the array platforms are most effective in applications where a large number of ligands with similar binding behavior for similar proteins are screened (for example using antibodies against specific targets as ligands). SPRi measurements are less suitable in methods with a broad variety of different types of ligands and binding properties, since it is challenging to find the optimal experimental conditions for each. The other multiplexed SPR systems, with multiple separate injectors and flow channels may increase throughput in such applications.

Advanced SPR technologies

Several adaptations to conventional SPR have been proposed and described to improve sensitivity or increase the evanescent field for biosensing. So far these applications have not been applied into commercial instrumentation and remain a research or diagnostic tool for academic environments. However, commercialization of these advanced SPR techniques would create a broad field of research in biosensing. So far, several publications have appeared, but the general applicability is still not achieved.

Long-range SPR (LRSPR) was mentioned as a potential alternative for cell sensing experiments. LRSPR has been successfully applied in cell sensing experiments, for example by cell stimulation under influence of lipopolysaccharides[53] or cellular responses to osmotic stress.[41] Furthermore, applications for blood group typing[61,62], leukemia biomarker detection in serum[63] or diagnosis of dengue infection by virus sensing in blood[64] have recently been described based on LRSPR. The principle of long-range SPR is to increase the propagation of surface plasmons further down the sensing solution, thereby increasing the sensitivity and evanescent field for measurements. The range increment is obtained by applying an additional layer onto the sensor surface, which allows for further propagation of the SP waves.

Localized SPR (LSPR) uses metallic nanoparticles or nanostructures, for example gold-covered nanoparticles, for SPR measurements.[65] Excitation of surface plasmons is generally done by fiber optics or waveguides.[66] Sensitivity is increased since the measurement is localized exactly on the gold nanoparticle where the interaction takes place.[67] However, this increased sensitivity can only be achieved when the light is positioned exactly on a single nanoparticle, rather than measuring the entire nanoparticle solution. On the other hand, LSPR allows for a portable SPR device which may be beneficial for several applications that require direct analysis in the field. LSPR has been applied to measure cell metabolites by immobilization of specific antibodies on a LSPR-nanochip. Cells are added to the antibody-immobilized sensor and the excretion of cell metabolites upon cell stimulation was measured in real-time.[67] Also functional immunoassays have been successfully developed with LSPR, even down to single molecule detection.[68]

A very interesting approach of sensor preparation is the *in situ* protein microarray first described by Ramachandran et al.[69] and more recently applied by Nand et al.[70], where the protein that is used as ligand is expressed in a cell-free system on the sensor surface and is instantly captured onto the sensor surface. The *in situ* expressed proteins were fused with a Tus-tag in the plasmid, which is directly captured by a Ter-DNA-oligo that is immobilized on the sensor surface. The high affinity Tus-Ter complex formation allows direct and specific capture of the expressed protein,[71,72] after which protein-protein interactions were measured on an SPRi platform. Such an approach is most interesting for proteins that are difficult to express and purify in the well-known expression systems. Also stability of the protein is less of an issue, since interaction measurements are directly performed after which the sensor is regenerated or discarded. Wide-spread applications of such *in situ* protein microarrays are most likely still far away from routine analysis, although it may be an interesting alternative for difficult applications.

One SPR-like technique was described by Rosman et al.[73] which encompasses a multiplexed sensor with aptamer functionalized gold nanorods, followed by measurement of spectral position of plasmon resonance of individual nanorods by dark-field spectroscopy. Although strictly speaking not exactly the same as SPR, it uses the same physical principles of creating surface plasmons at the interface of a dielectric interface. Randomly deposited nanorods result in an unmapped sensor which records all binding events, and only after analyte injection the target nanoparticle is identified. In our opinion, this technology can only be applied when absolutely no cross-reactivity or a-specific binding is observed. Furthermore, plasmon shifts showed a relatively large variation, which still lacks the general

use for a precise and reliable sensor based on these types of nanorods. Nevertheless, further miniaturization from microscale down to nanoscale will probably be further improved in the future.

Other promising label-free techniques

So far the focus was on SPR and SPRi, although other techniques, based on label-free measurements, are available nowadays. Label-free measurements are most often based on a transducer that generates an optical or electrical signal, which can be measured. Quite a few label-free techniques for protein interaction measurements or cell interactions measurements exist; we will highlight only a few recently introduced techniques for label-free interaction measurements.

Probably the most commonly used technique next to SPR is interferometry, which is for example applied in biolayer interferometry (BLI) in the Octet systems. Interferometry-based methods rely on the interference of light waves that are sent out.[74] In BLI two propagating waves from a white light source are simultaneously shone on a biosensor surface. When these two waves are in phase with each other, the total amplitude of the wave is doubled. Upon binding of a protein to the biosensor, one of the two waves has a different path length and the two waves will become out of phase, causing an interference that can be measured by an optical detector.

In imaging reflectrometric interferometry a change in optical thickness of the biosensor is measured based on a change in amplitude and phase of reflected polarized beams, similar to BLI / interferometry.[75] An array of proteins with up to thousands of spots is prepared, and light of a single defined wavelength is used followed by measurement of the intensity change of the reflected light due to mass accumulation. The technique is less sensitive to temperature shifts and the detection range is much wider, up to several micrometers compared to the few nanometers evanescent field in SPR. The system has been tested on an aptamer-protein interaction system and has been demonstrated on multistep antigen-antibody interactions, both providing kinetic data which were in agreement with previously published data on these interactions.[75]

Multi-parametric cell profiling on a dual biosensor has been demonstrated by Michaelis et al.[76] The combination of SPR and impedance measurements on a single biosensor was employed to study cell shape changes (by impedance measurements) and mass accumulation (by SPR) simultaneously. To this end, an SPR biosensor was modified in such

a way that is holds two electrodes that are needed for impedance measurements. In this set-up the settling and spreading of cells on the sensor surface have been studied, followed by intracellular events (i.e. cytoskeleton disruption) after introduction of a toxin.

Photonic crystal optical biosensors are plastic plates in the bottom of well microplates designed in such a way that normal white light is shone onto the bottom of the plate. When properly designed a single wavelength is reflected which is detected by a spectrophotometer. Binding events (association of molecules or cells) influence the reflected wavelength, and this wavelength shift is measured as binding. This principle can be applied in high-throughput, by using 96, 384 or 1536-well microplates, which can for example be illuminated by normal white light and detected by multiple detection heads. An 8-detection head system was available through SRU biosystems (the BIND reader), although in the past 5-6 years no more publications have appeared for this system. A review by Shamah et al.[77] describes several applications of the technique, ranging from receptor activation to cellular adhesion assays, stem cell differentiation and even to single-cell measurements.

Ellipsometry is another label-free technique for measuring protein interactions. It uses monochromatic light which is linearly polarized followed by transformation to elliptically polarized light. When reflecting from a sensor surface the light becomes linearly polarized again and can be detected by a CCD camera for example. The intensity of the reflected light changes upon binding events. This change can be translated to a quantitative binding signal. The technique has been applied in imaging format as well, where a microfluidic system is used to increase the throughput. The technique has been applied in a variety of detections, such as antigen-antibody binding and biomarker detection.[74]

Portable devices

SPR measurements on cell phones have been explored in recent years.[78,79] Preechaburana et al.[79] were the first to report on the use of a smart phone for SPR measurements. A disposable device was attached to the screen of the smart phone and the camera of the phone was used for detection. Binding of β-microglobulin to an immobilized anti-β-microglobulin antibody could be detected in this set-up, either directly or by using a secondary antibody for signal enhancement. Liu et al.[78] applied fiber-optics that were connected to the cell phones' flash light as a light source and to the camera as the detector for SPR measurements. A measurement, control and reference channel were created in a silica capillary that was coated with a gold film to obtain the generation of surface plasmons. Protein A – IgG binding events have been measured with this portable set-up.

The use of smart phones as diagnostic tools is rapidly evolving, and may become one of the most interesting point-of-care testing devices in the near future. Although SPR measurements on disposable platforms have been proven, using cell phones for illumination and detection, the general applicability in a biopharmaceutical environment will probably not be possible in the near future. Sensitivity, reproducibility and robustness probably have to be improved in order to comply with regulatory guidelines in biopharmaceutical development.

References

1. Wassaf, D., Kuang, G., Kopacz, K., Wu, Q. L., Nguyen, Q., Toews, M., Cosic, J., Jacques, J., Wiltshire, S., Lambert, J., Pazmany, C. C., Hogan, S., Ladner, R. C., Nixon, A. E., and Sexton, D. J. High-throughput affinity ranking of antibodies using surface plasmon resonance microarrays. Anal.Biochem. 15-4-2006; 351(2): 241-253

2. Abdiche, Y. N., Lindquist, K. C., Stone, D. M., Rajpal, A., and Pons, J. Label-free epitope binning assays of monoclonal antibodies enable the identification of antigen heterogeneity. J.Immunol.Methods 31-8-2012; 382(1-2): 101-116

3. Ouellet, E., Lund, L., and Lagally, E. T. Multiplexed surface plasmon resonance imaging for protein biomarker analysis. Methods Mol.Biol. 2013; 949 473-490

4. Ladd, J., Taylor, A. D., Piliarik, M., Homola, J., and Jiang, S. Label-free detection of cancer biomarker candidates using surface plasmon resonance imaging. Anal.Bioanal.Chem. 2009; 393(4): 1157-1163

5. Xu, H., Gu, D., He, J., Shi, L., Yao, J., Liu, C., Zhao, C., Xu, Y., Jiang, S., and Long, J. Multiplex biomarker analysis biosensor for detection of hepatitis B virus. Biomed.Mater.Eng 2015; 26 Suppl 1 S2091-S2100

6. Chavane, N., Jacquemart, R., Hoemann, C. D., Jolicoeur, M., and De, Crescenzo G. At-line quantification of bioactive antibody in bioreactor by surface plasmon resonance using epitope detection. Anal.Biochem. 15-7-2008; 378(2): 158-165

7. Jacquemart, R., Chavane, N., Durocher, Y., Hoemann, C., De, Crescenzo G., and Jolicoeur, M. At-line monitoring of bioreactor protein production by Surface Plasmon Resonance. Biotechnol Bioeng. 1-5-2008; 100(1): 184-188

8. Kyo, M., Usui-Aoki, K., and Koga, H. Label-free detection of proteins in crude cell lysate with antibody arrays by a surface plasmon resonance imaging technique. Anal.Chem. 15-11-2005; 77(22): 7115-7121

9. Usui-Aoki, K., Shimada, K., Nagano, M., Kawai, M., and Koga, H. A novel approach to protein expression profiling using antibody microarrays combined with surface plasmon resonance technology. Proteomics. 2005; 5(9): 2396-2401

10. Fernandes, P., Carvalho, F., and Marques, M. P. Miniaturization in biotechnology: speeding up the development of bioprocesses. Recent Pat Biotechnol. 2011; 5(3): 160-173

11. Bergander, T., Nilsson-Valimaa, K., Oberg, K., and Lacki, K. M. High-throughput process development: determination of dynamic binding capacity using microtiter filter plates filled with chromatography resin. Biotechnol.Prog. 2008; 24(3): 632-639

12. Chhatre, S and Titchener-Hooker, N. J. Review: Microscale methods for high-throughput chromatography development in the pharmaceutical industry. J Chem Technol Biotechnol 13-2-2009; 9(84): 927-940

13. Garcia, C. D., Hadley, D. J., Wilson, W. W., and Henry, C. S. Measuring protein interactions by microchip self-interaction chromatography. Biotechnol Prog. 2003; 19(3): 1006-1010

14. Deshpande, K., Ahamed, T., van der Wielen, L. A., Horst, J. H., Jansens, P. J., and Ottens, M. Protein self-interaction chromatography on a microchip. Lab Chip. 21-2-2009; 9(4): 600-605

15. Patel, R, Johnson KK, Andrien B A, and Tamburini P P. IgG subclass variation of a monoclonal antibody binding to human Fc-gamma receptors. American Journal of Biochemistry and Biotechnology 17-7-2013; 9(3): 206-218

16. Rosenfeld, R., Bangio, H., Gerwig, G. J., Rosenberg, R., Aloni, R., Cohen, Y., Amor, Y., Plaschkes, I., Kamerling, J. P., and Maya, R. B. A lectin array-based methodology for the analysis of protein glycosylation. J.Biochem.Biophys.Methods 10-4-2007; 70(3): 415-426

17. Pilobello, K. T., Krishnamoorthy, L., Slawek, D., and Mahal, L. K. Development of a lectin microarray for the rapid analysis of protein glycopatterns. Chembiochem. 2005; 6(6): 985-989

18. Chen, S., LaRoche, T., Hamelinck, D., Bergsma, D., Brenner, D., Simeone, D., Brand, R. E., and Haab, B. B. Multiplexed analysis of glycan variation on native proteins captured by antibody microarrays. Nat.Methods 2007; 4(5): 437-444

19. Kuno, A., Uchiyama, N., Koseki-Kuno, S., Ebe, Y., Takashima, S., Yamada, M., and Hirabayashi, J. Evanescent-field fluorescence-assisted lectin microarray: a new strategy for glycan profiling. Nat.Methods 2005; 2(11): 851-856

20. Wang, H., Li, H., Zhang, W., Wei, L., Yu, H., and Yang, P. Multiplex profiling of glycoproteins using a novel bead-based lectin array. Proteomics. 2014; 14(1): 78-86

21. Sterner, E., Flanagan, N., and Gildersleeve, J. C. Perspectives on Anti-Glycan Antibodies Gleaned from Development of a Community Resource Database. ACS Chem.Biol. 15-7-2016; 11(7): 1773-1783

22. Berkowitz, S. A., Engen, J. R., Mazzeo, J. R., and Jones, G. B. Analytical tools for characterizing biopharmaceuticals and the implications for biosimilars. Nat.Rev.Drug Discov. 29-6-2012; 11(7): 527-540

23. Treon, S. P., Hansen, M., Branagan, A. R., Verselis, S., Emmanouilides, C., Kimby, E., Frankel, S. R., Touroutoglou, N., Turnbull, B., Anderson, K. C., Maloney, D. G., and Fox, E. A. Polymorphisms in FcgammaRIIIA (CD16) receptor expression are associated with clinical response to rituximab in Waldenstrom's macroglobulinemia. J.Clin.Oncol. 20-1-2005; 23(3): 474-481

24. Koene, H. R., Kleijer, M., Algra, J., Roos, D., von dem Borne, A. E., and de, Haas M. Fc gammaRIIIa-158V/F polymorphism influences the binding of IgG by natural killer cell Fc gammaRIIIa, independently of the Fc gammaRIIIa-48L/R/H phenotype. Blood 1-8-1997; 90(3): 1109-1114

25. Norton, N., Olson, R. M., Pegram, M., Tenner, K., Ballman, K. V., Clynes, R., Knutson, K. L., and Perez, E. A. Association studies of Fcgamma receptor polymorphisms with outcome in HER2+ breast cancer patients treated with trastuzumab in NCCTG (Alliance) Trial N9831. Cancer Immunol.Res. 2014; 2(10): 962-969

26. Zhuang, Y., Xu, W., Shen, Y., and Li, J. Fcgamma receptor polymorphisms and clinical efficacy of rituximab in non-Hodgkin lymphoma and chronic lymphocytic leukemia. Clin.Lymphoma Myeloma.Leuk. 2010; 10(5): 347-352

27. Bibeau, F., Lopez-Crapez, E., Di, Fiore F., Thezenas, S., Ychou, M., Blanchard, F., Lamy, A., Penault-Llorca, F., Frebourg, T., Michel, P., Sabourin, J. C., and Boissiere-Michot, F. Impact of Fc{gamma}RIIa-Fc{gamma}RIIIa polymorphisms and KRAS mutations on the clinical outcome of patients with metastatic colorectal cancer treated with cetuximab plus irinotecan. J Clin.Oncol. 1-3-2009; 27(7): 1122-1129

28. Concetti, F. and Napolioni, V. Insights into the role of Fc gamma receptors (FcgammaRs) genetic variations in monoclonal antibody-based anti-cancer therapy. Recent Pat Anticancer Drug Discov. 2010; 5(3): 197-204

29. Liu, D., Tian, Y., Sun, D., Sun, H., Jin, Y., and Dong, M. The FCGR3A polymorphism predicts the response to rituximab-based therapy in patients with non-Hodgkin lymphoma: a meta-analysis. Ann.Hematol. 2016; 95(9): 1483-1490

30. Wu, J., Edberg, J. C., Redecha, P. B., Bansal, V., Guyre, P. M., Coleman, K., Salmon, J. E., and Kimberly, R. P. A novel polymorphism of FcgammaRIIIa (CD16) alters receptor function and predisposes to autoimmune disease. J.Clin.Invest 1-9-1997; 100(5): 1059-1070

31. Bruhns, P., Iannascoli, B., England, P., Mancardi, D. A., Fernandez, N., Jorieux, S., and Daeron, M. Specificity and affinity of human Fcgamma receptors and their polymorphic variants for human IgG subclasses. Blood 16-4-2009; 113(16): 3716-3725

32. Gregory, S. G., Barlow, K. F., McLay, K. E., Kaul, R., Swarbreck, D., Dunham, A., Scott, C. E., Howe, K. L., Woodfine, K., Spencer, C. C., Jones, M. C., Gillson, C., Searle, S., Zhou, Y., Kokocinski, F., McDonald, L., Evans, R., Phillips, K., Atkinson, A., Cooper, R., Jones, C., Hall, R. E., Andrews, T. D., Lloyd, C., Ainscough, R., Almeida, J. P., Ambrose, K. D., Anderson, F., Andrew, R. W., Ashwell, R. I., Aubin, K., Babbage, A. K., Bagguley, C. L., Bailey, J., Beasley, H., Bethel, G., Bird, C. P., Bray-Allen, S., Brown, J. Y., Brown, A. J., Buckley, D., Burton, J., Bye, J., Carder, C., Chapman, J. C., Clark, S. Y., Clarke, G., Clee, C., Cobley, V., Collier, R. E., Corby, N., Coville, G. J., Davies, J., Deadman, R., Dunn, M., Earthrowl, M., Ellington, A. G., Errington, H., Frankish, A., Frankland, J., French, L., Garner, P., Garnett, J., Gay, L., Ghori, M. R., Gibson, R., Gilby, L. M., Gillett, W., Glithero, R. J., Grafham, D. V., Griffiths, C., Griffiths-Jones, S., Grocock, R., Hammond, S., Harrison, E. S., Hart, E., Haugen, E., Heath, P. D., Holmes, S., Holt, K., Howden, P. J., Hunt, A. R., Hunt, S. E., Hunter, G., Isherwood, J., James, R., Johnson, C., Johnson, D., Joy, A., Kay, M., Kershaw, J. K., Kibukawa, M., Kimberley, A. M., King, A., Knights, A. J., Lad, H., Laird, G., Lawlor, S., Leongamornlert, D. A., Lloyd, D. M., Loveland, J., Lovell, J., Lush, M. J., Lyne, R., Martin, S., Mashreghi-Mohammadi, M., Matthews, L., Matthews, N. S., McLaren, S., Milne, S., Mistry, S., Moore, M. J., Nickerson, T., O'Dell, C. N., Oliver, K., Palmeiri, A., Palmer, S. A., Parker, A., Patel, D., Pearce, A. V., Peck, A. I., Pelan, S., Phelps, K., Phillimore, B. J., Plumb, R., Rajan, J., Raymond, C., Rouse, G., Saenphimmachak, C., Sehra, H. K., Sheridan, E., Shownkeen, R., Sims, S., Skuce, C. D., Smith, M., Steward, C., Subramanian, S., Sycamore, N., Tracey, A., Tromans, A., Van, Helmond Z., Wall, M., Wallis, J. M., White, S., Whitehead, S. L., Wilkinson, J. E., Willey, D. L., Williams, H., Wilming, L., Wray, P. W., Wu, Z., Coulson, A., Vaudin, M., Sulston, J. E., Durbin, R., Hubbard, T., Wooster, R., Dunham, I., Carter, N. P., McVean, G., Ross, M. T., Harrow, J., Olson, M. V., Beck, S., Rogers, J., Bentley, D. R., Banerjee, R., Bryant, S. P., Burford, D. C., Burrill, W. D., Clegg, S. M., Dhami, P., Dovey, O., Faulkner, L. M., Gribble, S. M., Langford, C. F., Pandian, R. D., Porter, K. M., and Prigmore, E. The DNA sequence and biological annotation of human chromosome 1. Nature 18-5-2006; 441(7091): 315-321

33. Bux, J., Stein, E. L., Bierling, P., Fromont, P., Clay, M., Stroncek, D., and Santoso, S. Characterization of a new alloantigen (SH) on the human neutrophil Fc gamma receptor IIIb. Blood 1-2-1997; 89(3): 1027-1034

34. Norris, C. F., Pricop, L., Millard, S. S., Taylor, S. M., Surrey, S., Schwartz, E., Salmon, J. E., and McKenzie, S. E. A naturally occurring mutation in Fc gamma RIIA: a Q to K127 change confers unique IgG binding properties to the R131 allelic form of the receptor. Blood 15-1-1998; 91(2): 656-662

35. Salmon, J. E., Millard, S., Schachter, L. A., Arnett, F. C., Ginzler, E. M., Gourley, M. F., Ramsey-Goldman, R., Peterson, M. G., and Kimberly, R. P. Fc gamma RIIA alleles are heritable risk factors for lupus nephritis in African Americans. J.Clin.Invest 1-3-1996; 97(5): 1348-1354

36. Szittner, Z., Bentlage, A. E., Rovero, P., Migliorini, P., Lorand, V., Prechl, J., and Vidarsson, G. Label-free detection of immune complexes with myeloid cells. Clin.Exp.Immunol. 2016; 185(1): 72-80

37. Suraniti, E., Sollier, E., Calemczuk, R., Livache, T., Marche, P. N., Villiers, M. B., and Roupioz, Y. Real-time detection of lymphocytes binding on an antibody chip using SPR imaging. Lab Chip. 2007; 7(9): 1206-1208

38. Stojanovic, I., Schasfoort, R. B., and Terstappen, L. W. Analysis of cell surface antigens by Surface Plasmon Resonance imaging. Biosens.Bioelectron. 15-2-2014; 52 36-43

39. Milgram, S., Bombera, R., Livache, T., and Roupioz, Y. Antibody microarrays for label-free cell-based applications. Methods 2012; 56(2): 326-333

40. Yanase, Y., Hiragun, T., Ishii, K., Kawaguchi, T., Yanase, T., Kawai, M., Sakamoto, K., and Hide, M. Surface plasmon resonance for cell-based clinical diagnosis. Sensors.(Basel) 11-3-2014; 14(3): 4948-4959

41. Vala, M., Robelek, R., Bockova, M., Wegener, J., and Homola, J. Real-time label-free monitoring of the cellular response to osmotic stress using conventional and long-range surface plasmons. Biosens.Bioelectron. 15-2-2013; 40(1): 417-421

42. Chabot, V., Cuerrier, C. M., Escher, E., Aimez, V., Grandbois, M., and Charette, P. G. Biosensing based on surface plasmon resonance and living cells. Biosens.Bioelectron. 15-2-2009; 24(6): 1667-1673

43. Shevchenko, Y., Camci-Unal, G., Cuttica, D. F., Dokmeci, M. R., Albert, J., and Khademhosseini, A. Surface plasmon resonance fiber sensor for real-time and label-free monitoring of cellular behavior. Biosens.Bioelectron. 15-6-2014; 56 359-367

44. Berthuy, O. I., Blum, L. J., and Marquette, C. A. Cancer-Cells on Chip for Label-Free Detection of Secreted Molecules. Biosensors.(Basel) 15-1-2016; 6(1):-

45. Stojanovic, I., van der Velden, T. J., Mulder, H. W., Schasfoort, R. B., and Terstappen, L. W. Quantification of antibody production of individual hybridoma cells by surface plasmon resonance imaging. Anal.Biochem. 15-9-2015; 485 112-118

46. Houngkamhang, N., Vongsakulyanon, A., Peungthum, P., Sudprasert, K., Kitpoka, P., Kunakorn, M., Sutapun, B., Amarit, R., Somboonkaew, A., and Srikhirin, T. ABO blood-typing using an antibody array technique based on surface plasmon resonance imaging. Sensors.(Basel) 9-9-2013; 13(9): 11913-11922

47. Schasfoort, R. B., Bentlage, A. E., Stojanovic, I., van der Kooi, A., van der Schoot, E., Terstappen, L. W., and Vidarsson, G. Label-free cell profiling. Anal.Biochem. 1-8-2013; 439(1): 4-6

48. Krombach, F., Munzing, S., Allmeling, A. M., Gerlach, J. T., Behr, J., and Dorger, M. Cell size of alveolar macrophages: an interspecies comparison. Environ.Health Perspect. 1997; 105 Suppl 5 1261-1263

49. Richards, J. O., Karki, S., Lazar, G. A., Chen, H., Dang, W., and Desjarlais, J. R. Optimization of antibody binding to FcgammaRIIa enhances macrophage phagocytosis of tumor cells. Mol.Cancer Ther. 2008; 7(8): 2517-2527

50. Guilliams, M., Bruhns, P., Saeys, Y., Hammad, H., and Lambrecht, B. N. The function of Fcgamma receptors in dendritic cells and macrophages. Nat.Rev.Immunol. 2014; 14(2): 94-108

51. Rosales, C and Uribe-Querol, E. Fc receptors: Cell activators of antibody functions. Advances in Bioscience and Biotechnology 16-4-2013;(4): 21-33

52. Jungi, T. W. and Hafner, S. Quantitative assessment of Fc receptor expression and function during in vitro differentiation of human monocytes to macrophages. Immunology 1986; 58(1): 131-137

53. Chabot, V, Miron, Y, Grandbois, M, and Charette, PG. Long range surface plasmon resonance for increased sensitivity in living cell biosensing through greater probing depth. Sensors and actuators B: Chemical 25-8-2012; 174 94-101

54. Vala, M, Etheridge, S, Roach, JA, and Homola, J. Long-range surface plasmons for sensitive detection of bacterial analytes. Sensors and actuators B: Chemical 28-8-2008; 139 59-63

55. Nguyen, H. H., Park, J., Kang, S., and Kim, M. Surface plasmon resonance: a versatile technique for biosensor applications. Sensors.(Basel) 5-5-2015; 15(5): 10481-10510

56. Helmerhorst, E., Chandler, D. J., Nussio, M., and Mamotte, C. D. Real-time and Label-free Bio-sensing of Molecular Interactions by Surface Plasmon Resonance: A Laboratory Medicine Perspective. Clin.Biochem.Rev. 2012; 33(4): 161-173

57. Kodoyianni, V. Label-free analysis of biomolecular interactions using SPR imaging. Biotechniques 2011; 50(1): 32-40

58. Ferrara, C., Grau, S., Jager, C., Sondermann, P., Brunker, P., Waldhauer, I., Hennig, M., Ruf, A., Rufer, A. C., Stihle, M., Umana, P., and Benz, J. Unique carbohydrate-carbohydrate interactions are required for high affinity binding between FcgammaRIII and antibodies lacking core fucose. Proc.Natl.Acad.Sci.U.S.A 2-8-2011; 108(31): 12669-12674

59. Hayes, J. M., Frostell, A., Cosgrave, E. F., Struwe, W. B., Potter, O., Davey, G. P., Karlsson, R., Anneren, C., and Rudd, P. M. Fc gamma receptor glycosylation modulates the binding of IgG glycoforms: a requirement for stable antibody interactions. J.Proteome.Res. 5-12-2014; 13(12): 5471-5485

60. Smelyanski, L. and Gershoni, J. M. Site directed biotinylation of filamentous phage structural proteins. Virol.J. 2011; 8 495-

61. Krupin, O., Wang, C., and Berini, P. Selective capture of human red blood cells based on blood group using long-range surface plasmon waveguides. Biosens.Bioelectron. 15-3-2014; 53 117-122

62. Tangkawsakul, W., Srikhirin, T., Shinbo, K., Kato, K., Kaneko, F., and Baba, A. Application of Long-Range Surface Plasmon Resonance for ABO Blood Typing. Int.J.Anal.Chem. 2016; 2016 1432781-

63. Krupin, O., Wang, C., and Berini, P. Detection of leukemia markers using long-range surface plasmon waveguides functionalized with Protein G. Lab Chip. 7-11-2015; 15(21): 4156-4165

64. Wong, W. R., Krupin, O., Sekaran, S. D., Mahamd Adikan, F. R., and Berini, P. Serological diagnosis of dengue infection in blood plasma using long-range surface plasmon waveguides. Anal.Chem. 4-2-2014; 86(3): 1735-1743

65. Puiu, M. and Bala, C. SPR and SPR Imaging: Recent Trends in Developing Nanodevices for Detection and Real-Time Monitoring of Biomolecular Events. Sensors.(Basel) 14-6-2016; 16(6):-

66. Guo, X. Surface plasmon resonance based biosensor technique: a review. J.Biophotonics. 2012; 5(7): 483-501

67. Endo, T., Yamamura, S., Kerman, K., and Tamiya, E. Label-free cell-based assay using localized surface plasmon resonance biosensor. Anal.Chim.Acta 5-5-2008; 614(2): 182-189

68. Mayer, K. M., Hao, F., Lee, S., Nordlander, P., and Hafner, J. H. A single molecule immunoassay by localized surface plasmon resonance. Nanotechnology. 25-6-2010; 21(25): 255503-

69. Ramachandran, N., Hainsworth, E., Bhullar, B., Eisenstein, S., Rosen, B., Lau, A. Y., Walter, J. C., and LaBaer, J. Self-assembling protein microarrays. Science 2-7-2004; 305(5680): 86-90

70. Nand, A., Singh, V., Perez, J. B., Tyagi, D., Cheng, Z., and Zhu, J. In situ protein microarrays capable of real-time kinetics analysis based on surface plasmon resonance imaging. Anal.Biochem. 1-11-2014; 464 30-35

71. Moreau, M. J. and Schaeffer, P. M. Differential Tus-Ter binding and lock formation: implications for DNA replication termination in Escherichia coli. Mol.Biosyst. 2012; 8(10): 2783-2791

72. Larsen, N. B., Hickson, I. D., and Mankouri, H. W. Tus-Ter as a tool to study site-specific DNA replication perturbation in eukaryotes. Cell Cycle 2014; 13(19): 2994-2998

73. Rosman, C., Prasad, J., Neiser, A., Henkel, A., Edgar, J., and Sonnichsen, C. Multiplexed plasmon sensor for rapid label-free analyte detection. Nano.Lett. 10-7-2013; 13(7): 3243-3247

74. Ray, S., Mehta, G., and Srivastava, S. Label-free detection techniques for protein microarrays: prospects, merits and challenges. Proteomics. 2010; 10(4): 731-748

75. Burger, J., Rath, C., Woehrle, J., Meyer, P. A., Ben, Ammar N., Kilb, N., Brandstetter, T., Proll, F., Proll, G., Urban, G., and Roth, G. Low-Volume Label-Free Detection of Molecule-Protein Interactions on Microarrays by Imaging Reflectometric Interferometry. J.Lab Autom. 1-7-2016; 2211068216657512-

76. Michaelis, S., Wegener, J., and Robelek, R. Label-free monitoring of cell-based assays: combining impedance analysis with SPR for multiparametric cell profiling. Biosens.Bioelectron. 15-11-2013; 49 63-70

77. Shamah, S. M. and Cunningham, B. T. Label-free cell-based assays using photonic crystal optical biosensors. Analyst 21-3-2011; 136(6): 1090-1102

78. Liu, Y., Liu, Q., Chen, S., Cheng, F., Wang, H., and Peng, W. Surface Plasmon Resonance Biosensor Based on Smart Phone Platforms. Sci.Rep. 10-8-2015; 5 12864-

79. Preechaburana, P., Gonzalez, M. C., Suska, A., and Filippini, D. Surface plasmon resonance chemical sensing on cell phones. Angew.Chem Int.Ed Engl. 12-11-2012; 51(46): 11585-11588

Chapter 7

SUMMARY

Summary

The rapid developments in the biopharmaceutical market, both for new biological entities and biosimilars, require the use of innovative analytical technologies to comply with demands for development of high-quality products and fast market approval. A typical biopharmaceutical process includes the following stages: discovery, early development, late development and manufacturing. During each of these stages, high-throughput screening technologies may be used to support those rapid developments. Surface plasmon resonance imaging (SPRi) is an example of such a high-throughput screening technology, which was demonstrated in several applications throughout the entire process development.

Analytical method development can be speeded up by SPRi screening technologies, such as finding the most optimal regeneration conditions for SPR-based methods as presented in **Chapter 2**. The most optimal regeneration buffer was determined from a total of 48 different buffers in a single measurement within 2 hours time. Especially in multiplexed SPR arrays it can be challenging to find the right regeneration buffer for a multitude of different ligands, which may all have different binding properties for the analytes. The buffer screening can dramatically speed up the method development for SPR analyses as a selection of potential regeneration buffers is determined with only a single SPR sensor in a single experiment.

The same principle of buffer screening was then applied to affinity chromatography screening, as presented in **Chapter 3**, where a protein A purification process was simulated and miniaturized. Rapid screening of the most optimal elution and wash buffers was performed within 1-2 days, which would normally require weeks to develop on small scale column. Furthermore, the ligand lifetime of the affinity chromatography was simulated in a miniaturized set-up and compared to lab scale column experiments. Results were highly comparable between the lab scale experiments and SPRi-based methods and demonstrated the applicability of such screening technology during process development. Especially the consumption of analyte and buffers was reduced up to 200-fold and on top of that the experimental time was reduced from several weeks to only 2 days.

Other important applications of the SPRi technology were demonstrated for biopharmaceutical product characterization, such as glycosylation and Fcγ receptor binding. **Chapter 4** describes the development of a lectin array to screen glycosylation fingerprints of recombinant human erythropoietin, which included the quantification of sialylation levels of rhEPO. Sialylation of rhEPO is one of the major Critical Quality Attributes (CQAs) of rhEPO, since the serum half-life largely depends on proper sialylation. Glycosylation

fingerprinting of five different brands of rhEPO was compared with the label-free lectin array. Development of the lectin array included the proper immobilization of lectins on a multiplexed sensor chip, followed by specificity and cross-reactivity determination for each of the selected lectins by analyses of neoglycoproteins and enzymatically remodeled glycoproteins such as transferrin and fetuin.

Proper Fc receptor binding is a CQA for most IgGs that are being developed as a biopharmaceutical, as it may influence the mechanism of action of the IgG (Fcγ receptors) and serum half-life (FcRn binding). A multiplexed screening assay for Fc receptor interactions of therapeutic IgGs was set up. Activity and stability at the sensor surface of low affinity Fcγ receptors (FcγRIIIa, FcγRIIIb, FcγRIIa and FcγRIIb) were relatively low in a direct coupling approach based on amine coupling. Therefore, in **Chapter 5** a more controlled and site-directed immobilization was developed, based on a minimal biotinylation of Fcγ receptors. A statistical design of experiments was performed to find the most optimal labeling conditions for Fcγ receptor biotinylation, resulting in active ligands at the surface with representative IgG binding properties. Mass spectrometric characterization of the biotinylated Fcγ receptors revealed that mainly double-biotinylated proteins reduced the ligand activity. Identification of the labeled amino acids showed that two major biotinylation sites are present in the Fcγ receptors, one of which is part of the active binding site for IgG binding. Labeling conditions could not be chosen such that this active binding site is not blocked by biotins, but by preventing the presence of a substantial amount of double-biotinylated fractions the chance of biotinylating in the active binding site was reduced. The major effect for double-biotinylation was due to a protein:biotin ratio of 1:2, as determined from the statistical design of experiments, and therefore protein:biotin ratio should be kept at 1:1 or even lower, e.g. 1:0.5. Incubation pH and incubation time, which were also part of the DoE, were not statistically significant for reduced ligand binding activity.

The optimized labeling approach was then applied to all low affinity Fcγ receptors and these were immobilized on a multiplexed SPRi sensor to screen for IgG quality based on Fc receptor binding in **Chapter 6**. The screening method was based on an active content measurement, where a reference sample was set to 100% activity and binding of stressed samples was calculated relative to this reference. Method optimization included the determination of IgG concentration range, accuracy and precision. The optimal IgG concentration range for FcγRI was different from the low affinity Fcγ receptors due to large differences in affinity for IgG binding. Furthermore, FcRn binding was not included on the

same screening sensor, because association of IgG to FcRn occurs at pH 6, while the other receptors bind at neutral pH (pH 7 - 7.5). Three separate screening methods were therefore used to profile the entire Fc region binding of IgGs; one multiplexed SPRi assay for the low affinity Fcγ receptors, an SPR single cycle kinetics method for FcγRI and a multi-cycle kinetics method for FcRn binding based on BLI. This combination of Fc receptor binding assays on three platforms provided the most optimal screening for IgG – Fc tail interactions. Differences in binding to one or more of the Fc receptors were detected under several stressed conditions. The main findings from stressed IgG samples showed that IgG deamidation reduced the binding to low affinity Fcγ receptors, while the binding to FcγRI and FcRn was not affected. Methionine oxidation at levels up to 7% did not impact binding to any of the Fcγ receptors. Deglycosylation of IgG affected the binding to each of the Fc receptors, while an aberrant fucosylation only changed the binding to FcγRIIIa and FcγRIIIb. The presence of aggregates in the samples had an avidity effect on each of the Fcγ receptors and altered the relative binding or binding kinetics. Together these results showed the applicability of these methods for CQA screening of IgGs in terms of Fc region binding.

In **Chapter 7** the main results are discussed and some applications that did not meet the requirements for high-throughput screening are included. An overview of the application of SPRi in the biopharmaceutical development process is provided, including examples of methods that have been successfully developed and methods that have been tested. Furthermore, an outlook on novel applications of SPRi that need more research was summarized. It was concluded that SPRi can be a valuable tool during process development and product characterization to increase sample throughput and to increase product knowledge in rapid screening methods. Other multiplexed SPR platforms, which are not based on the imaging of an entire sensor array, may be useful for several applications, whereas true screening arrays are best performed on SPRi systems. All results together show that there is not a single multiplexed SPR system, or other label-free instrument, that is the best for all intended applications. Depending on the purpose and the method set-up, a different instrument may be beneficial to use. However, in general, it will be possible to develop most applications on a SPRi system, although the multiplexing capabilities may not always be fully utilized. As with any analytical method, the instrumental possibilities and limitations should be balanced against the requirements for an intended application.

SAMENVATTING

Samenvatting

De huidige snelle ontwikkelingen in de biofarmaceutische wereld, zowel voor nieuwe biologische medicijnen als de zogenoemde "biosimilars", vereisen het gebruik van innovatieve analytische technieken om te voldoen aan de eisen voor producten van goede kwaliteit en voor snelle goedkeuring tot de markt. Een typisch biofarmaceutisch proces bestaat uit de volgende fasen: ontdekking, vroege ontwikkeling, late ontwikkeling en productie. Tijdens alle fasen kunnen 'high-throughput screening' technieken gebruikt worden om deze snelle ontwikkelingen te ondersteunen. Surface plasmon resonance imaging (SPRi) is een voorbeeld van zo'n screening-techniek, en het gebruik hiervan is aangetoond in diverse applicaties tijdens het gehele ontwikkelingstraject.

Analytische methodeontwikkeling kan versneld worden door het gebruik van de SPRi screening-techniek, bijvoorbeeld bij het vinden van de meest optimale regeneratiecondities voor methoden gebaseerd op SPR zoals beschreven in **Hoofdstuk 2**. De meest optimale regeneratiebuffer uit een totaal van 48 verschillende buffers werd gevonden in een enkele meting in 2 uur tijd. Zeker in multiplex SPR-methoden kan het een uitdaging zijn om de juiste regeneratiebuffer voor een groot aantal verschillende liganden te vinden, omdat deze allemaal andere bindingseigenschappen voor het product (analiet) kunnen hebben. De buffer screening zoals omschreven kan daardoor een grote tijdswinst opleveren voor de methode ontwikkeling van SPR analyses omdat een selectie van potentiële regeneratiebuffers snel is gemaakt met een enkele SPR meting op een sensor.

Ditzelfde principe van bufferscreening is daarna toegepast op een affiniteitschromatografiescreening in **Hoofdstuk 3**, waarbij een protein A zuiveringsproces is gesimuleerd en geminiaturiseerd. Een snelle screening van de meest optimale elutiebuffers en wasbuffers is uitgevoerd binnen 1-2 dagen, terwijl dit weken zou duren wanneer dit op kleine kolomschaal ontwikkeld moet worden. Daarnaast is er een simulatie uitgevoerd om de levensduur van het affiniteitsligand te testen in een geminiaturiseerde opzet en deze is vergeleken met kolom experimenten op labschaal. De resultaten tussen de kolommen en de SPRi methode waren vergelijkbaar en dit toont de toegevoegde waarde aan van de screening-techniek tijdens procesontwikkelingen voor biofarmaceutische producten. Daarnaast moet er benadrukt worden dat de hoeveelheid materiaal die nodig was met een factor 200 is gereduceerd, en dat bovendien de experimentele tijd kon worden teruggebracht van enkele weken tot 2 dagen.

Andere belangrijke toepassingen van SPRi zijn aangetoond voor de product karakterisatie van biofarmaceutische middelen, bijvoorbeeld voor glycosylering en Fcγ receptor-binding. In **Hoofdstuk 4** is een lectine-array ontwikkeld om het

"glycosyleringsprofiel" van recombinant humaan erythropoietin (rhEPO) te kunnen screenen. Deze methode kon bovendien de sialyleringsniveau's van rhEPO kwantificeren, wat belangrijk is voor de kwaliteit van het product. Sialylering van rhEPO is een van de 'kritische kwaliteitskarakteristieken' (CQAs) omdat de halfwaardetijd van rhEPO in bloed mede wordt bepaald door de juiste sialylering. Glycosyleringsprofielen van vijf verschillende merken rhEPO zijn met elkaar vergeleken op de lectine-array. De ontwikkeling van de lectine array omvatte verder de juiste immobilisatie van lectines op de multiplex sensor, gevolgd door een bepaling van specificiteit en kruisreactiviteit voor elk van de geselecteerde lectines door middel van neoglycaan-eiwit-analyse en enzymatisch gemodelleerde glycaan-eiwitten zoals transferrine en fetuine.

Een juiste Fc receptorbinding is een van de CQAs voor de meeste IgGs die ontwikkeld worden als biofarmaceutisch middel, omdat deze het werkingsmechanisme van het IgG kunnen beïnvloeden (in geval van Fcγ receptoren) of omdat deze belangrijk zijn voor de halfwaardetijd in bloed (in geval van FcRn). Daartoe is een multiplex screeningassay voor Fc receptor-interacties voor therapeutische IgGs opgezet. De activiteit en stabiliteit op het sensoroppervlak van de laag-affiene Fcγ receptoren (FcγRIIIa, FcγRIIIb, FcγRIIa en FcγRIIb) zijn relatief laag wanneer ze gekoppeld worden door middel van directe amine-koppelingschemie. Daarom is in **Hoofdstuk 5** een meer gecontroleerde en gerichte immobilisatie ontwikkeld, die gebaseerd is op een minimale biotinylering van Fcγ receptoren. Een statistisch experiment ontwerp ("design of experiments", ofwel DoE) is uitgevoerd om de meest optimale labeling condities voor Fcγ receptor biotinylering te bepalen, wat uiteindelijk resulteerde in actieve liganden op het oppervlak met representatieve IgG-bindingseigenschappen. Karakterisatie van de gebiotinyleerde Fcγ receptoren met behulp van massaspectrometrie liet zien dat voornamelijk dubbel-gebiotinyleerde eiwitten voor een reductie in ligand activiteit zorgden. Identificatie van de gelabelde aminozuren resulteerde in twee locaties op de Fcγ receptoren die voornamelijk gebiotinyleerd werden, en waarvan één onderdeel uitmaakt van een van de actieve bindingsplekken voor IgG. De labelingcondities konden niet zodanig worden aangepast dat deze specifieke locatie niet geblokkeerd werd door biotine, maar door labeling condities zodanig te kiezen kon wel worden voorkomen dat er substantiële hoeveelheden dubbel-gebiotinyleerd materiaal werden gevormd en hiermee werd wel de kans om de actieve plek te blokkeren verminderd. Het belangrijkste effect voor dubbele biotinylering in een eiwit werd veroorzaakt door de eiwit:biotine ratio van 1:2 te gebruiken, dat bepaald is uit het DoE, en daarom wordt aangeraden om deze ratio op 1:1 of lager (bijvoorbeeld 1:0.5) te houden. De incubatie-pH en incubatietijd, die ook werden

meegenomen in het experimenteel ontwerp, gaven statistisch geen significant effect op verminderde bindingsactiviteiten van de Fcγ receptoren.

De geoptimaliseerde labelingcondities zijn vervolgens toegepast op alle laag-affiene Fcγ receptoren om deze te kunnen immobiliseren op een multiplex SPRi-sensor, die in **Hoofdstuk 6** gebruikt is om de IgG-kwaliteit te kunnen screenen gebaseerd op Fc receptorbinding. De screeningmethode was gebaseerd op een meting van actieve hoeveelheid, waarbij een referentiemonster op 100% activiteit werd gezet en de binding van gestreste monsters berekend is relatief aan dit referentiemonster. De methodeoptimalisatie die is uitgevoerd omvatte onder andere de bepaling van de optimale concentratiespanne van IgG, accuratesse en precisie. De optimale IgG concentratie voor FcγRI was anders dan die voor de laag-affiene Fcγ receptoren door grote verschillen in affiniteit voor IgG-binding. Daarnaast kon de FcRn-binding niet worden toegevoegd op dezelfde sensor omdat associatie van IgG aan FcRn plaatsvindt bij pH 6, terwijl dit op pH 7 – 7.5 ligt voor de overige laag-affiene Fcγ receptoren. Daarom waren er drie aparte screening methoden nodig om het volledige Fc bindingsprofiel van IgGs te kunnen meten; een multiplex SPRi-assay voor laag-affiene Fcγ receptoren, een SPR 'single-cyclus kinetiek' methode voor FcγRI en een 'multi-cyclus kinetiek' methode voor FcRn binding gebaseerd op biolayer interferometrie (BLI) metingen. De combinatie van deze Fc bindingsassays gaf de meest optimale screening wanneer men kijkt naar efficiënt instrument gebruik en de methode-kwalificaties. Verschillen in binding aan een of meerdere Fc receptoren kon worden gemeten bij diverse vormen van stress op het IgG. De belangrijkste bevindingen van gestreste IgG-monsters lieten zien dat deamidatie voor een afname in binding op de laag-affiene Fcγ receptoren zorgt, terwijl binding aan FcγRI en FcRn niet beïnvloed werd. Methionine-oxidatie tot een maximum van 7% had geen invloed op de binding aan alle Fc receptoren. Deglycosylatie van IgG veranderde de binding aan alle Fc receptoren, terwijl afwijkende fucosyleringspatronen alleen voor verschillen in binding op FcγRIIIa en FcγRIIIb zorgen. De aanwezigheid van aggregaten in de monsters resulteerde in aviditeitseffecten op alle Fcγ receptoren en veranderde daardoor de relatieve binding of de bindingskinetiek. Al deze resultaten samen geven duidelijk de meerwaarde aan voor deze screeningstechnieken om snel de CQAs van IgGs te kunnen bepalen als het gaat om Fc receptorbinding.

In **Hoofdstuk 7** zijn vervolgens de belangrijkste resultaten besproken en werden daarnaast enkele mogelijkheden genoemd die hier niet tot de gewenste kwaliteitseisen voor high-throughput-screening hebben geleid. Een overzicht van de toepasbaarheid van SPRi gedurende het gehele proces van biofarmaceutische ontwikkeling is geschetst, waarbij

voorbeelden zijn genoemd van de beproefde methoden en van de overige methoden die zijn getoetst. Daarnaast is er een visie op de toekomst gegeven met betrekking tot verdere ontwikkelingen voor vernieuwende applicaties voor SPRi die nog verder onderzocht dienen te worden. De conclusie luidt dan ook dat SPRi een heel waardevolle techniek kan zijn om procesontwikkeling te versnellen en meer inzicht te geven in productkarakterisatie. Andere multiplex SPR-platformen, die niet gebaseerd zijn op het imaging-principe, kunnen daarnaast prima gebruikt worden voor diverse van de genoemde toepassingen, waarbij voor echte screening-analysemethodes toch zeker uitgeweken moet worden naar SPRi-systemen. Al deze resultaten samen laten zien dat er niet een enkel multiplex SPR-systeem is dat de beste keuze zal zijn voor alle mogelijke applicaties. Afhankelijk van de vraagstelling en hoe de methode opgezet dient te worden, dient een afweging gemaakt te worden voor het type instrument dat het beste gebruikt kan worden. Ondanks dat in het algemeen de meeste toepassingen op ieder SPRi-instrument ontwikkeld kunnen worden, zal er niet altijd volledig gebruik gemaakt worden van de capaciteiten van het systeem en kan het zinvol zijn een ander systeem te gebruiken. Zoals voor iedere analytische techniek nodig is, zullen mogelijkheden en beperkingen van het systeem afgewogen moeten worden en getoetst moeten worden aan de vereisten voor de uiteindelijke toepassing.

DANKWOORD

Na al die jaren werken aan mijn promotieonderzoek en het afronden van het proefschrift, is het dan eindelijk tijd om ook het dankwoord op papier te gaan zetten. Want het resultaat van al mijn werk was mij nooit in mijn eentje gelukt, en daarom is dit het moment om iedereen te bedanken die een bijdrage heeft geleverd en mij gesteund heeft.

Als eerste zijn dat natuurlijk mijn drie begeleiders die een bedankje verdienen. **Michel**, dankzij jou kwam er 4,5 jaar geleden de mogelijkheid om dit prachtige project binnen Synthon uit te gaan voeren. Jouw eeuwige optimisme en energie zorgden ervoor dat ik zelf ook bleef geloven in een succesvol einde van dit project. In jouw drukke agenda is altijd plek voor een extra overleg of een snel antwoord op een stuk wat ingediend moet worden. Waar haal je toch al die tijd vandaan! **Richard**, ondanks de afstand met Enschede, nam je regelmatig de tijd om te bellen en te vragen hoe een en ander vorderde. In het begin heb je me direct de diepgaande technische kennis van SPR proberen bij te brengen, ondanks dat ik niet altijd meteen begreep wat je bedoelde. Door jou heb ik heel veel geleerd van de technische kant van de SPR techniek en het IBIS instrument. **David**, officieel pas in het laatste jaar mijn derde begeleider geworden, maar stiekem al ruim 2 jaar langer heel nauw betrokken bij al mijn plannen en de uitvoering daarvan. Jij zorgde er voor dat ik nooit genoegen nam met de data en de tekst die ik al op papier had staan (101 comments op een draft paper van 9 A4-tjes, need I say more…). Jouw kritische blik op alles wat ik gedaan heb heeft ervoor gezorgd dat ik nu hopelijk ook nog een stuk kritischer ben geworden op mijn eigen werk, op een goede manier dan toch.

Roel, heel erg bedankt dat je vanaf het begin af aan mij de mogelijkheid hebt geboden om binnen Synthon een promotieonderzoek te gaan starten. Dankzij jouw overtuiging en enthousiasme, heb ik de stap durven nemen om samen met Michel te gaan kijken wat er mogelijk was binnen Synthon.

Uiteraard wil ik alle collega's van de **vakgroep bioproceskunde** bedanken. Ondanks dat ik nauwelijks ooit aanwezig ben geweest op Biotechnion en later Radix, heb ik wel de nodige input gehad op AIO-dagen. Uiteraard wil ik hier ook **René** nog even een extra woord van dank geven. Jij was in het begin mijn begeleider naast Michel, maar nadat Michel professor werd ben jij gestopt als begeleider voor mijn project. Ik heb wel de nodige hulp uit jouw hoek gehad in de eerste 2 jaar waarvoor dank. **Miranda** en **Marina**, dank jullie wel voor jullie snelle antwoorden op al mijn 'moeilijke' administratieve vragen. Als je, zoals ik, je promotie niet binnen de vakgroep doet, zijn er toch de nodige dingen die lastig te vinden zijn, zeker zonder jullie hulp.

Het 'ACCESS'-project team, **Louis**, **Mathieu**, **Dirk**, **Marc**, **Ciska**, **Xiao**, verdient hier ook een warm dankjewel. Tijdens alle bijeenkomsten door de jaren heen hebben jullie ervoor gezorgd dat ik af en toe ook op een andere manier naar mijn onderzoek en resultaten ging kijken; vanuit andere invalshoeken zagen jullie dingen die ik als vanzelfsprekend aannam. Verder wil ik mijn vier studenten (**Jeroen**, **George**, **Mark** en **Eef**) bedanken voor hun bijdrages aan mijn onderzoek en daarbij natuurlijk ook voor hun eigen studie de nodige ervaring hebben opgedaan. Daarnaast zijn er ook nog enkele studenten die helemaal niet mijn student waren maar wel voor mooie resultaten hebben gezorgd die ik kon gebruiken voor mijn publicaties. Dankjewel **Sanne** en **Eefje**.

In mijn beginjaren bij Synthon ben ik begonnen bij de Bioanalytische groep, en tijdens alle jaren dat ik met mijn promotie bezig was, mocht ik toch gezellig met jullie koffiepauze blijven houden. Bedankt voor de afleiding van de serieuze zaken als ik dat nodig had: **Jaap, Peter, Wietske, Robbin, Sjoerd, Husniye, Vera, Edgar, Marijn, Marieke, Marius, Raymond, Dongyuan, Petra** en **Chiel.** En een extra bedankje voor **Eline** en **Wendy** die een heleboel analyses voor mij gedaan hebben als dat nodig was. Daarnaast nog een speciaal bedankwoord voor **Mark**, voor het meedenken bij de uitdagingen die ik moest zien te overwinnen, en voor de hulp bij de diverse MS experimenten en hoe ik die het beste kon gebruiken in mijn publicaties.

Verder wil ik ook nog **Stefanie** en **Jan** bedanken voor het meehelpen bij het maken van de Fc receptoren. Daarnaast had ik in de laatste paar maanden nog even een uitstapje naar de USP afdeling omdat ik zo nodig zelf cellen wilde gaan kweken. Dank je wel **USPers** dat ik jullie lab mocht gebruiken. En daarbij ook mijn enorme dank aan **Rob** en **Lisette** voor het goed verzorgen van mijn cellen op de woensdagen en met Kerst, want ja… ik was wel vrij met de feestdagen. **Zeban**, ik waardeer je interesse in mijn cellenwerk en dat je direct openstond voor mogelijkheden binnen jullie groep. Helaas is het niet meer verder van de grond gekomen maar hopelijk kunnen we in de toekomst hier nog aan verder werken.

Dan is er nog een afdeling binnen Synthon die ik graag wil bedanken, namelijk de protein interaction groep van de preklinische afdeling**: Karin, Cindy, Ellen, Jochem, Jos, Tinie, Myrthe, Rachel, Benny, Ingrid** en **Ruud**. De laatste 2,5 jaar mocht ik te gast zijn in jullie werkoverleg wat mij enorm heeft geholpen bij het beter begrijpen en opzetten van mijn eigen SPR analyses.

Natuurlijk wil ik al mijn DSP collega's van Synthon hier bedanken voor alle steun door de jaren heen. Alhoewel ik weinig met de diverse DSP-werkzaamheden van doen had,

zorgden de praatjes met velen van jullie ervoor dat ik ook steeds beter de DSP-kant van ons werk ben gaan begrijpen, maar ook de nodige niet-werkgerelateerde dingen kon bespreken. **Kim, Maria, Bram, Bram en Bram, Bas, Guy, Shadee, Diane, Thomas, Man, Meng, Hetty, Ruud, Sanne, Susana, Walter, Xiaonan, Yorick, Niels, Ernst, Rien, Bert** en **Erik**. En natuurlijk onze ex-DSP'ers die een andere uitdaging hebben gevonden: **Manfred** en **Ferdi**. En ook nog even een speciaal woord van dank aan **Daniëlle**, voor het luisterende oor wanneer ik dat nodig had (zeker in de moeilijkere tijden), voor je enthousiasme om de buffers op de IBIS te gaan testen, wat uiteindelijk tot een mooi resultaat heeft geleid.

Een extra dankjewel voor **Lonnie**, **Jozefi** en **Judith** voor de gezellige wandelingen tijdens de lunchpauzes, waardoor ik ook elke dag even mijn gedachten kon verzetten in de buitenlucht. Judith, jammer dat je bent weggegaan bij Synthon; ik vond je een leuke, gezellige collega. Maar ik ben blij dat je een nieuwe uitdaging hebt gevonden, en we blijven ook in de toekomst gewoon regelmatig bijkletsen buiten werktijd.

Dan wil ik ook alle volleybalmaatjes die ik in vijf jaar bij Invicta heb gehad (23 in totaal…. Zou het aan mij liggen?, een volleybalteam bestaat toch uit 8-10 personen….), maar in het bijzonder nog even een extra dankjewel voor **Annet, Marike, Maringa, Astrid, Anne, Carolien, Paula, Ellen** die het wel het langste hebben volgehouden met mij ☺. Dank jullie wel voor alle gezellige volleybal-uurtjes waarin ik even niet aan mijn werk hoefde te denken.

Vivian, alle leuke dingen buiten werk en promotie om zorgden ervoor dat ik in de weekenden weer kon opladen. De gezellige avondjes uit, bioscoop-bezoekjes, feestjes en spelletjes-avonden zorgen ervoor dat ik niet altijd met werk bezig ben. En uiteraard ook voor mijn vriendinnen uit home-town America; ondanks dat we elkaar nog maar weinig spreken en zien sinds ik verhuisd ben, vind ik het altijd weer gezellig als we samen zijn: **Annelies, Marloes, Ivon, Mieke, Lieke, Esther, Jenny, Marloes** en **Thea**. Daarnaast wil ik ook mijn schoonouders **Theo** en **Angelika** bedanken voor de oprechte interesse in mijn onderzoek en de voortgang gedurende alle jaren.

Mark, **Jeroen, pap** en **mam**, ondanks dat jullie vaak de vraag moesten stellen hoe het ging met mijn 'studie' en 'afstuderen' en jullie het inhoudelijk hebben opgegeven wat ik nu eigenlijk doe, hebben jullie me wel altijd weten te steunen en interesse getoond in hoe het allemaal ging. Juist doordat het niet altijd over mijn werk hoeft te gaan maar we ook gewoon gezellige familie-dingen konden doen; dat werkt altijd beter om je werk even los te laten.

Als laatste mijn allerliefste **Frank**, jij bent altijd een steunpilaar als het nodig is en jij had er vertrouwen in dat ik kon doen wat ik moest doen. Dank je wel voor alle lieve woorden, humor en steun, en dat je er voor me was in de moeilijkste tijden. Nu jij nog je studie afronden en dan hebben we straks weer alle tijd voor elkaar. En niet te vergeten, mijn grootste kleine vriendje, **Jesper**, en binnenkort je nieuwe 'partner-in-crime' die we hopelijk snel gaan leren kennen. Door jou besef ik elke dag weer dat er nog een leven is naast het promoveren. Je maakt me aan het lachen om de stomste, kleinste dingen, omdat dat nu eenmaal is wat peuters doen. Heerlijk om zo zonder zorgen naar de wereld te kunnen kijken en die te ontdekken, en er zo voor te zorgen dat ik ook even alle zorgen vergeet na een drukke werkdag.

ABOUT THE AUTHOR

Karin Lubbers-Geuijen was born on 21 August 1985 in Roggel, The Netherlands. In 1997 she started secondary school at the Dendron College in Horst, where she received her VWO diploma ("profiel *Natuur en Gezondheid*") in 2003. In that year she started studying Analytical chemistry at the Hogeschool van Arnhem and Nijmegen, where she received her Bachelor's degree in 2006. She finalized her BSc degree with an internship and graduation at Analab SA, Santiago, Chile on a method development for illegal growth-promoting agents using LC-MS. In 2006 she started her MSc study Analytical biochemistry at the Vrije Universiteit in Amsterdam. She received her MSc degree in 2008, after performing her Master thesis at Synthon BV, Nijmegen in 2007-2008, focusing on method development for analyses of chiral molecules based on several analytical techniques.

In 2008 she started working at the Bioanalytical department within Synthon Biopharmaceuticals BV, Nijmegen, where she was responsible for method development and characterization of biopharmaceuticals, mainly based on chromatographic, electrophoretic and mass spectrometric techniques.

In 2012 she started her PhD research within Synthon Biopharmaceuticals BV, Downstream Processing department and at Wageningen University, chair group Bioprocess Engineering. The research involved the application of surface plasmon resonance imaging in different areas of biopharmaceutical development. The results of this PhD research are described in this thesis.

In May 2017 she finalized her PhD research and continued working within Synthon Biopharmaceuticals BV.

LIST OF PUBLICATIONS

K.P.M. Geuijen, R.B.M. Schasfoort, R.H. Wijffels, M.H.M. Eppink (2014). High-throughput and multiplexed regeneration buffer scouting for affinity-based interactions. Analytical Biochemistry (454) 38-40

K.P.M. Geuijen, L.A. Halim, H. Schellekens, R.B.M. Schasfoort, M.H.M. Eppink (2015). Label-Free Glycoprofiling with Multiplex Surface Plasmon Resonance: A Tool To Quantify Sialylation of Erythropoietin. Analytical Chemistry 87 (16) 8115-8122

K.P.M. Geuijen, D.F. Egging, S. Bartels, J. Schouten, R.B.M. Schasfoort, M.H.M. Eppink (2016). Characterization of low affinity Fcgamma receptor biotinylation under controlled reaction conditions by mass spectrometry and ligand binding analysis. Protein Science 25 (10) 1841-1852

K.P.M. Geuijen, D.E.J.W. van Wijk-Basten, D.F. Egging, R.B.M. Schasfoort, M.H.M. Eppink (2017). Rapid buffer and ligand screening for affinity chromatography by multiplexed Surface Plasmon Resonance imaging. Biotechnology Journal, accepted June 2017

K.P.M. Geuijen, C. Oppers-Tiemissen, D.F. Egging, P.J. Simons, L. Boon, R.B.M. Schasfoort, Michel H.M. Eppink (*submitted*). Rapid screening of IgG quality attributes: effects on Fc receptor binding

OVERVIEW OF COMPLETED TRAINING ACTIVITIES

Discipline specific		
Multivariate and Principal Component Analysis (Minitab)	Nijmegen	2013
Advanced Proteomics	Wageningen	2013
Online and At-line analytical technologies	Londen	2013
Protein characterization, biopharmaceutical development and biotechnology	Amsterdam	2013
Mini-symposium farewell Hans Tramper *	Wageningen	2014
Developments in protein interaction analysis	San Diego	2014
Netherlands biotechnology congress	Ede	2014
Biomolecular interaction analysis: From molecules to cells*	Porto	2014
Label-free technologies *	Boston	2015
Biosimilar master class ‡	Utrecht	2015
SensorCon One	Salt Lake City	2015
NBV Symposium Cell and Fermentation technology ‡	Leiden	2016
Microscale separations and bioanalysis ‡	Noordwijkerhout	2017
General		
VLAG PhD week	Baarlo	2013
Project and time management	Wageningen	2013
Scientific writing	Wageningen	2014
Teaching and supervising MSc students	Wageningen	2014
PhD workshop carousel	Wageningen	2015
Presenting with impact	Wageningen	2015
Efficient writing strategies	Wageningen	2015
Optionals		
Preparation of research proposal	Wageningen	2012
EFRO project ACCESS meetings	Netherlands	2012-2016
DSP department meetings	Nijmegen	2012-2016
Teaching		
BSc course Biorefinery	Wageningen	2013-2015

* Poster presentation
‡ Oral presentation

This research was financially supported by the "Europees Fonds voor Regionale Ontwikkeling (EFRO) voor Oost-Nederland (Gelderland and Overijssel)".

The work in this thesis was conducted at Synthon Biopharmaceuticals BV, Nijmegen, the Netherlands